Characterization and estimation of high frequency channel with multiple antenna system

Krishnan, Kuramesh

Award date:
2013

Awarding institution:
Coventry University
M S Ramaiah University of Applied Sciences

CHARACTERIZATION AND ESTIMATION OF HIGH FREQUENCY CHANNEL WITH MULTIPLE ANTENNA SYSTEM

By

KUMARESH KRISHNAN

December - 2013

A thesis submitted in partial fulfilment of the University's requirements for the Doctor of Philosophy

Coventry University in collaboration with
M. S. Ramaiah School of Advanced Studies

CERTIFICATE

This is to certify that the Doctoral Dissertation titled "Characterization and Estimation of High Frequency Channel with Multiple Antenna System" is a bonafide record of the work carried out by Mr. KUMARESH KRISHNAN in partial fulfilment of requirements for the award of Doctor of Philosophy Degree of Coventry University

December - 2013

Dr.Govind R Kadambi
Director of Studies
M.S.Ramaiah School of Advanced Studies, India

Dr.James Brusey
Supervisor
Coventry University, UK

ACKNOWLEDGEMENTS

The successful completion of any task would be incomplete without complementing those who made it possible and whose guidance and encouragement ensured its success. I am overwhelmed at this point of time to express my sincere and heartfelt gratitude to all those who were involved with me in the successful completion of my research work.

This research work has benefited from the help of many individuals. The discussion sessions with, and guidance of, **Prof. Govind R. Kadambi,** Pro-Vice Chancellor**,** M. S. Ramaiah University of Applied Sciences (MSRUAS)**,** Bangalore, were key to a well-sustained motivation for realizing and improvising my research results. I profusely thank him for the same.

I am thankful to **Dr. James Brusey,** Coventry University, U.K, for accepting to be my CU supervisor, for his thought provoking suggestions and also key inputs provided during my thesis preparation.

With deep sense of gratitude and indebtedness, I acknowledge the support, guidance and encouragement rendered by, **Prof. S.R. Shankapal**, Vice Chancellor, MSRUAS. While his advices have been a source of inspiration, his suggestions and feedback proved to be valuable course correctors throughout the tenure of my research work at MSRUAS.

I would like to thank **Prof. M.D Deshpande,** MSRUAS, for providing necessary resources, facilities and an excellent environment conducive to research work. His politeness and conduction of research reviews are worthy of emulation.

I take this opportunity to express my gratitude to **Dr. Peter White**, Professor, Coventry University, U.K. During the review meetings, his suggestions and directions have helped me a lot in understanding the purpose of research. I am ever grateful to him for his kindness and patient listening during review meetings.

It is also my pleasant duty to thank **Dr. Girish Chandra**, TCS, **Dr. Narasimhan,** NAL, and my colleague **Mr. A.N. Chakrapani Y Rao,** BEL for their feedback, suggestions and guidance during the reviews.

I would like to express my heartfelt gratitude **Mr. Michael Allen**, Research Fellow, Cogent Computing Applied Research Centre, Coventry, U.K for his generous support and encouragement during my stay at Coventry, U.K.

I avail this opportunity to extend my thanks to Management of Bharat Electronics Limited, Bangalore, who generously facilitated in all my academic endeavours. Without their support, motivation and co-operation, it would have been impossible to complete the research work successfully.

I wish to express my warm and sincere thanks to all the teaching and non-teaching staff of MSRSAS who directly or indirectly have been of great help in my research work

I would also thank my parents for their unconditional love and support without which nothing would have been possible.

I take this opportunity to express my deepest and unconditional love to my family members without whom my research work would have not seen the light of the day. I am forever indebted to them and very sincerely acknowledge their forbearance during this period. Their support has steadfastly sustained my motivation to culminate all my doctoral research work into this thesis.

Last, but certainly not the least, I offer my most humble submission and thanks to ALMIGHTY GOD for his grace and immeasurable blessings.

TABLE OF CONTENTS

LIST OF TABLES

LIST OF FIGURES

NOMENCLATURE

$n(k)$	AWGN at time index k
E_s	Total energy of symbol transmitted
$H(k)$	$M \times N$ MIMO channel matrix
$\|.\|$	Absolute Value
N_0	Noise Variance
ρ	Transmitted Signal to Noise ratio (SNR)
B	Bandwidth of the signal in Hz.
C	Channel Capacity
$I(.:.)$	Mutual Information
$E(.)$	Expectation
ε	% outage probability
$C_{out,\varepsilon}$	Outage capacity
η	Received SNR
G	Tap Gain Function
J	Cost function
δ	Delta
τ	Time Delay
σ^2	Variance
I	Identity Matrix
f_D	Doppler frequency (shift)
$q(.)$	Proposal Distribution

ABBREVIATIONS

ACF	Auto Correlation Function
AR	AutoRegressive
AWGN	Additive White Gaussian Noise
BER	Bit Error Rate
BLOS	Beyond Line-of-Sight
BPSK	Binary Phase Shift Keying
CDMA	Code Division Multiple Access
CK	Chapman-Kolmogorov
CSI	Channel State Information
ECM	Electronic Counter Measure
EKF	Extended Kalman Filter
EKPF	Extended Kalman Particle Filter
FDMA	Frequency Division Multiple Access
FEC	Feed-forward Error Coding
FFT	Fast Fourier Transform
FIR	Finite Impulse Response
FOT	Frequency of Optimum Transmission
GSF	Gaussian Sum Filter
HF	High Frequency
IDFT	Inverse Discrete Fourier Transform
IEKF	Iterated Extended Kalman Filter
IIR	Infinite Impulse Response
i.i.d	independent and identical distributed
LLPF	Local Linearization Particle Filter
LMS	Least Mean Square
LUF	Lowest Usable High Frequency
MAC	Multiplication-Accumulation Computation
MCMC	Markov Chain Monte Carlo
MI	Mutual Information
ML	Maximum Likelihood

MIMO	Multiple Input Multiple Output
MIMO-HF	Multiple Input Multiple Output High Frequency
M-QAM	M-ary Quadrature Amplitude Modulation
MSE	Mean Square Error
MUF	Maximum Usable Frequency
NG	Non-Gaussian
NL	Non-Linear
OFDM	Orthogonal Frequency Division Multiplexing
OFDMA	Orthogonal Frequency Division Multiplexing Access
PDF	Probability Density Function
P.D	Positive Definite
PF	Particle Filtering
PSD	Power Spectral Density
QPSK	Quadrature Phase Shift Keying
QoS	Quality of Service
RB	Recursive Bayesian
RBE	Recursive Bayesian Estimation
RLS	Recursive Least Square
RR	Residual Resampling
SDMA	Space Division Multiple Access
SER	Symbol Error Rate
SHF	Super High Frequency
SID	Sudden Ionospheric Disturbances
SIS	Sequential Importance Sampling
SISO	Single Input Single Output
SIMO	Single Input Multiple Output
SM	Spatial Multiplexing
SMC	Sequential Monte Carlo
SNR	Signal to Noise Ratio
SPF	Sigma Point Filters
SR	Systematic Resampling

STC	Space-Time Coding
STBC	Space-Time Block Codes
STTC	Space-Time Trellis Code
TDMA	Time Division Multiple Access
UHF	Ultra High Frequency
UKF	Unscented Kalman Filter
V-BLAST	Vertical Bell Labs Layered Space Time
VHF	Very High Frequency

ABSTRACT

This thesis presents the development of an efficient and adaptable simulation model for characterization and estimation of MIMO-HF channel subjected to impairments, such as multipath fading, system non-linearity and non-Gaussian noise. Under channel characterization and modelling, this thesis proposes the extension of conventional Watterson model for SISO to MIMO-HF channel incorporating the associated spatial correlation and the non-linearity of the system. The novelty of the developed model lies in the capability of its impulse response to emulate nearly the practical HF channel by incorporating the cited adverse channel impairments. This thesis proposes the modelling of MIMO-HF channel through the computationally efficient IIR /AR filter approach instead of conventional FIR filter. The generic and the versatile features of IIR filter-based approach for modelling the HF channel impairments have been demonstrated by its application to both SISO and MIMO-HF systems.

Within the purview of channel estimation for improved reliability and enhanced data rate of the MIMO-HF communication link, this thesis proposes a novel PF based channel estimation technique for HF communication links subjected to multipath fading and system non-linearity. The PF based channel estimation algorithm proposed in thesis for MIMO-HF is shown to closely approximate the impulse response of the channel induced by the channel impairments. The improved channel estimation facilitates the effective utilization of system resources to ensure enhanced capacity and reliability of HF links. Although one can conceive an idea of invoking the PF concept devoid of EKF, this thesis attempts to adopt a unified approach wherein PF and EKF schemes are combined to realize better posterior density functions, thereby improving the accuracy in channel estimation. The advantageous and desirable features derived by invoking the proposed PF formulation over the conventional RLS have also been addressed. This thesis also addresses the effects of spatial correlation, system non-linearity and the non-Gaussian noise on the proposed PF based channel estimation algorithm. The expected improvement in the receiver performance in lieu of improved channel estimation algorithms, as well as replacement of conventional SISO with MIMO, is validated through the performance parameters such as capacity and reliability.

CHAPTER 1

INTRODUCTION

1.1 Introduction and Motivation

For several decades now, HF ionospheric radio has been a reasonably simple and effective mode of communication for range spanning from less than 100 miles (the upper limit of the range of VHF and UHF Line-of-Sight radio) to many thousands of miles (world-wide). HF radio has been particularly useful where cable communication is impractical if not impossible: for communication with aircraft, ships, and other mobile units as well as for communication with temporary and remote ground stations.

Despite the introduction of satellite services, interest remains in HF data communications, due largely to its cost advantage and freedom from 'third party' controlled equipment's. Compared to satellite radio communication, the HF ionospheric radio communication is superior under disaster conditions. For the reasons of efficiency and reliability, HF ionospheric radio can be a backup to the more vulnerable satellite radio. It is imperative that reliability is an important performance attribute of HF ionospheric radio communication.

HF communication systems continue to thrive even in an era of ever increasing demand for higher data rates. This goal is predominantly challenging for systems that have both power and bandwidth limitations as well insistence on realization of the system performance with an affordable computational complexities. For the realization of higher data rate, the conventional Single Input Single Output (SISO) communication has limitations of requirement of wider bandwidth or higher order modulation types. Hence, there is need for a new technology that does not insist on higher bandwidth for a given data rate. Multiple antenna systems fetch a significant enhancement to data rate and system capacity. Multiple antenna systems, typically known as Multiple Input Multiple Output (MIMO) systems, are designed to improve communication performance significantly. To achieve robustness in the communication system, various diversity

techniques are used. These include time diversity (different time slots and channel coding), frequency diversity (different channel frequency band, spread spectrum, and Orthogonal Frequency Division Multiplexing (OFDM)), and also spatial diversity. Spatial diversity requires the use of multiple antennas at the transmitter or the receiver end. Multiple antenna technology can also be used to increase the data rate (spatial multiplexing) instead of improving robustness. The MIMO systems rely on architectures such as spatial multiplexing, transmit diversity and beam-forming to enhance the quality of transmission, data rates and received signal gain as well as reduced interference. In practice, these techniques are used separately or in combination depending on the channel condition. The promise of higher data rates with increased spectral efficiency makes MIMO attractive especially in HF communications where systems operate in rich multipath environments.

MIMO technology has been a broad topic of research for the past few decades. Research by Winters, Paulraj, Telatar, and Foschini [Winters 1994, Foschini 1998, Telatar 1999, Paulraj 2004] has shown the potential of MIMO systems in improving the robustness, directive gain, reduction of the probability of interception and enhanced throughput using combination of diversity and multiplexing techniques. Both diversity and multiplexing techniques are of specific relevance to many non-commercial bands, apart from commercial bands, of frequency. Some non-commercial applications that are of direct relevance to government agencies are Disaster Communication and Tactical Communication scenarios. In general the main objectives of MIMO technology are:

- To provide improved reliability of communication links
- To offer increased capacity and coverage compared to conventional single antenna
- To enhance the capability of ad-hoc network compared to existing conventional systems

Primarily, research in MIMO systems is focused on short- range communication within the VHF, UHF and SHF bands. Only little research has been conducted towards exploiting MIMO technology for long-range communication in HF band [Gunashekar 2009, Stangeways 2006]. The multipath fading associated with a rich scattering

environment forms an essential channel characteristic feature requirement to exploit the MIMO technique. Due to limitation of conventional SISO HF communication in terms of coverage and capacity in the presence of multipath, MIMO technology finds its application in HF communication to enhance the existing capabilities.

The understanding of HF channel propagation is important in the design, deployment and management of the resources (Bandwidth, power, and system computation) to achieve a reliable system performance (date rate, BER, SNR). For providing a realistic MIMO-HF system performance in the design process, channel characterization and a model that can accurately describe the propagation (transmission) medium are essential. Characterization of the HF channel requires both the measurements based on performance parameters as well as simulations that precede the measurement. Channel simulations are used to verify the validity of the designed communication system performances in the laboratory by incorporating channel impairments (such as delay, attenuation, multipath fading, and system non-linear effect and non-Gaussian noise scenario) of a practical HF communication channel. For the design and performance optimization of HF communication systems, accurate and realistic MIMO-HF channel modelling with multipath fading phenomenon associated with HF channel parameters (delay spread, Doppler spread) along with non-linearity of the HF system as well as non-Gaussian noise are crucial. They are applicable to both SISO and MIMO systems.

Various approaches for characterizing and modelling the HF channel are available in the literature. Among them, Watterson model is considered to be more prominent because of its simplicity and analytical nature. The pioneer work of Watterson [Watterson 1970] has been considered a practical way of representing the HF channel model and it is specifically referred to as Watterson model. This model assumes the amplitude variation of the channel to follow a Rayleigh distribution. Further, the Doppler spread on each of its multipath is assumed to exhibit Gaussian power spectrum. In brief, the representation of the Watterson channel model can be visualized as an ideal tapped delay line, where at each tap and delay line, signal gets multiplied with tap-gain function that is accumulated recursively. The tap-gain functions are filtered to produce a

Gaussian Doppler spread in the power spectrum of multipath propagation. The tap-gain function to characterize the channel parameter can be realized either by Finite Impulse Response (FIR) filter or Infinite Impulse Response (IIR) filter. The guaranteed accuracy and computational efficiency of channel characterization depend on whether it involves FIR or IIR. The FIR approximation of a channel model often requires a large number of tap coefficients, and the order of the filter increases with the increased sampling frequency (bandwidth) of the signal. It is well known that IIR filters can capture the system dynamics (time variants, Doppler spread) with fewer parameters (tap coefficients and order of filter) as compared to FIR filters [Radenkovic 2003]. The analytical response of channel modelling using IIR/Auto Regressive (AR) filter has better approximation for a wide range of Doppler spectrum with minimum order of filter and hardware resources [Baddour 2005]. The IIR configuration has a relative advantage of smaller silicon chip area and lower power consumption compared to FIR. This is attributed to the sufficiency of lower order of IIR configuration to retain the optimal accuracy and therefore has become a more preferred choice for hardware implementation of channel simulators.

The channel parameters that characterize the channel conditions have an effect on the transmission of the data. The effects of channel conditions on the transmitted data must be estimated to recover the transmitted information correctly. Often, the estimation of channel parameters is based on an approximate underlying channel model for the radio wave propagation. Channel estimation is a challenging task in receiver design since the accuracy of the channel estimation technique plays a major role in evaluating the performance of the system. The role of channel estimation is directed to counter the effects of variation of statistical channel parameters (such as delay spread, Doppler spread) for achieving an acceptable system performance, as specified by the designers.

Channel estimation based on supervised methods of signal detection algorithms requires the knowledge of channel impulse response, which is usually estimated by using the known training (mid-amble) symbols in the middle of the transmission burst. In general, there are two types of estimation approaches: Classical and Bayesian. In the classical

estimation, the vector (received time samples) to be estimated is viewed as deterministic, but unknown. In Bayesian estimation, the estimate is determined based on the Probability Density Function (PDF) of the received samples.
Several supervised channel estimation techniques based on adaptive filters, including Least-Mean-Square (LMS), Extended Kalman Filter (EKF) and Recursive-Least-Square (RLS) [Haykin.1996] are almost linear tracking methods. These linear methods cannot perfectly track or estimate the HF channel associated with non–linearity and non-Gaussian noise. To deal with both the non–linearity as well as non-Gaussian noise, Particle Filtering (PF) [Gordon 1993] is emerging as a powerful method for sequential signal processing, with a wide range of applications in science and engineering [Djuric 2003]. PF is a Sequential Monte Carlo (SMC) methodology [Wang 2004], where the basic idea is the recursive computation of relevant probability distributions using the concept of important sampling and approximation of probability distributions with discrete random measures.

The overall performance of HF system depends significantly on the effective utilization of resources. The critical utilization of resources depends on the choice of channel estimation technique and the estimation technique must prevail even under adverse channel conditions such as system non-linearity, time varying multipath fading and non-Gaussian noise environments. In view of these considerations and the inability of the conventional estimation techniques to fulfil the requirements of the context, an alternative approach to develop adaptive channel estimation technique for the HF channel invoking the principle of Bayesian forecasting will be of practical importance. Channel estimation based on PF is an ideal choice to deal with the system non-linearity and non-Gaussian noise scenarios [Bergman 1999, Arulampalam 2002, and Doucet 1998]. Reported research in [Haykin 2004] revealed that the PF can offer performance improvement of the MIMO wireless channel above that of the UHF band.

In the design of reliable and high data rate HF communication systems, the following aspects demand further research on:

Channel Characterization and Modelling:

It necessary to benchmark the performance of designed HF communication system in practical scenario by subjecting the system for various channel impairments. To emulated the practical HF channel impairment in laboratory following feature are necessary,

- Computationally efficient simulation module for HF channel characterization and modelling that is valid for both SISO as well as MIMO configurations.
- Impulse response (Transfer function) of the channel model which can emulate near practical HF channel by incorporating channel impairments comprising multipath fading, system non-linearity and non-Gaussian noise.

Channel Estimation:

To mitigate the effect of channel impairments in the receiver, channel estimation technique is employed to estimate the effects of channel impairments. These channel impairment information is utilize by subsequent module in receiver to recovery the transmitted symbols. The following feature is required for channel estimation is necessary,

- Extension of channel estimation algorithms from conventional SISO to MIMO system to take advantage of potential benefits, such as diversity and multiplexing gain , as well as to counter the effects of rich multipath HF environment for the improved reliability and enhanced data rate.
- HF channel estimation algorithms that can deal with the non-linearity of the system, channel impairments as well as non-Gaussian noise scenario.

The focus of the proposed thesis is to address and resolve the research issues listed under both channel characterization and channel estimation.

The goal of computationally efficient approach for HF channel characterization and modelling is realized through the application of the IIR Filter/AR approach to model the HF channel impairments instead of conventional FIR filter. The generic and the versatile features of the IIR filter based approach for modelling the HF channel impairments have been demonstrated by its application to both SISO and MIMO-HF system.

Mathematical models of the statistical parameters of the HF channel such as delay spread, Doppler spread, attenuation and frequency shift have been developed and realized through computationally efficient schemes to emulate near practical HF channel. The developed mathematical models have been proved to be applicable to both SISO and MIMO system configurations.

For enhanced reliability of the HF communication link, this thesis analyses the channel estimation algorithm with the joint application of MIMO and PF techniques to counter the channel impairments. The thesis also substantiates the utility of MIMO approach in the realization of higher data rate of the system as well.
Similar to MIMO serving the stated twin objectives of both enhanced reliability and higher data rate, this thesis demonstrates the objectives of PF in not only ensuring increased reliability but also its capability to deal with system non- linearity and non - Gaussian noise scenario. Although one can invoke the PF concept devoid of EKF, this thesis attempts a unified approach wherein PF and EKF schemes have been combined to realize better posterior density functions resulting in improved channel estimation. The expected improvement in the receiver performance in lieu of improved channel estimation algorithms as well as replacement of conventional SISO with MIMO systems evaluated through the system parameters like data rate and reliability have also been analysed in this thesis.

1.1.1 Objectives of the Thesis

Channel characterisation and modelling play important role in the realization of desired system performance of MIMO-HF systems. In particular, it is always desirable that channel characterisation and modelling should closely approximate the practical MIMO-HF channel. Channel simulator/modelling are an effective tool to analyse the effects of hostile channel parameters on the system performance in laboratory.

An efficient and adaptive channel estimation technique that can prevail over the commonly prevalent non-linearity of system, time varying multipath fading and non-Gaussian noise environments in a HF channel is an important need for effective

utilization of resources as well as in the design of a HF communication system featured with reliability and high data rate. Another research aspect of equal significance is the requirement to develop efficient adaptive (recursive) techniques for channel estimation to mitigate the imperfections in the transmission caused by both the non-linearity of system and time-varying HF channel to enhance the capacity and the reliability of a HF link.

From the above research perspectives, this thesis addresses the following questions:

(1) Given an SISO-HF channel model, what are the modifications necessary for its extension to a MIMO-HF configuration?

(2) Given such an enhanced HF channel model which can cater for both SISO and MIMO configurations, can the developed model be imparted the capability to handle the adverse scenario such as multipath fading, system induced non-linearity and non- Gaussian noise?

(3) Can the channel model thus developed be used in a real–time channel estimation algorithm and will such an algorithm enhance the capacity and reliability even in the presence of realistic interference?

This thesis envisages to address the answers to the above listed research questions through the realization of the following objectives:

1. To analyse an appropriate scheme for incorporating the short term multipath parameters in the characterisation and modelling of MIMO-HF channel associated with the non-linearity of system, non-Gaussian noise and spatial correlation
2. To explore the feasibility of extending the existing Watterson SISO-HF channel model to MIMO-HF channel model
3. To propose and validate the computationally efficient HF channel modelling applicable to both SISO and MIMO configurations

4. To develop and implement a PF based robust channel estimation technique for effective utilization of system resources leading to the enhanced capacity as well as reliability of HF links under adverse channel impairment catering to both the SISO and MIMO configurations
5. To analyse the feasibility of applying the developed PF based channel estimation technique from the perspective of real time applications to MIMO-HF channel

1.2 Organization and Outline of the Thesis

A succinct description of the organization of the chapters of the thesis is as follows.

In chapter 2, an introduction and review of HF channel characterisation and estimation followed by MIMO principles are presented. Chapter 3 discusses a survey on non-linear filtering technique followed by sub-optimal non-filtering that serves as basis for Particle Filtering. Chapter 4 presents a computationally efficient approach for modelling the HF channel with both SISO and MIMO configurations. An analysis of the effects of small scale fading, system induced non-linearity and non-Gaussian noise on Particle filtering based channel estimation algorithm is discussed in chapter 5. A summary and assessment of the research findings of the thesis are presented in chapter 6.

CHAPTER 2

INTRODUCTION TO MIMO SYSTEMS FOR HF CHANNEL COMMUNICATION

Wireless systems continue to strive for ever increasing higher data rates. This goal is predominantly challenging for systems that have both power and bandwidth limitations as well insistence on realization of the system performance with an affordable computational complexities. As conventional communication has limitation in using more bandwidth or higher order modulation types, there is need for new technology. Multiple antenna systems give a significant enhancement to data rate and channel capacity. Multiple antenna systems are typically known as Multiple Input Multiple Output (MIMO) systems and are designed to improve communication performance significantly. To achieve robustness in the communication system, different diversity techniques are used. These include time diversity (different timeslots and channel coding), frequency diversity (different channel frequency band, spread spectrum, and Orthogonal Frequency Division multiplexing), and also spatial diversity. Spatial diversity requires the use of multiple antennas at the transmitter or the receiver end. Multiple antenna technology can also be used to increase the data rate (spatial multiplexing) instead of improving robustness. The MIMO system relies on techniques such as spatial multiplexing, transmit diversity and beam-forming to enhance the quality of transmission, data rates and received signal gain as well as to reduce interference. In practice, these techniques are used separately or in combination depending on the channel condition. The promise of higher data rates with increased spectral efficiency makes MIMO especially attractive in wireless communications where systems operate in rich multipath environments

The research community has extracted the inherent potential benefits of MIMO in various aspects for wireless communications in both civilian and commercial systems through the pioneering contributions of [Foschini 1996], [Paulraj 2003] and [Telatar 1999]. MIMO technology has promised to enhanced capacity and reliable communication links for future wireless communication systems. Perhaps even more striking feature of MIMO is that just a few years after its invention, the technology seems to have poised for its

applications is large-scale standards-driven commercial wireless products and networks such as broadband wireless access systems, Wireless Local Area Network (WLAN), Third/Forth generation (3G/4G) networks and beyond.

HF data rates are currently too low to support reliable video or other data-intensive communication because of low bandwidth allocations and challenging propagation conditions. While recent efforts [Daniels 2013, Scheible 2014] have resulted in new waveforms designed for wider bandwidths and higher data rates, the highest rates are achievable only in the most favourable conditions. These conditions cannot prevail consistently due to the inherent variability of the HF channel. Further, enhancing data rates with HF through bandwidth expansion is increasingly difficult given the scarcity of acquirable HF spectrum as well as the challenges in forcing a change in international spectrum policy.

While prior work in academic and non-academic (commercial) research has suggested that HF sky-wave channels can support MIMO processing [Gunashekar 2009, Strangeways 2006, Tomei 2013, and Scheible 2014], prior experimental studies have made impractical assumptions for tactical communications [Ndao 2011]. For example, [Ndao 2011] has assumed antennas that are spatially separated by many wavelengths (tens of meters) at both the transmitter and receiver. A flexible tactical HF MIMO solution cannot afford this separation of antennas. [Daniels 2013] demonstrated the feasibility of MIMO-HF in a small-array configuration for Near-Vertical Incidence Sky-wave (NVIS) links. Future HF MIMO systems will exploit both diversity and spatial multiplexing through smart adaptive processing. Due to the limitation of conventional HF SISO communication in terms of coverage and capacity in the presence of multipath, MIMO technology finds itself as an alternative to enhance the existing capabilities of HF communication.

Channel characterisation and modelling play important role in the realization of desired system performance of MIMO-HF systems. In particular, it is always desirable that channel characterisation and modelling should closely approximate the practical MIMO-

HF channel. Channel simulator is an effective tool to analyse the effect of hostile channel parameters on the system performance in laboratory.

Channel estimation is a critical subsystem of a receiver block to counter the effect of channel impairment on the receiver performance. Channel estimation is a challenging task in receiver design since the accuracy of the channel estimation technique plays major role in evaluating the performance of a system. Basically, the HF channel is not only time-variant but also dynamic in nature and is also subjected to multipath propagation, mobility, local scattering of environment and static or dynamic change in the locations of transmitter and receiver. Because of the inherent varying nature of HF channel, transmitted signals are more likely to be subjected to detrimental effects before reaching to the receiver. The role of channel estimation is directed to counter the effects of variation of statistical channel parameters (such as means, variance, delay spread, Doppler spread) for achieving the acceptable system performance as specified by the designers.

In this chapter three topics are discussed. An introduction to HF channel and implications of characterization of HF channel is presented. This is followed by a discussion on MIMO concept as applicable to HF communication and signal processing to achieve both capacity gain and reliability. The review of HF channel characterization and estimation is the third topic of significance for this chapter.

2.1 HF Communications

Radio frequency range spanning 3 to 30 MHz is classified as High Frequency (HF) or shortwave or sky-wave communication for long distance communication. HF communication offers lower reliability and band limited data transmission compared to other wireless communication usually meant for medium and long range communication. When compared to other wireless communication such as satellite and terrestrial communication, HF communication is not vulnerable to Electronic Counter Measure (ECM) and destruction since it does not need huge infrastructure as compared to cellular mobile; Intermediary infrastructure is not required between the transmitter and receiver . Due to this advantageous feature, HF communication becomes the preferred

mode during emergency scenario, natural calamities/disaster and other unpredicted situation applications [NTIA 1998].

The phenomenon of refraction of HF radio waves from the ionosphere is referred as sky-wave propagation or communication. Suitability of ionospheric portion of spectrum for medium and long communication varies greatly with a complex combination of following factors [Harris Co. 1996, NTIA 1998]:

- Sunlight/darkness at site of transceiver
- Transmitter/receiver proximity
- Season
- Sunspot cycle
- Solar activity
- Polar aurora

In addition, other factors that affect the given HF communication are

- Maximum Usable Frequency (MUF)
- Lowest Usable High Frequency (LUF) and a
- Frequency of Optimum Transmission (FOT)

The impact of HF radio propagation on channel characterization, application of HF communication, inherent benefits of HF technology and challenges in HF communication are discussed in the next section.

2.1.1 Relevance of HF Radio Propagation on Channel Characterization

The characterization of a communication channel depends on radio propagation phenomena. The characteristics of HF channel model to be invoked in subsequent chapter are based on the short-term fading and dispersive effect of the HF sky-wave path. This effect is modelled as tapped delay line model for HF channel by [Watterson 1970]. The various propagation phenomena [Cannon 2002, Harris Co.1996] that define the channel characteristics discussed in detail in subsequent sections are:

- Ionospheric physics
- Radio Wave absorption anomalies
- Radio noise in HF band
- Propagation modes
- Short term loss factors
- Dispersive characteristics

I. Ionosphere

The structure of the ionosphere, its different layers, height of layers and ion density within the layers, constitute the essential parameters to define the HF sky-wave propagation [Watterson 1970, Cannon 2002, and Harris Co.1996]. This sub-section is meant to summarize ionospheric characteristics that affect HF sky-wave propagation. Figure 2.1 shows the phenomena of radio propagation. There are two modes of propagation namely ground wave and sky-wave propagation. Ground wave has four components such as direct, surface, reflected from the earth and refraction due to atmosphere [Harris Co.1996]. Sky waves travel Beyond Line-Of-Sight (BLOS). At certain frequencies, sky-waves act as repeater such that radio waves are refracted/bent, returning to earth hundreds or thousands of miles away depending on density of ionisation of the layer, frequency, angle at which wave enters the layers, time duration and atmospheric conditions. The medium for sky-wave is the ionosphere. The distribution of ionospheric medium is classified into various regions as shown in the Figure 2.2.

D region exists between 30 to 55 miles (48 to 88 Kms) above the earth only during day-time with less reflection of HF radio wave. The D region has the ability to refract signals at low frequencies. High frequencies pass through it with only partial attenuation. The major limiting factor in this region is the lower limit on the achievable LUF. This shortcoming is attributed to ionic collisions that eventually lead to absorption of sky-wave. The absorption is proportional to the amount of ionization of D layer. Higher the ionization, greater will be the energy loss suffered by the radio waves as they pass through the D layer. Absorption is thus most pronounced at mid-day. D layer absorption

increases rapidly following a large solar flare, disrupting HF communications for up to several hours. Since the absorption factor is inversely proportional to square of operating frequency [Harris Co.1996], there is a lower limit below which sky-wave propagation ceases to be effective.

E region ranges from 60 to 90 miles (96 to 144 Kms) above the earth only during day-time. The E region has the ability to refract signals at high frequencies (up to about 20 MHz) than refracted by the D region. The absorption in E region is relatively less when compared to D region. Reflection of sky-wave in this layer is due to the scattering phenomena caused by irregularities in ion density due to turbulence and from meteor trails leading to sporadic propagation characteristics. A sporadic E layer can greatly increase the radio wave frequencies that the E layer is able to reflect. However, it can also be pose a problem, as it may prevent such frequencies from reaching the F layer which supports propagation to a greater range in a single hop than does the E region.

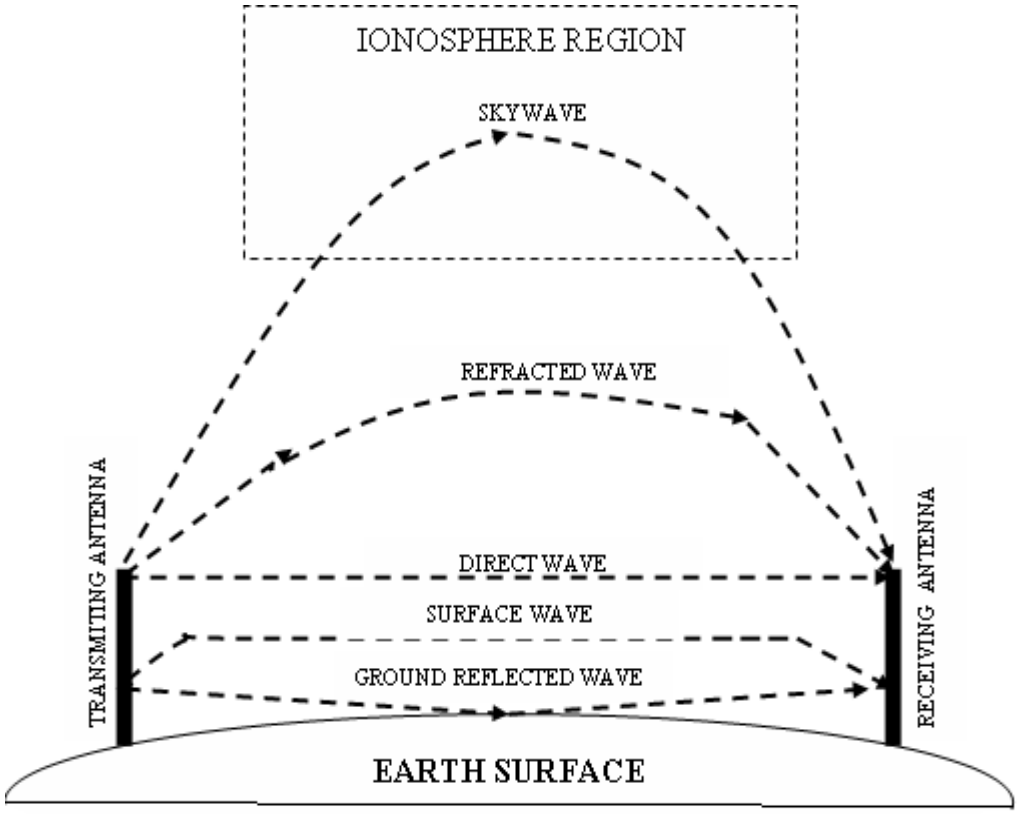

Figure 2.1 : Propagation paths

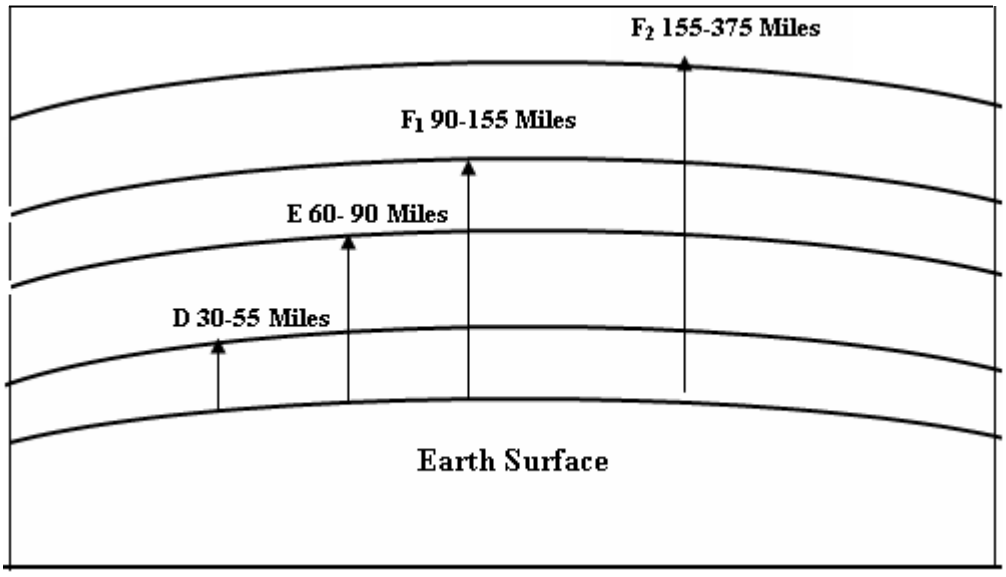

Figure 2.2 : Regions of the ionosphere

F region is sub-divided into F1 and F2 regions. F1 region exists during day-time at a height of about 90 to 155 miles (144 to 250 Kms) above the earth. During night time this F1 region gets merges with F2 region. F2 region operates from about 155 to 375 miles (250 to 603 Kms) during night-time and extends to 400 miles during the day. In general F region provides the refraction necessary to bend the radio wave back to earth for long distance communication. This refraction process (refractive index) is a function of ion density and frequency. F2 region sets an upper limit on the operating frequency (MUF), with the frequency below MUF getting reflected to earth. For frequencies above MUF, HF radio waves will penetrate the F layer and is not reflected back to earth.

II. Natural Phenomena

Natural Phenomena cause inconsistent propagation and are usually associated with high absorption. The time and duration of the high absorption cannot be predicted *apriori*. The duration of high absorption can last for few minutes to days during which time, the sky-wave path is rendered unusable. This effect depends on the geographical location. Some of the natural phenomena which lead to the high absorption are highlighted below.

Solar Activity

Solar Activity is due to the variation of ionized regions caused by Sun's intensity or solar disturbance. The variations which significantly affect the HF sky-wave propagation are: the eleven-year cyclic sunspot activity, solar eruption/flares, and particle radiation. The impact of ionic density variation that changes the parameters such as MUF, D and E regions' absorption, and LUF. A long term effect of ionic density variation includes the long term path loss.

Sudden Ionospheric Disturbances (SID)

SID occurs in D and E regions during day-time due to solar eruption. Its impact results in attenuation/absorption of signal and hence complete loss of link in communication. The SID is treated as long-term power fading. Usually it lasts anywhere from ten minutes to several hours and is relatively steady.

Magnetic Storms

The effect of magnetic storms is similar to that of SID effect. Magnetic storms are caused by particle radiation from the sun. The significant impact of magnetic storms on the ionospheric channel is long term power fading which may last for several days. The magnetic storm has two fold effects, namely reduction in ion density of F2 layer which reduces the MUF and the increased absorption in D and E regions.

III. Radio Noise

In all radio communications, the limiting factor is the ability to receive weak signals against the background noise. This background noise is ambient noise generated by external environment, which is characteristic of the HF band. In effect, this noise is embedded along the received signal via the antenna along with the wanted signals, which limit the performance of receiver.

The ambient noise environment is classified into two parts namely irreducible residual ambient noise which is constant in any particular location, and incidental noise from

man-made sources. The combination of these two noises determines the minimum usable signal level. A detailed discussion of radio noise is presented in chapter 4.

IV. Propagation Path or Mode

Radio Path

The HF radio path is established either by ground wave or sky-wave via reflections from layers in ionosphere. Diffused scattering from atmosphere (such as troposcatter or meteor scatter) can also lead to HF radio path. HF signals reaching a given receiver may arrive by any of the several paths, as shown in Figure 2.3. A signal which undergoes a single reflection is called a "one-hop" signal. A "two-hop" signal would imply that it undergoes two reflections between the ground and the ionospheric layer. Likewise, a "multihop" signal undergoes multiple reflections. The layer at which the reflection occurs is usually indicated, also, as "one-hop E" , "two-hop F", and so on.

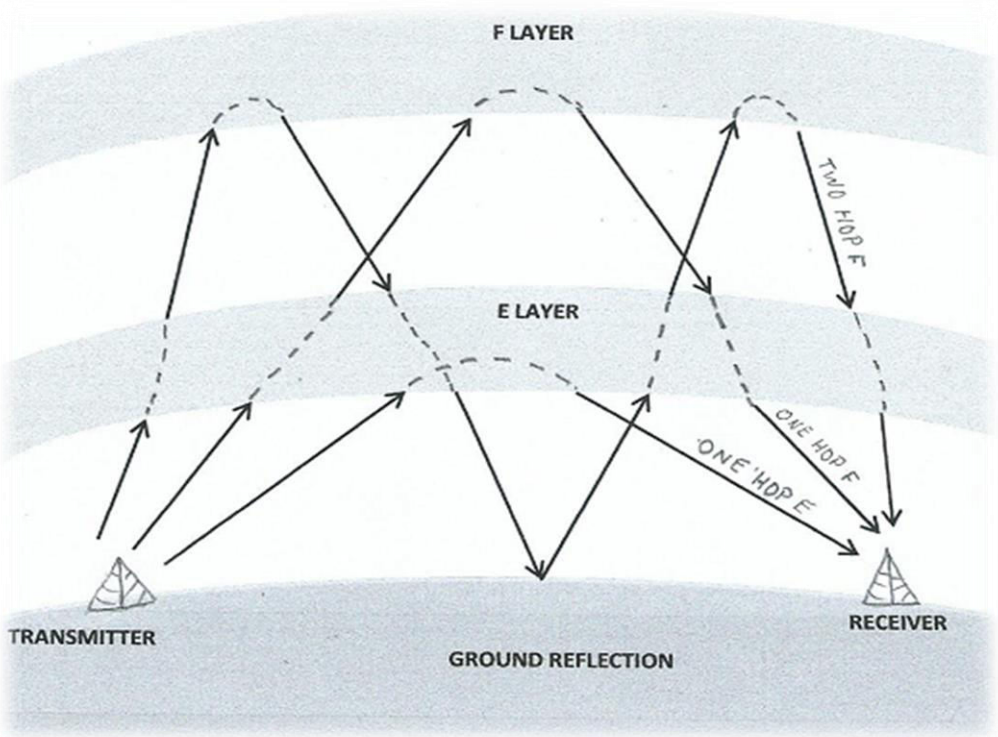

Figure 2.3 :Various paths by which a sky-wave signal might be received

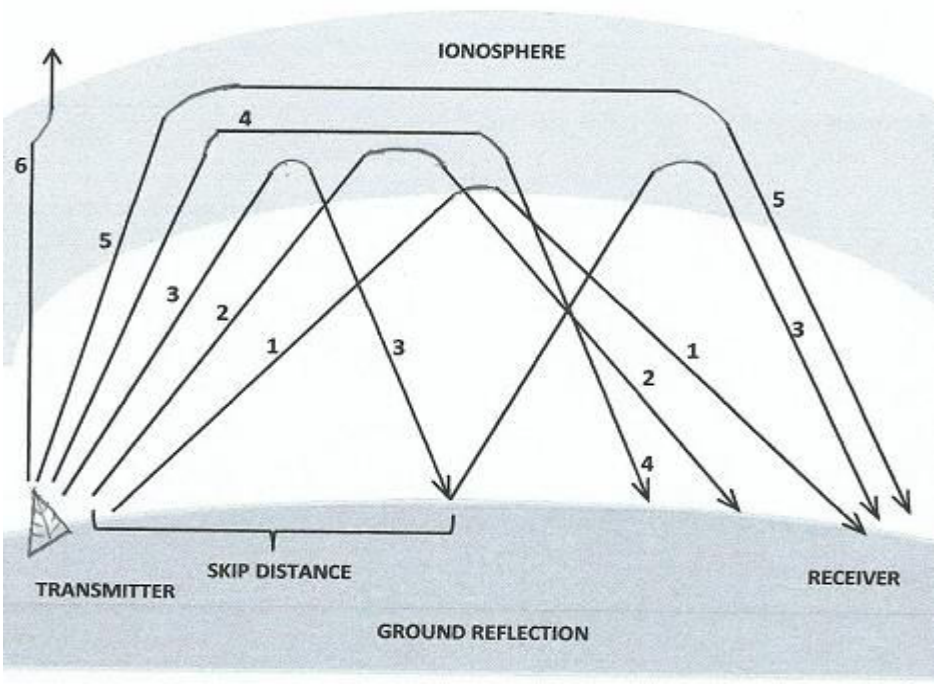

Figure 2.4 : Signal paths for a fixed frequency with varying angles of incidence

Figure 2.4 shows how radio waves may reach a receiver via several paths through one layer. The radio signal reaches the receiver via two or more paths (multipath propagation) through a single or multiple ionospheric layers by multi-hop between ionosphere and earth. The various angles at which radio signal strikes the layer are represented by dark lines and designated as rays 1 through 6.When the angle is relatively low with respect to the horizon (ray 1), there is only a slight penetration of the layer and the propagation path is long. When the angle of incidence is increased (rays 2 and 3), the rays penetrate deeper into the layer but the range of these rays decreases. When a certain angle is reached (ray 3), the penetration of the layer and angle of refraction are such that the ray is first returned to Earth at a minimal distance from the transmitter. However, that ray 3 still manages to reach the receiving site on its second refraction (called a hop) from the ionospheric layer. As the angle is increased still more (rays 4 and 5), the radio signal penetrates the central area of maximum ionization of the layer. These rays are refracted rather slowly and are eventually returned to Earth at great distances. As the angle approaches vertical incidence (ray 6), the ray is not returned at all, but passes through the layer.

The signal dispersion in a multipath propagation is due to:

- Multiple hop
- Multilayer propagation
- Paths with low and high angle
- Ordinary and extraordinary rays from one or more paths

For HF channel model, reflecting sky-wave is considered for analysis via multiple path or modes and reflection mechanism. Here mode refers to resolvable path of the signal between transmitter and receiver. Normally, this mode is modelled as tapped delay filter [Finite Impulse Response (FIR) or Infinite Impulse Response (IIR)] for channel characterization. The co-efficient of tap delay filter controls the channel parameters such as number of modes or paths, time delay between the modes, time spread and relative amplitude of the signal.

Loss Factors

For HF propagation the medium path attenuation is caused by beam spreading, absorption in the D, E and F1 layers. Also, absorption due to ground reflections during multiple hop paths results in long term loss factor having both daily variation and a seasonal variation. This long term medium loss exhibits under log-normal distribution. The long term medium loss is not considered in modelling the path loss and it is usually considered in the analysis of link budget.

Slight variation in path distance with a mode or between the modes is referred to as fading and it causes short term loss. This loss is accommodated in the channel model either as Rayleigh or Rician distribution.

Doppler Shift

Doppler shift is the variation in the carrier frequency of the HF wave subjected to ionic density variations. It occurs due to turbulence in the F2 or sporadic E reflecting layer. The Doppler shift in HF channel shows a typical variation of 1 to 5 Hz.

Delay Spread

Delay spread occurs due to multiple copies of transmitted signal received at the receiver and it is a function of the power received via different ionospheric paths of different path lengths. The time delay difference between the various copies received is referred as delay spread. This effect is an important parameter for HF channel model and it stimulates various single or multiple hops. The typical delay spread varies from 1 to 5 msec.

A detailed description of characterization of HF channel is covered in chapter 4.

2.1.2 Inherent Benefits of HF Technology

I. Long range communications capability

HF radio can communicate over long distances involving thousands of miles. It can also be used for purposes of emergency communication. HF communication provides access to points outside of the communication network area. HF communication systems do not rely on land-based infrastructure, such as land-line telephone, cellular and satellite communication. During disaster in an area or in situations warranting emergency operations, HF communication is the only alternative means of long range communication.

II. No requirement of infrastructure and low cost of ownership

HF radio communication network does not require major infrastructure. It may require fewer infrastructures compared to telephone land lines, cellular telephone and satellite telephones. Typically HF radio user requires devices such as radio and associated antennas. This is sufficient to communicate in the midst of an emergency situation. In setting up a HF communication facility within the geographical boundary of a country/region or locality, consideration must be given for installing the repeater or critical emergency contact points at appropriate places to increase the range of communication. For the scenario that involves the communication outside the country, appropriate treaty or license agreement between the two nations is required to have an uninterrupted communication between the HF radio users. Apart from the lesser

infrastructure requirement, HF communication provides economically viable solution for emergency wireless communication valid for the lifetime as compared to other modes of communication, since it involves only one time initial investment rather than the periodic equipment rental cost and cost involved in making a call.

2.1.3 Challenges in HF Communication

The performance of HF communication is widely dependent on how best the system is designed to mitigate the effects of channel propagation. For example to compensate the free space losses and attenuation in various ionosphere layers, an appropriate choice of antenna gain and increase in transmitted power are required. Apart from this, appropriate choice of the signalling waveform is required to a greater extent to compensate effect of radio channel distortion such as multipath, Doppler effect and other distortions. The signalling waveform includes the modulation techniques, error-correction code, interleaving, and other related issues. In the initial phase of a HF system design, channel simulator or characterization is required to analyse the system performance. The complex ionosphere channel is a considerable challenge for the designer to assess HF radio system and the designer's success depends on a good understanding of the multipath as well as Doppler characteristics.

Next section explains the concept of MIMO as applicable to HF communication and signal processing to achieve both capacity gain and reliability of communication link.

2.2 Principles of MIMO

Main objective for any wireless communication system design is to achieve considerable improvement in power as well as spectral efficiency relative to existing communication system. The limitation in achieving better power and spectral efficiency mainly depends on the characteristics of the wireless channel. Although there is considerable improvement in both power and spectral efficiency by various predecessor technologies, such as TDMA, FDMA, CDMA and to OFDMA. MIMO technology involves space-time coding and the constellation (modulation) process provides significant improvement in spectral efficiency, reliability and quality of links [Foschini 1998]. Initially, smart

antennas technology was employed in multiple antennas at the receiver to exploit the receive diversity. Later on, this technology has been extended to MIMO concept where both transmit and receive antennas exploit the advantage of both space and time diversity gain, and the linear increase in channel capacity with number of antennas without increasing the power and bandwidth. The importance of MIMO technology can be attributed to its ability to deal with multipath scenario, which hitherto was considered as an undesirable feature in conventional systems. MIMO system under rich scattering environment the individual channels realised between respective transmitters and receiver virtually constitute independently fading channels. The spectral efficiencies associated with MIMO channels are based on the premise that rich scattering environment provides independent transmission paths between individual transmit and receive antennas. Research of Jack Winters [Winters 1994] is considered as pioneering in MIMO technology, which describes ways of sending data from multiple users over same frequency/time channel using multiple antenna technique both at transmitter and receiver. Thereafter, several academicians, scientists and engineers have made significant contribution in the field of MIMO technology [Winters 1994, Tarokh 1999, Foschini 1998, Gunashekar 2009, and Paulraj 2003]. From the functionality perspective, MIMO technology can be configured into three categories such as Precoding, Spatial Multiplexing (SM) and Diversity coding [Gesbert 2003, Naguib 1998]. The concept of MIMO communications systems are addressed in the next section.

2.3 MIMO Communication Systems

A basic block diagram of a MIMO wireless with M transmit antenna (TX_1, ------TX_M) and N receive antennas (RX_1, -----, RX_N) is depicted in Figure 2.5. A data stream of L_b information bits $b(l)$ is de-multiplexed into M independent sub-streams at the transmitter. Each sub-stream data is mapped using a modulation scheme (BPSK, QPSK, M-QAM, etc.) to form transmits symbols. These mapped symbols are encoded into M dimensional STC across the transmit antenna at k the interval to form transmitted $s(k)$ symbols. These symbols $s(k)$, are transmitted across the MIMO fading channel $H(k)$ and is also subjected to AWGN $n(k)$, where l and k represents the bit and symbol period index respectively.

On the receiver side, the signal $r(k)$ received across N antennas is processed for demodulation and is decoded to estimate the bit $\hat{b}(l)$ using MIMO receiver signal processing block.

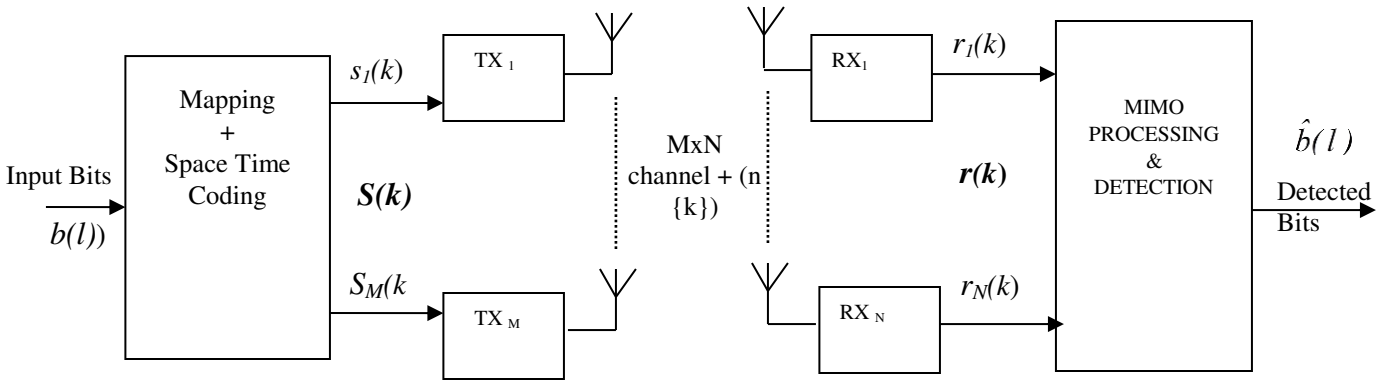

Figure 2.5: Basic diagram of a wireless MIMO system

Under the assumption of symbol-synchronization and ideal timing, general MIMO system can be represented using Equation (2.1)

$$r(k) = \sqrt{\frac{E_S}{M}}\, H(k)s(k) + n(k) \tag{2.1}$$

Where,

$r(k) = [r_1(k),\ r_2(k), \ldots\ldots\ldots r_N(k)]^T$ is the vector of received symbols.

$s(k) = [s_1(k),\ s_2(k), \ldots\ldots\ldots s_M(k)]^T$ denotes transmitted symbols with normalized average energy $E[|s_i|^2] = 1$

E_s the total energy of symbol transmitted, which is independent of the number of transmit antennas,

$H(k)$ represents the $M \times N$ MIMO channel at respective symbol index k, given as follows

$$H(k) = \begin{bmatrix} h_{11}(k) & h_{12}(k) & \cdots & h_{1M}(k) \\ h_{21}(k) & h_{22}(k) & \cdots & h_{2M}(k) \\ \vdots & \vdots & \vdots & \vdots \\ h_{N1}(k) & h_{N2}(k) & \cdots & h_{NM}(k) \end{bmatrix} \tag{2.2}$$

h_{nm} correspond to the complex channel gain between transmit antenna m and receive antenna n

$n(k) = [n_1(k),\ n_2(k), \ldots\ldots\ldots n_{NM}(k)]^T$ is the vector of independent and identically distributed (i.i.d) of complex additive white Gaussian noise sample with variance N_0.

If quasi-static channel is assumed for transmission, it would mean that channel $H = H(k)$ is constant over a whole burst

$$R = \sqrt{\frac{E_s}{M}}\, HS + N \quad , \tag{2.3}$$

Where,

R is received symbol of dimension N × K,

S is transmitted symbol of dimension M × K, and

N is noise sample of dimension N × K.

2.4 Capacity of Multiple Antenna Systems

The analysis of channel capacity in multiple antennas proves the enhanced spectral efficiency capability of a MIMO system. An inspiration for capacity analysis of multiple antenna systems can be derived through the research of [Foschini 1996 and Telatar 1999]. The Figure 2.6 shows different configuration modes of a multiple antenna system. This section facilitates a review on the capacity analysis of various MIMO configurations and it amply shows that there is dramatic increase in capacity by using MIMO technology.

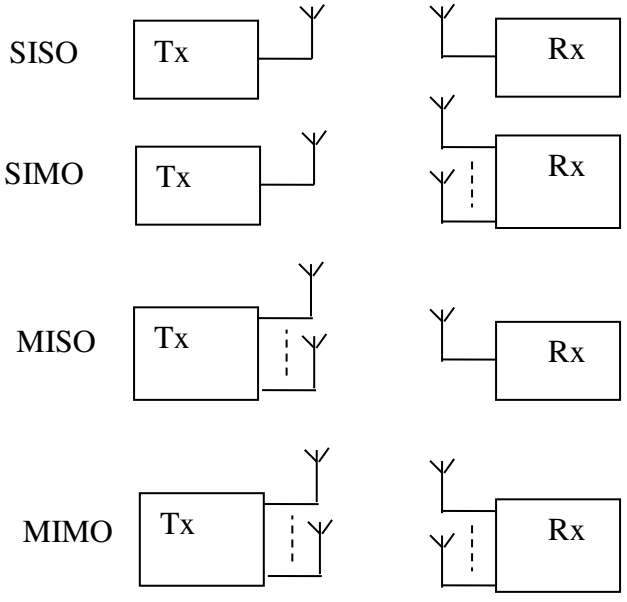

Figure 2.6: Different modes of multiple antenna configurations

2.4.1 Capacity for Single-Input Single-Output (SISO) Channel

The channel capacity or spectral efficiency C_{SISO} , of a SISO communication system for power constraint AWGN channel is defined as the maximum achievable error free transmission data rate [Shannon 1948]

$$C_{SISO} \approx B.\log_2(1+\rho) \quad bps \tag{2.4a}$$

Capacity for given RF channel of bandwidth B is given as

$$C_{SISO} \approx B.\log_2(1+\rho) \quad bps/Hz \tag{2.4b}$$

Where,

$\rho = {}^{E_s}/_{N_0}$ denotes the Signal to Noise Ratio (SNR) of the wireless system,

B is bandwidth of the signal in Hz.

2.4.2 Capacity for Single-Input Multiple-Output (SIMO) Channel

With N receive antennas, the average signal power at the receiver is N^2 times the individual power. There is an N- fold increase in Noise power also. Overall increase in SNR given as

The increase in SNR is N times the SNR of SISO channel is given as

$$SNR_{SIMO} \approx \frac{N^2.E_S}{N.N_0} = N.\rho \tag{2.5}$$

Thus, the channel capacity C_{SIMO} for this SIMO system for given bandwidth is approximately equal to

$$C_{SIMO} \approx B.\log_2(1+N.\rho) \quad bps/Hz \tag{2.6}$$

2.4.3 Capacity for Multiple-Input Single-Output (MISO) Channel

With M transmit antennas, the signal power is divided into M transmitter branches. Signal is coherently added to result in an M-fold increase in SNR as compared to SISO. But noise power is same as in the SISO case because of the single receiver antenna. Thus, the overall increase in SNR is approximately given as

$$SNR_{MISO} \approx \frac{M^2.(\frac{E_S}{M})}{N_0} = M.\rho \tag{2.7}$$

Thus, the channel capacity of MISO channel for given bandwidth is approximately equal to

$$C_{MISO} \approx \log_2(1 + M.\rho) \quad bps/Hz \tag{2.8}$$

2.4.4 Capacity for MIMO Channels

The derivation of MIMO channel capacity bound has significance in defining the effective throughput and it is still an active research area of interest. There are many research publications only devoted only for capacity analysis and performance limits for various MIMO channel configurations. The two most widely used approaches, based on deterministic and random channel assumption are summarized in this section [Foschini 1996, Telatar 1999, Paulraj 2003, Biglieri 1998 and Marzetta 1999].

a) Deterministic MIMO Channel

The generalized capacity of deterministic MIMO channel is defined by Equation (2.9) [Telatar 1999]

$$C = \underset{f(s)}{max}\, I(s;r) \qquad bps/Hz \tag{2.9}$$

Where,

'r' is received symbol

's' is transmitted symbols

$f(s)$ is the probability density function (pdf) of s and

$I(s;r)$ is the mutual information between *s* and *r,* which can be expressed as

$$I(s;r) = H(r) - H(r|s) \tag{2.10}$$

where,

$H(r)$ is the differential entropy of *r* and

$H(r|s)$ means the conditional differential entropy of *r* given that *s* is known.

Mutual Information (MI) is a measure of uncertainty about one random variable(s) given the knowledge of another variable(r) over noisy channel. High mutual information indicates a large reduction in uncertainty; low mutual information indicates a small reduction; and zero mutual information between two random variables means the variables are independent. However, MI is a measure ideally suited for analysing

communication channels to find the dependence of the received signal (r) and transmitted signal (s) over the noisy channel for given bandwidth.

Since the vectors *s* and *n* are independent, Equation (2.10) simplifies to

$$I(s;r) = H(r) - H(n) \tag{2.11}$$

The maximization of the mutual information $I(s;r)$ implies maximizing differential entropy $H(r)$, which occurs when *s* is a Zero Mean Circularly Symmetric Complex Gaussian (ZMCSCG). The distribution of $I(s;r)$ is completely characterized by its covariance matrix R_{ss} . The differential entropies $H(r)$ and $H(n)$ given in [Paulraj 2003] are

$$H(r) = \log_2 det(\pi e R_{rr}) = \log_2 det\left(\pi e\left(N_0 I_N + \frac{E_s}{M} H R_{ss} H^H\right)\right) \qquad bps/Hz \tag{2.12}$$

and

$$H(n) = \log_2 det(\pi e N_0 I_N) \quad bps/Hz \tag{2.13}$$

Therefore, the MIMO channel capacity can be evaluated through [Telatar 1999]

$$C = \underset{Tr(R_{ss})}{max} \log_2 det\left(I_N + \frac{\rho}{M} H R_{ss} H^H\right) \qquad bps/Hz \tag{2.14}$$

Where $Tr(R_{ss}) = M$ limits the transmitted symbol energy.

$\det(.)$ denotes determinant of matrix

$Tr(.)$ denotes trace of matrix

The capacity C in Equation (2.14) is often referred to as the error-free spectral efficiency or the data rate per unit bandwidth that can be sustained reliably over the MIMO channel.

If CSI is not known at the transmitter, then capacity for independent equi-powered transmitted signal is given as

$$C = \log_2 det\left(I_N + \frac{\rho}{M} H H^H\right) \qquad bps/Hz \tag{2.15}$$

After performing Eigen decomposition on HH^H , the Equation (2.15) can be expressed as

$$C = \sum_{i=1}^{r_c} \log_2\left(1 + \frac{\rho}{M}\lambda_i\right) \qquad bps/Hz \tag{2.16}$$

Where,

r_c is the rank of the channel and

$\lambda_i (i = 1,2, \ldots \ldots \ldots . r_c)$ are the positive Eigen values of HH^H.

Equation (2.16) expresses the capacity of the MIMO channel as the sum of the capacities of r_c SISO channels, each having the gain λ_i and a transmit energy of $\frac{E_S}{M}$.

Further, if the elements of H satisfy both $\left\|H_{i,j}\right\|^2 = 1$ and full-rank MIMO channel of $M = N = r_c$, then capacity of the MIMO channel is

$$C = M \log_2(1 + \rho) \qquad bps/Hz \tag{2.17}$$

The MIMO capacity for above case is therefore M times the scalar SISO channel capacity. All the above mentioned capacity values can be improved if the channel or some of its statistics parameters are known at the transmitter side [Foschini 1996].

b) Random MIMO Channel

Random MIMO channel *H* means randomly time-varying channel capacity. This channel capacity is given by its time average. Two capacity values calculated for a random MIMO channel are based on ergodic and outage channel capacity [Cho 2010]. The ergodic capacity is given as

$$C = E\left[\log_2 \det\left(I_N + \frac{\rho}{M} H R_{ss} H^H\right)\right] \qquad bps/Hz \tag{2.18}$$

Where

E(.) denotes expectation

The outage capacity quantifies the capacity that will be guaranteed with an assured level of reliability. For a chosen ε % -outage probability, outage capacity $C_{out,s}$ is defined as the information rate that is guaranteed for (100 - ε) % of the channel realizations. It means $P\left(C \leq C_{outg}\right) = \varepsilon$ % [Cho 2010, Biglieri 1998].

Figure 2.7 shows the 10%-outage capacity values for random MIMO-HF fading channels with M = N and no CSI at the transmitter side. Water-filling capacity structure has been assumed for the simulation results. As it can be noticed from the Figure 2.7, the capacity increases reasonably with the number of transmit antennas.

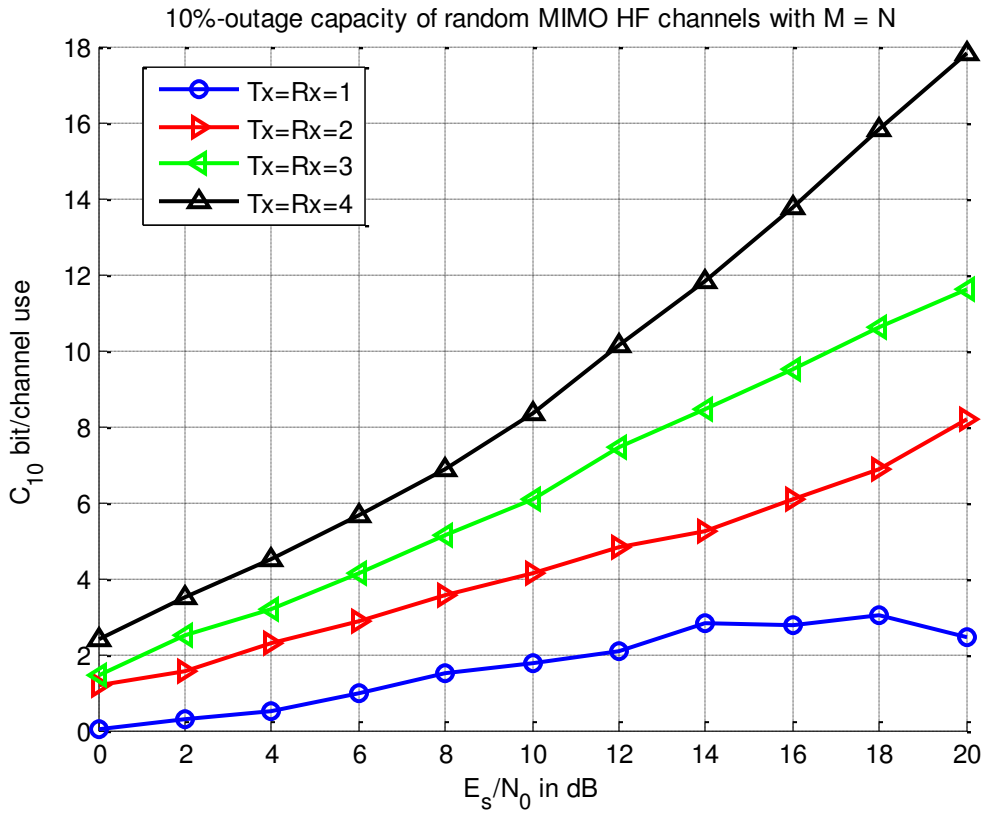

Figure 2.7: 10%-outage capacity of random MIMO channels with M = N

2.5 Space-Time Coding (STC) Techniques

The effective utilization of MIMO capacity to achieve the theoretical bound depends on the STC technique employed. The STC technique performs coding in both space and time domains. Because of this, STC technique utilizes the correlation between signal transmitted from various antennas at different time periods [Vucetic 2003, Alamouti 1998]. The advantage of STC is that it provides both transmit diversity gain and power gain over spatially uncoded system for the same bandwidth.

In reference to Figure 2.5, STC technique does show how the information bits $b(l)$ are mapped into the transmitted symbol S. Assuming $L_c = L_b$, data bits are mapped using a modulation scheme (example – BPSK, QPSK, M-QAM) having constellation of B points leads to data symbols $d(n)$,

Where,

L_c is number of coded transmitted bits

L_b is number of uncoded transmitted bits

n ranges from 1 to $N_c = {}^{L_c}/_{q}$ and

$q = \log_2 B$, represents the modulation order.

B is number of points of a constellation

These N_c symbols are processed by a space time coder which adds redundant parity symbols of $MK - N_c$ resulting in $M \times K$ transmitted symbols S. The effective data rate of the channel is ${}^{L_b}/_{K} = {}^{qN_c}/_{K} = qr_s,$ where $r_s = {}^{N_c}/_{K}$ the spatial code rate and K is number time index in the frame.

If any forward error coding technique of rate r_t is used before symbol mapper i.e., $L_c = L_b/r_t$ and $N_c = L_c/(qr_t)$, then the effective data rate is expressed as

$$\frac{L_b}{K} = \frac{L_b r_t}{K} = \frac{qN_c r_t}{K} = qr_s r_t \tag{2.19}$$

The spatial rate r_s varies from 0 (infinite coding diversity) to M (full multiplexing) based on the choice of STC scheme. The following subsections show the structures and benefits of the most commonly used STC techniques.

2.5.1 Spatial Multiplexing

Spatial Multiplexing (SM) technique processes different information of data in the parallel streams by transmitting simultaneously over M transmit antennas by exploiting multipath. The receiver processes the M spatial streams signal to recover the transmitted information. The optimal detection is quite complex and several sub-optimal low-complexity detectors ranging from zero forcing to complex soft a*posteriori* probability detection can be implemented to recover the transmitted data. Higher capacity gain can be achieved based on the radio frequency conditions and users' proximity to the base station. With increase in data rate at short distance, both spectral and power efficiency can be achieved significantly.

Basic block diagram of an uncoded SM system commonly known as Vertical Bell Labs Layered Space Time (V-BLAST) is shown in Figure 2.8. The information bits are mapped to a constellation mapper (QPSK, QAM) resulting in symbols s. and these symbols are streamed into M parallel sub-streams. These parallel streams are transmitted

independently at a spatial rate of $r_s = M$. The effective signalling rate due to this symbol transformation is qM bits per symbol transmission period, where, q is modulation order.

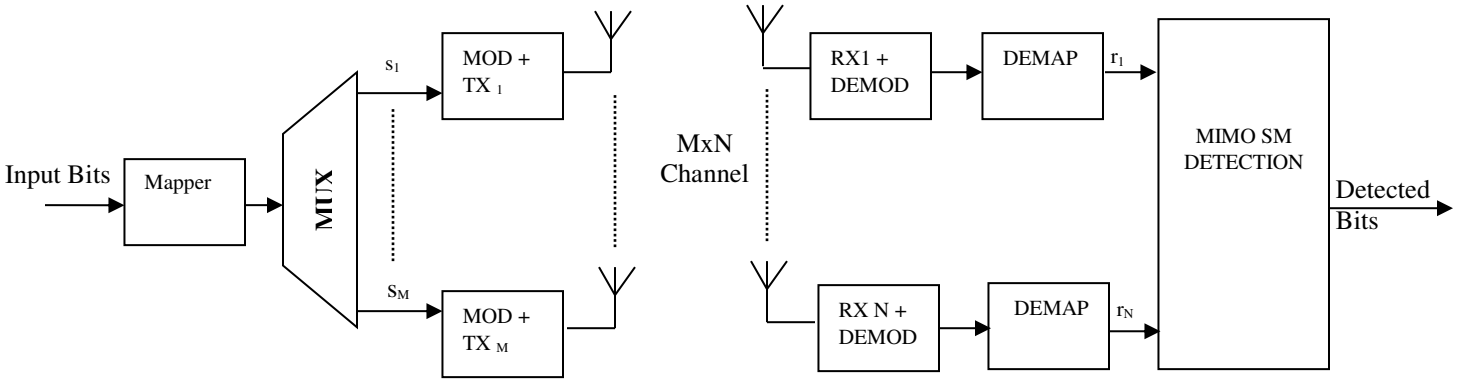

Figure 2.8 : Diagram of an uncoded N ×M spatial multiplexing MIMO system

2.5.2 Space-Time Block Codes

The space-time coding scheme by [Tarokh 1999], is essentially a jointly design of coding, modulation scheme, transmit and receive diversity. This scheme can be operated on the block of input symbols commonly referred as Space-Time Block Codes (STBC) or operate on one input symbol at a time (like Traditional Trellis Code Modulation) is referred as Space – Time Trellis Code (STTC).

Initially STBC scheme is proposed by [Alamouti 1998] where the coding scheme is designed to achieve transmit diversity with two transmit and a receive antennas. Later on, this scheme was modified by [Tarokh 1999] to improve both the capacity and diversity performance and it is known as STBC. For example, in a 2x2 antenna STBC structure, the transmitted symbol stream is divided into pairs s = [s_1, s_2] that are mapped into a 2x2 matrix S_A, which is defined as

$$S_A = \begin{pmatrix} s_1 & -s_2^* \\ s_2 & s_1^* \end{pmatrix} \tag{2.20}$$

The first and second columns of S_A represents the symbols transmitted at t_1 and t_2 time index. The row index represents the antenna space. The signals at the receiver antenna for symbol time indices 1 and 2 are given by Equation (2.21)

$$y = \begin{bmatrix} r_1 \\ r_2^* \end{bmatrix} \tag{2.21}$$

Where,

$$r_1 = \sqrt{\frac{E_s}{2}}\, h_1 s_1 \; + \; \sqrt{\frac{E_s}{2}}\, h_2 s_2 \; + \; n_1 \tag{2.22}$$

$$r_2 = \sqrt{\frac{E_s}{2}}\, h_1 s_2^* \; + \; \sqrt{\frac{E_s}{2}}\, h_2 s_1^* \; + \; n_2 \tag{2.23}$$

and h_1 and h_2 are the complex channel coefficients (gains) between respective transmit and receive antennas. The channel is assumed as quasi-static over period of symbol transmission.

The relationship between the received vector y, channel matrix H_{eff}, noise vector n and transmitted symbols s can be expressed as system Equation (2.24),

$$y = \sqrt{\frac{E_s}{2}} \begin{bmatrix} h_1 & h_2 \\ h_2^* & -h_1^* \end{bmatrix} \begin{bmatrix} s_1 \\ s_2 \end{bmatrix} + \begin{bmatrix} n_1 \\ n_2^* \end{bmatrix} = \sqrt{\frac{E_s}{2}}\, H_{eff} s + n \tag{2.24}$$

where $s = [s_1 \quad s_2]^T$,

$n = [n_1 \quad n_2]^T$,

H_{eff} is the effective channel matrix that is orthogonal, there by

$H_{eff}^H H_{eff} = \|h\|_F^2 \, I_2$.

If $z = H_{eff}^H y$, then

$$z = \sqrt{\frac{E_s}{2}}\, \|h\|_F^2 \, I_2 s + \tilde{n} \tag{2.25}$$

Where.

$\tilde{n}$ is a vector of noise samples having zero-mean and with covariance value defined as $E\{\tilde{n}\tilde{n}\} = \|h\|_F^2 N_0 I_2$. Therefore Equation (2.25) can be simplified as

$$z_i = \sqrt{\frac{E_s}{2}}\, \|h\|_F^2 \, I_2 s_i \; + \; \tilde{n}_i \, , \qquad i = 1, 2, \tag{2.26}$$

Equation (2.26) can be considered as two individual detection tasks to estimate the symbols. The received SNR value η corresponds to each symbol is given by,

$$\eta = \frac{\|h\|_F^2 \rho}{2} \tag{2.27}$$

If $E(\|h\|_F^2) = 2,$ the SNR at detection will be η= ρ,

Where $\rho = \frac{E_S}{N_0}$ is the SNR of the STBC system and is also referred as the SNR per transmitted symbol for the Alamouti scheme [Tarokh 1999, Durgin 2003].

Further, the Alamouti Scheme can be extended to higher MIMO antenna configurations using Orthogonal Space Time Block Coding (OSTBC). An example of such coding scheme, which can achieve a diversity gain on $M \times N$ for M=4 orthogonal code structure is given in Equation (2.28) with spatial rate of r_s =1 [Su 2003, Gesbert 2003]

$$S_{STBC} = \begin{bmatrix} s_1 & -s_2 & -s_3 & -s_4 \\ s_2 & s_1 & s_4 & -s_3 \\ s_3 & -s_4 & s_1 & s_2 \\ s_4 & s_3 & -s_2 & s_1 \end{bmatrix} \tag{2.28}$$

2.5.3 Space-Time Trellis Codes

Space – Time Trellis Code (STTC) techniques are effectively a joint design of FEC, modulation scheme, transmit and receive diversity to mitigate the effects of fading for multi-antenna system [Tarokh 1999]. Figure 2.9 shows Trellis structure with QPSK, 4 state STTC for M=2 transmit antennas. Each Trellis state node has 'A' groups of symbols to transmit, where A is modulation symbols or constellation size. These codes are designed to maximize the coding gain and diversity gain which in turn depends on Trellis structure and number of receive antennas. Maximum Likelihood (ML) sequence estimation based on Viterbi decoder is used to decode the transmitted frame at the receiver.

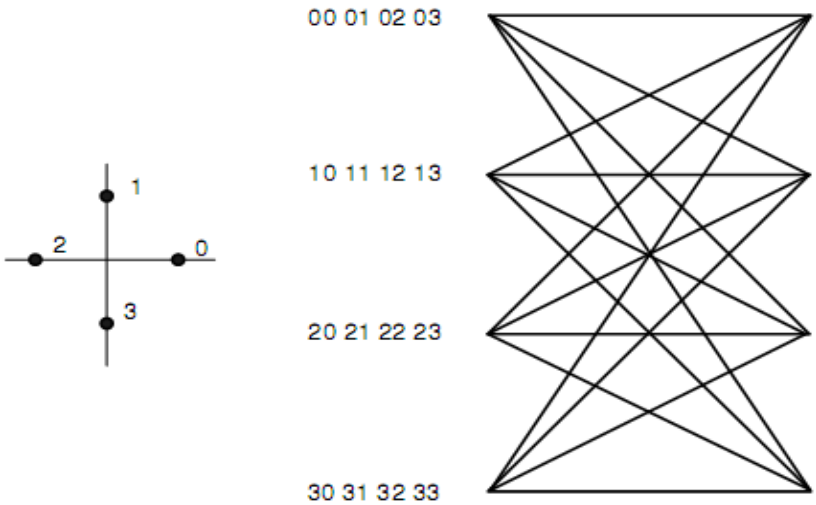

Figure 2. 9: Trellis diagram for a QPSK, 4-state STTC code with M = 2

2.6 Need of MIMO Approach for HF Communication

Basically the MIMO concept is limited to the UHF band and above by exploiting the rich scattering effects. Primarily the MIMO technology is used to improve spectral efficiency and reliability of communication system [Paulraj 2004, Foschini 1998, and Telatar 1999]. HF propagation is prone to fading as a consequence of multipath effects and provides rich scattering environment. The application of MIMO for HF would be an ideal choice to exploit the effect of fading in useable form to improve the capacity and reliability of HF system. The efforts of the past research pertaining to the topic with a focus on exploiting MIMO technique within the HF bands have been rather limited. In open literature, the limited contributions are evident through [Ndao 2009, Strangeways 2007, Xu 2004, Gunashekar 2007, Brine 2010, Alvarez 2011, Daniels 2013, Scheible 2014, and Fabrizio 2000].

The non-ideal characteristics of ionospheric channels such as severe linear distortion; fast channel time variations, propagation effects, the high interference levels and severe fading impose constraints on the achievable high-data-rate of transfer over HF channel [Eleftheriou 1987, Clark 1989]. The increase in demand for higher capacity and reliable adaptive links for HF channel [Clark 1989, Eleftheriou 1987, and Brine 2010] has motivated the researchers to investigate the time, frequency and spatial dimensions of signal transmission. Thus, signal transmission with multi-dimensional approach has emerged as a powerful paradigm to meet these demands. MIMO communication systems offer significant capacity gain compared to conventional SISO systems by exploiting the spatial dimension [Gunashekar 2007]. MIMO communication is an emerging technology offering significant promise for high data rates and mobility required for the next generation HF communication systems.

The next section presents a Review of HF channel characterization and estimation.

2.7 Review of HF Channel Characterization and Estimation

The understanding of radio propagation is important in the design, deployment and management of the resources (Bandwidth, power, and system computation) to achieve the reliable system performance (Date rate, BER, SNR). For providing the realistic system performance in the design process, channel models that can be accurately described, the propagation channels are essential. The propagation of radio channel describes the nature of the environment.

Radio propagation is heavily site-specific and can vary significantly depending on the terrain, velocity of the mobile terminal, frequency of operation, interference sources, and other dynamic factors. Accurate characterization of the radio channel through key parameters (such as multipath fading parameters: delay spread, Doppler spread, etc.) and a mathematical model are important for predicting signal coverage, achievable data throughput, specific performance attributes of alternative signalling and reception estimation schemes, analysis of interference from different sources of the systems, and for determining the optimum location for installing the base station.

The essence of propagation of the radio channel plays important role in the design of any wireless communication system. Achieving the near ideal system performance depends upon the available resources (such as bandwidth, power). For higher system performance, one needs to pay for the computational complexities. The system performance depends on the dynamics of channel parameters which determine the magnitude of computational complexities. In addition, channel characterization plays vital role in both network planning as well as mitigation of radio interference. In general, characterization of channel is broadly classified into large-scale and Small-scale fading channel [Sklar 1997a]. The small-scale characterization is usually invoked to improve the receiver designs and to combat the impairment attributed to multipath environment. The parameters that are under the purview of small scale characterization include delay spread, angular spread, coherence bandwidth, Doppler spread, and correlation properties. The significance of large-scale characteristics plays its role in analysis of geographical coverage as well as interference of commissioned communication system.

Channel estimation is a critical component of a receiver block to counter the effect of channel impairment on the receiver performance. Channel estimation is a highly challenging task in receiver design since the accuracy of the channel estimation technique plays a major role in evaluating the performance of a radio system. Basically, the HF channel is highly dynamic in nature and is also subjected to time, multipath propagation, mobility, local scattering environment and static or dynamic change in the locations of transmitter and receiver. Because of the inherent varying nature of HF channel, transmitted signals are more likely to be subjected to detrimental effect before reaching to the receiver. The role of channel estimation is directly related to counter the effect of variation of statistical channel parameters (such as means, variance, delay spread, Doppler spread) so as to ensure that acceptable system performance is achieved as specified by the designers.

Both HF channel characterization and estimation are active research areas with the expectation for near-zero or minimal error rate to facilitate enhanced acceptability of the complete transceiver system. In this chapter, a review of channel characteristics and estimation pertaining to HF channel is presented with a view to highlight the novelties and the limitation of the techniques that are already being widely used. An attempt has been made to bring out the contributions of the proposed thesis to overcome some of the significant shortcoming of the existing techniques related to HF channel characterization and estimation.

This chapter presents a review on channel characterization and estimation technique for HF channel. An introduction to HF channel characterization and its literature review will be discussed. This will be followed by a review on channel estimation techniques with emphasis on HF channel.

2.7.1 HF Channel Characterization

The sky-wave HF channel characterization is important to evaluate the performance of a communication system prior to its deployment. Channel characterization enables the user or designer to predict signal coverage, achievable data rate and quality of link, which in turn leads to adaptive selection of various transmitter parameters such as power level,

modulation index, coding rate, preamble structure to compensate the undesired attributes of small-scale channel impairments. Channel characterization is used mainly in laboratory to analyse signalling waveform integrity such as feed-forward error, modulation, interleaver, preamble structure, synchronization, channel estimation and other associated blocks needed to realize transceiver system [Sklar 1997a, 1997b]. The feasibility of successful utilization of a given waveform integrity depends on the channel parameters defining the channel characteristics.

The typical characteristic feature of a HF sky-wave communication channel is that it is highly noisy. Combination of anisotropic and inhomogeneous dispersive nature of HF channel leads to both deterministic as well as stochastic parameters of ionospheric channel and subjected to both slow and fast fading in various latitudes [Cannon 2002]. It is difficult to model exactly the ionospheric nature of HF channel. In general asymptotic and numerical methods are employed in modelling the significant channel parameters to realize the ionospheric HF channel characteristic. Consideration of multipath propagation effects is a must and constitutes one of the significant features of characterization of channel. The replicas of the transmitted signal at receiver after undergoing multiple reflections from the various ionospheric layers associated with sky-wave propagation are referred to as multipath effects.

The effectiveness of the analysis of complex nature of ionospheric channel characterization hinges on the level of invoking the depth of underlying principles of small scale channel impairments of radio propagation. The characteristic and behaviour of the channel determine the quality of communication systems. The assessment of this quality is subjective in due consideration of the degree of the dynamic nature of the channel. Models of the signal distortions caused by the ionosphere are important because they facilitate the design and testing of radio system via their incorporation in channel characterization. The review presented in this chapter is aimed to address the characterization of ionospheric channel.

I. HF Channel Model and Review

Various ways of modelling the HF channel are available in the literature. Among them, Watterson model is considered as more prominent because of its simplicity and analytical nature. The pioneering work of Watterson [Watterson 1970] is a practical way of representing the HF channel model and it is specifically referred to as "Watterson model". This model assumes the amplitude variation of channel to follow a Rayleigh distribution and the Doppler spread on each of its multipath has Gaussian power spectrum. Watterson model does not assume a particular type of distribution for the delay spread. In brief, representation of Watterson channel model can be visualized as an ideal tapped delay line, where at each tap and delay line, signal gets multiplied with tap-gain function $G_i(t)$ and accumulated recursively. Each tap-gain function is defined [Watterson 1970] as

$$G_i(t) = \tilde{G}_{ia}(t)exp(j\pi v_{ia}t) + \tilde{G}_{ib}(t)exp(j\pi v_{ib}t) \quad (2.29)$$

Where,

Subscripts a and b represent the two possible magneto-ionic components.

v_i denotes Doppler shifts,

Tilde sign (~) indicates that the G terms are sampled functions of two independent complex Gaussian ergodic random processes, each with zero mean values as well as independent real and imaginary components with equal RMS values. Such complex sequences exhibit Rayleigh fading. The tap-gain functions are filtered to produce a Gaussian Doppler spread in the power spectrum of multipath propagation.

In Clarke's model of representing a wireless channel, wide-sense stationary isotropic scattering signal is generated using a single correlated sequence of Rayleigh distribution [Clarke 1968]. Practically scattering encountered in the environment is non-isotropic in nature which affects the second order statistics of the channel and this constitutes the primary reason for not invoking the Clarke's model for HF channel analysis. Emulating the equivalent fading scenarios is an essential feature for channel characterization and this necessitates an input in the form of complex Gaussian sequences. The cross-correlation operation on the complex Gaussian sequence exhibits the Rayleigh

distribution. In the literature, a number of different algorithms have been proposed for the generation of correlated Rayleigh random variates ([Young 2000, Loo 1991, H¨oher 1992, Verdin 1993, and Pop 2001]). The most popular among these channels to simulate generate random variates is based on:

- Sum-of-Sinusoids
- White Noise Filtering method
- Inverse Discrete Fourier Transform (IDFT) algorithm.

[Pop 2001] which has addressed the modelling of the sum-of-sinusoids algorithm that encountered abnormal variation in stochastic behaviour and also shows that classical Jakes simulator [Jeruchim 1992] generates the fading signal which is not wide sense stationary. Subsequently [Zheng 2002] and [Zheng 2003], have analysed the stationarity problem of sum-of-sinusoids to maintain accuracy of the correlation statics. Channel modelling based on IDFT technique has high quality and accuracy in generating the fading coefficient [Young 2000]. IDFT requires all input samples to generate the channel characteristics with single Fast Fourier Transform [FFT] operation. This in turn would in effect imply that IDFT algorithm is not suited for real time processing. Also, the memory requirement and intensive computation for generation of large number of variates are rather high and hence this technique is not feasible in general.

On the other hand, white noise filtering method is realized generally either by Finite Impulse Response (FIR) Filter or Infinite Impulse Response (IIR) Filter. This method guarantees accuracy and computational efficiency of channel characterization based on FIR or IIR selection. FIR approximation of a channel model often requires a large number tap coefficients, and the order of the filter increases with the increase of the sampling frequency of signal. It is well known that IIR filters can capture the system dynamics with fewer parameters (tap coefficients and order of Filter) as compared with FIR filters [Radenkovic 2003]. In [Delmas 2000], it is discussed that realistic radio channels often exhibit long tails of weak leading and trailing terms in its impulse response. In the case of FIR filters, this leads to channel under-modelling effects and degradation of modelling performance. IIR or AutoRegressive (AR) channel representation can reduce the effect of modelling errors.

Practically, narrow-band filter is used to characterize the Doppler spectrum of the channel modelling with a very sharp roll off and infinite attenuation in stop-band region. To realize this specification of narrowband filter, it is impractical to have a FIR filter with large number of taps. But for same specification, IIR filter would need lesser number of taps and has an advantage of ease of implementation. It requires fewer hardware resources in term of silicon space, storage and computation time compared to a FIR filter. Feedback structure of All-pole or Auto-Regressive (AR) or IIR filter allows steeper Doppler frequency roll offs and cater for smooth flat response under irrational magnitude response with minimum order compared to a FIR filter [Komninakis 2003, Baddour 2005 and Alimohammad 2007]. Analytic response of channel modelling using AR filter has better approximation for wide range of Doppler spectrum with minimum order of filter and hardware resources [Baddour 2005]. IIR configuration has relative merit of smaller chip (ASIC) area and lower power consumption compared to that of FIR. This is attributed to the sufficiency of lower order of IIR configuration to retain the optimal accuracy and therefore has become a more preferred choice for hardware implementations of channel simulators [Malik 2009, Alimohammad 2007 and Alimohammad 2012]. Initially application of the AR model was for Kalman based channel estimation technique to predict both short and long range dynamics of fading channel [Eyceoz 1998, Wu 2000]. Later AR model technique has been extended by [Wu 2000, Zhang 2000] to realize channel simulator. It is found that [Zhang 2000] and [Colman 1997] use low order AR process to realize the correlation statistics of channel. The realized accuracy of correlation statistics falls short to ensure the desired channel response. This can be attributed to the numerical instability of statistical parameters resulting in its failure to model statistical parameter of channel. This has restricted the scope of applicability of AR models. [Baddour 2005] has demonstrated the simple AR modelling structure with correlated narrowband Rayleigh variates and also considering non-isotropic Rayleigh random process. [Baddour 2005] also addresses numerical stability problems of [Colman 1997, Zhang 2000].

Numerous HF channel simulators have been developed based on the Watterson HF channel model [Watterson 1970, Mastrangelo 1997]. In current literature, the HF channel

modelling is based on FIR Filter [Watterson 1970, Mastrangelo 1997]. The limitation of such a model is its inability to accurately represent the important statistical characteristics of the channel both in the frequency and the time domain. With various critical analysis of work of various authors, it is found that work pertaining to modelling of channel HF channel is only based on FIR filters. It is essential to address AR approach for accurately generate band-limited Gaussian random processes to characterize the HF channel. This thesis proposes to extend the application of [Baddour 2005] to characterize Doppler spectrum of HF channel. Thus far, in all the research work pertaining to modelling of HF channel, only the Single Input Single Output (SISO) scenario has been considered.

Most of the application of MIMO Communication is predominantly centred around the ultra-high frequency band (3.1- 10.6 GHz) to provide significant improvement in capacity without increasing the bandwidth. Inherently desired feature of highly rich scattering feature for MIMO application is found in ionospheric HF channel [Gunasheker 2007, Abbasi 2009]. In the literature, there have only limited attempts to explore the concept of MIMO to HF channel despite knowing the potential advantages of MIMO. In order to improve the through capacity and reliability of HF link, it is essential to characterize the MIMO-HF channel. Modelling of MIMO-HF channel is an important entity in the channel characterization. There seems to be no research in open literature to model MIMO-HF channel and, therefore, one of the contributions of this thesis is to address the modelling of a HF channel.

2.7.2 HF Channel Estimation

In order to improve the performance of HF communication system in term of reliability and effective data rate, channel parameters have to be monitored periodically. One of the significant challenges in HF communication is that channel is highly dynamic nature both in time and frequency. The data transmission through the HF channel is highly influenced by the various layers within the ionosphere. The ionosphere medium which is anisotropic, inhomogeneous, time and space variant. These severe physical constraint cause distortion and dispersion of transmitted signals both in time and frequency domains [Arikan 2004].

Before transmitting the information from transmitter end, snapshot of channel response is necessary. Knowing the channel response in advance, adaptive resource allocation can be scheduled between the various subsystems of communication. Adaptive resources such as coding, modulation rate, power level, preamble scheme can be adjusted to the prevalent channel conditions which lead to better utilization of the radio resources. Channel estimation or prediction of the Channel State Information (CSI) is a crucial integral part of the communication system for the extraction of the channel parameter. Channel estimation/prediction of the rapidly HF channel fading enables to improve the link reliability and capacity throughput [Ekman 2002, Johnson 1997] thereby amply demonstrating the utility of channel estimation/prediction.

Performance of channel estimation algorithms is related to the extraction of the statistical information of small scale propagation channel. Different techniques [Clark 1989, Tugnait 2000] have been proposed to exploit these statistics for better channel estimates.

Channel estimation, along with most synchronization procedures, is itself a major and historical topic of research in the realm of HF communications system. As such, innumerable novel channel estimators have already been proposed and a relative comparison of various estimators has been performed can be found in literature. One of the obvious reasons for such an activity surrounding channel estimation is that there does not exist a universal measure of performance to rate a given channel estimation with respect to the other. Instead, several different selection criteria such as computational complexity, Mean Square Error (MSE) of the estimate, robustness against outage channel environment, and an optimal processing memory requirement have to be factored into the decision process of selection of a channel estimator.

I. Review on HF Channel Estimation Methods

Channel estimation of ionospheric propagation is typically very costly in either time or memory or both. Most of the practical available channel estimation schemes are based on either Least Mean Square (LMS) algorithm or one of the Kalman based Recursive Least Square (RLS) algorithms as means for estimating the HF link. A Kalman filter assumes

that the channel performs a degree-1 Markov process on the signal [Clark 1989, Eleftheriou 1987, Boroujeny 1996], which is a valid assumption for both time invariant and random-walk channels. Thus, Kalman filter is optimum for either of the two channel conditions, in sense that it can give the minimum MSE in the adaptive adjustment of the receiver. Normally HF channel cannot be modelled as degree-1 Markov process, and computer-simulation tests, in fact, have confirmed that the conventional Kalman filter, together with its more previous developments is not optimum for a typical HF channel [Clark 1989, Eleftheriou 1987, and Boroujeny 1996]. Further the Kalman filter is limited to Gaussian stationary process. [Liu 2002] improved the channel estimate by applying tracking techniques using Kalman filtering.

Initial work for improving the channel estimate by applying tracking techniques were performed using Kalman filtering [Liu 2002]. Kalman-based systems necessarily require a state model of the HF channel system. These systems modelled the channel with a static AR process and additive channel noise with a Gaussian distribution. [Komninakis 2002] has shown that low-order AR model based channel representation is prone to error at high SNRs. In effect a model mismatch occurs between the AR channel model and the actual channel itself. In order to overcome this deficiency, it becomes a necessity to increase the order (and necessarily the overall complexity) of the state Equation. Realistically HF channel is subjected to the conditions of system non-linearity, non-stationary fading and non-Gaussian noise. This was demonstrated by channel sounding measurements of typical HF environments [Clark 1989, Eleftheriou 1987, and Boroujeny 1996] and it becomes almost a must to replace the Kalman filter with PF [Arulampalam 2002].

A significant challenge to engineers and scientists is to find efficient methods for on-line, real-time estimation and prediction of the dynamic parameters of the systems from the sequential observations. Most of dynamical systems in applications such as HF communication systems and navigation are non-linear and non-Gaussian. However, there seems to be no effective algorithm with a universal appeal to treat non-linear and non-Gaussian system. Recently, researchers have begun to concentrate on a new class of filtering methods based on the Sequential Monte Carlo (SMC) approach.

Particle Filtering (PF) is a class of sequential Monte Carlo methodology used for Bayesian filtering. Discrete approximation of any probability density consists of weights and states $\left\{w_t^{(i)}, x_t^{(i)}\right\}_{i=1}^{N}$,

where

w is weight

x is state

t is time instants

N is the number of particle, vary from $i = 1,..., N$.

These states with associated weights are used to form an approximated Probability Density Function (PDF) in a structured approach [Arulampalam 2002]. In filtering context, the dynamics of the particles represent a particular state. These particles are propagated over time through Monte Carlo simulation to obtain new particles and their weights. The importance of particle filter will be felt when an analytical form cannot be realized for the required posterior PDF of system.

The basic principle of PF lies in the recursive computation of appropriate probability distributions using the concepts of importance sampling and approximation of probability distributions with discrete random measures. PF has drawn attention of many researchers in various fields including those in signal processing, statistics, and econometrics. This interest stems from its potential to cope with non-linear and /or non-Gaussian scenario [Djuri´c 2003, Hoang 2013]. Based on the ideas of sequential importance sampling and the use of Bayesian theory, PF is predominantly useful in dealing with non-linear and non-Gaussian problems. The underlying principle of the PF is the approximation of relevant distributions with random measures composed of particles (samples from the space of the unknowns) and their associated weights

The overall performance of HF channel has significant dependence on effective utilization of resources. The critical utilization of resources depends on the choice of channel estimation technique and the estimation technique must prevail even under adverse channel conditions such as system non-linearity, time varying multipath fading

and non-Gaussian noise environments. In view of these considerations and the inability of the conventional estimation techniques to fulfil the requirements of the context, an alternative approach to develop adaptive channel estimation technique for the HF channel invoking the principle of Bayesian forecasting will be of practical importance and relevance. Channel estimation based on Particle Filtering is an ideal choice to deal with non-linear and non-Gaussian scenarios [Bergman 1999, Arulampalam 2002, Hoang 2013 and Doucet 1998]. Reported research in [Haykin 2004] revealed the performance improvement of PF for MIMO wireless channel above UHF band. This thesis investigate channel estimation techniques based on PF for time varying HF channel to mitigate the effect of channel impairment along with non-linear and non-Gaussian noise conditions. The thesis also addresses the application of PF based estimation technique applicable to MIMO-HF channel, also which seems to have not been attempted in open literature thus far. Although one can conceive an idea of invoking the PF concept of devoid of Extended Kalman Filter (EKF), this thesis attempts to adopt a unified approach wherein PF and EKF schemes have been combined to realize better posterior density functions. The expected improvement in the receiver performance evaluated through the system parameters like data rate and reliability is also addressed in this thesis.

2.8 Conclusion

This chapter is intended to facilitate a review of topics, namely HF channel, MIMO and the characterization as well as the estimation for MIMO-HF channel. Under HF communication, the importance of the HF ionosphere medium for the radio communication is highlighted. The significant effects on the HF radio waves exerted by various layers in ionosphere are also discussed with requisite details. The most important effects, such as absorption factor, scattering phenomenon, limit in useable operation frequency, radio noise, path loss, Doppler shift, delay spread and other statistical parameters related to characterization have been reviewed rather concisely. The characterization of HF channel to include the effects of the above cited parameters and the role of HF channel characterization in the design of HF system are highlighted.

Inherent benefit of HF technology is its utility in long range communication with reduced infrastructure requirement and low cost compared to other wireless systems. Finally, the

significant challenge in HF communication is that the performance of the HF communication system is widely dependent on the technique to mitigate the effects of channel on the signal waveform. Hence signal waveform is a prominent deciding factor in the HF communication system design which (signal waveform) depends on the characterization of HF channel itself.

MIMO constitutes the second topic of this chapter. Under it, the principles of MIMO and its potential capability to enhance the performance of a communication system are addressed. The various configuration modes of MIMO to improve reliability and capacity such as Precoding, spatial multiplexing and diversity coding have been discussed. The precoding technique is used to enhance the reliability and to improve capacity along with MIMO technique. Spatial multiplexing and diversity coding address the throughput and diversity enhancement respectively. Capacity analysis for multiple antenna system based on deterministic and random channels is described for MIMO system to emphasize the capacity enhancement with varying number of transmit and receive antennas. Under space-time coding, three structures/techniques such as SM, STBC and STTC are discussed. SM is used to achieve higher capacity gain when there is user's proximity to the base station, thereby both spectral and power efficiency can be achieved significantly. The structure of STTC has an advantage of full coding gain over STBC. However in both STTC and STBC, there is full diversity gain. The disadvantage of STTC is that it is extremely hard to design and generally requires encoders and decoders of high complexities. Finally the reasoning for extending the MIMO technology for the present HF communication is highlighted in view of its imminent potential to offer significant improvement in terms of both capacity and reliability.

The last topic of this chapter is a review on HF channel characterization and estimation for MIMO communication. The channel characterization of a HF communication which is an important and topic of hot pursuit of research has a significant role with the expectation for near zero or minimal error rate in performance quantification of a complete transceiver. A realistic and robust channel characterization shall consider the channel impairments of various geographical terrains like urban, suburban, rural and

hilly. The limitations associated in the application of FIR channel model and its inadequacy to represent the dynamic characteristics of the channel parameters has been highlighted. Through literature survey featured with requisite details and relevance of it to address the realistic scenario elicited earlier, this chapter brings out the need to pursue the AR model in the characterization of the HF channel model with both SISO and MIMO configurations.

Over the past few decades, the extended Kalman filter has become a standard and widely used technique in varied engineering disciplines involving estimation algorithm for non-linear systems. However, recently, novel and more accurate non-linear filters have been proposed as more accurate alternatives to the extended Kalman filter within the framework of state and parameter estimation. Like most new algorithms, probably the non-linear filtering methods are not widely known or well understood and therefore their application has been rather limited. In the past, most of the research on HF channel estimation has been rather limited to linear and Gaussian noise scenario even though the realistic scenario would comprise both the non-linear and non-Gaussian noise. In this thesis, relevance and application of PF, which is a recent class of the non-linear filtering algorithms is investigated for its advantageous feature to handle the HF channel estimation under non-linear and non-Gaussian scenario. For the intended purpose for better posterior density function, this thesis also attempts to unify the applications of both extended Kalman and PF even though the two are differently motivated and still derived under the framework of recursive Bayesian filtering.

CHAPTER 3

NON- LINEAR FILTERING: RECURSIVE BAYESIAN ESTIMATION

Estimation of the parameter/state of the non-linear stochastic process of any dynamical system is considered as a non-linear filtering problem. These classes of non-linear processes in general are very widely common in integrated navigation, radio communication, radar/sonar surveillance, and satellite orbit/attitude estimation. To be more specific, channel estimation of non-linearity of system along with HF channel impairments is of particular interest to this thesis. A greater emphasis of this thesis is the estimation of system non-linearity along with HF channel associated with frequency non-selective dispersive characteristics. Since this thesis contemplates the channel characterization of HF channel with MIMO antenna replacing the conventional SISO, space-time coding also needs to be incorporated. The MIMO-HF channel is usually subjected to channel impairments, system induced non-linearity and/or non-Gaussian noise. The characterization of HF channel subjected to system induced non-linearity and non-Gaussian conditions is not a routine as well as straight forward task. It calls for more innovative estimation and prediction techniques to characterize the dynamic systems from the sequential observation (received signals). In general recursive Bayesian (RB) approach is considered as the best method to address the optimal non-linear filtering [Djuric 2003]. The Novelty of RB estimation lies in the determination of the Probability Density Function (PDF) of the state vector which completely describes the non-linear system based on available measurement. Kalman filter provides optimal closed form solution only for linear system with Gaussian process and noise. RB based optimal solution for non-linear filtering is not an easy task since it requires infinite dimensional processes. For practical aspect the exact formulation of an optimal solution for non-linear filtering is considered as not a prudent choice. Rather than an exact formulation, an approximation to the optimal solution to non-linear filtering is a reality. From a modelling view point, approximation to the optimal solution to non-linear filtering can be realized through the following:

1. Analytical approximation non-linear filter,
2. Direct numerical approximation non-linear filter

3. Sampling-based non-linear filter
4. Gaussian mixture non-linear filter
5. Simulation-based non-linear filter

Among the above 5 categories of approximation to optimal solution of non-linear filtering, analytical approximation approach is widely used in practical applications. Extended Kalman filter is a class of analytical approximate non-linear filter. Extended Kalman analytically approximated with only the first order Taylor series expansion is featured with narrow region of stability. In view of such a narrow region of stability, it is unable to handle completely the system dynamics that are usually non-linear [Gelb 1974]. Thus, the purpose of this chapter is to carry out research on non-linear filtering techniques which perform better than conventional extended Kalman Filter. This chapter presents a brief introduction to Recursive Bayesian Estimation (RBE) to deal with the non-linear filtering techniques. It is pertinent to point out that the subsequent chapters invoke extensively the recursive Bayesian techniques. RBE is followed by the discussion on sub-optimal non-filtering technique which serves as a fundamental basis for PF. The novel studies on optimal solution to non-linear filtering pursued through PF constitute the main focus of this chapter.

3.1 Recursive Bayesian Estimation

The Bayesian approach of estimating the state x_k for given measurement $Y_k = \{y_1, y_2, \ldots\ldots, y_k\}$ is to derive the Posterior Distribution/Density Function (PDF) $p(x_k|\, Y_k)$ for x_k conditional on the measurement Y_k. Optimal estimation is obtained if the density $p(x_k|\, Y_k)$ is known. Otherwise the conditional expectation of x_k with Y_k is calculated and is given in Equation (3.1)

$$\hat{x}_k = E(x_k|Y_k) = \int x_k p(x_k|Y_k) dx_k \tag{3.1}$$

The Equation (3.1) can be extended to estimate the PDF of the state $p(x_k|Y_k)$ instead of state x_k only. Therefore evaluation of the conditional PDF $p(x_k|Y_k)$ plays vital role in filtering theory.

The posterior density of the state x_k is calculated based on Baye's theorem which states:

$$p(x|y) \propto p(x)p(y|x) \tag{3.2}$$

One of the difficulties in evaluating the $p(x_k|Y_k)$ is computational intensive operations involved in higher dimensional integration of Equation (3.1). This can be avoided by using sequential scheme which means

$$p(x_1, x_2, \ldots\ldots x_k|\, Y_k) \propto \mathrm{p}(x_1, x_2, \ldots\ldots x_k|\, Y_{k-1}) p(y_k|x_k) \qquad (3.3)$$

The marginally integrating out $x_1, x_2, \ldots\ldots\ldots, x_{k-1}$ gives

$$p(x_k|Y_k) \propto p(x_k|Y_{k-1})\, p(y_k|x_k) \qquad (3.4)$$

Applying Markov process, the Equation (3.4) leads to

$$p(x_k, x_{k-1}|Y_{k-1}) = p(x_{k-1}|Y_{k-1}) p(x_k|x_{k-1}) \qquad (3.5)$$

Where, x_{k-1} can be integrated to give an Equation for $p(x_k|Y_{k-1})$ in terms of $p(x_{k-1}|Y_{k-1})$. Therefore the densities of the interest are updated recursively to either take account of a new observation or to consider an estimate of the future state of the system leads to probability *prediction* or the Chapman-Kolmogorov equation and update equation following while the probability *prediction* equation or the Chapman-Kolmogorov equation is represented as

$$p(x_k|Y_{k-1}) = \int p(x_k|x_{k-1}) p(x_{k-1}|Y_{k-1}) dx_{k-1} \qquad (3.6)$$

The update equation is represented by

$$p(x_k|Y_{k-1}) = c_k p(y_k|x_k) p(x_k|Y_{k-1}) \qquad (3.7)$$

Where c_k is the normalizing factor defined as

$$c_k = \left(\int p(y_k|x_k) p(x_k|Y_{k-1}) dx_k\right)^{-1} \qquad (3.8)$$

A Recursive Bayesian Estimation Algorithm for the filtering problem is formulated through the above prediction and correction equations and is illustrated in Figure 3.1. By invoking Bayesian Formula, update Equations (3.7) takes the compact form given by Equation (3.9).

$$p(x_k|Y_k) = \frac{p(y_k|x_k) p(x_k|Y_{k-1})}{p(y_k|Y_{k-1})} \qquad (3.9)$$

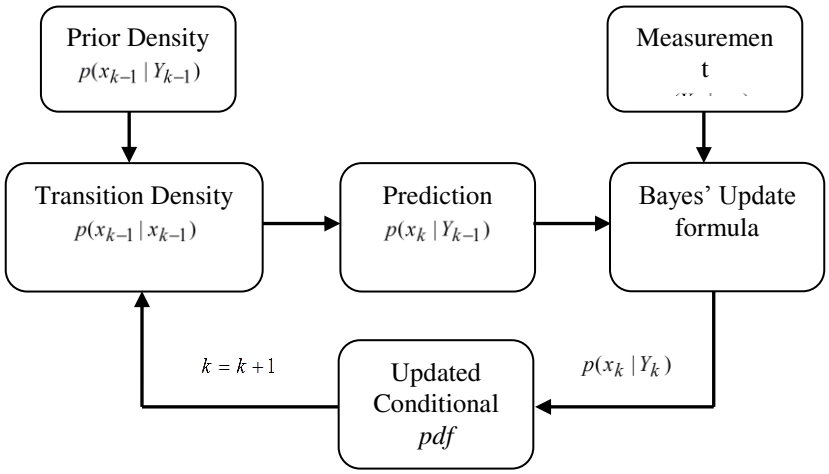

Figure 3.1: Prediction and update stages for the recursive Bayesian estimation

3.2 Analytical Approximations in Non-Linear Filtering

The solution to the recursive Bayesian estimation discussed in previous section consists of a set of three integral equations which is computed recursively. There are various classes of problems for which these equations are tractable. One such important class of problem is where state and observation equations are linear and their noise distribution is Gaussian. In such a case, Equations (3.6) - (3.7) can be solved based on the Kalman filter [Kalman 1960]. For other class of problems involving non-linear state and observation equations associated with non-Gaussian noise distribution, generally it is difficult to derive recursive relationship either in closed-form or numerically. Thus, generally approximate filtering solutions are needed to be evaluated to analyse the same.

Extended Kalman Filter (EKF) is considered as first approximate non-linear filter that linearizes the system and observation equations with the assumption of a priori distribution as Gaussian. The EKF uses the Kalman filter method to obtain estimates of mean and covariance of state equation. By using EKF, state estimation is approximated for the conditional mean and variances which leads to two sources of inaccuracy [Arulampalam 2002, Haykin 1996]. The first source of inaccuracy is the linearization of the non-linear system dynamic at each time step. The second source of inaccuracy is due to the assumption of Gaussian distribution for non-linear system while estimating mean

and covariance, that results in-correct value of state estimation. Thus non-linearities in the system model result in non-Gaussian posterior and prior distributions at each time index, and the calculated mean and covariance matrix will be approximations to the true quantities. The solutions to the problems associated with the above non-linearities have been addressed by various scientists and engineers [Athans 1968] based on truncating the higher order terms (from second order) in the expansion of system equation. [Julier 1995, 1997] has discussed Unscented Kalman Filter (UKF), which is an effective method for non-linear state estimation compared to EKF. These techniques are called as Sigma Point Filters (SPFs) and belong to the simulation based non-linear filters.

Most of non-linear filtering method (EKF, UKF) are based on local linearization of the non-linear system equations or local approximation of the probability density of the state variable. These methods are considered as effective algorithms for dealing with both non-linear and non-Gaussian system. The Gaussian Sum Filter (GSF) is also the extension of EKF used for non-linear and/or non-Gaussian filtering problem, which approximates the a-*posterior* density function by linear weighted sum Gaussian densities [Alspach 1972]. GSF is reasonably suitable for posterior functions of multimodal densities and requires heavy computational load to model accurately the non-Gaussian density [Fearnhead 1998].

The other approach to deal with the non-linear and non-Gaussian filtering is to evaluate the posterior density at the sequence of grid points prescribed in the sample space [Bucy 1970], or approximate the posterior density by splines or by step functions [Kramer 1988]. The advantages of the above approximation are that they simplify the process of integration involved in the recursive Bayesian solution. But computational load increases exponentially as the dimension increases and calculation at each grid point of distribution is non-trivial [Sorenson 1971].

More recently, much attention is given to new class of non-linear/non-Gaussian filtering methods based on sequential Monte Carlo approach [Arulampalam 2002, Gordon 1993, Doucet 1998, and Hoang 2013]. The sequential Monte Carlo is based on simulation

method that uses the Monte Carlo simulation in order to solve on-line estimation and prediction problems. The sequential Monte Carlo approach is also referred as the bootstrap filtering [Gordon 1993] or the condensation algorithm [Cormick 2000] or the particle filtering [Carpenter 1999]. The flexible nature of the Monte Carlo simulation renders more adaptive feature to estimate the state [Arulampalam 2002, Ristic 2004]. This thesis proposes research on the channel estimation based on PF with extended Kalman filter as proposal distribution for dealing with non-linear and non-Gaussian system, which is discussed in chapter 5.

The most commonly used the Extended Kalman Filter (EKF) based on analytical approximated non-linear filter along with non-linear least square estimation are discussed in the next section.

3.2.1 Non-Linear Least-Squares Estimation

Consider the following continuous discrete non-linear equations,

$$\dot{x}(t) = f(x,t) + w(t) \tag{3.10}$$

$$y_k = h(x_k,k) + v_k \tag{3.11}$$

Where, $x_k \in R^n$ is the $n\times1$ state vector,

$y_k \in R^m$ is the $m\times1$ observation vector.

$f(x,t)$ is the non-linear continuous function of the state

$h(x_k,t)$ is discrete non-linear function

$w(t) \in R^q$ is the $q\times1$ state noise process vector and

$v_k \in R^s$ is the $s\times1$ additive measurement noise vector.

Noise vectors are assumed to be zero-mean Gaussian processes

$$E[w(t)w^T(s)] = \delta(t-s)Q(t), \quad E\left[v_k v_j^T\right] = \delta_{kj}R_k \tag{3.12}$$

The basic principle of the least-squares method is to optimally estimate the state which minimizes the sum of the squares of the residues. The residue is denoted as

$$\vartheta_k = y_k - h(x_k,k) \tag{3.13}$$

Where,

y_k referred as the actual observations or true observations.

If the nominal trajectory of the system is $\hat{x}_k$, then the measurement function $h(x_k, k)$ can be approximated by using the Taylor-series expansion

$$h(x_k) = h(\hat{x}_k) + \frac{\delta h}{\delta x}\Big|_{x_k=\hat{x}_k} (x_k - \hat{x}_k) + higher\ order\ term \tag{3.14}$$

Where, $h(\hat{x}_k)$ is the estimated value of the observation at the value $\hat{x}_k$, and the gradient matrix H_k, also known as the Jacobian matrix and is defined as

$$H_k \equiv \left[\frac{\delta h}{\delta x}\Big|_{\hat{x}_k}\right] \tag{3.15}$$

If one assumes that the current estimates of the state x_c are denoted by

$$x_c = [x_{1c}, x_{2c}, \dots\dots, x_{nc}]^T \tag{3.16}$$

Then the current estimate is related to the estimates $\hat{x}_k$ by an unknown set of corrections Δx

$$\hat{x}_k = x_c + \Delta x \tag{3.17}$$

If correction component Δx is sufficiently small, then it is possible to solve for an approximation to the updated x_c with an improved estimate of $\hat{x}_k$ using Equation (3.17). With this assumption, the function $h(\hat{x}_k, k)$ can be linearized about x_c,

$$h(\hat{x}_k) \approx h(x_c) + H\Delta x \tag{3.18}$$

After the correction of measurement residue Δx it can be linearly approximated by

$$\Delta y \equiv y_k - h(\hat{x}_k) \approx y_k - h(x_c) - H\Delta x \tag{3.19}$$

Where,

$\Delta x = \hat{x}_k - x_c$ is the differential correction, and

The residual before the correction is defined as

$$\Delta y_c \equiv y_k - h(x_c) \tag{3.20}$$

The implication of the weighted least-squares estimation is to minimize the weighted sum of the squares of the measurement residues given by the cost function J.

$$J = \frac{1}{2}\Delta y^T W \Delta y = \frac{1}{2}[y_k - h(\hat{x}_k)]^T W [y_k - h(\hat{x}_k)] \tag{3.21}$$

Where, W is a $m \times m$ symmetric weighting matrix used to weight the relative importance of each measurement. The strategy for determining the differential corrections Δx is to select the particular corrections that lead to the minimum sum of

squares of the linearly predicted residuals J_p. The measurement residues can be approximated in terms of Δy_c by using Equation (3.19), and the cost function is rewritten by

$$J_p = \frac{1}{2}[\Delta y_c - H\Delta x]^T W[\Delta y_c - H\Delta x] \tag{3.22}$$

The minimization of J_p in Equation (3.22) is equivalent to the minimization of J in Equation (3.21). For the minimization of J_p, the following conditions should be satisfied

Necessary Condition

$$\nabla_{\Delta x} J_p = \frac{\delta J_p}{\delta \Delta x} = H^T W H \Delta x - H^T W \nabla y_c = 0 \tag{3.23}$$

Sufficient Condition

$$\nabla^2_{\Delta x} J_p = \frac{\delta^2 J_p}{\delta \Delta x_i \delta \Delta x_j} = H^T W H > 0, \ (postive\ definite\ ) \tag{3.24}$$

From the necessary condition, the normal equation can be obtained

$$H^T W H \Delta x = H^T W \nabla y_c \tag{3.25}$$

Finally, the explicit solution for solving the weighted least-squares problem applicable for solving Δx is represented by

$$\Delta x = (H^T W H)^{-1} H^T W \Delta y_c \tag{3.26}$$

Because of the non-linearities in the non-linear function, this process of non-linear estimation must be iterated until the solution converges, i.e., Δx approaches zero.

The complete non-linear least-squares algorithm is summarized in Figure 3.2. To begin with the algorithm, an initial guess Δx of the current estimates is required. A stopping condition with an accuracy dependent tolerance for the minimization of J is given by

$$\delta J = \frac{|J_i - J_{i-1}|}{J_i} < \frac{\varepsilon}{\|W\|} \tag{3.27}$$

Where i is the iteration number and ε is a prescribed small value. If the judgment criterion in Equation (3.27) is not satisfied, the update procedure is iterated with the new estimate as the current estimate until the process converges.

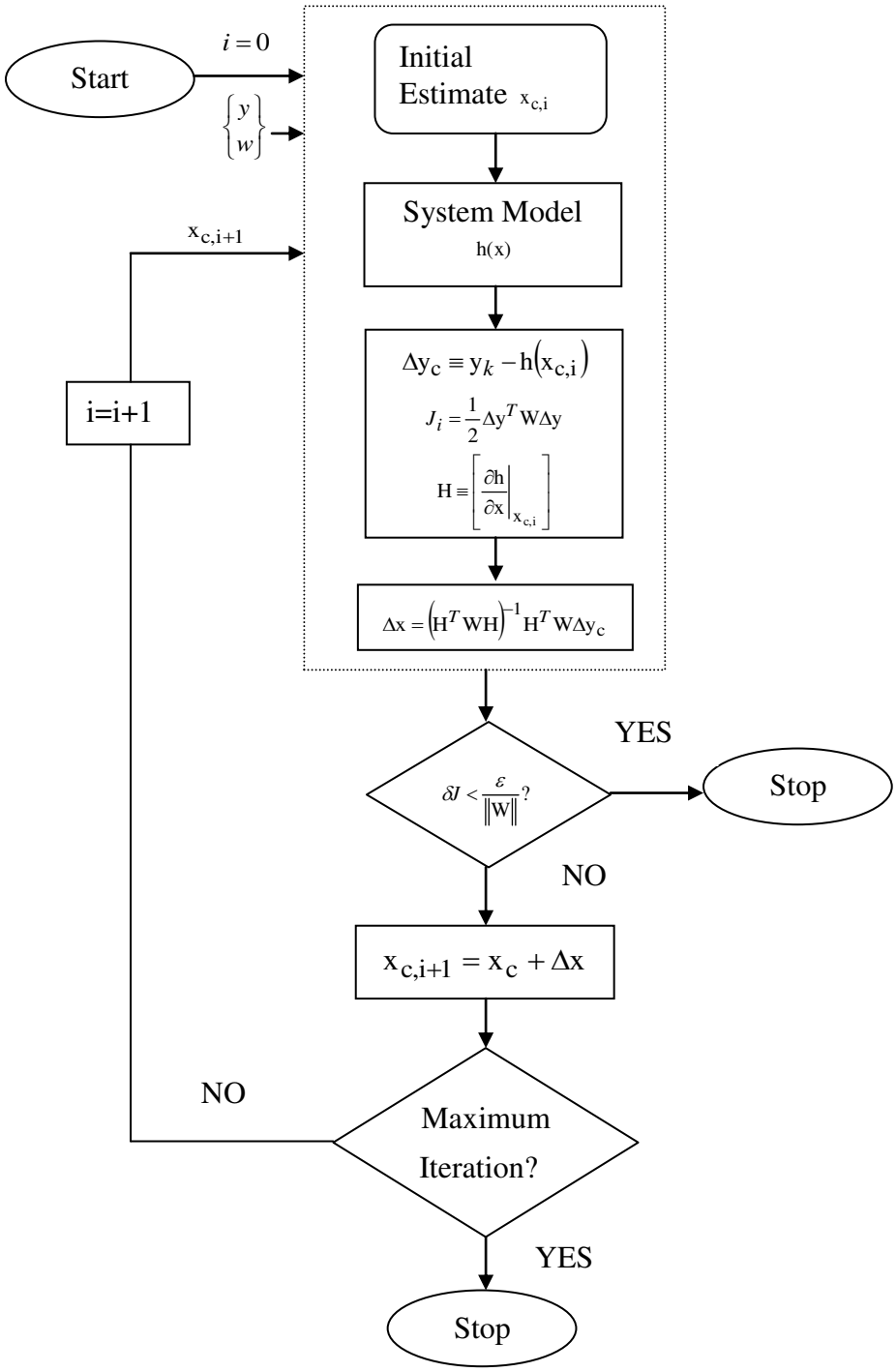

Figure 3.2: Non-linear least square differential correction

3.2.2 Extended Kalman Filter

This section discusses the concept of EKF from the Bayesian perspective for the development of algorithms to estimate the state vectors invoking the concept highlighted in [Frost 1971]. Discrete-time non-linear equations can be of the form

$$x_{k+1} = f(x_k, w_k, k) \tag{3.28}$$

$$y_{k+1} = h(x_k, k) + v_k \tag{3.29}$$

Where,

$\mathrm{x}_k \in R^n$ is the $n \times 1$ state vector,

$\mathrm{y}_k \in R^m$ is the $m \times 1$ observation vector.

$w_k \in R^q$ is the $q \times 1$ state noise process vector and

$\mathrm{v}_k \in R^s$ is the $s \times 1$ additive measurement noise vector.

$f(x_k, w_k, k)$ is the non-linear discrete function of the state

$h(x_k, t)$ is discrete non-linear function of the observation

Further it is assumed that the noise vectors are zero-mean Gaussian processes and

$$E\left[\mathrm{w}_k \mathrm{w}_j^T\right] = \delta_{kj}\mathrm{Q}_k, \quad E\left[\mathrm{v}_k \mathrm{v}_j^T\right] = \delta_{kj}\mathrm{R}_k, \quad E\left[\mathrm{v}_k \mathrm{w}_j^T\right] = 0, \quad \forall k, j \tag{3.30}$$

The EKF provides the minimum variance estimate of the state based on statistical information about the dynamic system model (Equations 3.28 and 3.29) and observations (Equations 3.29). Given a system model and initial state and covariance values, the EKF propagates the first two moments (mean and covariance) of the distribution of x_k recursively. Then, along with imperfect measurements (in the presence of noise), the EKF updates the estimates of the state vector and the covariance vector. The update is done through the Kalman gain matrix, K, which comes from minimizing the weighted scalar sum of the diagonal elements of the covariance matrix. Thus, the EKF method has a distinctive *predictor-corrector* structure, which is similar to the recursive Bayesian relationships stated in Equations (3.6) ~ (3.7).

The EKF is based on the analytical Taylor series expansion of the non-linear systems and observation equations about the current estimated value x_k. Thus, for non-linear models, the predicted state estimate and covariance are approximated by [Shalom 2001]

$$\hat{\mathrm{x}}_{k+1}^{-} = \mathrm{f}\left(\hat{\mathrm{x}}_k, k\right) \tag{3.31}$$

$$\mathrm{P}_{k+1}^{-} = \mathrm{F}_k \mathrm{P}_k \mathrm{F}_k^T + \mathrm{Q}_k \tag{3.32}$$

Where,

F_k is the Jacobian matrix of f evaluated about $\hat{\mathrm{x}}_k$.

The update equations are written as

$$\hat{\mathrm{x}}_{k+1}^{+} = \hat{\mathrm{x}}_{k+1}^{-} + K_{k+1}\upsilon_{k+1} \tag{3.33}$$

$$\mathrm{P}_{k+1}^{+} = \mathrm{P}_{k+1}^{-} - K_{k+1}\mathrm{P}_{k+1}^{vv}K_{k+1}^{T} \tag{3.34}$$

Where,

υ_{k+1} is the innovative vector, which is equal to the difference between the actual and the predicted observations, and is given by

$$\upsilon_{k+1} = \mathrm{y}_{k+1} - \hat{\mathrm{y}}_{k+1}^{-} = \mathrm{y}_{k+1} - \mathrm{h}\left(\hat{\mathrm{x}}_{k+1}^{-}, k+1\right) \tag{3.35}$$

The covariance of the innovation vector is evaluated as

$$\mathrm{P}_{k+1}^{vv} = \mathrm{P}_{k+1}^{yy} + \mathrm{R}_{k+1} \tag{3.36}$$

Where,

P_{k+1}^{yy} is the output covariance.

The Kalman gain K_{k+1} is computed by

$$K_{k+1} = \mathrm{P}_{k+1}^{xy}\left(\mathrm{P}_{k+1}^{vv}\right)^{-1} \tag{3.37}$$

Where,

P_{k+1}^{xy} is the cross-correlation matrix predicted between $\hat{\mathrm{x}}_{k+1}^{-}$ and $\hat{\mathrm{y}}_{k+1}^{-}$.

The PDF in the Bayesian recursion are related to the optimal terms in the EKF algorithms given in [Arulampalam 2002]

$$p\left(\mathrm{x}_k \mid \mathrm{Y}_k\right) = N(\mathrm{x}_k; \hat{\mathrm{x}}_k, \mathrm{P}_k) \tag{3.38}$$

$$p\left(\mathrm{x}_{k+1} \mid \mathrm{Y}_k\right) = N(\mathrm{x}_{k+1}; \hat{\mathrm{x}}_{k+1}^{-}, \mathrm{P}_k^{-}) \tag{3.39}$$

$$\approx N(\mathrm{x}_{k+1}; \mathrm{f}\left(\hat{\mathrm{x}}_k\right), \mathrm{F}_k \mathrm{P}_k \mathrm{F}_k^T + \mathrm{Q}_k) \tag{3.40}$$

$$p(\mathrm{x}_{k+1} \mid \mathrm{Y}_{k+1}) = N(\mathrm{x}_{k+1}; \hat{\mathrm{x}}_{k+1}, \mathrm{P}_{k+1}) \tag{3.41}$$

$$\approx N(\mathrm{x}_{k+1}; \hat{\mathrm{x}}_{k+1}^{-} + K_{k+1}\upsilon_{k+1}, \mathrm{P}_{k+1}^{-} - K_{k+1}\mathrm{P}_{k+1}^{vv}K_{k+1}^{T}) \tag{3.42}$$

Where $N(\mathrm{x}; m, P)$ denotes a Gaussian density with argument x, mean m, and covariance P. The recursive Bayesian relations of the predictor-corrector structure for the EKF can be represented by the block diagram shown in Figure. 3.3. The specific algorithm of the EKF formulated in terms of the innovation vector υ_k and covariance terms P_k^{vv} is summarized in Table 3.1.

It is pertinent to note that in the EKF algorithm, the state distribution is approximated through the first-order linearization of the non-linear functions by a Gaussian random variable. These approximations can introduce large errors in the true mean and covariance.

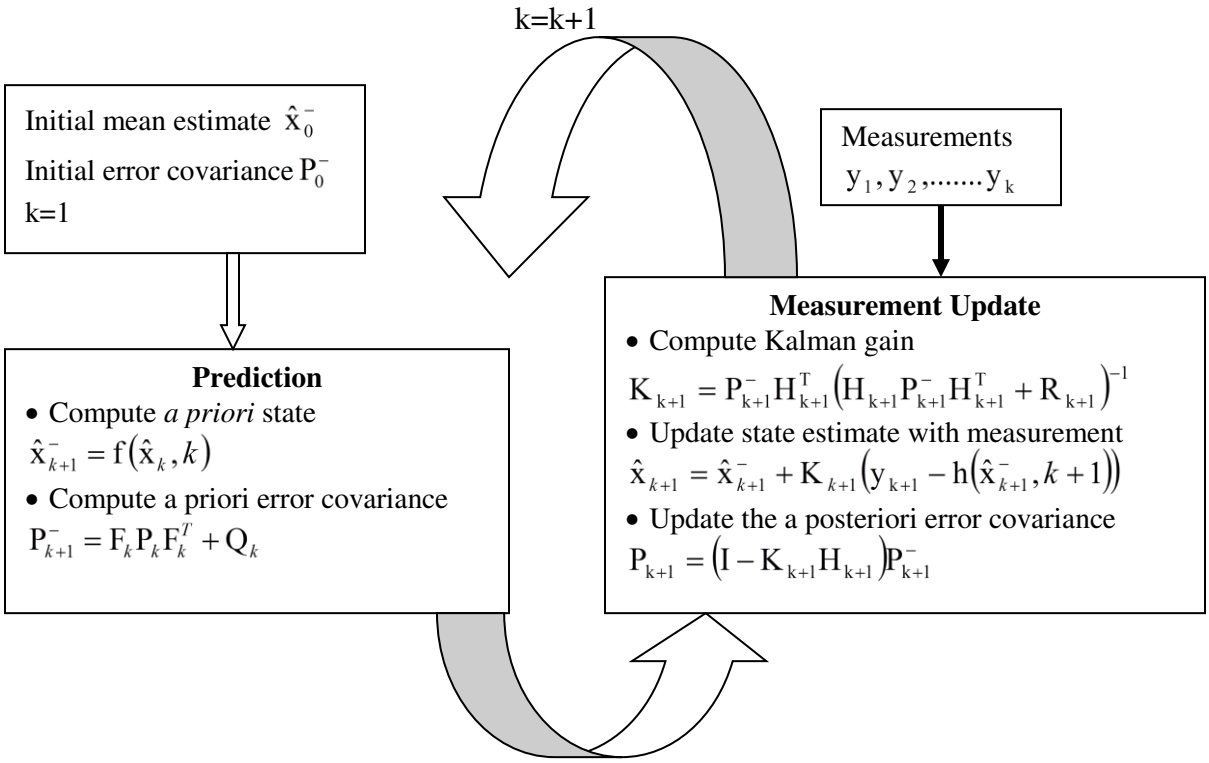

Figure 3.3:Diagram of predictor-corrector form of the extended Kalman filter

Table 3.1 Extended Kalman Filter Algorithms

Initialization:

$$\hat{\mathrm{x}}_0 = E[\mathrm{x}_0]$$
$$\mathrm{P}_0 = E\left[(\mathrm{x}_0 - \hat{\mathrm{x}}_0)(\mathrm{x}_0 - \hat{\mathrm{x}}_0)^T\right]$$

State Propagation:

$$\hat{\mathrm{x}}_{k+1}^{-} = \mathrm{f}(\hat{\mathrm{x}}_k, k)$$
$$\mathrm{P}_{k+1}^{-} = \mathrm{F}_k \mathrm{P}_k \mathrm{F}_k^T + \mathrm{Q}_k$$

Observation Propagation:

$$\hat{\mathrm{y}}_{k+1}^{-} = \mathrm{h}(\hat{\mathrm{x}}_{k+1}^{-}, k+1)$$
$$\mathrm{P}_{k+1}^{vv} = \mathrm{H}_{k+1} \mathrm{P}_{k+1}^{-} \mathrm{H}_{k+1}^T + \mathrm{R}_{k+1}$$
$$\mathrm{P}_{k+1}^{xy} = \mathrm{P}_{k+1}^{-} \mathrm{H}_{k+1}^T$$

Update:

$$\mathrm{K}_{k+1} = \mathrm{P}_{k+1}^{xy} \left(\mathrm{P}_{k+1}^{vv}\right)^{-1}$$
$$\mathrm{P}_{k+1}^{+} = \mathrm{P}_{k+1}^{-} - \mathrm{K}_{k+1} \mathrm{P}_{k+1}^{vv} \mathrm{K}_{k+1}^T$$
$$\hat{\mathrm{x}}_{k+1}^{+} = \hat{\mathrm{x}}_{k+1}^{-} + \mathrm{K}_{k+1} \upsilon_{k+1}$$

where (-) denotes a "propagated" value, (+) denotes a "updated" value

Q_k = System model error matrix, R_k = Measurement error matrix

3.3 Principles of Particle Filtering

Approximated Gaussian filtering discussed in previous section is efficient for linearization of non-linear systems. EKF is one class of approximated Gaussian filtering discussed in previous section. The other categories of it include the Iterated Extended Kalman Filter (IEKF), the Gaussian Mixture Filter (GMF), and the Sigma Point Filter (SPFs) [Julier 1995, Ito 2000]. But most of practical communication systems are dynamical in nature and are associated with both non-linear and non-Gaussian noise. The state estimation techniques under non-linear and non-Gaussian noise scenario pose challenges for the scientists and engineers in their pursuit for an optimal and efficient method for real time estimation and prediction of dynamical system from the sequential observations. To date, there is no algorithm which can be branded as "universally effective" for dealing non-linear and non-Gaussian systems. However, recently there is lot interest and attention towards a new class of filtering method based on the sequential Monte Carlo (SMC) approach under the class of simulation-based filter [Doucet 1998]. Initially SMC method has been introduced in fields of physics, statistics and automatic control. Later this approach found its application in almost all fields of engineering. Earlier implementation of SMC was based on simple plain Sequential Importance Sampling (SIS) step which constitutes basic form of SMC filters. The practical utilization of resampling technique in SMC led to the major contribution for non-linear and non-Gaussian class of filtering [Gordon 1993]. The SMC approach is commonly known as Bootstrap filtering [Gordon 1993], the Condensation algorithm [Cormick 2000], and the PF [Carpenter 1999]. The flexible nature of the Monte Carlo simulation finds it application in target tracking system [Arulampalam 2002, Ristic 2004].

3.4 Optimal Recursive Bayesian Estimation

Considering the non-linear state space model, the objective is to estimate the posterior probability density for the state based on the observation,

$$x_{k+1} = f(x_k, w_k, k) \tag{3.43}$$

$$y_{k+1} = h(x_k, k) + v_k \tag{3.44}$$

Where,

$x_k \in R^{n\times 1}$ is the state vector,

$y_k \in R^{m\times 1}$ is the observation vector,

$f(x_k, w_k, k)$ is the non-linear discrete function of the state

$h(x_k, t)$ is discrete non-linear function of the observation

$w_k \in R^{q\times 1}$ and $v_k \in R^{r\times 1}$ are the process and measurement noises respectively.

Let $X_k = (x_0, x_1, \dots\dots\dots, x_k)$ and $Y_k = (y_0, y_1, \dots\dots\dots, y_k)$ be the vectors of states and observations up to time step k. If there is an assumption that w_k and v_k are both independent and have known density distributions, .then the state of the system is a Markov process

$$p(X_k) = p(x_0)\prod_{i=1}^{k} p(x_i|x_{i-1}) \tag{3.45}$$

and the measurements Y_k are conditionally independent given the states X_k

$$p(Y_k|\, X_k) = \prod_{i=1}^{k} p(y_i|x_i) \tag{3.46}$$

Obviously the size of these expressions grows as time evolves if we were to calculate everything from initial time k=0. To estimate the *a-posterior* in real time, one needs k samples to determine the estimation at time $k+1$.

The following recursive equations are used [Doucet2000]

$$p(x_{k+1}|Y_k) = \int p(x_{k+1}|x_k)\, p(x_k|Y_k)dx_k \tag{3.47}$$

$$p(x_{k+1}|Y_{k+1}) = \frac{p(y_{k+1}|x_{k+1})p(x_{k+1}|Y_k)}{p(y_{k+1}|Y_k)} \tag{3.48}$$

The initial a posterior density $p(x_0|y_0)$ is obtained by

$$p(x_0|y_0) = \frac{p(y_0|x_0)p(x_0)}{p(y_0)} \tag{3.49}$$

The Equation (3.47) is called the *time update* equation (*or prediction*) and the second Equation (3.48) is called the *measurement update* equation. The likelihood probability density $p(y_k|x_k)$ in Equation (3.48) is computed by the *a-priori* measurement noise density $p(v_k)$ and the measurement Equation (3.44). And similarly, the *state transition* density $p(x_{k+1}|x_k)$ in Equation (3.47) is calculated by using the a priori process noise density $p(w_k)$ as well as the dynamic equation (Equation (3.43)).

Depending upon the characteristics of the system, there are different methods of estimating $p(x_k|\, Y_k)$ because closed form solution for $p(x_k|\, Y_k)$ are intractable due to the integration in Equation (3.47). In general there are three different cases of filtering, namely linear-Gaussian, non-linear Gaussian, and non-linear/non-Gaussian. For the linear-Gaussian case where both system dynamic as well as measurement equations are linear, it's a-*prior* initial state and noise sequence are Gaussian. In this case, the Bayesian estimation Equations (3.47) and (3.48) lead to Kalman filtering approach. For second case where system equations are non-linear with Gaussian distribution assumption, solution is provided by sub-optimal recursive approach. Finally for non-linear and non-Gaussian case, the solution for optimal Bayesian equations is solved by SMC approach. PF derived within a unified frame-work of the sequential importance sampling algorithm is discussed in subsequent sections.

3.5 Particle Filtering

In SMC techniques filtering is achieved by recursively generating a set of weighted samples of the state variables. Each sampled particle has some degree of information about the observation state. The weighted samples form an estimate of the desired posterior distribution. For every time instant, the samples are more and more likely to drift away from the real state implying that their corresponding weight tends to zero. To avoid this, normally the sample with smaller weight will be discarded and those with larger weight will be multiplied and considered. Therefore the implementation of the PF consists of three operations.

1) Generation of particle (Sampling step)
2) Particle weight computation (Importance step)
3) Resampling

The first two steps form the Sequential Importance Sampling (SIS) algorithm. The SIS filter along with the resampling is termed as the generic particle filter.

3.5.1 Sequential Importance Sampling

The discrete-time non-linear model equation is of the form

$$x_{k+1} = f(x_k, k) + w_k \tag{3.50}$$

$$y_k = h(x_k, k) + v_k \tag{3.51}$$

Where the process w_k and measurement noises v_k are assumed to be independent with known densities

$$w_k \sim p_{w_k}(.), \quad v_k \sim p_{v_k}(.) \tag{3.52}$$

For the Markov process, the state distribution function is expressed by

$$p(X_k) = p(x_0)\prod_{i=1}^{k} p(x_i \mid x_{i-1}) \tag{3.53}$$

Where $p(x_0)$ is prior distribution of the state at time $k = 0$. The observations are conditionally independent given the states

$$p(Y_k \mid X_k) = \prod_{i=1}^{k} p(y_i \mid x_i) \tag{3.54}$$

Posterior is represented as total PDF because the model is non-linear and non-Gaussian. Total PDF is evaluated by recursive Monte Carlo simulation. The recursive equation for the estimation of PDF is given by

$$p(X_k \mid Y_k) = \frac{p(y_k \mid X_k, Y_{k-1})p(x_k \mid X_{k-1}, Y_{k-1})}{p(y_k \mid Y_{k-1})} p(X_{k-1} \mid Y_{k-1}) \tag{3.55}$$

$$= \frac{p(y_k \mid x_k)p(x_k \mid x_{k-1})}{p(y_k \mid Y_{k-1})} p(X_{k-1} \mid Y_{k-1}) \tag{3.56}$$

The particle filter utilizes the discrete version of large number of samples to estimate the density function. Let $\{X_k^{(i)}\}_{i=1}^{N}$ be the sample drawn from the posterior density. Then the expression for the estimate of the posterior is

$$\hat{p}(X_k \mid Y_k) = \frac{1}{N}\sum_{i=1}^{N} \delta(X_k - X_k^{(i)}) \tag{3.57}$$

Where,

$\delta(X_k)$ is the Dirac delta function.

All the samples collected by the posterior density are drawn and selectively considered such that weighted sum is equal to unity. In order to satisfy the law of total probability, the estimate has to multiplied by $1/N$.

These estimates can be used to calculate different moments of the posterior. For example the expectation and covariance are given as

$$\hat{\mathrm{x}} = E\{\mathrm{x}\} = \int \mathrm{x}\, p(\mathrm{x}) d\mathrm{x}$$

$$= \int \frac{1}{N} \sum_{i=1}^{N} \delta\left(\mathrm{x} - \mathrm{x}^{(i)}\right) \mathrm{x} d\mathrm{x}$$

$$= \frac{1}{N} \sum_{i=1}^{N} \mathrm{x}^{(i)} \tag{3.58}$$

$$\mathrm{P} \approx \int \frac{1}{N} \sum_{i=1}^{N} \delta\left(\mathrm{x} - \mathrm{x}^{(i)}\right) \delta(\mathrm{x} - \hat{\mathrm{x}}) \delta(\mathrm{x} - \hat{\mathrm{x}})^T d\mathrm{x}$$

$$= \frac{1}{N} \sum_{i=1}^{N} \left(\mathrm{x}^{(i)} - \hat{\mathrm{x}}\right)\left(\mathrm{x}^{(i)} - \hat{\mathrm{x}}\right)^T \tag{3.59}$$

Since the posterior is unknown, sample has to be drawn from known probability density $q(\mathrm{X}_k \mid \mathrm{Y}_k)$. Bayes's rule provides

$$q(\mathrm{X}_k \mid \mathrm{Y}_k) = q(\mathrm{x}_k \mid \mathrm{X}_{k-1}, \mathrm{Y}_{k-1}) q(\mathrm{X}_{k-1} \mid \mathrm{Y}_k) \tag{3.60}$$

$$= q(\mathrm{x}_k \mid \mathrm{X}_{k-1}, \mathrm{Y}_k) q(\mathrm{X}_{k-1} \mid \mathrm{Y}_{k-1}) \tag{3.61}$$

To estimate the posterior, these samples are associated with so called *important weight*

$$w_k^{(i)} = \frac{p\left(\mathrm{X}_k^{(i)} \mid \mathrm{Y}_k\right)}{q\left(\mathrm{X}_k^{(i)} \mid \mathrm{Y}_k\right)} = c_k \frac{p\left(\mathrm{y}_k \mid \mathrm{x}_k^{(i)}\right) p\left(\mathrm{x}_k^{(i)} \mid \mathrm{x}_{k-1}^{(i)}\right)}{q\left(\mathrm{x}_k^{(i)} \mid \mathrm{X}_{k-1}^{(i)}, \mathrm{Y}_k\right)} w_{k-1}^{(i)} \tag{3.62}$$

Where,

$c_k = p(\mathrm{Y}_{k-1}) / p(\mathrm{Y}_k)$.

Only the relative relationship between the weights is important and c_k can therefore be neglected. Hence the weight equation can be written as

$$w_k^{(i)} = w_{k-1}^{(i)} \frac{p\left(\mathrm{y}_k \mid \mathrm{x}_k^{(i)}\right) p\left(\mathrm{x}_k^{(i)} \mid \mathrm{x}_{k-1}^{(i)}\right)}{q\left(\mathrm{x}_k^{(i)} \mid \mathrm{X}_{k-1}^{(i)}, \mathrm{Y}_k\right)} \tag{3.63}$$

Efficient choice to draw the sample from the state propagation density is

$$q(\mathrm{x}_k \mid \mathrm{X}_{k-1}, \mathrm{Y}_k) = q(\mathrm{x}_k \mid \mathrm{x}_{k-1}) \tag{3.64}$$

Then, the corresponding weight update equation becomes

$$w_k^{(i)} = w_{k-1}^{(i)} p\left(\mathrm{y}_k \mid \mathrm{x}_k^{(i)}\right) \tag{3.65}$$

The new estimate of the posterior $p(\mathrm{X}_k \mid \mathrm{Y}_k)$ for the sample drawn from $q(\mathrm{x}_k \mid \mathrm{X}_{k-1}, \mathrm{Y}_k)$ along with the importance weights is given by

$$\hat{p}(\mathrm{X}_k \mid \mathrm{Y}_k) = \sum_{i=1}^{N} \overline{w}_k^{(i)} \delta\left(\mathrm{X}_k - \mathrm{X}_k^{(i)}\right) \tag{3.66}$$

Where,

$$\overline{w}_k^{(i)} = \frac{w_k^{(i)}}{\sum_{j=1}^{N} w_k^{(j)}} \tag{3.67}$$

Then, the estimated mean value $\hat{\mathrm{x}}_k^+$ and covariance P_k^+ are computed in terms of the current state x_k and the importance weights $\overline{w}_k^{(i)}$

$$\hat{\mathrm{x}}_k^+ = E\{\mathrm{x}\} = \sum_{i=1}^{N} \overline{w}_k^{(i)} \mathrm{x}_k^{(i)} \tag{3.68}$$

$$\mathrm{P}_k^+ = \left\{ \left[\mathrm{x}_k - E\{\mathrm{x}_k\}\right]\left[\mathrm{x}_k - E\{\mathrm{x}_k\}\right]^T \right\} \tag{3.69}$$

$$\approx \sum_{i=1}^{N} \overline{w}_k^{(i)} \left(\mathrm{x}_k^{(i)} - \hat{\mathrm{x}}_k^+\right)\left(\mathrm{x}_k^{(i)} - \hat{\mathrm{x}}_k^+\right)^T \tag{3.70}$$

3.5.2 Resampling

The weights of most of the samples drawn will be almost zero as time evolves [Carpenter 1999] signifying that they do not contribute much to the posterior estimation. Basically the estimate in the region of interest is not accurate as most of the samples may not contribute significantly. This phenomenon is known as degeneracy problem in the SIS particle filter [Arulampalam 2002]. Next section discusses the methods to ascertain the occurrence of degeneracy and an effective way of resolving the degeneracy.

i. Effective Sample Size

Effective sample size is a method to measure how well the samples are distributed across the region of interest. Comparison of the covariance of the set of samples drawn from the posterior with that obtained through the method of importance sampling provides measurement of the sampling efficiency. This in turn will provide the expression for the effective sample size. Effective sample size can be estimated by [Bergman 1999]

$$\hat{N}_{eff} \approx \frac{1}{\sum_{i}\left(\overline{w}_k^{(i)}\right)^2} \tag{3.71}$$

If all the sample weights are equal, the effective sample size will be N. Lower threshold is chosen for effective sample size when the samples are widely spread. Normally the threshold is fixed as $N_{th} = 2N/3$. When the samples depart away from the state, their weights decrease and are referred as degeneracy [Arulampalam 2002]. There by the effective sample size decreases eventually leading to $N < N_{sh}$. At this situation among a new set of N samples drawn from $\left\{X_k^{(i)}\right\}$, samples with associated weight nearing zero have to be replaced and such a replacement is from resampling of the chosen distribution. The probability of finding such replacement for degeneracy samples with $X_k^{(i)}$ is $\overline{w}_k^{(i)}$. Now the new set of samples is drawn from the estimate of the posterior and all the weights should therefore be set to 1/N. This means that only the samples with higher weights will be considered leading to the cluster of samples concentrated in the interesting region. The flow for replacement of degeneracy samples is described in Figure 3.4.

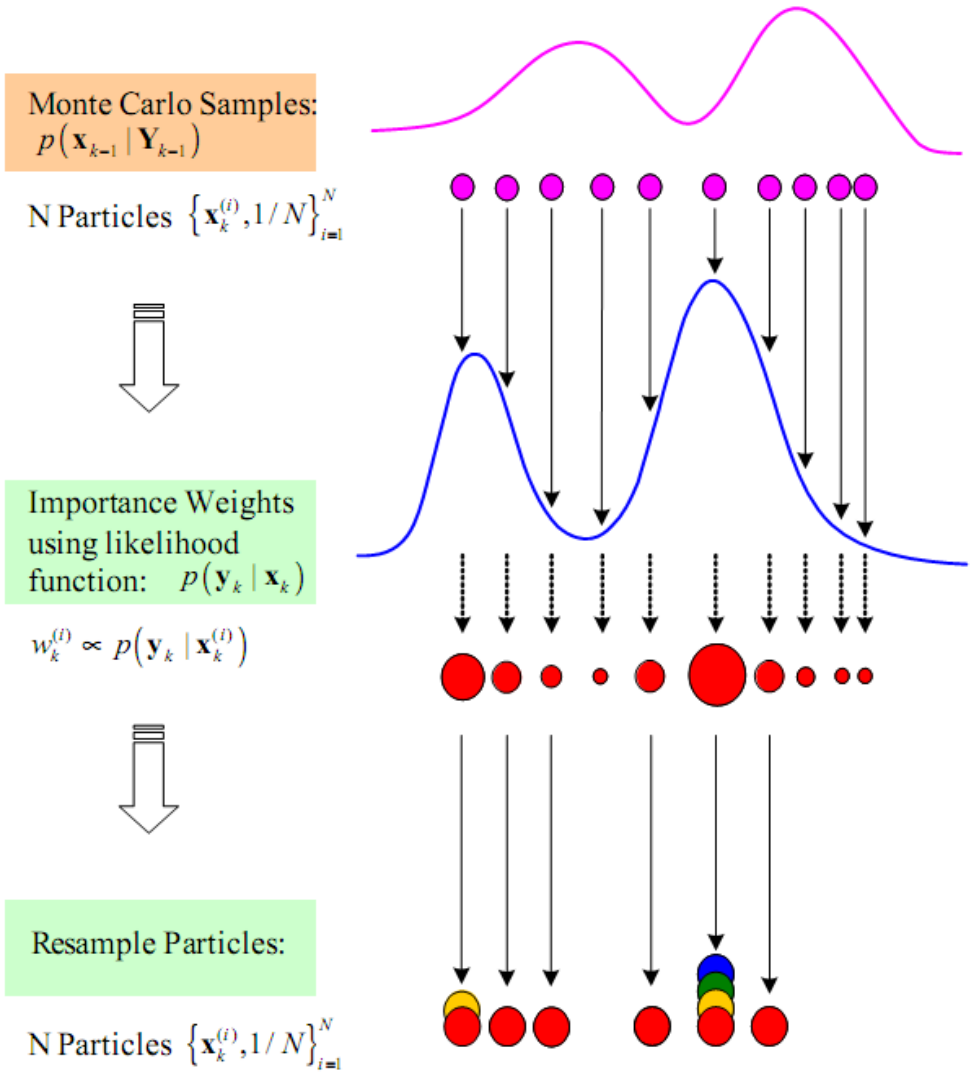

Figure 3.4: Systematic diagram for generic Particle filtering

ii. Resampling Algorithms

Resampling technique is a method to mitigate the effects of the degeneracy sample. The basic principle of resampling technique is to eliminate particles with lesser weights and to concentrate on particles with large weights. The following section describes three resampling algorithms.

Simple Random Resampling

In this method, N independent and identical distributed (i.i.d) random variables are generated from the uniform distribution. They are sorted in ascending order and compared with cumulative sum of normalized weights [Ristic 2004]. Initially the threshold is calculated based on cumulative sum of the normalized weights in any order. Then for the each index i (i=1 to N)

1. Uniform random number u_i between 0 and 1, u_i = U[0, 1] is drawn
2. Search algorithm (binary search) is used to identify the position of u_i within the thresholds
3. The resampled index is set according to the index of the location of u_i

This technique although simple is not computationally efficient. The discussion of computationally efficient techniques is to follow.

Residual Resampling (RR)

The principles of this technique are as follows

1. $s_i = \left\lfloor N\overline{w}_k^{(i)} \right\rfloor$ copies of $\mathrm{x}_k^{(i)}, i = 1, \cdots, n,$ are retained where $\overline{w}_k^{(i)}$ is the renormalized weight of $w_k^{(i)}$. Let $N_r = N - \sum_{i=1}^{n} s_i$
2. N_r samples i.i.d drawn from $\mathrm{x}_{1:k}^{(i)}$ with probabilities proportional to $N\overline{w}_k^{(i)} - s_i$ $i = 1, \cdots, N$ are obtained
3. The summation weight is reset to 1 implying $\overline{w}_k^{(i)} = 1/N$ for $i = 1, \cdots, N$,

The residual resampling is superior over the random resampling since it also provides reduced variation in the estimates [Liu 1998, Bergman 1999].

Systematic Resampling (SR)

This efficient technique uses a minimum variance method [Liu 1998] in which uniform distribution U [a, b] is utilized on the interval [a, b]. In this method each value u_i is independently drawn by using the following scheme

$$u_1 \sim \mathrm{U}[0,1/N] \tag{3.72}$$

$$u_i = u_1 + \frac{i}{N} \tag{3.73}$$

The systematic resampling algorithm is described in Table 3.2.

Table 3.2 Systematic Resampling Algorithm

1. Initialization at time $i = 1$
   - Set $c_1 = 0$
2. For $i = 2, \cdots, N$
   - Construct $c_i = c_{i-1} + w_k^i$
3. Set I = 1
4. Draw a starting point
   - $u_1 \sim \mathrm{U}[0,1/N]$
5. For $j = 1, \cdots, N$
   - Construct $u_j = u_1 + (j-1)/N$
   - While $u_j > c_i$
     - $i = i + 1$
   - Otherwise
     - assign sample: $\mathrm{x}_k^j = \mathrm{x}_k^i$
     - assign weight: $w_k^j = 1/N$

3.6 Generic Particle Filter Algorithm

The concept discussed in section 3.5 is considered as a motivation of how particle filter works. Table 3.3 illustrates the algorithmic summary of the particle filter or SIS with resampling stage. Choice of the proposal or importance distribution is a most critical design issue while implementing the particle filter. The Figure 3.4 shows the overall procedure for the generic PF algorithms.

The initial samples are drawn from the prior distribution and the corresponding weights are calculated from the measurement. For the each iteration the samples are drawn from the selected importance distribution. Accordingly their weight is updated from the selected proposal distribution of the drawn samples.

Table 3.3 Generic Particle Filter (PF) Algorithm

- Initialization: at time $k = 0$
  1. For $i = 1, \cdots, N$
     - Sampling from the prior $\mathrm{x}_0^{(i)} \sim p(\mathrm{x}_0)$
  2. For $i = 1, \cdots, N$,
     - Calculate $w_0^{(i)} = p(\mathrm{y}_0 \mid \mathrm{x}_0^{(i)})$
     - Calculate the total weight $w_T = \sum_i^N w_0^{(i)}$
     - Normalize $w_0^{(i)} = w_T^{-1} w_0^{(i)}$
- Prediction and Update: For each time $k \geq 1$
  1. For $i = 1, \cdots, N$,
     - Sample $\mathrm{x}_k^{(i)} \sim q(\mathrm{x}_k \mid \mathrm{X}_{k-1}^{(i)}, \mathrm{Y}_k)$
     - Calculate the importance weights

$$w_k^{(i)} = w_{k-1}^{(i)} \frac{p(\mathrm{y}_k \mid \mathrm{x}_k^{(i)}) p(\mathrm{x}_k^{(i)} \mid \mathrm{x}_{k-1}^{(i)})}{q(\mathrm{x}_k^{(i)} \mid \mathrm{X}_{k-1}^{(i)}, \mathrm{Y}_k)}$$

2. Calculate the total weight $w_T = \sum_i^N w_k^{(i)}$

3. For $i = 1, \cdots, N$,

   - Normalize $w_k^{(i)} = w_T^{-1} w_k^{(i)}$

4. If $\left(N_{eff} < N_{th}\right)$, then Choose either (a) or (b)

   - (a) Apply resampling algorithm
   - $\left[\left\{ \mathrm{x}_k^{(i)}, w_k^{(i)} \right\}_{i=1}^N \right]$ = Resample(RR, SR) $\left[\left\{ \mathrm{x}_k^{(i)}, w_k^{(i)} \right\}_{i=1}^N \right]$
   - (b) Apply resampling algorithm
   - Set the weights, $w_k^{(i)} = 1/N$

3.6.1 Sequential Importance Resampling Particle Filtering

Sequential Importance Resampling (SIR) approach is proposed by [Gordon 1993] and it is special case of SIS algorithm. The SIR algorithm can be derived from the SIS algorithm by an appropriate choice of the importance density and the resampling step. The optimal proposal distribution which minimizes the variance on the importance weight is given by [Doucet 2000, Liu 1998]

$$q\left(\mathrm{x}_k \mid \mathrm{x}_{1:k-1}, \mathrm{y}_{1:k}\right) = p\left(\mathrm{x}_k \mid \mathrm{x}_{1:k-1}, \mathrm{y}_{1:k}\right) \tag{3.74}$$

But sampling from this proposal distribution is impractical for arbitrary densities. Thus efficient choice of the importance density is the transition prior density

$$q\left(\mathrm{x}_k \mid \mathrm{x}_{1:k-1}, \mathrm{y}_{1:k}\right) = p\left(\mathrm{x}_k \mid \mathrm{x}_{k-1}\right) \tag{3.75}$$

The sample is drawn from this proposal in the form of

$$\mathrm{x}_k^{(i)} \sim p\left(\mathrm{x}_k \mid \mathrm{x}_{k-1}^{(i)}\right) \tag{3.76}$$

The procedure for generating a sample $\mathrm{x}_k^{(i)}$ is achieved by

- First generating a process noise sample $\mathrm{v}_{k-1}^{(i)} \sim p_v\left(\mathrm{v}_{k-1}\right)$ where p_v is the pdf of the noise v_{k-1}

- Then, substituting the samples $\mathrm{x}_{k-1}^{(i)}$ and $\mathrm{v}_{k-1}^{(i)}$ into the dynamic system function, i.e., $\mathrm{x}_k^{(i)} = \mathrm{f}\left(\mathrm{x}_{k-1}^{(i)}, \mathrm{v}_{k-1}^{(i)}\right)$.

The update equation for the weights is given by

$$w_k \propto w_{k-1} p\left(\mathrm{y}_k \mid \mathrm{x}_k\right) \frac{p\left(\mathrm{x}_k \mid \mathrm{x}_{k-1}\right)}{q\left(\mathrm{x}_k \mid \mathrm{x}_{k-1}, \mathrm{y}_{1:k}\right)} \tag{3.77}$$

For this particular choice of the importance density in Equation (3.75), the corresponding weight update equation becomes

$$w_k^{(i)} \propto w_{k-1}^{(i)} p\left(\mathrm{y}_k \mid \mathrm{x}_k^{(i)}\right) \tag{3.78}$$

It is noted that since resampling in the SIR algorithm is applied at every time step, the prior weights are all equal to $w_{k-1}^{(i)} = 1/N$. Thus the update weight is given by

$$w_k^{(i)} \propto p\left(\mathrm{y}_k \mid \mathrm{x}_k^{(i)}\right) \tag{3.79}$$

The SIR PF algorithm is illustrated in Table 3.4.

Table 3.4 SIR Particle Filter Algorithm

- Initialization: at time $k = 0$
  1. For $i = 1, \cdots, N$
     - Sampling from the prior $\mathrm{x}_0^{(i)} \sim p\left(\mathrm{x}_0\right)$
  2. For $i = 1, \cdots, N$,
     - Calculate $w_0^{(i)} = p\left(\mathrm{y}_0 \mid \mathrm{x}_0^{(i)}\right)$
     - Calculate the total weight $w_T = \sum_i^N w_0^{(i)}$
     - Normalize $w_0^{(i)} = w_T^{-1} w_0^{(i)}$
- Prediction and Update: For each time $k \geq 1$
  1. For $i = 1, \cdots, N$,
     - Sample $\mathrm{x}_k^{(i)} \sim p\left(\mathrm{x}_k \mid \mathrm{x}_{k-1}^{(i)}\right)$
     - Calculate the importance weights $w_k^{(i)} = p\left(\mathrm{y}_k \mid \mathrm{x}_k^{(i)}\right)$

2. Calculate the total weight $w_T = \sum_{i}^{N} w_k^{(i)}$

3. For $i = 1, \quad \cdots, \quad N$,

   - Normalize $w_k^{(i)} = w_T^{-1} w_k^{(i)}$

4. Apply resampling algorithm

   - $\left[\left\{ x_k^{(i)}, w_k^{(i)} \right\}_{i=1}^{N} \right]$ = Resample(RR, SR) $\left[\left\{ x_k^{(i)}, w_k^{(i)} \right\}_{i=1}^{N} \right]$

3.6.2 Improving Particle Filters

The resampling is helpful to minimize the effect of degeneracy. But all particles with higher weights will not contribute to any additional information resulting in a form of undesirable redundancy. This is usually referred to as sample impoverishment [Freitas 1998]. To mitigate the effect of particle degeneracy and sample impoverishment, various variants of particle filter algorithm have been proposed. These variants or methods in general are classified into the following categories

- Choice of Proposal Distribution

In this method choosing an optimal importance density involves maximizing the effective sample size $\widehat{N}_{eff}$. In turn the optimal density function minimizes the variance of the weight $\overline{w}_k^{(i)}$ [Doucet 2000]. But evaluating optimal important density involves multi-dimensional integral which is not tractable in real time application.

- Local Linearization

In this method the optimal importance density can be approximated by incorporating the current measurement through a bank of standard non-linear filters [Doucet 2000, Merwe 2000]. This technique performs better than SIR filters.

- Regularization

Regularization is a technique to mitigate the sample impoverishment. A modified PF algorithm in which resampling process is performed based on kernel-based density estimation can be potential solution to mitigate the effect of the sample impoverish [Carlin 1992].

- Markov Chain Monte Carlo (MCMC)

This method is relatively a simple way to generate the samples from any probability distribution. It is also potential solution for sample impoverishment in resampling step as well as regularization scheme [Freitas 1999].

- Rao-Blackwellization

Some models for characterizing a system may have linear dynamic and can be estimated using a conventional Kalman filter. The combination of Kalman filter with particle filter will reduce the number of particles needed to obtain a given level of performance and also reduce the variance of Monto Carlo (MC) estimate [Nordlund 2002]. Specific description of above methods is discussed in the following sections

3.6.3 Local Linearization Particle Filter

The sample degeneracy of SIS algorithm is due to the increase in variance of the importance weight over a time. To reduce the sample degeneracy, the optimal importance density can be approximated by incorporating the most current measurement through a bank of the standard non-linear filter such as Extended Kalman filter (EKF) or unscented Kalman filter [Doucet 2000, Merwe 2000]. The importance of the process is to ensure that neither the likelihood of the sample lies in one of the tails of the prior distribution nor it is too much narrow due to small measurement. The Figure 3.5 illustrates how to incorporate the current observation into the proposal distribution and move the samples to the regions of high likelihood.

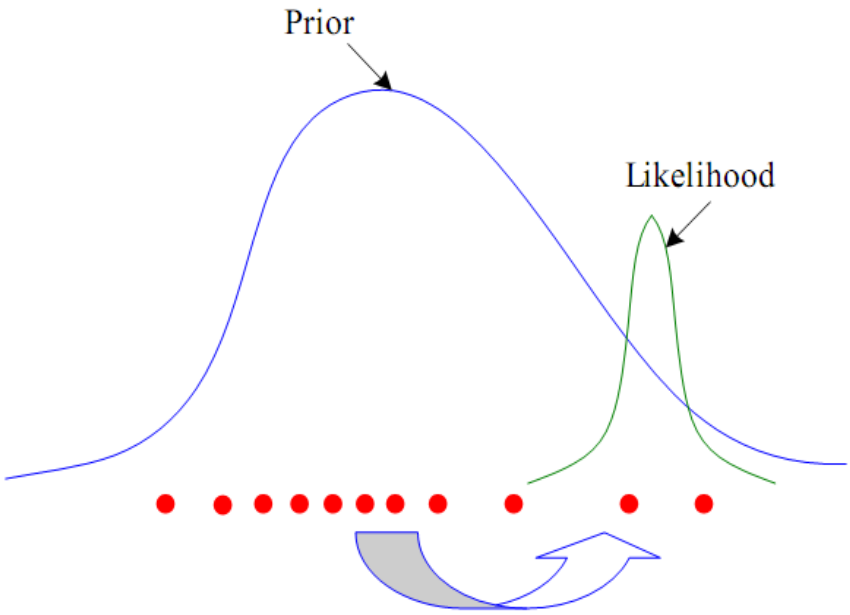

Figure 3.5: Concept for moving samples to regions of high likelihood

The underlying principle of the concept illustrated in Figure 3.5 is to use a separate non-linear filter like, EKF (i), where individual particle index i in order to generate and propagate a Gaussian importance distribution

$$q\left(\mathrm{x}_k^{(i)} \mid \mathrm{x}_{k-1}^{(i)}, \mathrm{y}_k\right) = N\left(\hat{\mathrm{x}}_k^{(i)}, \hat{\mathrm{P}}_k^{(i)}\right) \tag{3.80}$$

Where $\hat{\mathrm{x}}_k^{(i)}$, and $\hat{\mathrm{P}}_k^{(i)}$ are estimates of the mean and covariance computed from EKF (i) at time k using measurement y_k. The proposed particle filter is generally referred to as the Local Linearization Particle Filter (LLPF) and is also called the Extended Kalman Particle Filter (EKPF) [Doucet 2000].

The local linearization method for approximation of the importance density propagates the particles towards the likelihood function, and subsequently the LLPF performs better than the SIR filter. The additional computational burden of using such an importance density is often offset by reduction in the required number of samples to achieve a level of performance. The Table 3.5 summarizes the generic algorithm of the LLPF. In this thesis, the available general framework of EKPF is invoked to derive the state estimation for MIMO–HF channel with non-linear characteristics as well as Gaussian and non-Gaussian noise distribution.

Table 3.5 Local Linearization Particle Filter (LLPF)

- **Initialization:** at time $k = 0$

  1. For $i = 1, \cdots, N$, sampling from the prior $\mathrm{x}_0^{(i)} \sim p(\mathrm{x}_0)$
  2. For each $i = 1, \cdots, N$, Calculate the weight $w_0^{(i)} = p\left(\mathrm{y}_0 \mid \mathrm{x}_0^{(i)}\right)$ and normalize $\overline{w}_0^{(i)} = \dfrac{w_0^{(i)}}{\sum_{j=1}^{N} w_0^{(j)}}$

- **Prediction and Update**: For each time $k \geq 1$

  1. For $i = 1, \cdots, N$, run { EKF}

  $$\left[\hat{\mathrm{x}}_{k-1}^{(i)}, \hat{\mathrm{P}}_{k-1}^{(i)}\right] = EKF\left(\hat{\mathrm{x}}_{k-1}^{(i)}, \hat{\mathrm{P}}_{k-1}^{(i)}\right)$$

  2. For $i = 1, \cdots, N$, draw a sample from importance density

  $\mathrm{x}_k^{(i)} \sim N\left(\mathrm{x}_k^{(i)}; \hat{\mathrm{x}}_k^{(i)}, \hat{\mathrm{P}}_k^{(i)}\right)$

  3. For each $i = 1, \cdots, N$, calculate $w_k^{(i)} = p\left(\mathrm{y}_k \mid \mathrm{x}_k^{(i)}\right)\overline{w}_{k-1}^{(i)}$ and normalize the importance weights $\overline{w}_k^{(i)} = \dfrac{w_k^{(i)}}{\sum_{j=1}^{N} w_k^{(j)}}$

  4. If resampling $\left(N_{eff} < N_{th}\right)$ then, set the weights $\overline{w}_{k-1}^{(i)} = 1/N$ and resample with $\left\{\mathrm{x}_k^{(i)}, \overline{w}_k^{(i)}\right\}$

- **Output**: the set of samples used to approximate the posterior distribution

  1. $\hat{p}\left(\mathrm{x}_k \mid \mathrm{Y}_k\right) = \sum_{i=1}^{N} \overline{w}_k^{(i)} \delta\left(\mathrm{x}_k - \mathrm{x}_k^{(i)}\right)$
  2. $\hat{\mathrm{x}}_k = \sum_{i=1}^{N} \overline{w}_k^{(i)} \mathrm{x}_k^{(i)}$
  3. $\hat{\mathrm{P}}_k = \sum_{i=1}^{N} \overline{w}_k^{(i)} \left(\hat{\mathrm{x}}_k - \mathrm{x}_k^{(i)}\right)\left(\hat{\mathrm{x}}_k - \mathrm{x}_k^{(i)}\right)^T$

3.7 Extended Kalman Particle Filter

In this method the proposal distribution is approximated to the optimal importance distribution by incorporating the most current measurement y_k through a bank of EKPF [Merwe 2000]. This method relies on the first order Taylor series expansion of the likelihood and transition distribution as well as a Gaussian assumption on all the random variables. EKF approximates the optimal mean square error estimator of the system state by calculating the conditional mean of the state for all the given observations. EKF is a recursive method of propagating the Gaussian approximation of the posterior distribution through time and combining it at each time step with the new observation. The Table 3.6 summarizes the generic algorithm of the EKPF.

Table 3.6 Extended Kalman Particle Filter (EKPF) Algorithm

- **Initialization:** at time $k = 0$

  1. For $i = 1, \cdots, N$, sampling from the prior $\mathrm{x}_0^{(i)} \sim p(\mathrm{x}_0)$
  2. For each $i = 1, \cdots, N$, Calculate the weight $w_0^{(i)} = p\left(\mathrm{y}_0 \mid \mathrm{x}_0^{(i)}\right)$ and normalize

$$\overline{w}_0^{(i)} = \frac{w_0^{(i)}}{\sum_{j=1}^{N} w_0^{(j)}}$$

- **Prediction and Update**: For each time $k \geq 1$

  1. For $i = 1, \cdots, N$, update the particles with the EKF

$$\hat{\mathrm{x}}_{k|k-1}^{(i)} = \mathrm{f}\left(\mathrm{x}_{k-1}^{(i)}\right)$$

$$\mathrm{P}_{k|k-1}^{(i)} = \mathrm{F}_k^{(i)} \mathrm{P}_{k-1}^{(i)} \left(\mathrm{F}_k^{(i)}\right)^T + \mathrm{Q}_k$$

$$K_{k|}^{(i)} = \mathrm{P}_{k|k-1}^{(i)} \left(\mathrm{H}_k^{(i)}\right)^T \left[\mathrm{H}_k^{(i)} \mathrm{P}_{k|k-1}^{(i)} \left(\mathrm{H}_k^{(i)}\right)^T + \mathrm{R}_k \right]^{-1}$$

$$\hat{\mathrm{x}}_k^{(i)} = \hat{\mathrm{x}}_{k|k-1}^{(i)} + K_{k|}^{(i)} \left(\mathrm{y}_k - \mathrm{h}\left(\hat{\mathrm{x}}_{k|k-1}^{(i)}\right)\right)$$

$$\mathrm{P}_{k|}^{(i)} = \mathrm{P}_{k|k-1}^{(i)} - K_{k|}^{(i)} \mathrm{H}_k^{(i)} \mathrm{P}_{k|k-1}^{(i)}$$

  2. For $i = 1, \cdots, N$, draw a sample from importance density

$$\mathrm{x}_k^{(i)} \sim N\left(\mathrm{x}_k^{(i)}; \hat{\mathrm{x}}_k^{(i)}, \hat{\mathrm{P}}_k^{(i)}\right)$$

3. For each $i = 1, \cdots, N$, calculate $w_k^{(i)} = p\left(\mathrm{y}_k \mid \mathrm{x}_k^{(i)}\right)\overline{w}_{k-1}^{(i)}$ and normalize the importance weights $\overline{w}_k^{(i)} = \dfrac{w_k^{(i)}}{\sum_{j=1}^{N} w_k^{(j)}}$

4. If resampling $\left(N_{eff} < N_{th}\right)$ then, set the weights $\overline{w}_{k-1}^{(i)} = 1/N$ and resample with $\left\{\mathrm{x}_k^{(i)}, \overline{w}_k^{(i)}\right\}$

- **Output**: the set of samples used to approximate the posterior distribution

1. $\hat{p}\left(\mathrm{x}_k \mid \mathrm{Y}_k\right) = \sum_{i=1}^{N} \overline{w}_k^{(i)} \delta\left(\mathrm{x}_k - \mathrm{x}_k^{(i)}\right)$

2. $\hat{\mathrm{x}}_k = E\left(\mathrm{x}_k \mid \mathrm{Y}_k\right) \approx \sum_{i=1}^{N} \overline{w}_k^{(i)} \mathrm{x}_k^{(i)}$

3.8 Conclusion

HF channel characterization is a non-linear stochastic process associated with frequency non-selective dispersive feature. This chapter is intended as a framework for chapter 5 that deals with HF channel estimation. A framework for formulating the mathematical equation to analyse non-linear state model and estimate the parameter/state of the non-linear stochastic process has been highlighted in this chapter.

Recursive Bayesian (RB) techniques which as considered as the best method to address the optimal non-linear filtering have been discussed. Novelty of RB lies in estimating the PDF of the state vector which describes characteristic of non-linear system based on available measurement. Though RB is optimal solution for non-linear filtering application, it involves the evaluation of the integrals of higher dimensions. Due to this complexity, an alternative approximated optimal solution is considered for practical application. Various approximated techniques have been discussed in this chapter. EKF, which is an example of analytical approximation techniques, has been formulated and discussed to address non-linear filtering. More recently much attention is being placed on new class of non-linear/non-Gaussian filtering methods based on Sequential Monte Carlo (SMC) approach. The SMC is based on simulation method that uses the Monte Carlo

simulation in order to solve on-line estimation and prediction problems have been highlighted. The concepts of SMC and resampling techniques which form the basis for invoking the Particle filtering to address non-linear and non-Gaussian class of filtering have been discussed in depth. Various aspects, such as the effect of particle degeneracy and sample impoverishment are addressed in this chapter. This chapter also highlights the significance of a combination of local linearization particle filter (sample impoverishment technique) and EKF in mitigating the effects of particle degeneracy. The mathematical formulation presented in this chapter will be of specific relevance for the performance analysis of HF channel estimation under non-linear and non-Gaussian noise dealt in chapter 5.

CHAPTER 4

ANALYTICAL MODELLING AND SIMULATION OF MIMO-HF CHANNEL

HF sky-wave is the medium of transmission in ionosphere through which long haul transmission is achieved with a low cost infrastructure. The refraction of HF waves in the ionized medium combined with ground reflection is responsible for propagation of signal over greater distances. In this process of propagation, the HF communication system exhibits low Signal to Noise Ratio (SNR), subjected to slow fading at mid-latitudes and fast fading at high and equatorial latitudes. Initially very low data rate approximately 75 bps was available for HF user. Gradually the data rates have increased significantly to 9.6 kpbs and beyond in a 3 kHz channel bandwidth due to advent of low cost digital signal processing. However, major limitation factor in the design of high data rate digital communication system for HF channel is coherence bandwidth which is typically estimated to be few kilohertz. Using wider channel bandwidth there is a considerable increase in data rate up to 64 kpbs [Cannon 2002] [Ndao 2011]. However, with reliability also a factor, the achievable data rate turns around 16kpbs. The performance parameters of HF channel discussed above are not competitive with pertinent system applications operating in VHF/UHF and higher band communication. A first realization of the HF system based on multiple antenna technology was by [Perrine 2005]. It was based on Single Input Multiple Output (SIMO) realizing a data rate of 30 kpbs in 9 kHz bandwidth. The developed HF system was tested over a 800 km link involving a four-channel receiving system. Later [Ndao 2011] simulated to demonstrate transmission of higher data rate of 80 kbps in a 9 kHz bandwidth and [Ndao 2013] demonstrated date rate 24.09 kbps in a 4.2 kHz bandwidth based on MIMO technology with polarization diversity.

The performance of sky-wave HF communication systems is dependent on its waveform design that is supposed to compensate propagation channel distortion effects such as path loss, multipath fading and Doppler effects. From HF environment perspective, channel is characterized as multipath time-varying environment that produces both time and frequency dispersion. The source of multipath is the reflections of signals from different

layers in the ionosphere which lead to multi-hop propagation. Hence the received signal contains several echoes or modes separated in time by few milliseconds (time/delay spread). The source of frequency (Doppler) shift and frequency spread is the fading encountered by each mode is due to the inherent nature of the ionospheric reflection. In general, BER, throughput and link reliability are some of performance metrics to evaluate a HF system. To validate the system performance, HF channel model or simulator is required to meet the compliance specific to the existing standards. Hence HF channel model /simulator is required to assess the performance metrics of the system. In view of the above mentioned complexities, ionospheric (HF) channel poses considerable challenge to the designers of new digital ionospheric radio systems. Their eventual success critically hinges on a good understanding of the radio-channel multipath and Doppler characteristics. Therefore modelling, measurement and characterization of the HF channel analyse its multipath and Doppler characteristics constitute a research initiative for the development of digital ionospheric communication systems.

Common methods used to evaluate the performance of HF communication system are based on theoretical analyses and experiential measurements. The available HF models [Proakis 1989, Rappaport 1996] derived through the theoretical analysis are not amenable from practical perspective. A primitive model for HF channel analysis consists of a single path with no fading or slow Rayleigh fading with relatively more emphasis on incorporating the time-spread (multipath) distortion and/or frequency-spread (fading) distortion. Although the above model is simplistic, it is surely not a realistic one since ionosphere exhibits non-stationary (time variant) features. The ionospheric environment to which an experimental measurement is subjected will not conform to the above simplistic model. The analysis of stationary ionosphere performed over various snap shots of time durations can still be helpful in arriving at the possible bounds for the variation of channel parameters. This calls for the development a HF channel simulator. The cumulative performance analysis of a stationary HF channel carried over considerable time duration through such a simulator has a reasonably good potential to closely approximate even a non-stationary HF channel. This chapter is aimed at the

development of a mathematical HF channel model applicable to both SISO and MIMO systems to analyse the practical scenario.

4.1 HF SISO Channel Model

The characteristic of HF signal varies as it propagates from the transmit antenna to the receive antenna. The characteristics depend upon the distance between the two antennas, the path(s) of the signal (refraction from the ionosphere layers), environment (building and other objections) around the path, mobility of Tx, mobility of Rx, and also mobility of channel as well as the climatic changes (summer/rain). Further the refractive and absorptive characteristics of the ionospheric layers depend strongly on radio frequency, latitude, and time of day, season, and the solar activity. Thus the profile of received signal can be obtained from that of transmitted signal if the model of transmission medium is available. This model of medium is referred as channel model. Further, the power profile of the received signal can be obtained by convolving the power profile of transmitted signal with impulse response of the given channel as follows.

$$y(t) = h(t) * x(t) + n(t) \tag{4.1}$$

Where,

$y(t)$ is received signal

$x(t)$ is transmitted signal

$h(t)$ is time varying impulse response of the channel

$n(t)$ is noise

t is variation in time.

The frequency response of Equation (4.1) is given as,

$$Y(f) = H(f).X(f) + N(f) \tag{4.2}$$

Where,

H(f) is channel response in frequency

X(f) is the frequency response of transmit signal

N(f) is the frequency response of Noise

Y(f) is frequency response of received signal.

The basic components required to characterize the channel model are path loss, shadowing, and multipath. The first two components are referred as large scale

propagation where as multipath is small scale propagation. The scope of this thesis is to deal with small scale propagation (multipath fading) [Sklar 1997a, b].

- ***Path loss*** *means reduction in power density of propagating signal. The difference between Tx power and Rx power is referred as path or transmission loss.*

HF signal propagated over ionospheric paths undergo energy losses before arriving at the receiver. Larger part of these energy losses is due to absorption in both the ionosphere and lower atmospheric levels. The two other types of losses which also significantly affect the ionospheric propagation of radio waves are ground reflection loss and free space loss.

Ground Reflection Loss

When propagation is accomplished via multihop refraction, RF energy is lost each time the radio wave is reflected from the Earth's surface. The amount of energy loss depends on the frequency of the wave, the angle of incidence, ground irregularities, and the electrical conductivity at the point of reflection.

Free space Loss

Normally, the major loss of energy is because of the spreading out (divergence) of the wavefront as it travels away from the transmitter. As the distance increases, the area of the wavefront spreads out, much like the beam of a flashlight. This means the amount of energy contained within any unit of area on the wavefront will decrease as distance increases. By the time the energy arrives at the receiving antenna, the wavefront is so widely spread, that only a very small fraction of the wavefront is incident on the receiving antenna.

The free space loss is given by

$$L_0(dB) = 32.4 + 20\log_{10} f_{MHz} + 20\log_{10} d_{km} \qquad (4.3)$$

where, L_0 is the free-space path loss, measured in decibels, f_{MHz} operating frequency in MHz and d_{km} is distance of separation between the transmitter and receiver in km.

The combined effects of absorption, ground reflection loss, and free space loss account for most of the energy losses of radio transmissions propagated by the ionosphere.

The thick dotted line in Figure 4.1 shows the received power as a function of the distance from the transmitter.

- ***Shadowing*** *quantifies the loss of transmitted signal*

When a radio wave encounters an obstacle, its wave is reflected /scattered or absorbed, causing a shadow beyond the obstacle. However, some waves does enter the shadow area because of diffraction. This effect is referred as shadowing. Diffraction is the ability of radio waves to propagate around sharp corners and bends around obstacles. For a given diameter of obstruction, the effect of diffraction is more pronounced for a radio wave with smaller wavelength and hence a larger attenuation of the received signal.

The dotted line in Figure 4.1 shows the received power as a function of the distance from the transmitter which includes both path loss and shadowing effects.

- ***Multipath fading***

Of many adverse effects of ionospheric propagation, elimination of signal fading is one of the most difficult task due to its unpredictable nature. Fading is the fluctuation of the signal amplitude. It is caused by several ionospheric phenomena such as ionic movements, rotation of the axes of the polarization ellipses and ionospheric absorption. It is difficult to obtain a signal of constant amplitude, and at times the signal will "fade out" when the amplitude of the incoming signal drops below the minimum detection level of the receiver. The variations in amplitude and phase of the received signal are called the multipath fading.

The types of fading can be broadly classified into the categories of multipath fading and single-path fading. In the extreme case of heavily disturbed ionospheric conditions, fading due to scintillation will occur and this can be regarded as an extreme case of multipath fading. Fading is a frequency selective phenomenon. The ionic movements in ionosphere which cause the fading induce relatively greater phase shift at a higher

frequency than at a lower frequency [Davies 1965].The relatively larger phase shift leads to faster fading.

Multipath fading occurs when there is more than one path for the signal to traverse between the transmitter and the receiver. Mostly it occurs when the Line of Sight (LoS) path is not available. Multiple paths also referred to as modes, can be generated within the ionospheric propagation channel by a combination of reflections at different layers of the ionosphere and multi-hop. Scattering of the signal by ionospheric irregularities can also contribute to multipath fading. Due to the differences in length of the different paths, the waves arriving at the receiver will have different phases. The differing phase amongst the multipath can lead to either constructive or destructive interference. Large scale irregularities within the ionosphere, such as a travelling ionospheric disturbance, have a behaviour that is time dependent, and therefore the interference behaviour varies with time. As a result, the total signal at the receiver, which is obtained by super-imposition of the signals from the different paths, displays the characteristic of fading over time.

The three components of the channel response are highlighted in Figure 4.1. The thick dashed line represents the path loss. The lognormal shadowing change of the total loss is shown by the thin dashed line. Finally the multipath results in variations shown by the solid thick line. The variation in received signal due to multipath is a function of the frequency.

The following terms are used to characterize the multipath fading.

- **Delay spread**

The maximum delay after which the power profile of the received signal at the receiver becomes negligible is referred as maximum *delay spread* τ_{max}. A large τ_{max} indicates a highly dispersive channel. For HF channel the delay spread values varies from 1ms to 5 ms.

- **Coherence time**

If the transmitter, receiver, or even the other objects in the channel dynamic, the channel characteristics change. The time period for which the channel characteristics can be assumed to be constant even though Tx, Rx and channel environment vary is referred as coherence time $(\Delta t)_c$. Measurement of coherence time is based on auto-correlation function. The value of coherence time for HF channel varies from 1 to 10 sec.

- **Coherence bandwidth**

For every channel parameter in the time domain, there is a corresponding (analogous) parameter in the frequency domain. The Fourier transform of the delay spread shows the frequency dependence of the channel characteristics. The frequency bandwidth over which the channel characteristics remain same is called coherence band-width. This also can be obtained based on autocorrelation function of delay spread. The coherence bandwidth is inversely related to the delay spread. The larger the delay spread means less is the coherence bandwidth and the channel is said to become more frequency selective.

- **Doppler spread**

The delay spread profile gives the statistical power distribution of the channel over time for a signal transmitted at a particular instant. Similarly, Doppler power spectrum gives the statistical power distribution of the channel for a signal transmitted at a particular frequency f. While the delay spread profile is caused by multipath whereas the Doppler spectrum/spread is caused by motion of the intermediate objects in the channel.

The Doppler power spectrum is nonzero for $(f - f_D, f + f_D)$,

Where,

f_D is the maximum Doppler spread.

The coherence time is the reciprocal of Doppler spread,

Coherence Time $\approx$ 1/Doppler Spread

Thus, if the transmitter, receiver, or the intermediate objects shift very fast, it implies the Doppler spread is large and the coherence time is small implying that the channel changes fast. This effect is referred as fast fading.

The relationship of all the channel parameter discussed above is illustrated in Figure 4.2. The subsequent section describes the characterization and modelling of HF channel based on above multipath parameter discussed.

Figure 4.1: Path loss, shadowing, and Multipath [Rappaport 1996]

Figure 4.2 : Relationships among the channel correlation functions and power density functions [Sklar 1997a]

4.1.1 HF Channel Characterization and Modelling

Ionosphere is an anisotropic, inhomogeneous, temporally and spatially dispersive, random time-varying channel which is non-stationary both in time and frequency. Ionospheric HF channel is typically characterized by multipath propagation and fading. Due to the anisotropic nature, electromagnetic wave entering into ionosphere region splits into two modes referred as ordinary and extraordinary. These two modes are orthogonal to each other and they recombine at the exit of the ionosphere. The signals from the transmitter propagate through these modes or paths to the receiver via single/multiple reflections from the E and F layers of the ionosphere. Since the transmission times over these paths or modes are different for different transmitted signals, the signal at the receivers may consist of several multipath components spread in time over an interval of several milliseconds resulting in variation of amplitude, phase and polarization of the signal received. The variation in height of ionospheric layers may increase or decrease with time and thereby contributing to different frequency (Doppler) shifts on each of the multipath components. The turbulence nature of ionosphere causes each component to exhibit differing Doppler spread (fading) and a resultant fading of the composite received signal. The cumulative effect of above may produce multiplicative signal distortion both in time and frequency [ITU-R 2000, Watterson 1970].

Figure 4.3 shows an example of power spectra of multipath component of received signal transmitted over the HF channel associated with four paths. The four paths in Figure 4.3 refer to one –hop E mode (1E), one-hop F mode (1F), two-hop F mode (2F), and a mixed mode (e.g. 1E ~ 1F). While two magneto-ionic (joint effect of atmospheric ionization and the earth's magnetic field upon the propagation of electromagnetic waves) components labelled as ‘a’ and ‘b’ in the 1E mode have the same frequency spreads, their frequency shifts are different and resolvable. For the other three modes, both the spreads and shifts of the magneto-ionic components are essentially the same and they appear as single entity. Hence the simulator designed to characterize the HF channel in terms of short-multiplicative distortion (short term fading) would consider the parameters such as the signal losses, time-spread and frequency spread. Moreover these parameters are

subjected to daily and seasonal changes. Geographical location also has the impact on these parameters.

Figure 4.3: Power spectra of multipath component over ionospheric channel [ITU-R 2000]

For modelling the HF channel, it is necessary to characterize the statistical behaviour of ionospheric channel by investigating the joint statistics of transmitted and received band-limited signal. Modelling should also incorporate the parameters of ionospheric channel such as coherence channel bandwidth, Doppler and multipath spread of signals. In order to model the HF channel, the correlation and covariance functions of linear time varying channel impulse response will be exploited to represent the near practical HF channel. The modelling of the channel is achieved through characterizing filter impulse response to meet requirement of the HF channel response by incorporating the multipath fading parameters based on certain assumptions for practical implementation. Either FIR or IIR filter can be used to characterize the HF channel.

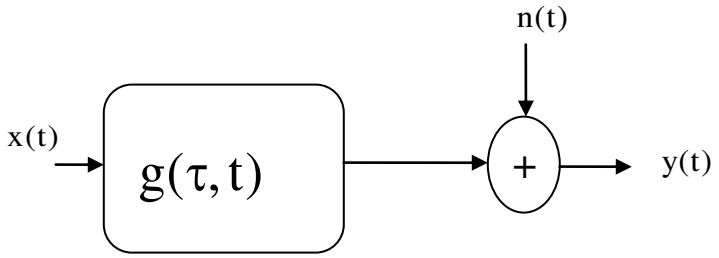

Figure 4.4: Generic model for multipath fading channel

Figure 4.4 shows the generic model of multipath channel. Where signal $x(t)$ is transmitted over a multipath channel. For discrete multipath propagation, the equivalent base-band channel response $g(\tau, t)$ can be defined as a function of two variables τ and *t*. The variable τ is considered to represent the effect of the channel delay and t represents the time instant. The received signal $y(t)$ is represented as

$$y(t) = \sum_{i=1}^{n} g(\tau_i, t)x(t - \tau_i) + n(t) \quad (4.4)$$

where,

$n(t)$is noise.

Due to the random nature of $g(\tau,t)$, the channel effects can be characterized by four important factors: the multipath delay spread, T_m, the coherence time, Δt_c, the coherence bandwidth, Δf_c, and finally the Doppler spread, β_d. The distortion of the signal *x(t)* transmitted through the HF channel can be correlated with the given information about these factors.

The detail discussion of characterisation of channel response $g(\tau, t)$ in term of tap-gain function is presented in Appendix I.

The Figure 4.5 shows the generation of tap-gain functions. The each tap –gain function is generated by passing White Gaussian Noise (WGN) through a filter (FIR or IIR) whose spectrum response (Gaussian shape) that replicates the impulse response of the HF channel. The cut-off frequency of the filter corresponds to the delay shift (Doppler shift). The separation of tap represents the delay spread of the channel.

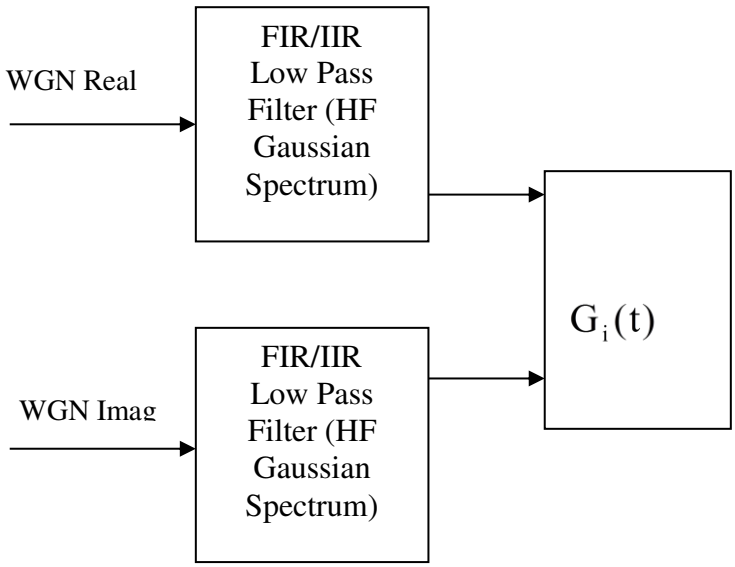

Figure 4. 5: Generation of tap–gain function

4.1.2 Implementation of Tap-Gain Function

The generation of tap-gain function can be achieved based on white noise filtering method. This method can generally be realized either by FIR or IIR Filter. The guaranteed accuracy and computational efficiency of channel characterization based White Noise Filtering method also depends on whether it involves FIR or IIR. FIR approximation of a channel model often requires a large number tap coefficients, and the order of the filter increases with the increased sampling frequency (bandwidth) of signal. It is well known that IIR filters can capture the system dynamics with fewer parameters (tap coefficients and order of filter) as compared with FIR filters [Radenkovic 2003]. In [Delmas 2000], it is discussed that realistic radio channels often exhibit long tails of weak leading and trailing terms in its impulse response. In the case of FIR filters, this leads to channel under-modelling effects and degradation of modelling performance. IIR or AutoRegressive (AR) channel representation can reduce the effect of modelling errors. In the reported literature on HF channel characterization, the channel modelling invoked FIR concept [Wheatley 2000]. To overcome the above referred under- modelling effects, in this thesis IIR is used in modelling the HF channel.

Practically narrowband filter is used to characterize the Doppler spectrum of the channel modelling with a very sharp roll off and infinite attenuation in stop-band region. To

realize this specification of narrowband filter, it is impractical to have a FIR filter even with large number of taps. But for same specification, IIR filter would need lesser number of taps and is has an advantage of ease of implementation. It requires fewer hardware resources in term of silicon space, storage and computation time compared to a FIR filter. Feedback structure of All-pole or Auto-Regressive (AR) or IIR filter allows steeper Doppler frequency roll offs and retains smooth flat magnitude response with minimum order compared to a FIR filter [Komninakis 2003, Baddour 2005]. Analytic response of channel modelling using AR filter has better approximation for wide range of Doppler Spectrum with minimum order of filter and hardware resources [Baddour 2005]. IIR configuration has relative advantage of smaller chip area and lower power consumption compared to that of FIR. This is attributed to the sufficiency of lower order of IIR configuration to retain the optimal accuracy and therefore has become a more preferred choice for hardware implementations of channel simulators [Malik 2009]. Initially application of the AR model was for Kalman based channel estimation technique to predict both short and long range dynamics of fading channel [Eyceoz 1998, Wu 2000]. Later AR model technique has been extended by [Wu 2000, Zhang 2000] to realize channel simulator. It is found that [Zhang 2000] and [Colman 1997] use low order AR process to realize the correlation statistics of channel. The realized accuracy of correlation statistics falls short to ensure the desired channel response. This can be attributed to the numerical instability of statistical parameters resulting in its failure to model statistical parameter of channel. This has restricted the scope of applicability of AR models. [Baddour 2005] has demonstrated the simple AR modelling structure with correlated narrowband Rayleigh variates as well as considering non-isotropic Rayleigh random process. [Baddour 2005] also addresses numerical stability problems of [Colman 1997, Zhang 2000] thereby enhancing the scope of applicability of AR models. HF channel does not exhibit an ideal Rayleigh fading. It approximates more closely to Gaussian random process. This thesis extends the research of [Baddour 2005] to consider HF channel exhibiting Gaussian distribution. The next section discusses the modelling of the tap-gain function based on AR model (IIR filtering approach) for Gaussian shape spectrum for HF channel has also been considered.

4.2 Autoregressive Modelling of Band-Limited Random Processes.

Auto-Regressive (AR) models are commonly used to approximate discrete-time random processes [Kay 1988]. This is due to the simplicity with which their parameters can be computed and due to their correlation matching property. A complex AR process of order p $(AR(p))$ can be generated via the time domain recursion

$$h[n] = -\sum_{k=1}^{P} a_k h[n-k] + w[n] \tag{4.5}$$

Where,

$w[n]$is a complex white Gaussian noise process with uncorrelated real and imaginary components has zero mean.

$h[n]$is the simulator output.

The AR model parameters consist of the filter coefficients $\{a_1, a_2, \ldots\ldots a_p\}$ and the variance σ_p^2 of the driving noise process $w[n]$. The corresponding Power Spectral Density (PSD) of the $\mathrm{AR}(p)$ process has the rational form [Baddour 2005]

$$S_{hh}(f) = \frac{\sigma_P^2}{\left|1+\sum_1^P a_k exp(-j2\pi fk)\right|^2} \tag{4.6}$$

Although the Doppler spectrum models proposed for radio communication are not rational, an arbitrary spectrum can be closely approximated by an AR model of sufficiently large order. The basic relationship between the desired model AutoCorrelation Function (ACF) $R_{hh}[k]$ and the $AR(p)$ parameters are given by [Kay 1988]

$$R_{hh}[k] = \begin{cases} -\sum_{m=1}^{P} a_m R_{hh}[k-m]\,, k \geq 1 \\ -\sum_{m=1}^{P} a_m R_{hh}[k-m] + \sigma_p^2\,, k = 0 \end{cases} \tag{4.7}$$

for $k = 1,2,\ldots\ldots\ldots, p$

In matrix form ,

$$R_{hh}a = -v \tag{4.8a}$$

Where

$$R_{hh} = \begin{bmatrix} R_{hh}[0] & R_{hh}[-1] & \dots & R_{hh}[-p+1] \\ R_{hh}[1] & R_{hh}[0] & \cdots & R_{hh}[-p+2] \\ \vdots & \vdots & \vdots & \vdots \\ R_{hh}[-p+1] & R_{hh}[-p+2] & \cdots & R_{hh}[0] \end{bmatrix}$$

$$a = [a_1, a_2, \dots \dots \dots a_p]^T$$

$$v = \left[R_{hh}[1]\, R_{hh}[2] \dots \dots \dots . R_{hh}[p]\right]^T \tag{4.8b}$$

and

$$\sigma_p^2 = R_{hh}[0] + \sum_{k=1}^{p} a_k\, R_{hh}[-k] \tag{4.9}$$

Given the desired ACF sequence, the AR filter coefficients can thus be determined by solving the set of p Yule–Walker equations in (4.8a). These equations can in principle be solved efficiently by the Levinson–Durbin recursion in O(p^2). Since R_{hh} is an autocorrelation matrix, it is positive semi-definite and can be shown to be singular only if the process is purely harmonic and consists of $p-1$ or fewer sinusoids [Haykin 1996]. In all other cases, the inverse R_{hh}^{-1} exists and the Yule–Walker equations are guaranteed to have the unique solution given as

$$a = -(R_{hh} + \varepsilon I)^{-1} v \tag{4.10}$$

Where,

a AR fading filter coefficients

I is a p × p identity matrix and

$\varepsilon \neq 0$ is a suitable diagonal matrix parameter that renders $(R_{hh} + \varepsilon I)$ non-singular and invertible.

The generated *AR(p)* process has the ACF [Kay 1988]

$$\widehat{R_{hh}}[k] = \begin{cases} R_{hh}[k], 0 \le k \le p \\ -\sum_{m=1}^{p} a_m \widehat{R_{hh}}\,[k-m],\ k > p \end{cases} \tag{4.11}$$

That is, the simulated process has the attractive property that its sampled ACF perfectly matches the desired sampled ACF up to lag p.

This section has addressed the generation of tap-gain function G of Figure 4.5 in term of 'a' AR filter coefficients. The next section considers HF noise.

4.3 HF Noise

To achieve reliable communication, the minimum signal level required (to operate above the noise) is a function of the ambient noise level. This is the usual constraint on all communication systems. Depending upon whether the channel is operating at frequencies which are lower or higher than the HF band (3-30 MHz), there will be a difference in the ambient noise source and level. At frequencies above the HF band, the ambient noise is generally a function of the receiver noise temperature or other noise associated with the receiver system. At frequencies in/lower than the HF band, communication is limited by external noise sources. This creates a severe problem for the HF communicator as the external noise sources, levels, and statistics, vary greatly depending on environment (rural Vs. urban), time of day, location of mid-path (latitude and longitude), and frequency of operation. Therefore, the HF channel models must include a provision for adding noise as appropriate and desired, to the signal when using the model for simulation. However, the noise sources are not included as an inherent feature of the in conventional channel model. The noise sources, such as Gaussian or impulsive, are external to the channel model. Due to the variation in external noise with respect to level, statistics, and frequency, the pre-programmed (determined) noise sources are added to the signal, independent of HF channel multipath fading. External noise sources which affect HF circuits may be classified into two general categories namely random and impulsive as shown in Table 4.1.

Table 4.1Classification of Noise in HF channel

Type	Atmospheric Sources	Equipment Sources
Random	▪ Distant Lighting ▪ Cosmic ▪ RF Interference	▪ Intrinsic Receiver Noise
Impulsive	▪ Local Lightning ▪ Man-Made ▪ RF Interference	▪ Power

In general, with currently available receiver [Mastrangelo 1997], the main noise contributors are atmospheric (in rural areas), and both atmospheric and manmade in urban areas. In these areas the main contributions are from lightning, both impulsive and random, and usually greatly exceed any cosmic or equipment thermal noise. The above noise can be modelled either as additive Gaussian or non-Gaussian noise model.

4.3.1 Gaussian Noise Model

The Gaussian distribution represents a cornerstone model in statistic and engineering. Apart from the mathematical simplicity of the model, the *central limit theorem* has given Gaussian distribution a privileged place through the history of statistics. This important theorem explains with just theoretical augments, the appearance of Gaussian statistics in real life. A simple formulation of it follows

Theorem 1 (Central Limit Theorem) *Let* $X_1, X_2, \ldots$ *be as sequence of i.i.d. random variables with zero mean and variance* σ^2. *Then, as* $N \to \infty$ *the normalized sum*

$$S_N = \frac{1}{\sqrt{N}} \sum_{i=1}^{N} X_i \tag{4.12}$$

converges almost to a zero- mean Gaussian variable with the same variance as X_i.

Conceptually, the central limit theorem explains the Gaussian nature of process generated from the superposition of many small and independent effects. This is the example case for the thermal noise, which are generated as the superposition of a large number of random independent interactions at the molecular level.

Intimately linked to the Gaussian model are the linear estimation methods. For example, given a set of i.i.d. Gaussian samples, it is a known fact that the optimal estimator of location is the sample mean. Traditionally, the central limit theorem has been a theoretical basis that favours the use of linear methods even in the conditions in which the non-Gaussian nature of the underlying process is evident.

The field of communications has not escaped to the "pervasiveness" of the Gaussian model. Although many significant processes found in communications are distinctly non-Gaussian, a large number of practical communication systems still exist with the "Gaussian (and liner)" assumption. A serious concern is that, in general, a system designed under the Gaussian assumption will show drastic performance degradations when the noise statistics depart to (even slightly) heavier-tailed (rapid decaying) models. This is well known for the linear estimators like the sample means, whose performance decreases from optimal in the Gaussian model, to significantly poor in the presence of impulsive contamination.

4.3.2 Non-Gaussian Models

The impulsive nature of the noise processes commonly found in wireless communication has been repeatedly noticed for more than 30 years. Non-Gaussian impulsive noise can arise in radio signals from any of a variety of impulsive sources (Local Lightning, Man-Made, RF Interference, and Power) as well as from certain instances of multipath propagation and multi-user. In order to model these processes, a wide variety of distributions with heavier-than-Gaussian tail (decay) have been proposed as viable alternatives to the Gaussian distribution. Mainly these models are based on distributions which, like the zero-mean Gaussian, are symmetric around zero. Usually, the usefulness of these models is determined by the trade-off between fidelity and complexity. On one hand, fidelity stands for more precise and efficient signal processing algorithms, while the complexity issue stands for simpler models from which more tractable (estimation) algorithms can be derived.

Although some practical processes might be better modelled by asymmetric distributions, this thesis concentrates only on symmetric models for following reasons.

(1) A large number of important noise and interference processes found in wireless communications are symmetric

(2) Asymmetric models may lead to a significant increase in the computational complexity of the associated signal processing

(3) Estimating the location of an asymmetric distribution requires either *a priori* information about the process or a subjective methodology to determine the "centre" of the distribution.

The most credited statistical- physical models for electromagnetic radio noise have been proposed by Middleton [Wang 2004]. Middleton proposed class A, B, and C models addressing cases where noise bandwidth is less or greater that the receiver bandwidth, or a linear combination of both, respectively. These models have direct physical interpretation and have been found to provide good fits to a variety of noise and interference measurements, including atmospheric noise. A simplified distribution commonly used in the modelling of impulsive noise is the *Gaussian mixture* or *contaminated Gaussian,* defined by an ε – contamination density function of the form

$$f(x) = (1 - \varepsilon)\, f_p(x) + \varepsilon\, f_c(x)\,, \tag{4.13}$$

Where both f_p and f_c are zero-mean Gaussian densities with variances σ_p^2 and σ_c^2 respectively. Gaussian mixture models have been popular in communications mainly because of their mathematical tractability and their ease of conceptual interpretation. The parameter ε can be interpreted as the amount of contamination allowed in the model. Since $f(x)$ is the sum of two Gaussian densities, it is easy to generate pseudo random Gaussian –mixture noise for computer simulation studies.

4.3.3 Non-linearity Distortion

Non-linear distortions in the transmitter produce inter-modulation components, some of which may fall in the frequency band of the signal. Such non-linear distortion components are similar to additive transmitter distortions. Like additive transmitter distortion, the non-linear components of the signals in (transmitter, channel and receiver) undergo the fading phenomenon. However the signal in the transmitter undergoes negligible fading as with an additive channel. The signal in the channel and the signal in the receiver undergo significant non-linear distortions like a multiplicative channel. If the non-linear distortions introduced by the transmitter module can be generated at a suitably low level relative to the input signal (say < -30 dB), which is usually the case, then distortion caused by the transmitter is unlikely to affect the system performance, and therefore, can be ignored.

The Bit-Error-Rate (BER) performance of a system with respect to receiver non-linear distortions depends not only on the amount of the non-linearity in the receiver but also on the type of multiplexing that is used. Frequency-multiplexed systems are far more susceptible to receiver non-linear distortions than single-pulse-train systems or concentrically multiplexed multiple-pulse-train systems [Watterson 1979]. In this thesis, the emphasis and interest are on non-linear distortion introduced by system. Figure 4.6 shows the system non-linearity with channel model. All physical devices have some degree of non-linearity and thus distort the signal transformation process. The elements of a linear equivalent circuit are derived from small variations about the DC operating point. Thus linearity of "small signal" means that the development is limited to the first order derivative. Likewise, a non-linear equivalent circuit can be defined by higher order derivatives.

System non-linearities are mainly due to Power Amplifiers (PA). PAs located at an access point of a downlink channel often operate close to saturation in order to achieve power efficiency. The models employed in the description of PAs are either static (memory less) or dynamic (models with memory). The non-linearity is due to power amplifier stage either transmitter or repeater. Some of non-linear models frequently used for simulation [Aseeri 2001, Jantunrn 2004]

$$r'(k) = tanh(r(k)) \tag{4.14a}$$

$$r'(k) = r(k) + 0.2r^2(k) - 0.1r^3(k) \tag{4.14b}$$

Equation (4.14a) corresponds to the non-linearity introduced due to saturation of amplifiers used in the transmission systems and Equation (4.14b) corresponds to the random non-linear distortion.

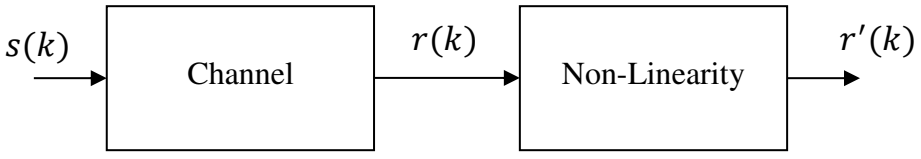

Figure 4.6: System non-linearity with channel model

4.4 AR Modelling for MIMO-HF Channel

In general, characterization and channel modelling, noise and non-linear distortion of SISO-HF channel discussed in the earlier sections of this chapter are applicable to MIMO channel. However, certain degree of signal correlation normally exists due to the multiple antennas at the transmitters and receivers. This correlation is a complicated function of the scattering environment and the antenna spacing [Kermoal 2002, Spirent 2011]. With a realistic assumption more de-correlated the signals between the antennas, the greater spectral advantage is obtained [Gunashekar 2007, Kermoal 2002]. The antenna spacing for MIMO is proportional to the wavelength (typically tens of meters at HF band) [Daniels 2013]. As a consequence, rich scattering environment such that the channel gains become independent and identically distributed (uncorrelated) is a distinct possibility. In such a scenario [Scheible 2014], each of the MIMO sub-channels can be described by the SISO characterization. A discussion on the AR modelling for characterization of MIMO-HF fading channel is presented in this section without spatial correlation effects. In subsequent section the spatial MIMO channel model is presented.

Figure 4.7 shows a typical MIMO communication system with M_t transmit antennas and N_r receiver antennas. The Space-Time (S-T) modem at the transmitter (Tx) encodes incoming bit stream using Alamouti's codes [Alamouti 1998]. The information bits are modulated and the signal is mapped across space and time (M_t transmit antennas). Thereafter, the S-T modem at the receiver (Rx) processes the received signal, which is subjected to time-varying HF fading channel. In addition, the received signal also experiences Inter Symbol Interference (ISI) under additive Gaussian / non-Gaussian noise. The received signal will be decoded on each of the N_r receiver antennas according to the transmitter's signaling strategy. The observed signal from i^{th} receiver at the discrete time index k is

$$r_k^i = \sum_{j=1}^{M_t} h_k^{i,j}(k,\tau)s_k^j + w_k^i, \quad i = 1, \ldots\ldots\ldots\ldots N_r \tag{4.15}$$

Where s_k^j is the transmitted symbol at the time index k,

τ is the delay variable

$h_k^{i,j}(k,\tau)$ is the channel impulse response between j^{th} transmitter and i^{th}

receiver of MIMO channel with correlated Rayleigh processes whose Doppler spectrum is characterized by Gaussian shape [Watterson 1970 and Mastrangelo 1997].

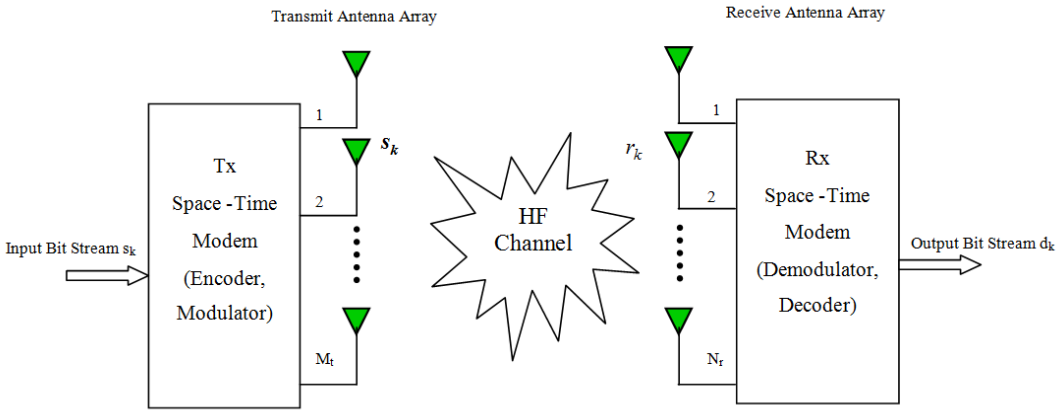

Figure 4.7: MIMO communication system

For simplicity $h_k^{i,j}(k,\tau)$ is written as $h_k^{i,j}$. For each time instance k, the (M_t x N_r) time-varying channel parameters have to be estimated with the following auto-correlation function

$$\left[R_h^{i,j}\right] = E\left[h_k^{i,j}\, h_l^{i,j^*}\right] = exp\left[2\left\{\pi f_d^{i,j} T(k-l)\right\}^2\right] \tag{4.16}$$

And normalized spectrum for each $h_k^{i,j}$ is given as

$$S_k(f) = \frac{1}{(2\pi)^{1/2} f_d^{i,j}} exp\left[-\frac{f^2}{2\left(f_d^{i,j}\right)^2}\right] \tag{4.17}$$

Where superscript * denotes the complex conjugate,

$f_d^{i,j}$ is the Doppler frequency shift for path between the j^{th} transmitter and i^{th} receiver,

T is the duration of each symbol.

In this thesis an Auto-Regressive (AR) modelling approach is considered for the generation of correlated Rayleigh processes whose Doppler spectrum is characterized by Gaussian shape [Watterson 1970, Mastrangelo 1997]. The analysis of [Baddour 2005] that treats the U shaped Doppler spectrum is extended to deal with the Gaussian shape of the Doppler spread of the HF channel. The implementation model for channel estimation $h_k^{i,j}$ can be approximated by following the AR process of order L:

$$h_k^{i,j} \approx \sum_{i=1}^{L} \alpha_{i,j,l} h_{k-l}^{i,j} + n_{i,j,k}\,, \tag{4.18}$$

Where $\alpha_{i,j,l}$ is l^{th} coefficient between j^{th} transmitter and i^{th} receiver and $n_{i,j,k}$ is zero-mean identical independent distribution (i.e.) complex Gaussian processes with variance given by

$$E\left[n_{i,j,k} n_{i,j,k}^{*}\right] = \sigma_{i,j,k}^2 \tag{4.19}$$

The procedure outlined in [Baddour 2005] has been adopted for the optimum selection of AR channel model parameters from correlation functions $R_h^{i,j}$. The additive noise (w_k^i Equation (4.15)) can be modeled either as a complex-Gaussian distribution $p(z) = N(z: 0, \sigma_w^2)$ with argument z, zero mean, and variance σ_1^2, or as the Middleton class-A noise model. This latter model has been used to model the impulsive noise commonly generated in wireless environment [Middleton 1977 and Wang 2004]. The probability density function of the noise model is given by

$$p(z) = (1-\epsilon)N(z: 0, \sigma_1^2) + \epsilon\, N(z: 0, \sigma_2^2) \tag{4.20}$$

Where $0 \leq \varepsilon \leq 1$. The first component $(1-\epsilon)N(z: 0, \sigma_1^2)$ represents the ambient background noise with probability $(1-\epsilon)$, while $\epsilon\, N(z: 0, \sigma_2^2)$ denotes the presence of an impulsive component occurring with probabilityε. In order to maintain a constant noise variance σ^2 for a particular SNR, the parameters ϵ, noise variance σ_1^2 and σ_2^2 are varied such that

$$\sigma_w^2 = (1-\epsilon)\sigma_1^2 + \epsilon\sigma_2^2 \tag{4.21}$$

Finally in Equation (4.21), if $\sigma_2^2 = 0$, then noise model reverts to the Gaussian distribution.

Equation (4.15) can be written in a matrix form for flat fading as

$$r_k = H_k s_k + w_k \tag{4.22}$$

Where r_k is the received matrix

H_k is the channel matrix

s_k is the transmitted symbol with time index k

w_k is the matrix with i.i.d. AWGN elements with variance σ_w^2.

An equal Doppler shift between transmitter and receiver's elements in MIMO system is assumed i.e. $f_d^{i,j} = f_d$.With these assumption matrix coefficients of the AR model of

Equation (4.18) can be replaced by scalar coefficients. The time-varying channel matrix can be described as

$$H_k = \alpha H_{k-1} + N_k \,, \tag{4.23}$$

Where N_k is a matrix with i.i.d. Gaussian noise elements with variance σ_n^2,

α is an AR coefficient modeled for HF fading channel.

Further, the Equations (4.22) and (4.23) can also be extended to frequency selective channel. In order to parameterize Equation (4.23), for time lag (τ), the autocorrelation of the channel fading process of Equation (4.16) is:

$$E\left[h_k h^*_{(k-\tau)}\right] = \exp(-2(\pi f_D \tau)^2)\, I, \tag{4.24}$$

Where, I is the identity matrix

τ is the time lag

f_D denotes the Doppler frequency (shift).

The Doppler shift is given by

$$f_D = \frac{v}{c}\, f_c \tag{4.25}$$

where, v is the vehicle speed or ionospheric variation

c is the speed of light

f_c is the carrier frequency

Substituting Equation (4.22) in Equation (4.23) for time lag $\tau = \{0, T_s\}$ yields

$$\alpha^2 + \sigma_n^2 = 1, \tau = 0 \tag{4.26}$$

$$\alpha = exp(-2\,(\pi f_D T_s)^2), \;\; \tau = T_s \tag{4.27}$$

where, $1/T_s$ is the sampling rate.

For example, if the normalized desired fading rate is $f_D T_s = 0.01$, then α = 0.998, and $\sigma_n^2 = 3.94\times10^{-3}$.

A final comment that illustrates the suitability of the channel model is in order. By projecting Equation (4.23) for τ time steps into the future, the expected value of a future channel state conditioned on the current value is given by

$$E\left[h_{(k+\tau)}|h_k\right] = \alpha^\tau h_k \tag{4.28}$$

For α value near unity, then $h_{(k+\tau)} \approx h_k$, i.e., the best guess about a future estimate is the current estimate. This is precisely what is assumed by sending periodic training codes over the wireless channel; once the channel has been estimated; it is assumed to remain

approximately constant until the next set of training data is sent. Significant changes over longer periods of time are expected. For $M_t = N_r = 1$, the MIMO configuration reduces to conventional SISO channel.

4.5 Spatial MIMO Channel Model

Modelling MIMO channel involves representation of a fading channel between transmitter and receiver array antennas with appropriate spatial correlation between elements of antenna arrays. Multiple antenna or MIMO system is usually expressed as an M_t x N_r combination, where M_t is the number of antennas at the transmitter, and N_r is the number of antennas at the receiver. The MIMO channel H which describes the transfer function (impulse response) between the receiver (Rx) and the transmitter (Tx) can be expressed as,

$$H = \begin{bmatrix} h_{11} & \dots & h_{1M} \\ \vdots & \ddots & \vdots \\ h_{N1} & \dots & h_{NM} \end{bmatrix} \tag{4.29}$$

Where, h_{NM} is the complex transmission coefficient from antenna at the M^{th} transmitter to N^{th} antenna at the receiver.

In a realistic fading environment, the signals at the transmitter and receiver antenna elements are correlated. Extensive measurements [Spirent 2011] have shown that the correlation is not constant, but varies significantly over a geographic area or mode of HF wave propagation. The correlation between antenna elements is a mathematical function related to the geometrical configuration of the local scattering and is a function of the Angular Spread (AS) of signal, Angle of Arrival (AoA), and the Direction of Travel (DoT).

It is assumed that all antenna elements in the two arrays have the same polarization and the same radiation pattern. The spatial complex correlation coefficient between antennas m_1 and m_2 at the transmitter (Tx) is given

$$\rho_{m_1,m_2}^{Tx} = \langle h_{m_1 n}, h_{m_2 n} \rangle \tag{4.30}$$

Where, $\langle a, b \rangle$ denotes the correlation coefficient between $'a'$ and $'b'$. From Equation (4.30), it is assumed that the spatial correlation coefficient of antennas at the Tx is independent of the antennas at the receiver. By the reciprocity theorem of antenna, the n elements at the Rx illuminate the same surrounding scatters and, therefore, also generate the same Power Azimuth Spectrum (PAS) at the Tx [Kermoal 2002]. The spatial complex correlation coefficient observed at the Rx is similarly defined in Equation (4.31) and assumed to be independent of m.

$$\rho_{n_1,n_2}^{Rx} = \langle h_{n_1 m}, h_{n_2 m} \rangle \tag{4.31}$$

Given Equations (4.30) and (4.31), one can define the following symmetrical complex correlation matrices at the transmitter and receiver of the MIMO system.

$$R_{Tx} = \begin{bmatrix} \rho_{11}^{Tx} & \cdots & \rho_{1M}^{Tx} \\ \vdots & \ddots & \vdots \\ \rho_{M1}^{Tx} & \cdots & \rho_{MM}^{Tx} \end{bmatrix}$$

$$R_{Rx} = \begin{bmatrix} \rho_{11}^{Rx} & \cdots & \rho_{1N}^{Rx} \\ \vdots & \ddots & \vdots \\ \rho_{N1}^{Rx} & \cdots & \rho_{NN}^{Rx} \end{bmatrix} \tag{4.32}$$

Spatial correlation matrix of the MIMO channel is the Kronecker product of the spatial correlation matrices at the Tx and the Rx and is defined as,

$$R = R_{Tx} \otimes R_{Rx} \tag{4.33}$$

Where, $\otimes$ represents the Kronecker product.

4.5.1 Generation of Correlated Channel Coefficients

Correlated channel coefficients h_{mn} are generated from zero-mean complex independent identically distributed (i.i.d.) random variables a_{mn} shaped by the desired Doppler spectrum such that

$$A = Ca \tag{4.34}$$

Where, $A_{NMx1} = [h_{11}, h_{12}, \ldots\ldots h_{1M}, h_{N1}, \ldots\ldots\ldots, h_{NM}]$ and $a_{NMx1} = [a_1, a_2, \ldots\ldots\ldots, a_{NM}]$. The symmetrical mapping matrix C results from the standard Cholesky factorization of the matrix $R = CC^T$ provided that C is non-singular.

The Kronecker product assumes that the individual cross terms are identical. This is not always a reasonable assumption. For instance, it assumes the correlation between receive antennas n_1 and n_2 measured at antenna m_1 is identical to the correlation measured at antenna m_2, and likewise, the correlation between transmit antennas $m_1$and m_2 measured at antenna m_2 is identical to the correlation measured at antenna n_2. For a 2x2 MIMO configuration, the Kronecker product is of the form:

$$E(h_{11}h_{12}^*) = E(h_{21}h_{22}^*)^* = \propto \quad (4.35a)$$

$$E(h_{11}h_{21}^*) = E(h_{12}h_{22}^*)^* = \beta \quad (4.35b)$$

For the purpose of simulation studies of this thesis, the above assumption is assumed to be valid. However, this assumption is not accurate for many conditions, including realistic antennas with pattern variations, branch imbalance between ports, and polarization effects. In these cases, a full correlation matrix with unique individual terms is required. Until recently, spatial correlation statistics of practical MIMO-HF antenna configurations were not available [Daniels 2013]. The values of α and β can be selected to represent different types of channels, and often real values in the range from 0-1 to capture the spatial correlation between the antenna arrays at the transmitter and the receiver of the MIMO system. One example set of values is shown in Table 4.2 [Spirent 2011].

Table 4.2 Correlation Scenarios

Low Correlation		Medium Correlation		High correlation	
α	β	α	β	α	B
0	0	0.3	0.9	0.9	0.9

.

4.6 Simulation Results and Analysis

The simulation results and analysis for characterizing the MIMO-HF channel based on the short term fading associated to HF channel is discussed in subsequent section. Modelling of tap-gain function to characterize channel parameter is implemented based on the AR structure. The comparison in generation of tap-gain function with FIR

structure, in terms of complexity and advantage is also highlighted in subsequent sub-sections.

4.6.1 HF Channel Characterization Simulation Result and Analysis

In this section, simulation results are presented for HF channel characterization. The following channel parameters have been considered to characterize the HF channel.

- Doppler Spread : 1 to 10Hz, shift in frequency 0 to ±2Hz.
- Multipath : 3 Path various 1 to 5ms, with two Magneto-ionic Component
- Sampling frequency : 300 Hz
- Tap-Gain generation : IIR compared with FIR
- Auto Regressive : Designed for Doppler spread having Gaussian spectrum required for HF channel.
- Channel noise : Gaussian and non-Gaussian
- Channel variation : Linear and system non-linearity.
- Antenna configuration : SISO and MIMO (2x2,4x4)

In discrete stationary channel model illustrated Figure A1.1 with three taps, $G_i(t)$ represents uncorrelated tap-gain function which is modelled for Doppler spread of Gaussian shape. The simulation results of auto-correlation for the corresponding tap-gain function of SISO channel is shown in Figures 4.8- 4.10. Equation (A1.12) has been invoked to simulate the tap-gain functions. In the simulation, the observation period of ACF was 5 sec. From the results shown in Figures 4.8- 4.10, it is noticed that the three multipath represented through the 3 tap-gain functions exhibit uncorrelated properties. From the Figures 4.8-4.10, it is observed that as observation time increases, the auto-correlation decreases and nearly approaches zero after an elapsed time. The difference in time corresponding to the peak value and a-prior set value (say 0.707 of the peak value) of ACF corresponds to the delay spread of the observation signal. The ACF for the composite channel response from the all the multipath is illustrated in Figure 4.11.

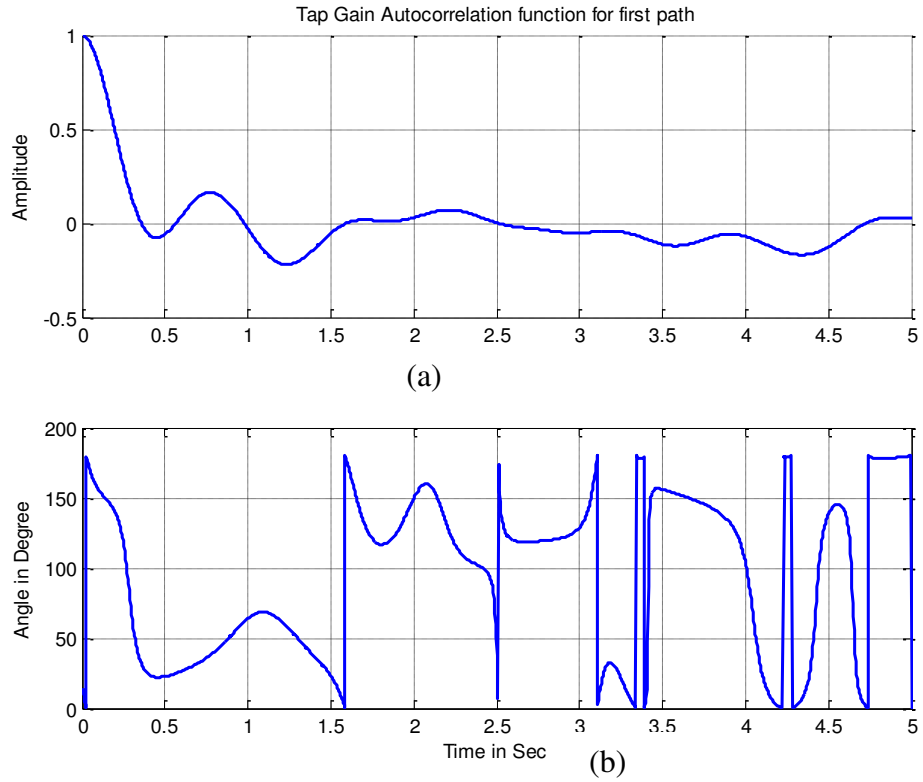

Figure 4.8: ACF for $G_1(t)$ (a) Amplitude (b) Phase

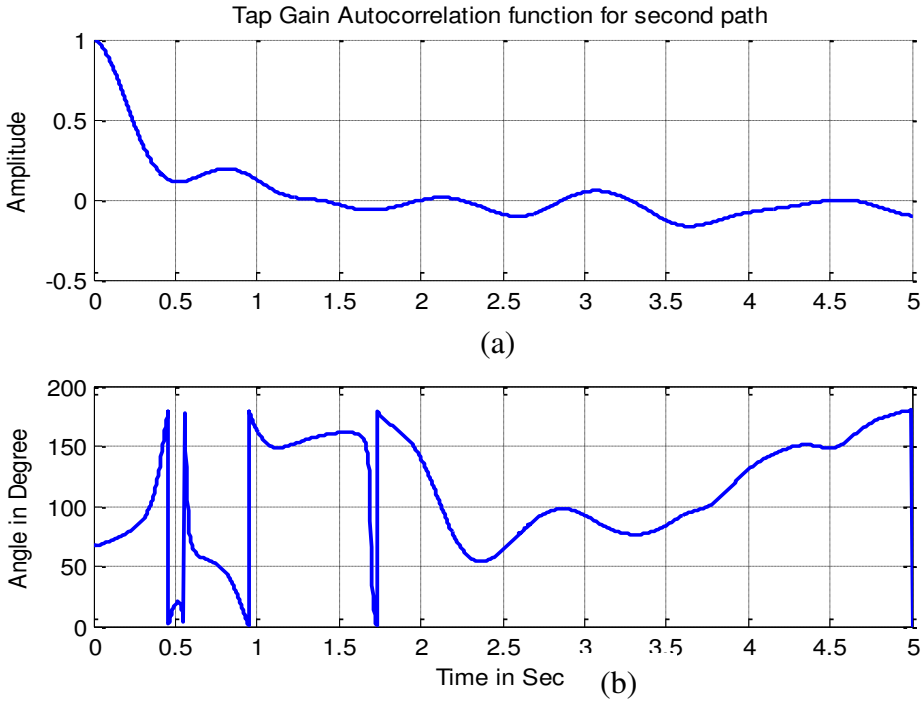

Figure 4.9: ACF for the $G_2(t)$ (a) Amplitude (b) Phase

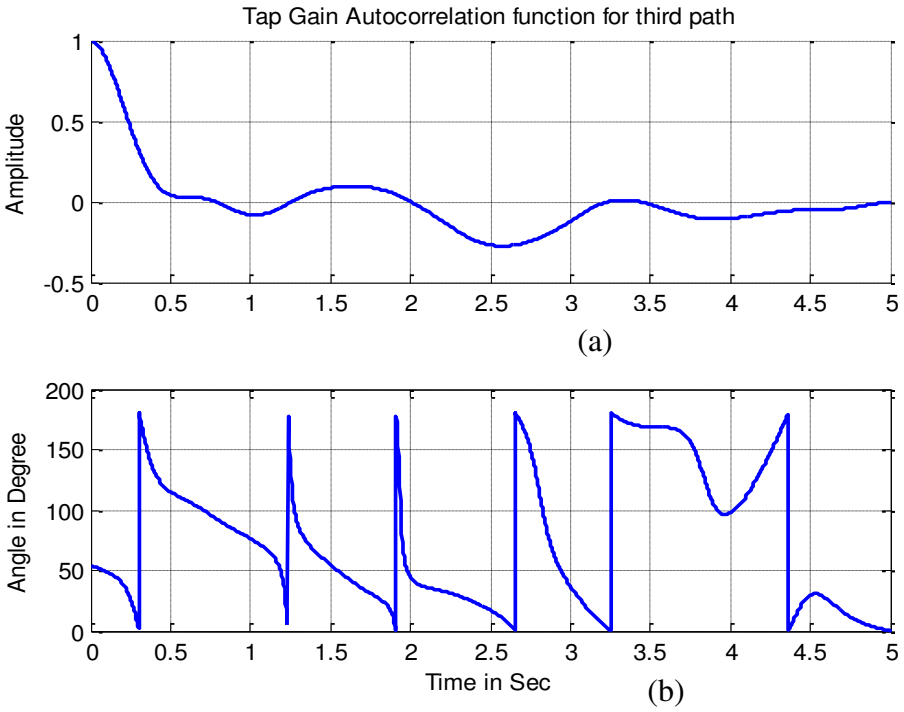

Figure 4.10: ACF for the $G_3(t)$ (a) Amplitude (b) Phase

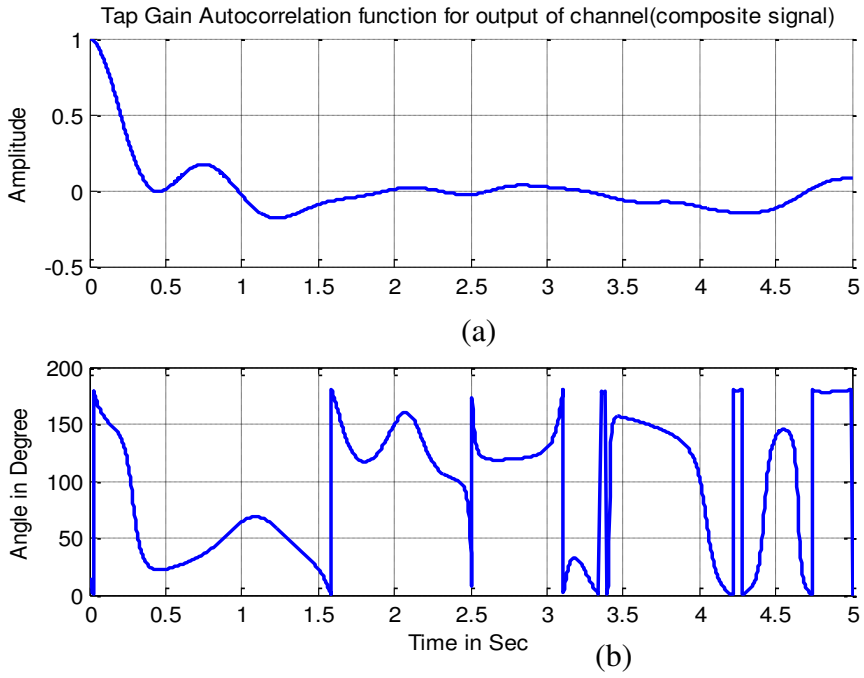

Figure 4.11: ACF for channel response $G_1(t) + G_2(t) + G_3(t)$, (a) Amplitude (b) Phase

Figures 4.12 illustrate the two dimensional ACF for first multipath. The corresponding results for the composite (all 3 multipath) are shown in Figure 4.13.

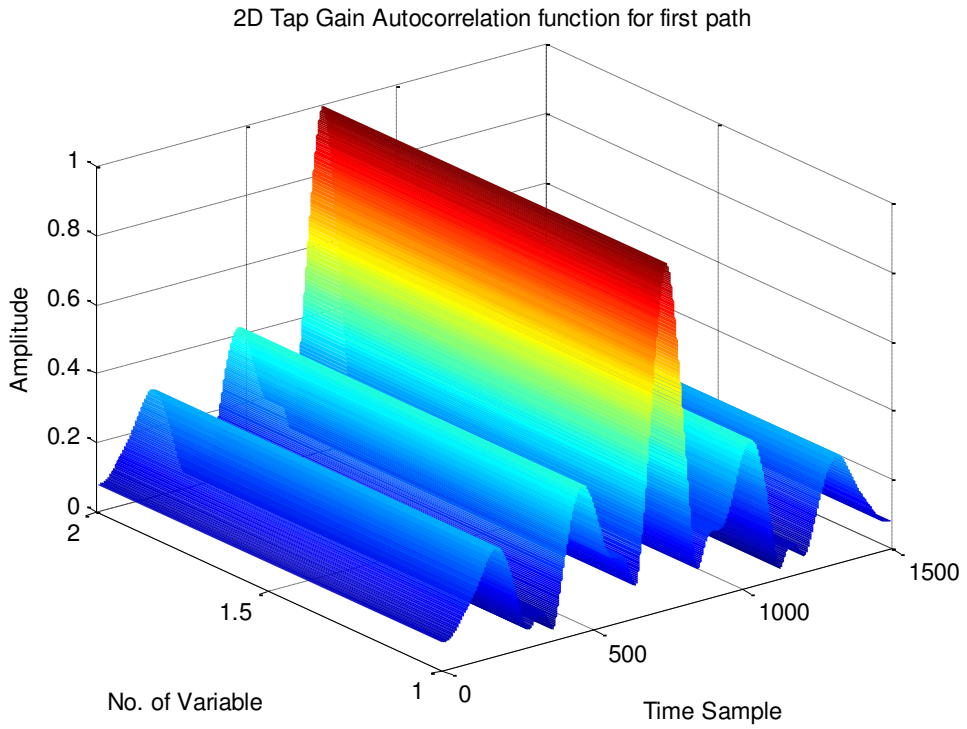

Figure 4. 12: 2D ACF for the $G_1(t)$

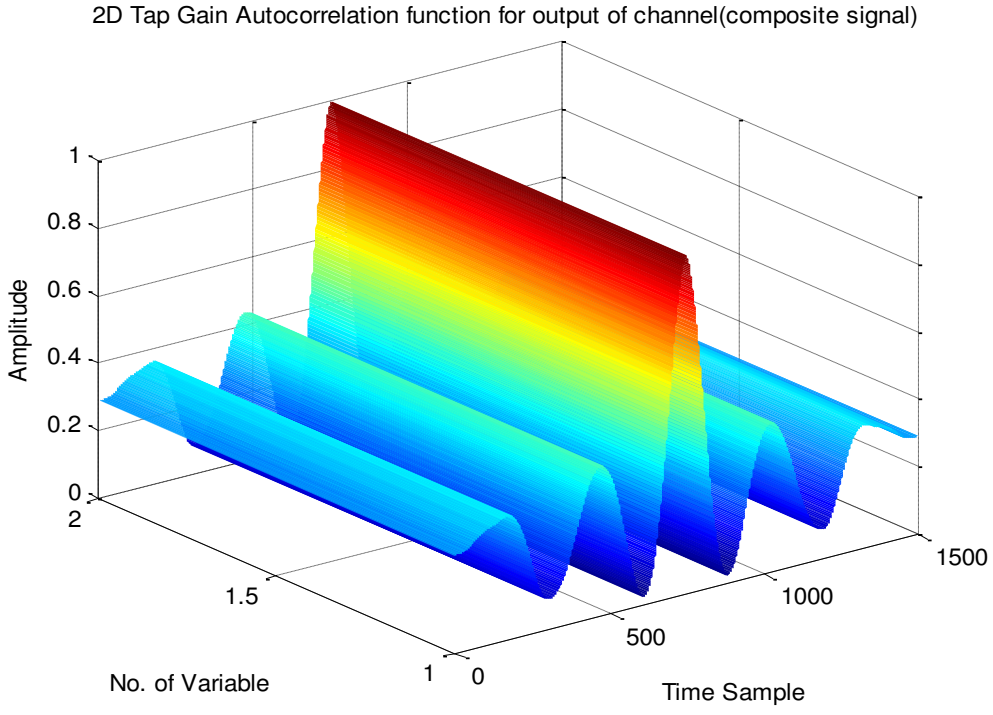

Figure 4.13: 2D ACF for channel response $G_1(t) + G_2(t) + G_3(t)$

From Figure 4.14, it is evident that cross-correlation between any two paths is small (around 0.1) and Figure 4.15 illustrates the 2D cross-correlation between two paths.

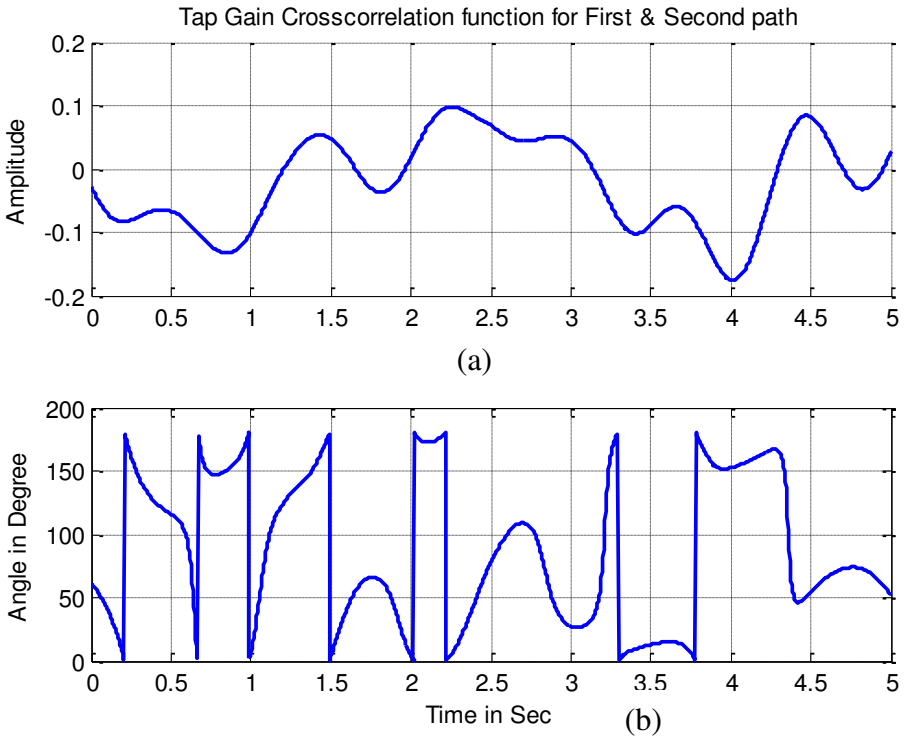

Figure 4.14: Cross correlation between $G_1(t)$ and $G_2(t)$

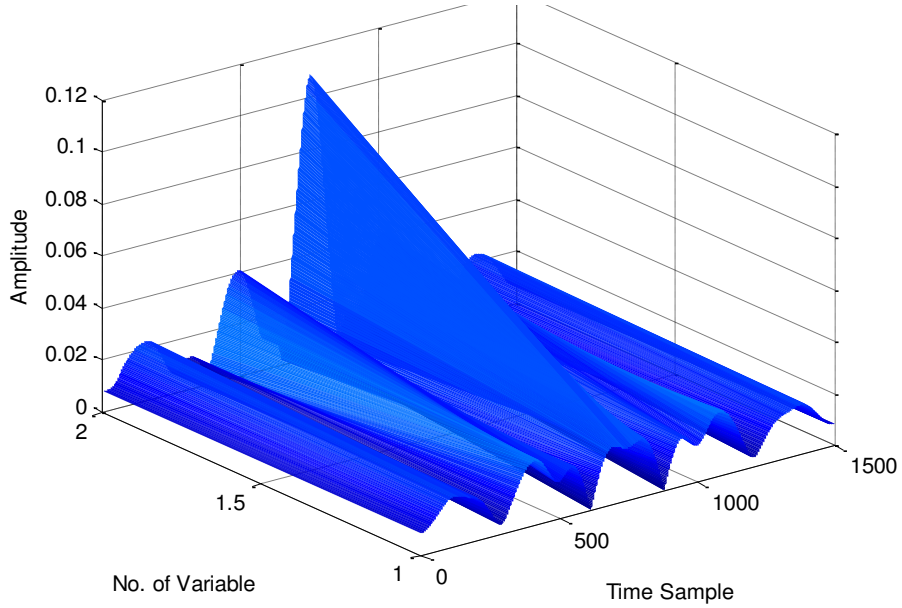

Figure 4.15: 2D Cross correlation between $G_1(t)$ and $G_2(t)$

Figure 4.16 illustrates the simulated Power Spectral Density (PSD) of ACF for single path shown in Figure 4.9. The simulated PSD is also compared with the tap-gain spectrum obtained through the Equation (A1.16). From Figure 4.18, it is evident that both simulated PSD and the tap-gain spectrum through Equation (A1.16) correlate very well over an amplitude range of about 55 dB. The tap-gain spectrum exhibits parabolic variation because of the logarithmic ordinate. The frequency span between the peak value and the -3 dB point of PSD or tap-gain spectrum corresponds to Doppler spread introduced by the HF channel.

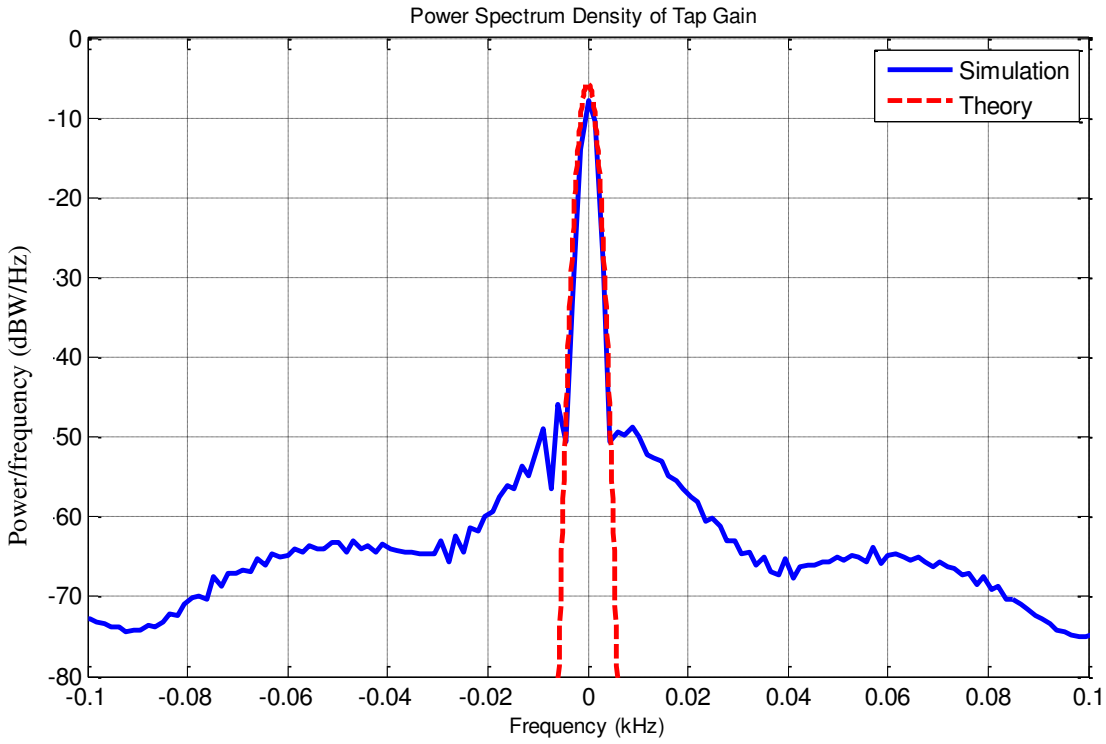

Figure 4.16 : PSD of tap-gain function with single path

Figure 4.17 illustrates PSD of ACF for single path of Figure 4.16 having two-magneto-ionic components. The simulated PSD for this scenario is also compared with the tap-gain spectrum obtained through the Equation (A1.16). From the results depicted in Figure 4.17, it is observed that both the simulated PSD and the tap-gain spectrum correlate well over an amplitude range of 55 dB. The spectral peaks corresponding to the

two magneto-ionic components are at 6 Hz and -7 Hz. Each of the two spectral peaks has a Doppler spread of 5 Hz.

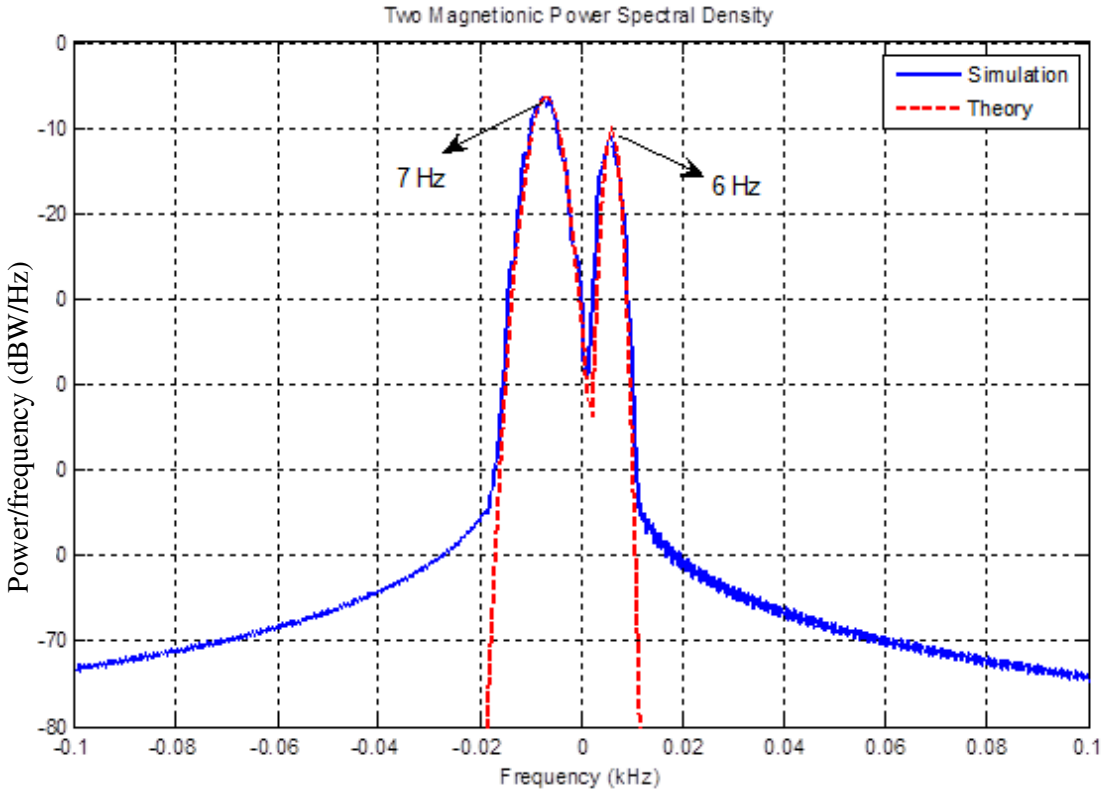

Figure 4.17: PSD of Tap-gain function with Two magnetic ionic component

Figure 4.18 illustrates the comparison of amplitude variation between linear and system non-linear with fading channel over a time period, three path losses of the three multipath being 0 dB, -4 dB, -7dB. The Doppler spread is 4Hz. The general inference from the results of Figure 4.20 is that non-linearity tends to give rise increased fluctuations in the peak amplitudes.

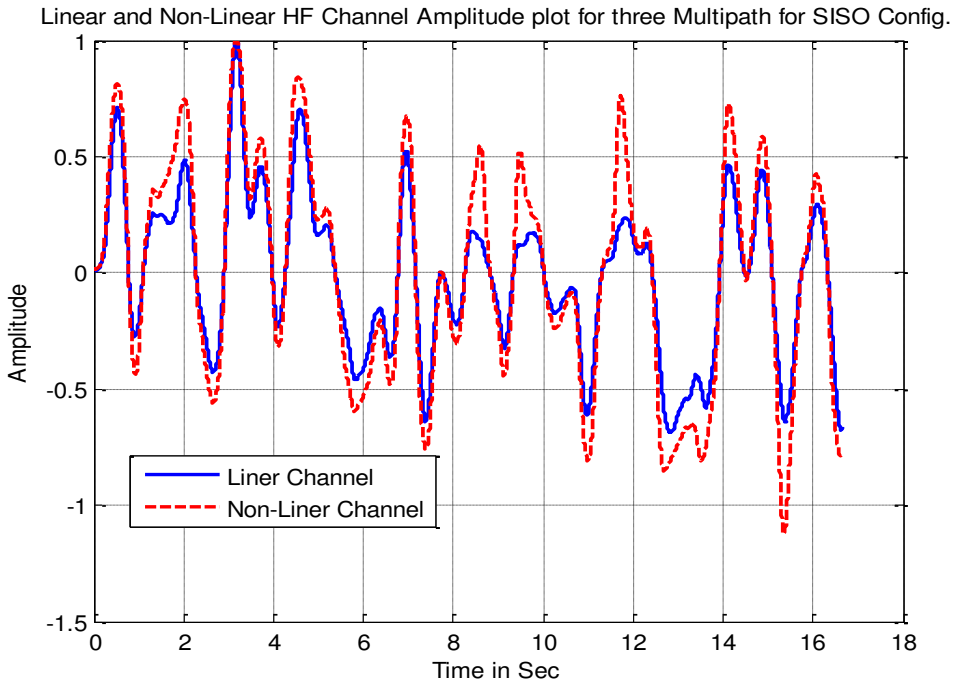

Figure 4.18: Comparison of Amplitude variation between Linear and system non-linearity with channel impairments for three Multipath for SISO Config.

A relative comparison of the influence of Gaussian and non-Gaussian noise on HF channel is illustrated in Figures 4.19 to 4.21. The noise PSD is shown Figure 4.19. It is pertinent to point out that noise PSD is independent of its distribution function.

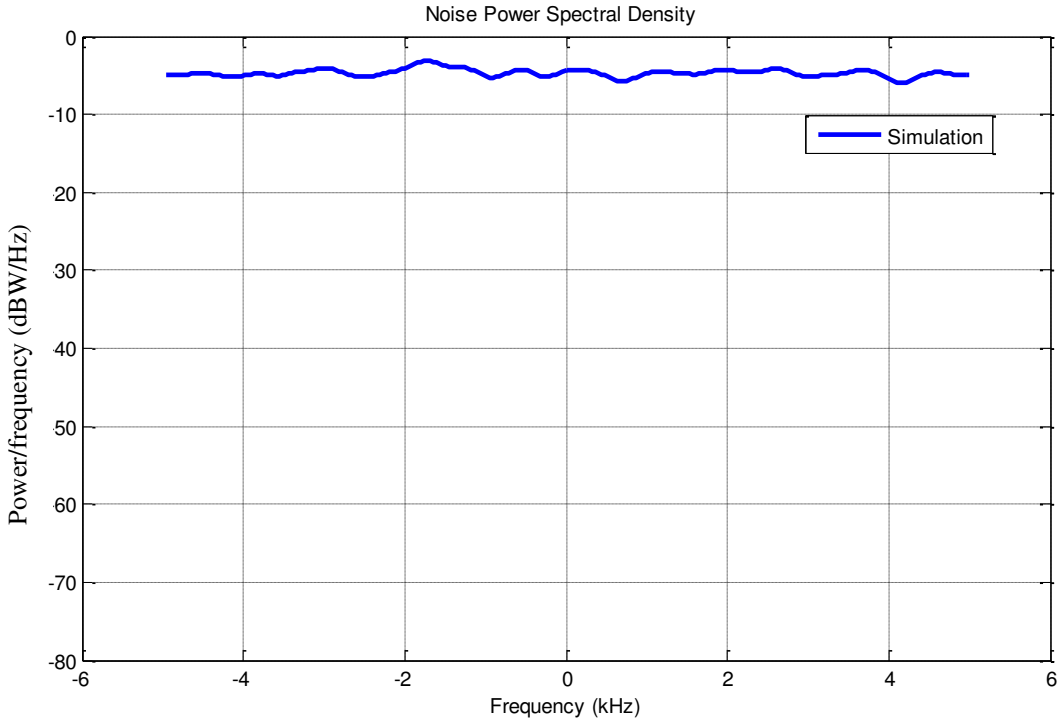

Figure 4.19: Noise power spectral density

The histogram for Gaussian and non-Gaussian noise distribution is shown in Figure 4.20. The results depicted in Figure 4.19 conforms the PDF of Gaussian function. Non-Gaussian distribution is simulated through a mixture of two Gaussian functions with identical zero mean and varying variance. Non-Gaussian distribution leads to asymmetry in the histogram. From the results of the Figure 4.21, it is easy to observe the impulsive nature of the amplitude variation introduced by non-Gaussian noise resulting in severe impairment in the estimation of desired signal.

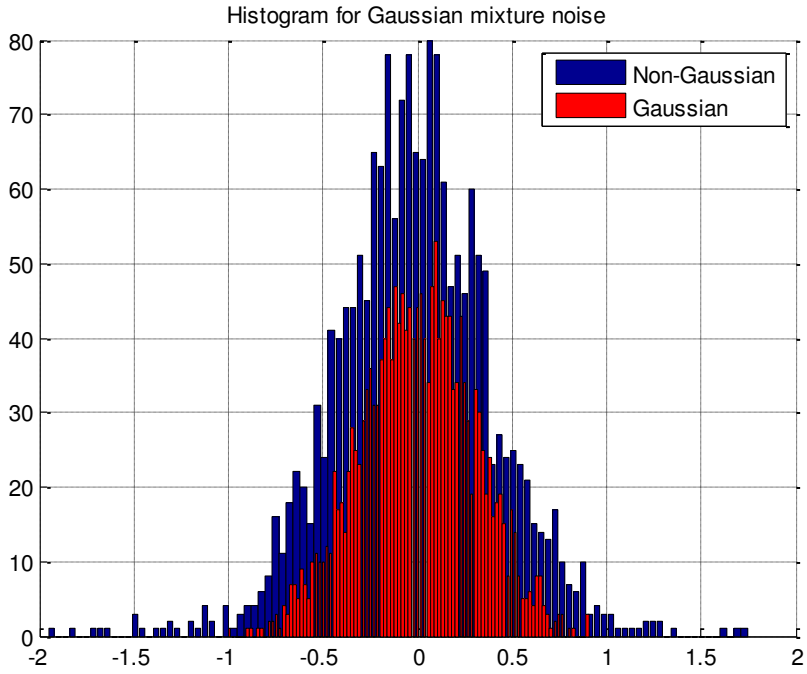

Figure 4.20: Histogram for Gaussian and non-Gaussian noise

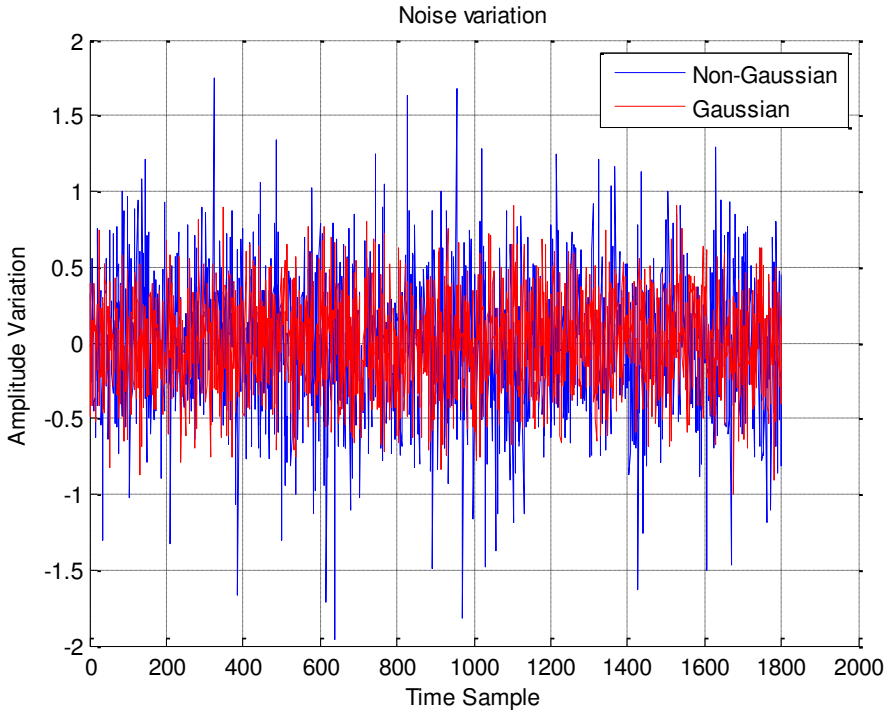

Figure 4.21 : Variation of Gaussian and non-Gaussian noise

For MIMO 2x2 configuration with flat fading is illustrated and it can be extended for higher configuration and frequency selectivity. The channel coefficient for 2x2 MIMO for single path is given as follows

$$H_{2x2} = \begin{bmatrix} h_{00} & h_{01} \\ h_{10} & h_{11} \end{bmatrix} \tag{4.36}$$

Where,

$H_{Tx,Rx}$ represents the channel matrix between Tx and Rx antennas, For 2x2 Configuration, the indices for both Tx and Rx vary from 0 to 1.

$h_{Tx,Rx}$ represents the individual elements of the channel matrix or the coefficients of the channel matrix.

The amplitude fluctuations of the channel coefficients of 2X2 MIMO channel are depicted in Figure 4.22. The simulation results shown in Figure 4.22 are based on the parameters used to simulate the results in Figure 4.8

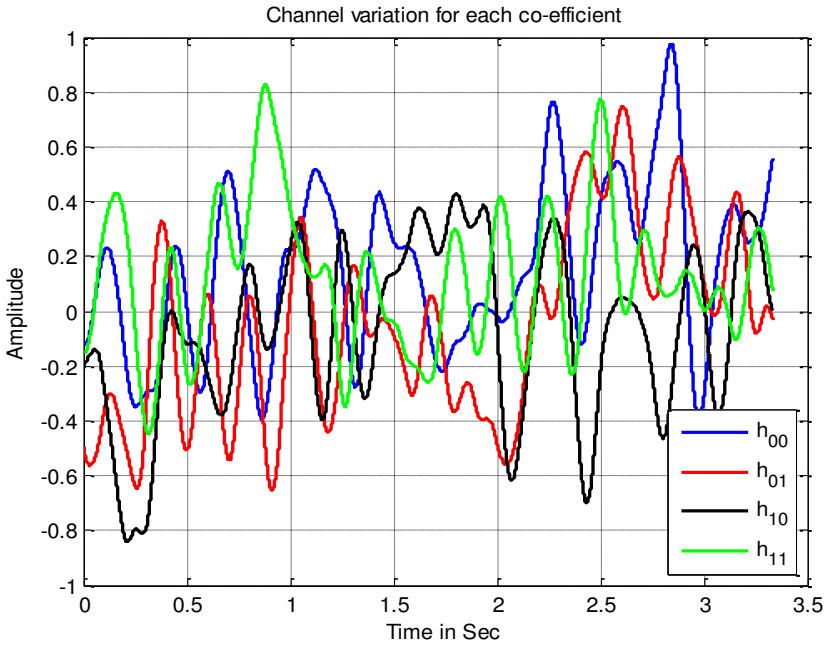

Figure 4.22: Channel variation for 2x2 MIMO configuration

Figure 4.23 illustrates the ACF of the 4 channel coefficients of 2X2 MIMO channel. The delay spread encountered by the 4 channel coefficients between Tx and Rx is almost the same and is around 40 msec.

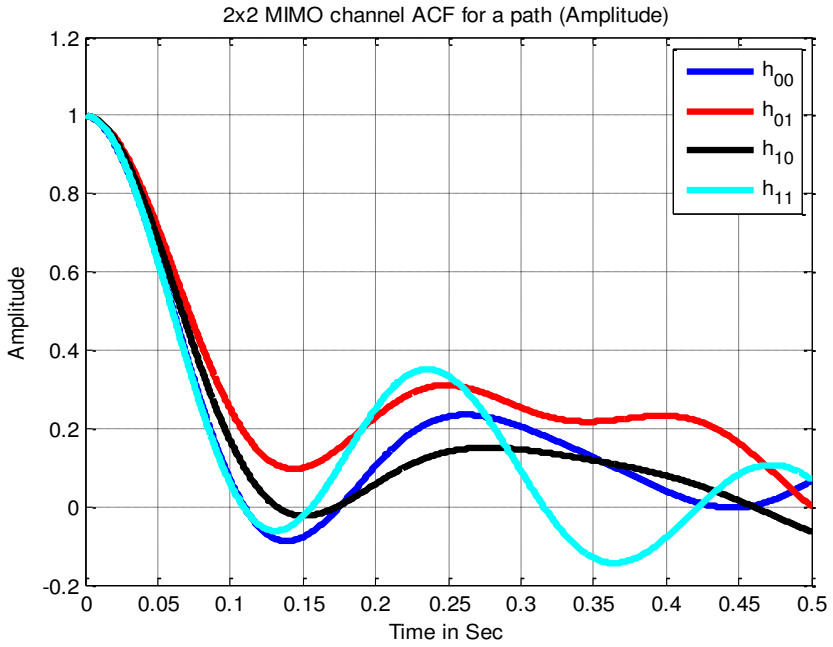

Figure 4.23 : ACF of Tap-gain function (Channel coefficient) for 2x2 MIMO .

The uncorrelated characteristics of the generated channel coefficients of 2X2 MIMO channel are shown in Figure 4.24 implying the presence of rich multipath scattering scenario.

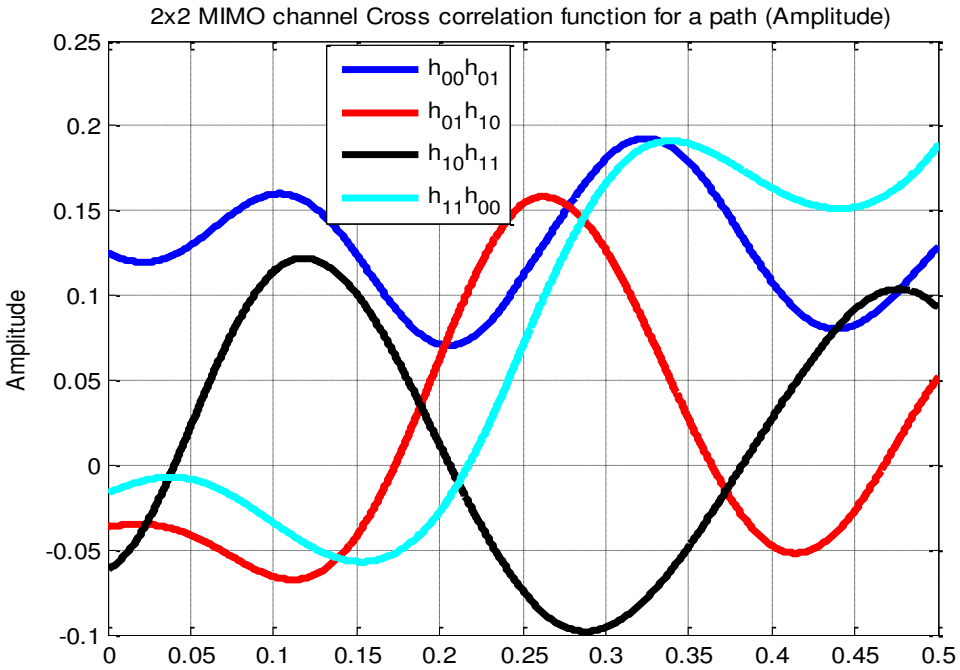

Figure 4.24 : Cross -correlation for 2x2 MIMO channel coefficient

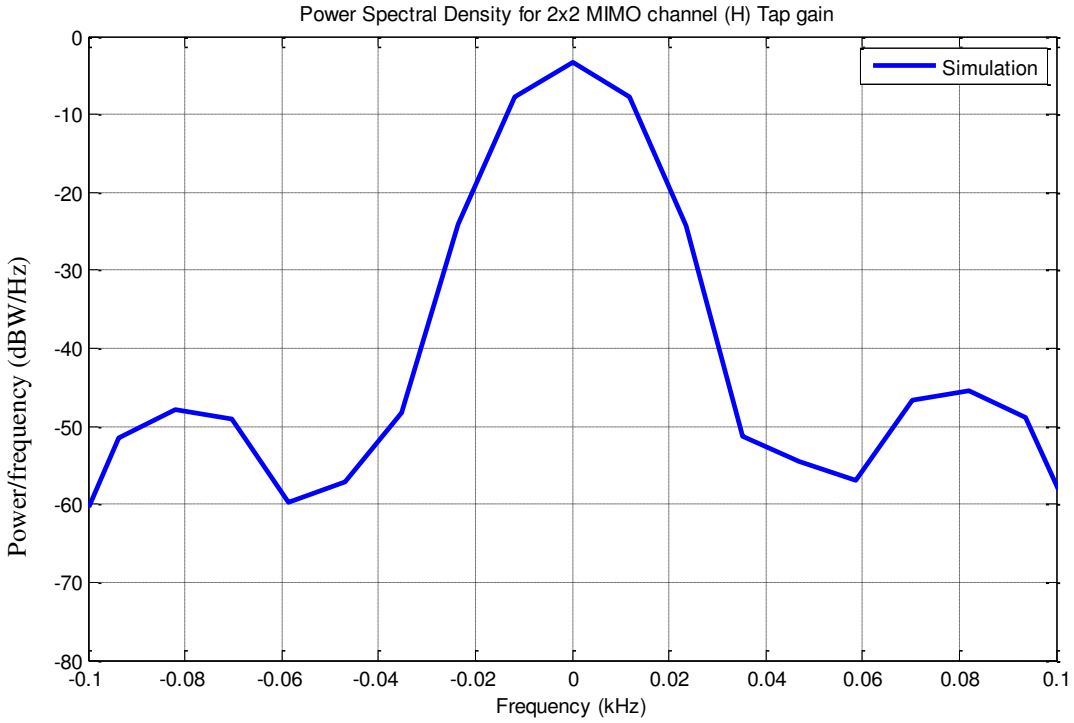

Figure 4.25: PSD for 2x2 MIMO channel with Doppler spread of 4 Hz

The PSD of 2x2 MIMO channel with a Doppler spread of 4 Hz for the all coefficients is shown in Figure 4.25. The PSD is derived through Fourier transform the ACF of the channel coefficients of Figure 4.23.

4.6.2 Complexity Analysis in Generation of Tap-Gain Function

The following section demonstrates the signification of AR (IIR) model over FIR model in terms of complexity of implementation . The following parameters are considered for the simulation of tap-gain functions of HF channel.

Doppler spread (f_d) : 1- 10Hz

Sampling frequency (F_s) : 300 Hz and 4000Hz

Tap-gain generation : AR and FIR method.

No. of tap-gains : 1 (can be generalized for any number)

Order of AR : Between 7 to 11

Order or length FIR : $N = Ceil(K\_qual * Fs/(f_d * 2)) + 1$, [Wheatley 2000]

where K_qual is the shape quality it consider to be 1.4 (larger the constant, the better the match).

Order of IIR : $N = Ceil\left[\frac{\log_{10}\left(\frac{A_{min}^2 - 1}{\varepsilon^2}\right)}{2 * \log_{10}\left(\frac{f_s}{f_d}\right)}\right]$ [Proakis 1997]

Where A_{min} is stopband gain, ε =0.3 to 0.5 passband gain, f_s stop band frequency & $f_s = f_d + 5$ is considered for the simulation

Table 4.3 shows the various test cases for which ACF and PSD for HF channel Tap-gain function is analysed for AR and FIR channel models.

Table 4.3 Test Case Simulation for ACF And PSD for Tap-Gain Function

Test Case	Doppler Spread (Hz)	Sampling Frequency (Hz)
A	10	300
B	1	300
C	10	4000
D	1	4000

Test Case A

Figures 4.26 and 4.27 illustrate the ACF and PSD for tap-gain function generated using AR (IIR) and FIR model for a path with Doppler spread 10 Hz and sampling frequency 300 Hz.

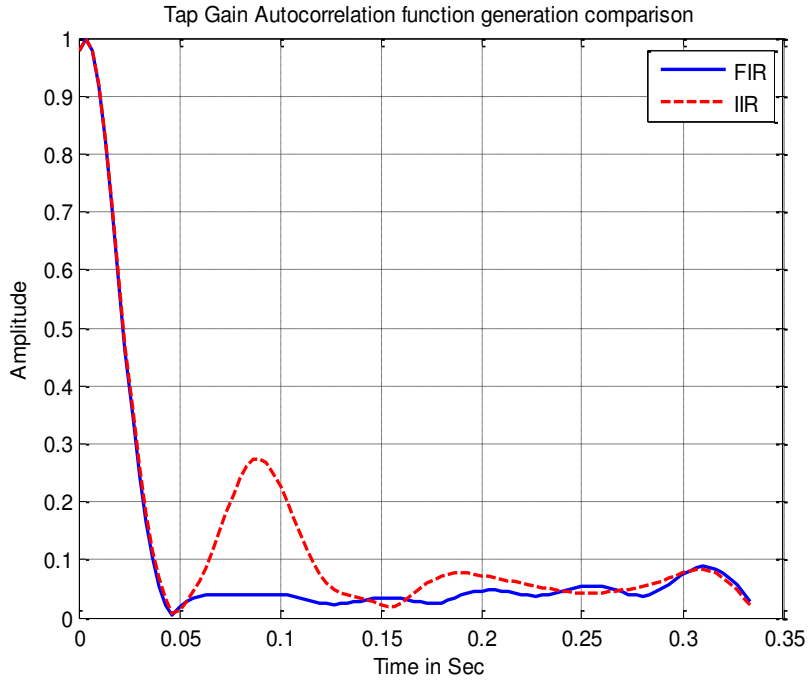

Figure 4.26: ACF of tap-gain function generated using AR and FIR with Doppler spread 10 Hz and sampling frequency 300 Hz

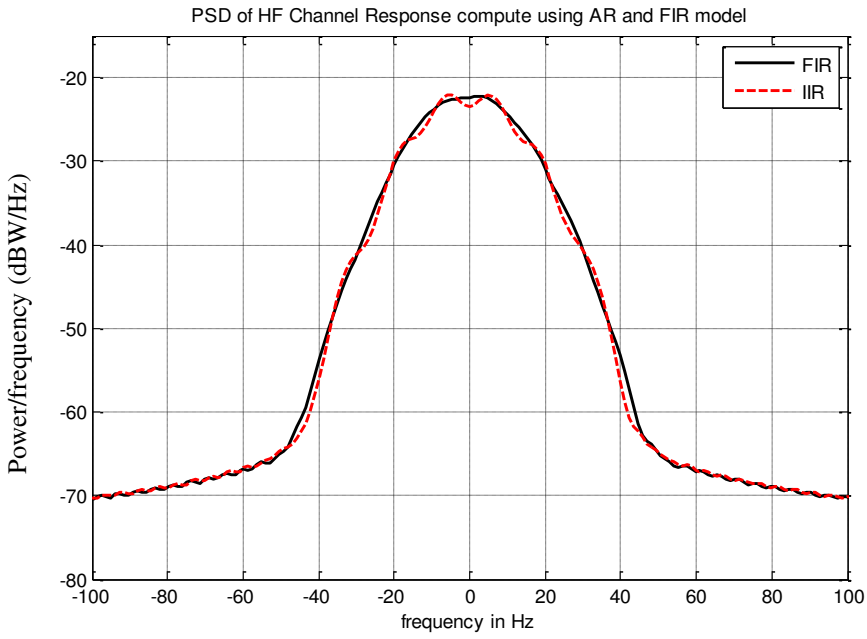

Figure 4.27: PSD of tap-gain function generated using AR and FIR models with Doppler spread 10 Hz and sampling frequency 300 Hz

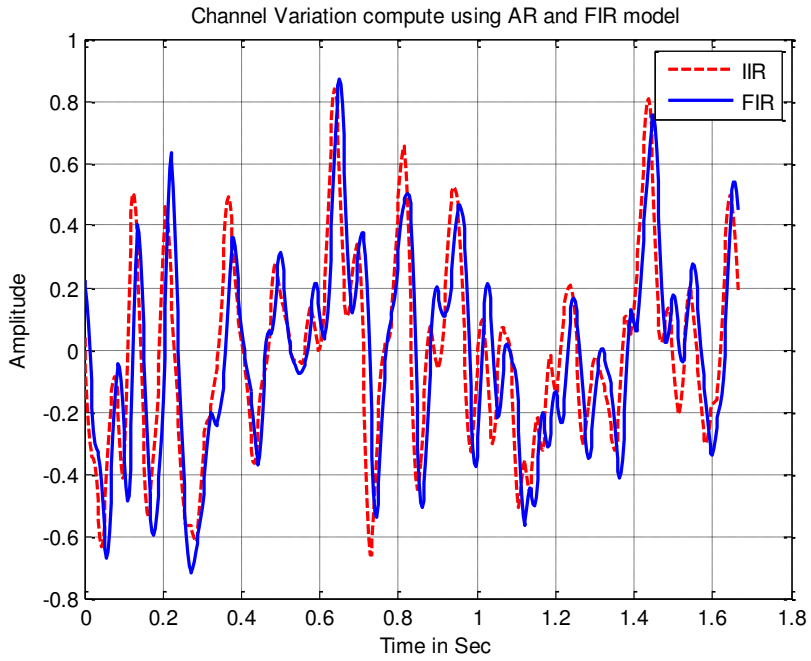

Figure 4.28: Channel variation for the tap-gain function generated using AR and FIR model with Doppler spread 10 Hz and sampling frequency

Test Case B

The ACF and PSD of the HF channel modelled through AR and FIR with a Doppler spread of 1 Hz and Sampling frequency 300 Hz are shown in Figures 4.29 and 4.30. The corresponding amplitude variations of the HF channel modelled through AR and FIR are shown in Figure 4.31.

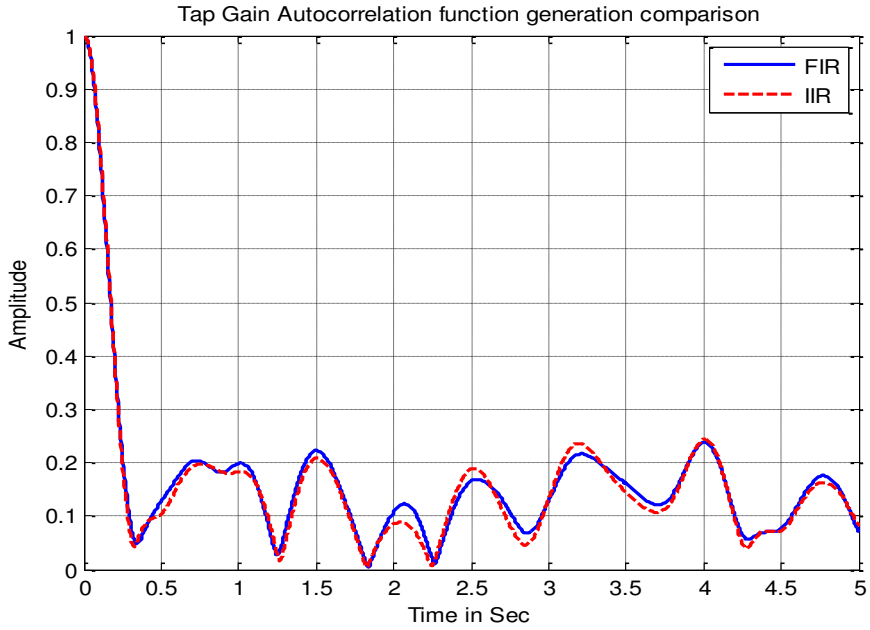

Figure 4.29: ACF of tap-gain function generated using AR and FIR with Doppler spread 1 Hz and sampling frequency 300 Hz

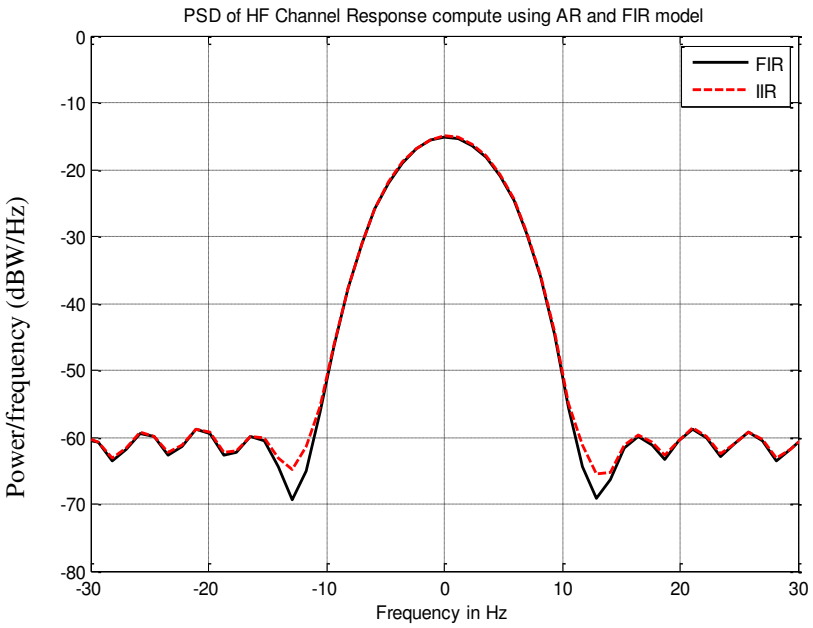

Figure 4.30: PSD of tap-gain function generated using AR and FIR with Doppler spread 1 Hz and sampling frequency 300 Hz

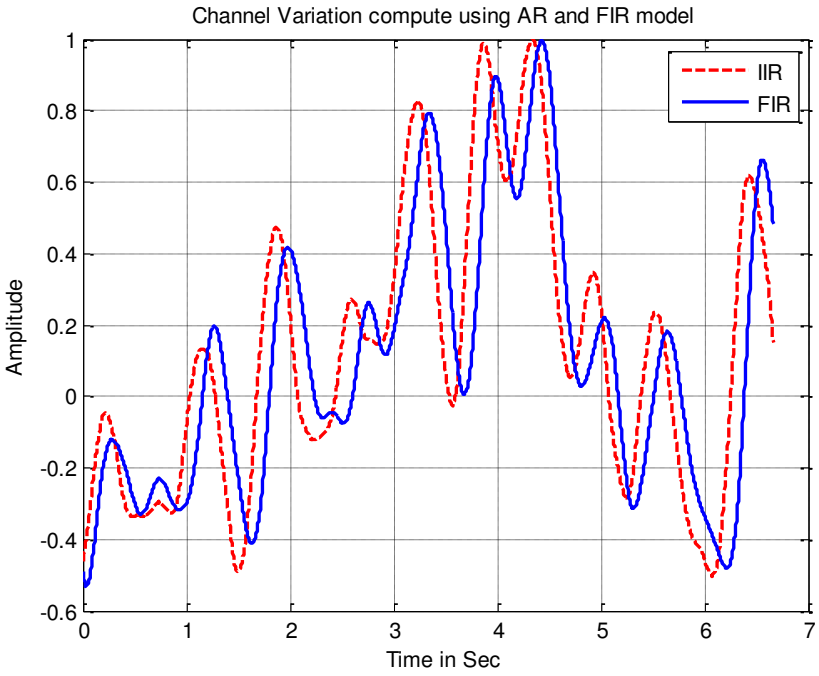

Figure 4.31: Channel variation for the tap-gain function generated using AR and FIR with Doppler spread 1 Hz and sampling frequency 300 Hz

The well-known FIR model for the modelling of HF channel has been invoked to channel modelling using AR (IIR). To characterize the HF channel associated with Doppler spread of 10 Hz and sampled at 300 Hz, the order of the tap-gain function for AR is found to be 9 while it is 226 for FIR. However, when the Doppler spread was reduced to 1 Hz with other parameters unaltered, the AR model showed no change in the order of Tap-gain function while FIR showed a significant variation from 226 to 24. It implies that FIR model would necessitate a rapid reconfiguration of the sources to cater the dynamic conditions of the channel represented through Doppler spread variations. The further advantage of reduced order of tap-gain functions required for the case IIR for the identical channel conditions is illustrated through relatively smaller delay as shown in Figures 4.28 and 4.31.

Test Cases C and D

From the results illustrated in Figures 4.32 to 4.37, it is noticed that simulated tap-gain functions using AR and FIR models show insignificant difference between them. The same results indicate that FIR model introduces a delay in generating the steady state tap-gain function. The referred delay is attributed to the increased order of FIR for the channel response.

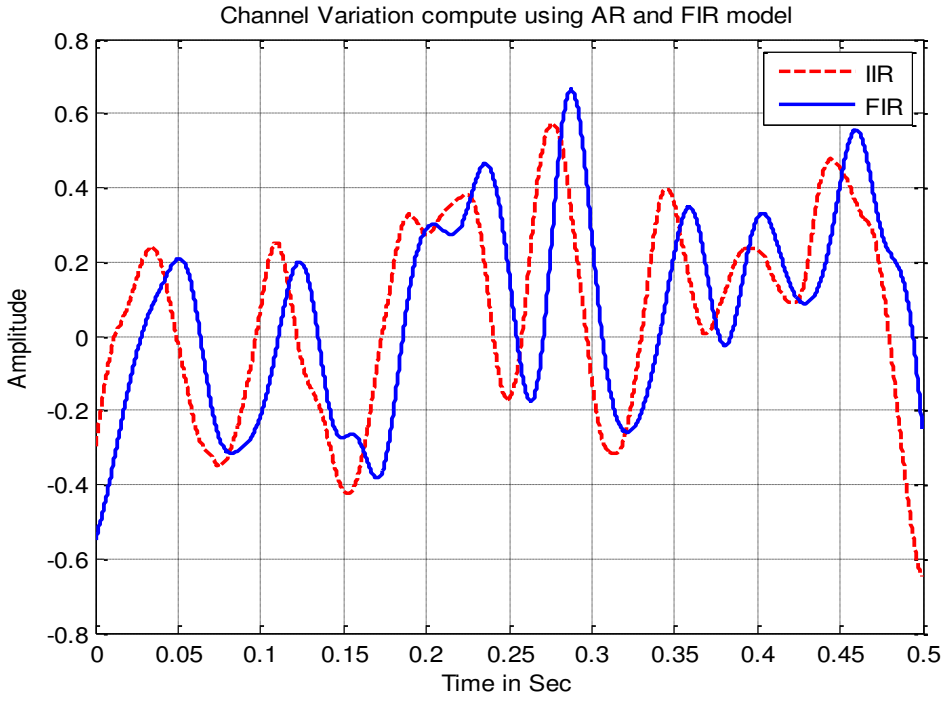

Figure 4.32 : Channel variations for the tap-gain function generated using AR and FIR with Doppler spread 10 Hz and sampling frequency 4000 Hz

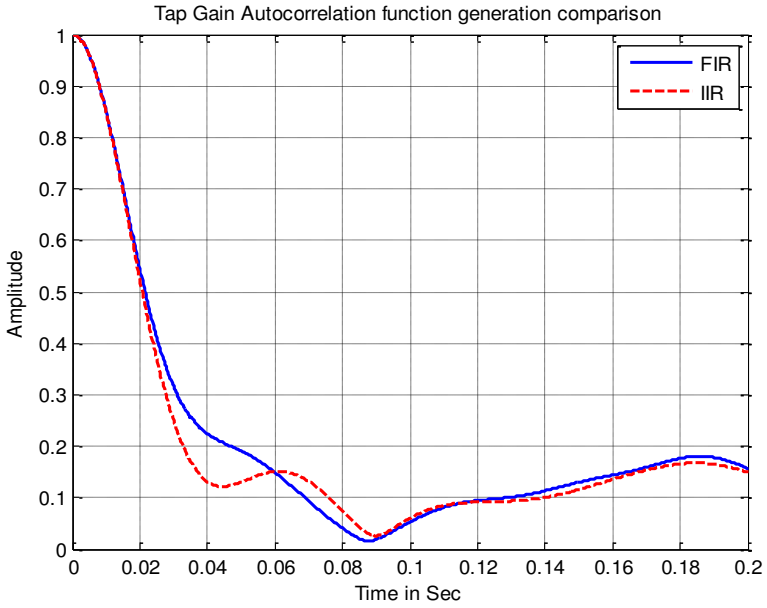

Figure 4.33: ACF of tap-gain function generated using AR and FIR with Doppler spread 10 Hz and sampling frequency 4000 Hz

To generate the HF channel response (for a Doppler spread 10 Hz and sampling frequency 4000 Hz) the order of AR model is 11 whereas the order for FIR is 301 with only the change of Doppler spread from 10 Hz to 1 Hz, for channel response the order for AR model remained at 9 while the order for FIR there was a significant increase in its order from 301 to 3001.

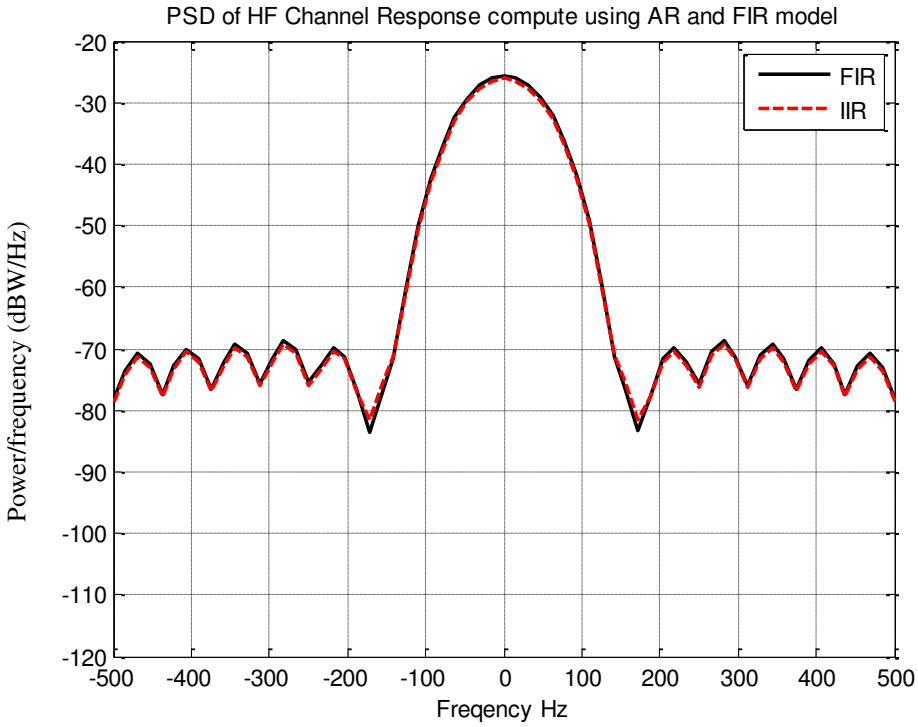

Figure 4.34: PSD of Tap-gain function generated using AR and FIR with Doppler Spread 10 Hz and Sampling frequency 4000 Hz

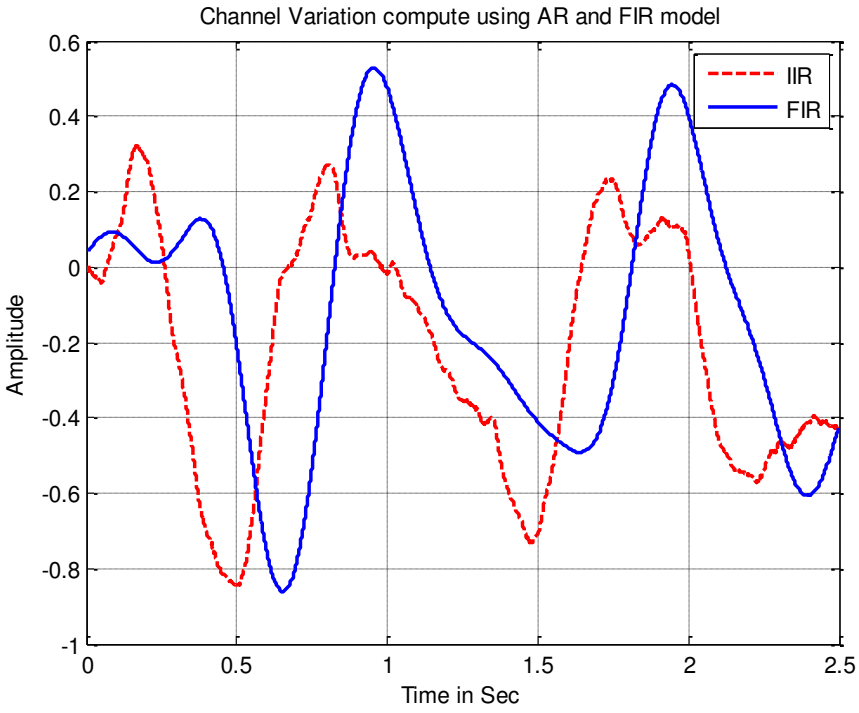

Figure 4.35 : Channel variation for the tap-gain function generated using AR and FIR with Doppler spread 1 Hz and sampling frequency 4000 Hz

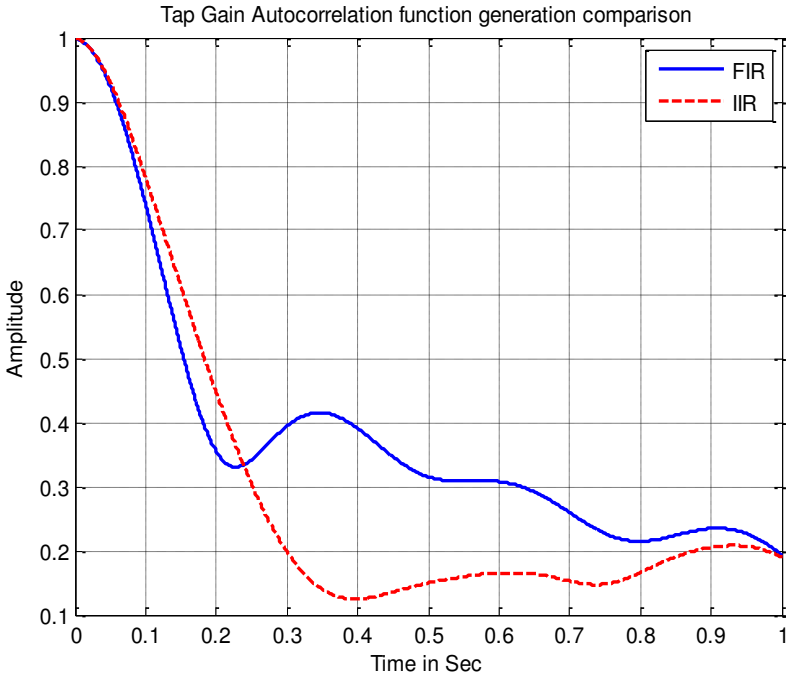

Figure 4.36 : ACF of tap-gain function generated using AR and FIR with Doppler spread 1 Hz and sampling frequency 4000 Hz

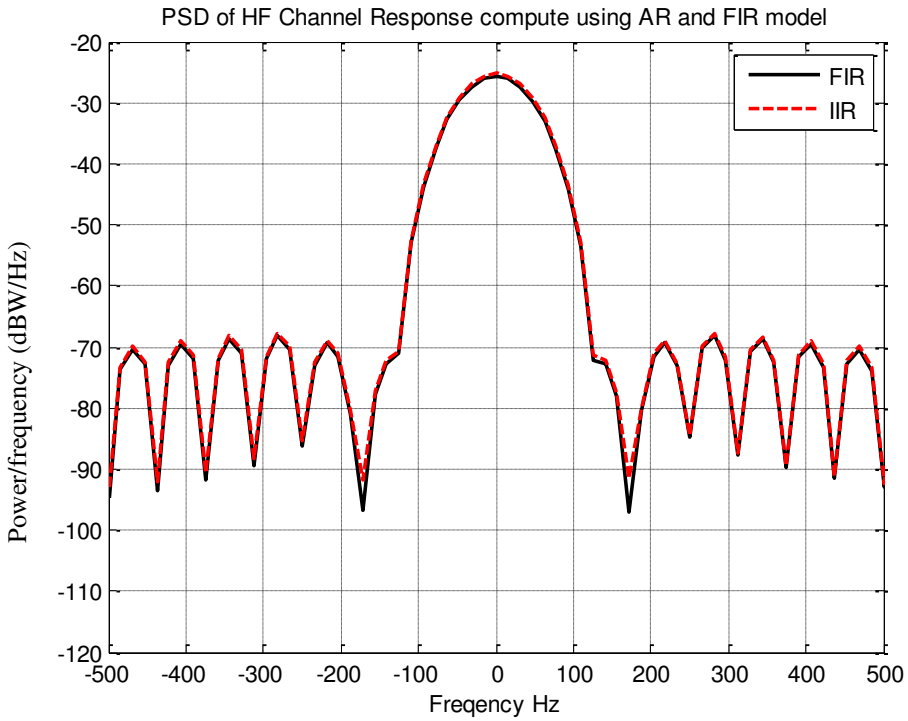

Figure 4.37 : PSD of tap-gain function generated using AR and FIR with Doppler spread 1 Hz and sampling frequency 4000 Hz

From Figures 4.32 and 4.35, it is seen that for higher sampling frequency the ACF generated using AR model shows smooth response and fast roll-off compared to the FIR model (Figure 4.32 and 4.35).

MATLAB Filter Design and Analysis Tools (FDAT) have been used to carry out a comparative analysis of complexities involved in characterizing HF channel using AR and FIR models. This involves importing respective filter coefficients to the FDAT. Table 4.4 illustrates the relative comparison between the AR and FIR filter for generation of a single tap-gain function for one sample.

Table 4.4 Test Case Comparison Simulation for Tap-Gain Function

Test case	Doppler spread (Hz)	Sampling frequency (Hz)	FIR order	IIR order
A	10	300	24	9
B	1	300	226	9
C	10	4000	301	11
D	1	4000	3001	9

Figure 4.38 depicts the comparison of computational complexities involved in the characterization of HF channel invoking AR and FIR models with FDAT for the test cases B discussed earlier. In particular, Figure 4.38 dwells the relative complexities in terms algebraic operations and memory storage (states). It is evident that AR modelling exhibits greater advantage over FIR in terms complexities from the point of computation as well as memory utilization.

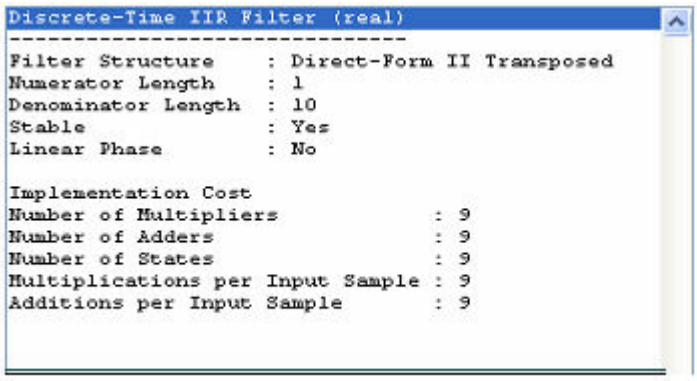

Figure 4.38 (a) AR

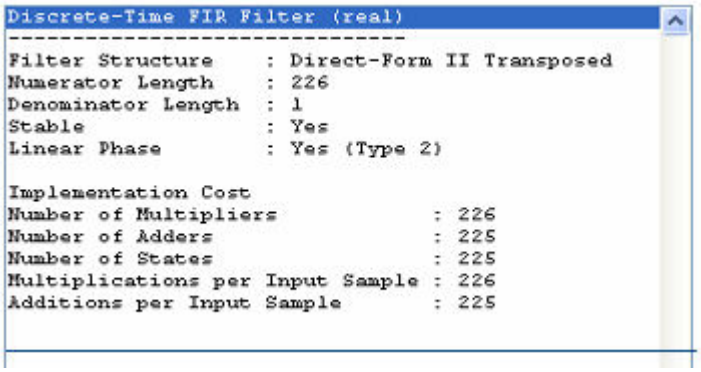

Figure 4.38 (b) FIR

Figure 4.38 : Comparison of relative complexities for generating a sample for tap-gain functions for test case B.

Figure 4.39 is analogous to Figure 4.38 except it is generated for test case C (Higher sampling frequency). Even in case of higher sampling frequency, AR modelling exhibits its lower computational burden compares to FIR.

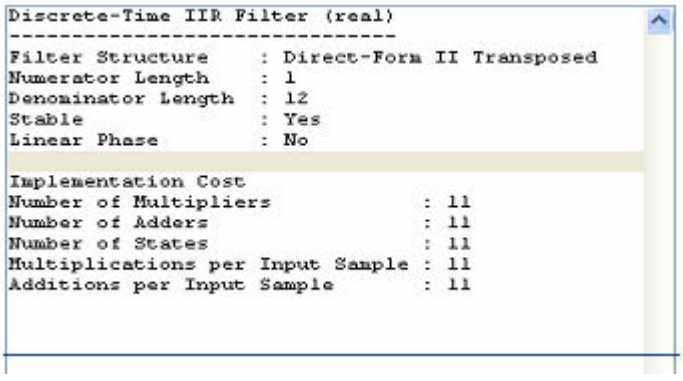

Figure 4.39 (a) AR

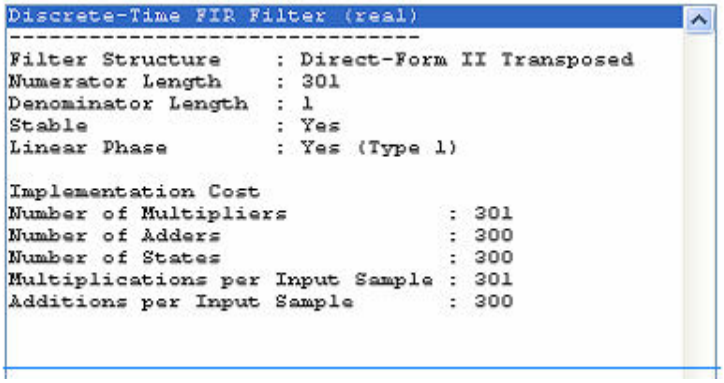

Figure 4.39 (b) FIR

Figure 4.39 :Comparison of relative complexities for generating a sample for tap-gain function for test case C

In order to highlight the difference in the requirement of order of the filter (for AR and FIR) to generate tap-gain functions, extensive simulations have been carried out for various combinations of Doppler spread and sampling frequencies. Figure 4.40 shows the comparison of the order of AR and FIR filter required to generate tap-gain function.

With the span of sampling frequencies extending from 300 Hz to 4000 Hz AR model requires an order of 11 to realize the specified channel parameters (Doppler spread of 1 to 10 Hz). The order of the filter varies from 3 to 11 only. For the identical scenario, the order of FIR varies from 24 to 3001 which surely is a much wider variation compared to AR model. It is pertinent to point that the increasing order of the filter is directly related to the complexities in hardware implementation. From the results of Figure 4.40 (a), it can be inferred that the AR model requires only 3 to 11 Multiplication-Accumulation Computation (MAC) compared 24 to 3001 MAC required by FIR. From Figure 4.40 (b), it is evident that swing in order of the filter with FIR is rather wide to meet the varying Doppler spread. The relatively narrow swing in the order of the filter with AR allows a flexibility to freeze a slightly higher filter order without undue implementation burden and yet satisfying a rather varying Doppler spread. The same cannot be said in case of FIR

The results of Figure 4.40 specifically pertain to a single tap-gain function of SISO. In case of SISO, the order of computations with both AR and FIR models will increase linearly with change in number of multipath. In a typical HF channel scenario [Watterson 1970], 3 multipath is considered to be sufficient for SISO. When MIMO replaces SISO for the channel characterization, the above discussed generation of tap-gain function of SISO has to be repeated for every individual channel coefficient of MIMO channel. For each channel coefficient, the tap-gain function need to generate as module. In general the MAC required implementing the tap-gain function for MIMO channel is given as

$$MAC_{MIMO} = 2^{max(Tx,Rx)} \text{ x (No. of Multipath) x (Order of AR or FIR)} \quad (4.37)$$

Considering the an example for MIMO 2x2, multipath path = 3, order of AR =11 and order of FIR = 301 (for Doppler spread =5 Hz and sampling frequency = 2000 Hz)

- MAC required for AR → 132 (Multiply and Adder)
- Time to compute for AR→ 66 msec
- MAC required for FIR→ 3612
- Time to compute for sequential AR→ 1806 msec.

It is observed from the results of the above example; there is an advantage with AR model in terms of resources utilization and computation time.

Table 4.5 shows the comparison of computational complexity (MAC) in evaluating the tap-gain function for SISO using the FIR and AR models. It is evident that AR model exhibits least computation complexity for varying parameters such as Doppler spread and sampling frequency.

Table 4.5 Comparison of MAC between FIR and AR Models to Evaluate Tap-Gain Function for SISO Configuration

Sampling frequency in Hz	Doppler spread in Hz	SISO (FIR)		SISO (AR)	
		Single tap	Three Multipath	Single tap	Three Multipath
300	10	24	72	11	33
	6	39	117	7	21
	2	114	342	4	12
	1	226	678	3	9
2200	10	166	498	11	33
	6	276	828	7	21
	2	826	2478	4	12
	1	1651	4953	3	9
4000	10	301	903	11	33
	6	501	1503	7	21
	2	1501	4503	4	12
	1	3001	9003	3	9

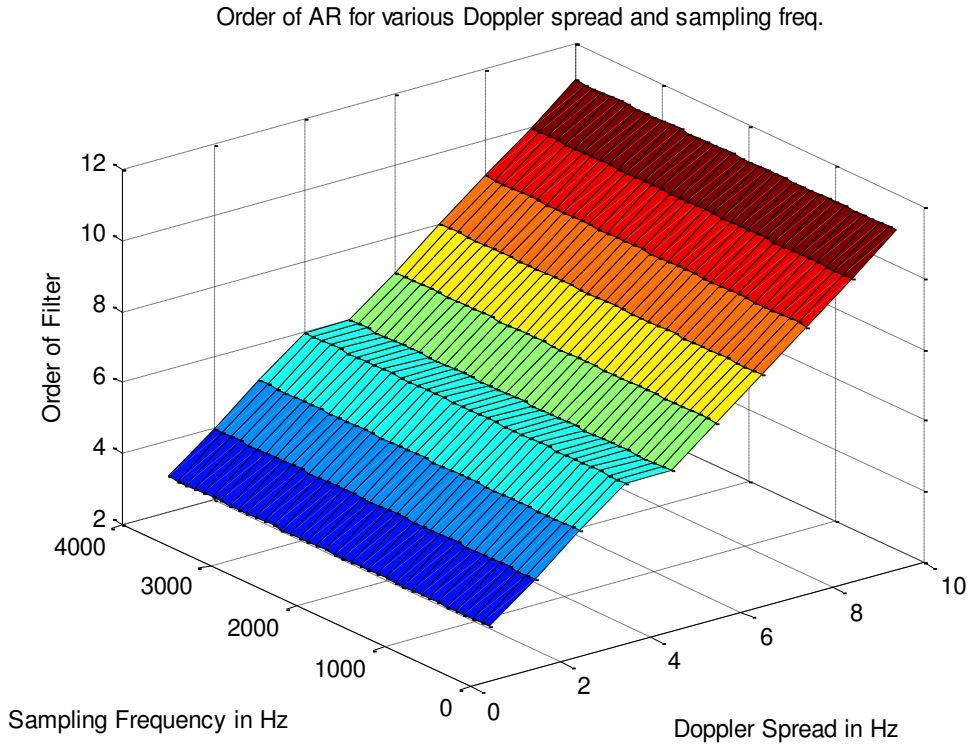

Figure 4.40 **(a)**

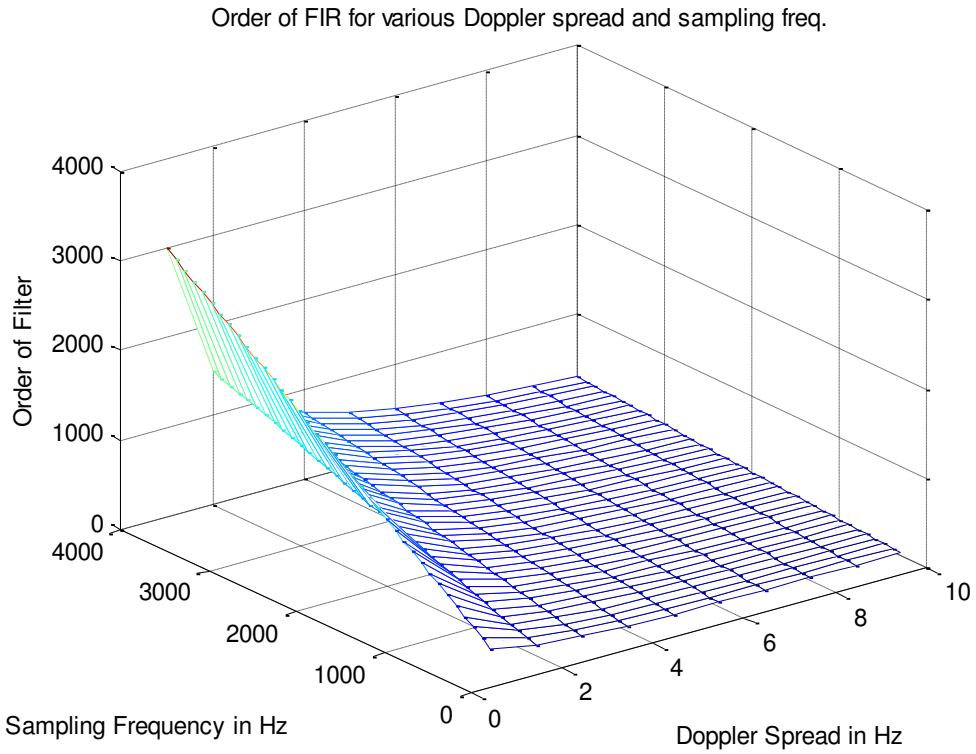

Figure 4.40 **(b)**

Figure 4.40: (a) AR (b) FIR order of filter for computing for various Doppler spread and sampling frequency

Table 4.6 is analogous to table 4.4 except that it is for MIMO configuration. Even with MIMO configuration also, AR model continues to have lower MAC requirements compared to FIR.

Table 4.6 MAC Comparison between FIR and AR to Evaluate Tap-Gain Function for MIMO Configuration

		2x2 MIMO (FIR)		2x2 MIMO (AR)	
Sampling frequency in Hz	**Doppler spread in Hz**	**Single path**	**Three multipath**	**Single path**	**Three multipath**
300	10	96	288	44	132
	6	156	468	28	84
	2	456	1368	16	48
	1	904	2712	12	36
2200	10	664	1992	44	132
	6	1104	3312	28	84
	2	3304	9912	16	48
	1	6604	19812	12	36
4000	10	1204	3612	44	132
	6	2004	6012	28	84
	2	6004	18012	16	48
	1	12004	36012	12	36

4.7 Conclusion

The random and unpredictable nature and the absence of definitive statistical characterization of various HF channel parameters have resulted in continued demand for improvement of channel model. The designer would desire a near real-time channel simulator to have fair statistical knowledge of channel conditions. SNR, Doppler spread and delay spread are the three significant channel parameters to characterize the Omni presence of multipath fading in a HF channel. Realistically, characterization of HF channel can be accomplished only through snapshot observations of desired parameters to retain the inherent random behavior of the channel. The accuracy of the HF system performance such as BER, throughput and link reliability depends upon the how well the system parameters have been captured through snapshot observations.

This chapter presents an analytical model to characterize the multipath fading phenomenon of HF channel associated with non-Gaussian noise and system non-

linearity. The presented analytical model is aimed to consider the collective impairment of the realistic HF channel due to non-linearity of the systems, multipath fading effects and non-Gaussian noise. In the proposed channel characterization scheme, Watterson channel model has been invoked to impart non-linear and random time varying features to capture both the time and frequency dispersion. The multipath fading phenomenon is modeled through multiple tap-gain functions to realize time dispersive nature of the channel. Each tap-gain function represents a multipath associated with a differing delay and gain. To capture the frequency dispersive nature of the channel, the tap-gain has been modeled so as to realize Gaussian Doppler power spectral function.

The non-stationary characteristics of the HF channel have been analyzed through the cumulative simulation invoking multiple snap shot observations of the channel. Each snap shot channel analysis represents the stationary nature of the channel. The cumulative simulation through stationary ionosphere channel performed over various snap shots of observations can still be helpful in arriving at the possible bounds for the variation of channel parameters. This in turn has a reasonably good potential to closely approximate even a non-stationary HF channel. Through extensive simulations, the feasibility of analysis of non-stationary HF channel has been demonstrated. The characterization of channel parameter through tap-gain function has been realized invoking White noise filtering method using FIR or AR models. This chapter also substantiates that the requirement of lower filter order by AR model does not result in any significant deviation in the characterization of the channel.

Practically, a narrowband filter is used to characterize the Doppler spectrum of the channel modelling with a very sharp roll off and infinite attenuation in stop-band region. To realize this specification of narrowband filter, it is impractical to have a FIR filter even with large number of taps. But for same specification, IIR filter would need lesser number of taps and thus has an advantage of ease of implementation The simulation studies on HF channel characterization presented in this chapter reveal that the change in Doppler spread has minor variation in change of order of the AR model. Further the

effect of change in the order of AR model is independent of the sampling frequency. The same is not true with the FIR model.

The effectiveness in selecting the FIR or AR depends on the parameters such as computation complexity, implementation time, dynamic memory allocation resource and resource dependency on dynamic range in selection of Doppler frequency and sampling frequency. With all these parameters, the simulation study of this chapter proves that AR is an ideal choice to characterize the given parameters of a HF channel.

Finally, the computational complexity involved in generating the AR function for different Doppler spread and sampling is demonstrated and its complexity varies exponentially with the selection MIMO configuration also discussed.

MIMO is an enabling technology in order to meet the growing demands for higher capacity and more reliable transmissions over harsh HF channels. The channel model needed in the development of a MIMO-HF system has to represent the signal dispersion in the three dimensions namely, angular, delay and Doppler domain, representing phase, time and frequency, respectively, and it appeared to be not available in open literature. This chapter proposes the formulation of an analytical model for the MIMO-HF channel. The validity of the proposed model to characterize the MIMO-HF channel has been established through extensive numerical simulations. The desirable feature of reduced computational complexities associated with the AR model in the characterization of HF channel has been established through an extensive simulation exercise involving varying combinations of channel parameters and sampling frequency with both SISO and MIMO configurations.

CHAPTER 5

MIMO-HF CHANNEL ESTIMATION BASED ON PARTICLE FILTERING

In a MIMO-HF system, the channel parameter estimation is crucial for the process of detection of the originally transmitted signal/data [Alvarez 2011]. Varieties of equalization and signal detection techniques have been developed for MIMO systems. The applicability of a particular signal detection technique is developed to suit a specific mode of MIMO operation, namely diversity or spatial multiplexing or combined. Regardless of the mode of MIMO system operation, most of the equalization/detection schemes require knowledge of the Channel State Information (CSI) to recover the original transmitted signal. With the usual assumptions associated with the channel estimation techniques, such as linearity, time invariance and near flat fading, it is more realistic to look for an efficient method of approximating the channel as closely as to the ideal one between the transmitter and receiver. Estimation of CSI is an essential component of the receiver design. Further, the efficiency of CSI estimation can affect the performance of the system in two different ways. It can introduce a channel estimation error leading to increased BER, which in turn affects the channel capacity. Also, the dedicated fractional bandwidth of the system for the transmission of pilots or training symbols is dependent on both the channel condition as well as the invoked CSI estimation technique.

The channel parameters that characterize the channel conditions will have effect on the transmission of the data. The effects of channel conditions on the transmitted data must be estimated in order to recover the transmitted information correctly. Often, the estimation of channel parameters is based on an approximate underlying channel model for the radio wave propagation. The receiver can precisely recover the transmitted data/information as long as it can keep track of the varying channel models. Earlier chapter 4 presented a detailed discussion on channel models for both SISO and MIMO-HF communication system.

There are the three main strategies for the design of channel estimation algorithms:

(1) **Supervised or training (Pilot) based methods:** A set of known information symbols are sent over the channel so that the receiver can estimate the channel.

(2) **Blind techniques**: The channel parameters are recovered from the statistical properties of the received information symbols up to some kind of ambiguity. A reduced number of training symbols is usually still needed to obtain an estimate.

(3) **Semi-Blind channel estimation**: A training matrix is used to allow a first estimate, which is improved using statistical properties of the received signal or information from already detected symbols.

Channel estimation based on supervised method for signal detection algorithms require the knowledge of channel impulse response, which is usually estimated by using the known training (mid-amble) symbols in the middle of the transmission burst. In HF environment the channel is time-variant, which makes the estimation task more difficult. In any communication wireless system and its derivatives, the time period between the transmission bursts is so long that the channel changes significantly from burst to burst and thus a separate channel estimation is needed for each individual burst. On the other hand, the channel effects during the short burst period are assumed to exhibit lesser variation, hence it is reasonable to assume block fading channel characteristics implying that the channel is assumed to be time-invariant during the burst, but is changing between the bursts.

In channel estimation theory, there are two general types of estimation approaches:

1) Classical estimation, and

2) Bayesian estimation.

In the classical estimation, the vector (received time samples) to be estimated is viewed as deterministic but unknown . The estimate is determined based on the Probability Density Function (PDF) of the received samples. In Bayesian estimation, the unknown vector is regarded as a random vector and prior information such as the mean, variance, and *a priori* PDF is used to determine the estimate.

Several pilot symbols assisted channel estimation schemes such as linear least squares (LS), Minimum Mean-Square-Error (MMSE) scaled LS and relaxed MMSE have been introduced in [Bazzi 2010] for providing the MIMO receivers with the CSI for large

diversity and multiplexing gains. Other channel estimation methods are based on the adaptive filters including Least-Mean-Square (LMS), Extended Kalman Filter (EKF) and Recursive-Least-Square (RLS) [Haykin 1996]. Because the channel estimation methods based on adaptive filters are almost linear tracking methods, these linear methods cannot track or estimate non-linear introduced by system and non-Gaussian-noised wireless channel perfectly. As a result, Particle Filtering (PF) [Gordon 1993] is emerging as a powerful method for sequential signal processing with a wide range of applications in science and engineering [Djuric 2003]. PF is a Sequential Monte Carlo (SMC) methodology [Wang 2004] where the basic idea is the recursive computation of relevant probability distributions using the concept of important sampling and approximation of probability distributions with discrete random measures.

A channel estimation method using PF for MIMO systems is presented in [Huber 2003]. The method uses PF to track channel under the assumption that the receiver has precise knowledge of the realization of the fading AR channel [Haykin 1996]. A channel tracking method using PF is proposed in [Chin 2002].

Accurate knowledge (or good estimate) of the underlying channel is essential for mitigating the effect of multipath and fading. If the channel estimates are not reliable, the performance of algorithms such as equalization and detection at the receivers degrade significantly. The overall performance of HF system has significant dependence on effective utilization of resources. The critical utilization of resources depends on the choice of channel estimation technique and the estimation technique must prevail even under adverse channel conditions such as non-linear, time varying and non-Gaussian noise environments. In view of these considerations and the inability of the conventional estimation techniques to fulfil the requirements of the context, an alternative approach to develop adaptive channel estimation technique for the HF channel invoking the principle of Bayesian forecasting will be of practical importance and relevance. Channel estimation based on PF is an ideal choice to deal with non-linear and non-Gaussian scenarios [Bergman 1999, Arulampalam 2002, and Doucet 1998]. Reported research in [Haykin 2004] revealed the performance improvement of PF for MIMO wireless channel above

UHF band. This chapter investigates channel estimation technique based on PF for time varying HF channel to counter the effect of channel impairment along with non-linear and non-Gaussian noise conditions. The chapter also addresses the application PF based estimation technique applicable to MIMO-HF channel also which seems to have not been attempted in open literature thus far. Although one can conceive an idea of invoking the PF concept of devoid of EKF, this chapter attempts to adopt a unified approach wherein PF and EKF schemes have been combined to realize better posterior density functions. The expected improvement in the receiver performance evaluated through the system parameters like data rate and reliability is also addressed in this chapter.

In this chapter both classical and Bayesian approaches to estimate the channel impulse response are presented. Recursive Least Squares (RLS) channel estimator is derived based on classical supervised methods are discussed. PF which falls under supervised Bayesian approach are discussed. However, the main emphasis of this chapter is on PF technique which falls under supervised Bayesian approach, which improves estimation accuracy by exploiting some prior knowledge of channel vector and even under adverse channel conditions such as non-linear, time varying and non-Gaussian noise environments.

5.1 Recursive Least Squares (RLS) Estimation

A simplified MIMO communication system with M_t transmits antennas and N_r receiver antennas to represent the channel estimation block is shown in Figure 5.1.

The Space-Time (S-T) modem at the transmitter (Tx) encodes incoming bit stream b_t using Alamouti's code. The information bits are modulated and signal is mapped for space and time across M_t transmit antennas is represented as vector s_t of dimension M_t .Thereafter, the S-T modem at the receiver (Rx) processes the received signal y_t of vector dimension N_r which is subjected to time-varying ionospheric (HF) fading channel represented by matrix H_t of dimensions N_r x M_t. The received signal will be decoded on each of the N_r receiver antennas according to the transmitter's signalling strategy and estimated information bit $\hat{b}_t$ is recovered based on the channel estimation $\hat{H}_t$ and detection process.

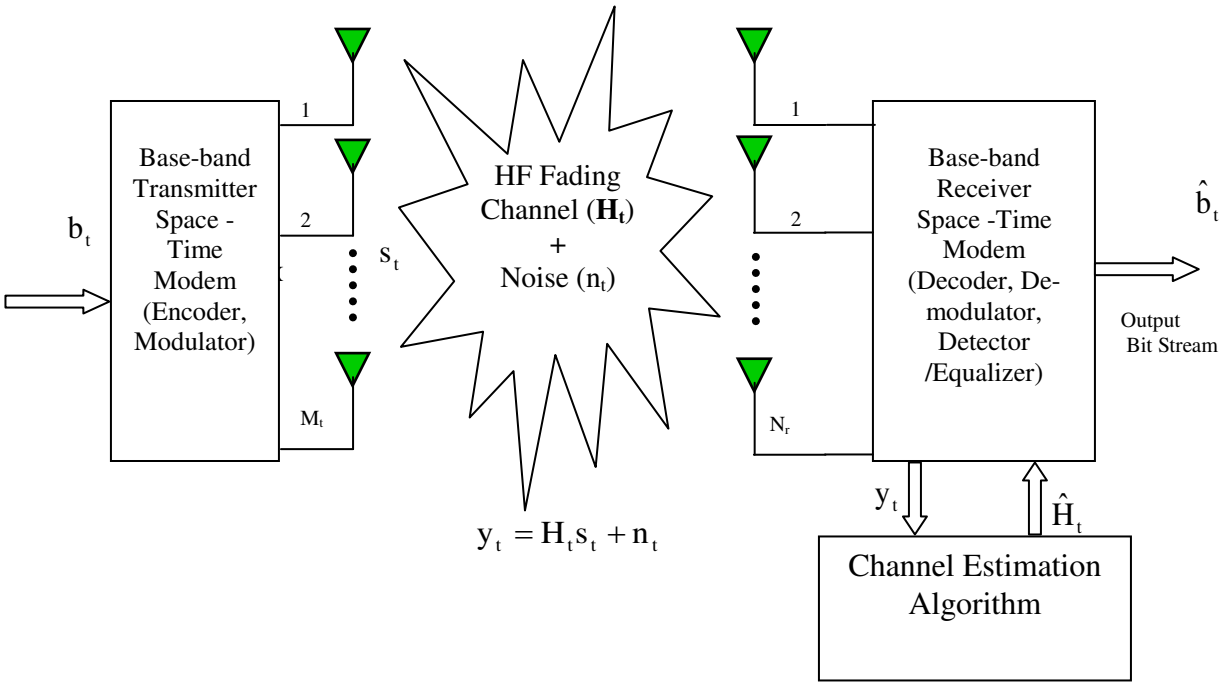

Figure 5.1: Simplified block diagram of MIMO-HF system to illustrate channel estimation scheme

The received signal at time instant t is represented as

$$y_t = H_t s_t + n_t \tag{5.1}$$

Where,

y_t is the received signal vector

H_t is the channel matrix

s_t stands for the transmitted signal vector

n_t denotes the noise vector

Recursive Least Squares (RLS) is an adaptive filter technique based on weighted linear least squares. RLS recursively finds the filter coefficients that minimize the cost function relating to the input signals. The cost function (C_t) is defined as weighted average of error squares and is represented at the time instant t as follows,

$$C_t = \sum_{k=1}^{t} \lambda^{t-k} \|y_k - H_t s_k\|^2$$

$$= \sum_{k=1}^{t} \lambda^{t-k} \left[(y_k - H_t s_k)^H (y_k - H_t s_k)\right], \tag{5.2}$$

Where,

λ is the forgetting factor (which assigns exponentially lesser weight to older error samples)

superscript *H* denotes the conjugate transpose operator.

k represent delay time index

The objective of channel estimation $\hat{H}_t$ is to minimize the Euclidian cost function $\|y_k - H_t s_k\|^2$. Therefore gradient of cost function of Equation (5.2) is calculated with respect to channel matrix and is given as

$$\frac{1}{2}\nabla_{H_t} C_t = \sum_{k=1}^{t} \lambda^{t-k}\left[\left(y_k - \hat{H}_t s_k\right)s_k^H\right] = 0, \tag{5.3}$$

Where,

$\hat{H}_t$ is estimate of H_t.

Equation (5.3) is evaluated for $\hat{H}_t$ as,

$$\hat{H}_t = \left(\sum_{k=1}^{t} \lambda^{t-k} y_k s_k^H\right)\left(\sum_{k=1}^{t} \lambda^{t-k} s_k s_k^H\right)^{} \tag{5.4}$$

Let $P_t = \left(\sum_{k=1}^{t} \lambda^{t-k} s_k s_k^H\right)$

$$Q_t = P_t^{-1}$$

$$R_t = \left(\sum_{k=1}^{t} \lambda^{t-k} y_k s_k^H\right)$$

$$\hat{H}_t = R_t Q_t \tag{5.5}$$

The Equation (5.5) is solved iteratively as follows

$$\begin{aligned} P_t &= \lambda P_{t-1} + s_t s_t^H, \\ R_t &= \lambda R_{t-1} + y_t s_t^H, \end{aligned} \tag{5.6}$$

Where Q_t is calculated iteratively by using the matrix inversion lemma [Karami2006] and can be written as

$$Q_t = \lambda^{-1} Q_{t-1} - \frac{\lambda^{-2} Q_{t-1} s_t s_t^H Q_{t-1}}{1 + \lambda^{-1} s_t^H Q_{t-1} s_t}. \tag{5.7}$$

As can be seen from Equation (5.7), the RLS algorithm assigns more weight to the current observations due to the forgetting factor λ. The RLS algorithm is also featured with faster convergence. The RLS algorithm is also very useful in applications where the environment varies randomly [Apolinário 2009] and is thus an appropriate choice for algorithms for HF channel estimation.

5.2 MIMO Channel Estimation based on Particle Filtering

MIMO transceivers operating in a fading channel with M_t transmit and N_r receives antennas are depicted in Figure 5.2. The incoming data stream b_t is encoded multiplexed and transmitted across the wireless (HF) channel. The channel decoder, the predictor module and filter that collectively implement the channel-estimation algorithm iteratively process the received signal y_t. The role of the receiver is to produce an estimate of the transmitted symbols s (t). The receiver performs the estimation of the transmitted sequence in the presence of an unknown channel parameter.

The state space representation of base-band communications model for a fading channel [Djuric 2003] can be written as:

$$x_t = f_t(x_{t-1}, u_t)$$
$$y_t = H_t s_t + v_t, \quad (5.8)$$

Where, y_t denotes the discrete time signal, received at the receiver at time instant t.

x_t is the state of the system comprising vectors of transmitted symbols s_t

H_t is coefficient of fading channel of dimension N_r x M_t

Further for simplicity the column vector h_t and matrix H_t of dimension N_r x M_t is related through $h_t = Vec\,(H_t)$

f_t is a known function which transforms the information bits x_t to the symbol s_t

s_t is the transmitted symbol of dimension M_t x 1

u_t and v_t are additive channel noise

The state of the system varies in time according to a known function f_t. It describes a Markov process driven by the additive channel noise u_t and v_t.

From the received signal y_t, the channel is estimated or the transmitted symbols are detected sequentially. This implies obtaining estimates of $p(h_t, s_t \,|y_{0:t})$, where $y_{0:t} = \{y_0, y_1, y_2 \ldots \ldots y_t\}$.

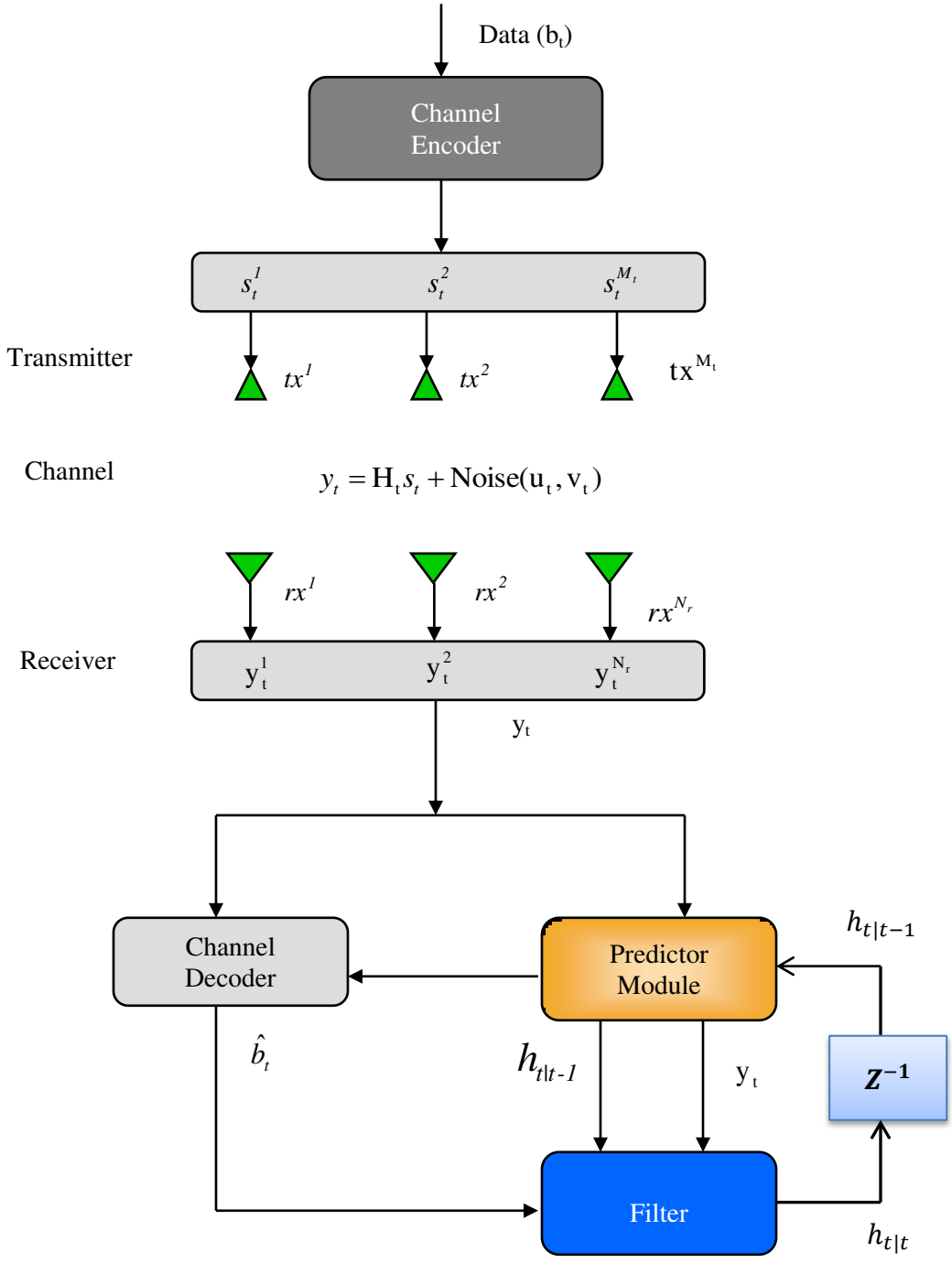

Figure 5.2: Proposed structure for HF channel estimation with multiple antennas

The signal y_t of Equation (5.8) can be rewritten as

$$y_t = x_t h_t + v_t, \tag{5.9}$$

Where x_t forms state sequence, which consists of transmitted symbol s_t and transition vector F (function of $f_t(t)$)

y_t forms observation sequence. Each state of y_t is represented by the previous M channel coefficients (h_t)

An important objective of the recursive estimation of Equation (5.9) is to infuse a level of confidence in accepting the validity of the channel coefficient h_t at time t, taking the past values of the given the data, $y_{1:t}$ up to time instant t. Thus recursive estimation demands the probability density function (pdf) $p(h_t, x_t \,|y_{0:t})$

Since the channel estimation essentially involves the estimation of the coefficient h_t, the pdf can be represented with a compact notation of $p(h_t \,|y_{0:t})$. It is assumed that the initial pdf is of the form $p(h_0|y_0) \equiv p(h_0)$.The pdf $p(h_t \,|y_{1:t})$ may be obtained recursively in two stages, namely the prediction and the update.

The prediction stage involves using the system Equations (5.8) and (5.9) with the assumption that pdf $p(h_{t-1} \,|y_{1:t-1})$ at time $t-1$ is available. The update state h_t will evolve over time t via the Chapman–Kolmogorov equation

$$p(h_t|y_{t-1}) = \int p(h_t|h_{t-1})\, p(h_{t-1}|y_{t-1})\, dh_{t-1} \tag{5.10}$$

Where $p(h_t \,|h_{t-1})$ describes how the state density y_t evolves with time t, and is defined by the state Equation (5.8). When the current observation y_t becomes available, prior pdf of Equation (5.10) gets updated through Bayes' rule resulting in

$$p(h_t|y_t) = \frac{p(y_t|h_t)\, p(h_t|y_{t-1})}{\int p(y_t|h_t)\, p(h_t|y_{t-1})\, dh_t} \tag{5.11}$$

Where $p(y_t \,|h_t)$ is the likelihood of receiving the observation y_t, given the state h_t. The denominator term in Equation (5.11) is necessary in order to keep the new estimate of the posterior properly normalized such that $\int p(h_t|y_t) dh_t = 1$, for all t. From the distribution function of Equation (5.11), channel estimate $\hat{h}_t$ can be obtained. In order to recursively evaluate the updates, the technique of importance sampling, is utilized, which is a general Monte Carlo (MC) method for sequential MC filters [Djuric 2003, Arulampalam 2002].

The concept of importance sampling is to represent the required posterior density function by a set of weighted particles:

$$p(h_t|y_t) \approx \sum_{l=1}^{L} w_t^l \delta(h_t - h_t^l) \tag{5.12}$$

Where L is the number of particles

$\delta(\cdot)$ denotes the Dirac delta function

h_t^l is the state of particle at time t.

The weights w_t^l are normalized such that at each time t.

$$\sum_{l=1}^{L} w_t^l = 1. \tag{5.12a}$$

As the number of particles increases to the larger value, the approximation in Equation (5.12a) converges to the true posterior pdf.

Proposal distribution $q(.)$ is a known distribution from way new particles are drawn and is given by

$$h_t \sim q(h_t|h_{t-1}^l, y_t) \tag{5.13}$$

In order to increase the sampling efficiency, extended Kalman filter is taken as the proposal distribution [Lee 2005].

Following the selection of the particles from Equation (5.13), the weights w_t^l for $l = 1.....L$ at time t are sequentially updated as follows [Djuric 2003],

$$w_t^l = w_{t-1}^l \frac{p(y_t|h_t^l)\, p(h_t^l|h_{t-1}^l)}{q(h_t^l|h_{t-1}^l, y_t)} \tag{5.14}$$

To monitor the degeneracy of weight or sample impoverishment, a measure called the effective sample size $\hat{N}_{eff}$ is adopted as defined in [Doucet 1998],

$$\hat{N}_{eff} = \frac{1}{\sum_{l=1}^{L} (w_t^l)^2} \tag{5.15}$$

Whenever $\hat{N}_{eff}$ is below a predefined threshold NT (typically NT = 2/3 L), a re-sampling procedure is performed. In particular, particles with low weights are discarded to form a subset of particles $\{h_t^p\}$. New particles $\{h_t^l\}$ are generated by re-sampling with

replacement particles from the subset $\{h_t^p\}$ with probability $Pr(h_t^l = h_t^p) = w_t^p$ to keep the parameter L constant. Now, the weights must be normalized by resetting them to $w_t^l = 1/L$. In a sequential filtering framework, the re-sampling procedure is almost inevitable. Re-sampling also introduces increased random variation into the estimation procedure. The channel estimation algorithm using PF can be succinctly summarized as follows.

For time steps t, t + 1, t + 2…

i) Starting from posterior estimate $p(.)$ for time t – 1, the mean and variance of posterior density function $N(m_{t-1}, P_{t-1})$ with mean m_{t-1} and variance P_{t-1} .

ii) The prior distribution is updated and then prediction is performed.

$$N(m_{t-1}, P_{t-1}) \rightarrow N(\hat{m}_t, Q_t) \tag{5.16}$$

Where estimated mean, $\hat{m}_t = m_{t-1}$ (5.17)

The variance of update with the process noise variance of σ_v^2

$$R_t = P_{t-1} + \sigma_v^2 I \tag{5.18}$$

The updated variance with the measurement noise of variance σ_u^2

$$Q_t = R_t + \sigma_u^2 I \tag{5.19}$$

$u_t = N(0, \sigma_u^2)$ is process noise.

$v_t = N(0, \sigma_v^2)$ is measurement noise.

iii) Posterior estimate for time t:

$N(m_t, Q_t) \rightarrow N(m_t, P_t)$

Where, $m_t = \hat{m}_t + R_t Q_t^{-1}[\hat{h}_t - (\hat{h}_{t-1} + \hat{m}_t)]$ (5.20)

The posterior variance is obtained through $P_t = R_t Q_t^{-1} \sigma_u^2$ (5.21)

The limiting behaviour of the recurrence relations of Equations (5.16) through (5.19) can be modified using convergence results as shown below.

$$t \rightarrow \infty, \begin{cases} K_t \overset{\Delta}{=} R_t Q_t^{-1} \rightarrow K \\ P_t \rightarrow P = K\sigma_u^2 \end{cases} \tag{5.22}$$

$$K = \frac{\alpha\left(\sqrt{1 + 4/\alpha} - 1\right)}{2} I = \xi I \tag{5.23}$$

$$\alpha = \frac{\sigma_v^2}{\sigma_u^2} \tag{5.24}$$

ξ denotes rate of adaptation and takes the value $0 \le \xi \le 1$.

iv) Once m_t and P_t are found out, the channel estimation h_t is performed using the method of importance sampling to predict the state density $p(h_t | y_{0:t})$, by propagating particles ℓ = 1, ..., L, from time t −1 to t using Equations (5.20) and (5.21),

$$h_t^l = h_{t-1}^l + \mu_t^l + n_t^l \tag{5.25}$$

Where $\mu_t^l = \mathrm{N}(m_t, P_t)$, n_t^l = noise variance.

5.3 Performance Comparison for MIMO-HF Channel Estimation under Non-Linear and Non-Gaussian Conditions

Achieving reliable communication over HF channels is known to be challenging particularly due to the hostile propagation medium. To tackle this problem, diversity techniques were shown to be promising. This section demonstrates through simulation results the benefits of diversity strategies when applied to MIMO. The performance gains in terms of capacity and Mean Square Symbol Error Rate (SER) are quantified using MIMO configuration in evaluating the channel estimation algorithm. MIMO-HF communication system adopted for performance analysis in this section is shown in Figure 5.3.

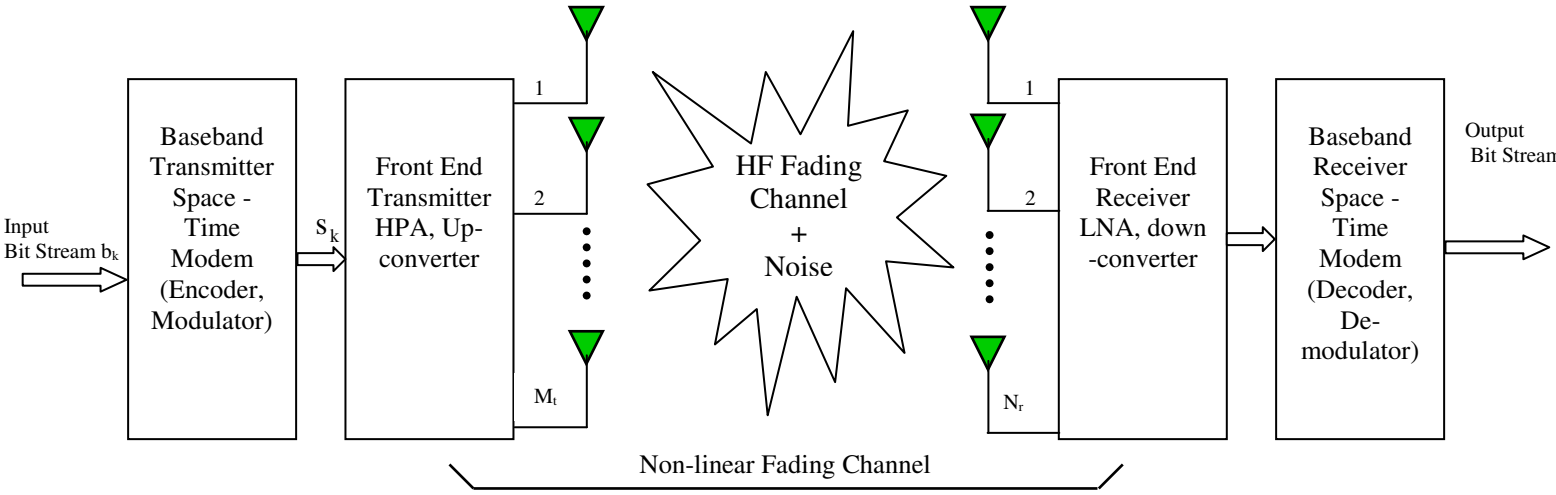

Figure 5.3: shows the system model adopted for performance analysis

The system consists of M_t transmits antennas with both base-band signal processing and front end transmitter. In base-band signal processing the information bit stream b_k at time k instant of bandwidth W, is encoded to symbol based on modulator selection In this thesis Binary or Quadrature Phase Shift Keying (BPSK/QPSK) is adopted for simulation. Then Space-Time (S-T) modem at the transmitter (Tx) encodes incoming symbol stream m_k to STBC using Alamouti's codes [Alamouti 1998] to represent as s_k. These symbols streams are further processed in front end transmitted for up-converting to desired transmitted frequency (3-30 MHz) and power level. Front end transmitter module consists of up-converter and high power amplifier module. For simulation purposes the front end module can be used or intermediate frequency of base-band signal without operating at high frequency and high power amplifier module is sufficient to realize the system. The impairment effects can comprise of:

i. Sensitivity
ii. Image rejection due to I/Q imbalance,
iii. Non-linear distortion due to power amplifier at the transmitter as well as Low Noise Amplifier (LNA) and mixer at the receiver
iv. Phase noise originating from random fluctuations or instability of the oscillators

For the purpose of simulation, the signal that is processed at the base band frequency at the transmitter block is subjected the HF channel model along with the collective impairments cited above. Therefore the resulting signal is considered to have been subjected to both the multipath fading channel and the cited impairments.

At the base-band receiver after processing at front end receiver N_r block, the signal is down converted to IF which is same as operating frequency of transmitted signal. Thereafter, the S-T modem at the receiver (Rx) processes the received signal which is subjected to time-varying ionosphere fading along with Inter Symbol Interference (ISI) effect. The received signal will be decoded on each of the N_r receiver antennas according to the signalling strategy of transmitters. The observed signal from i^{th} receiver at the discrete time index k is

$$r_k^i = \sum_{j=1}^{M_t} h_k^{i,j}(k,\tau) s_k^j + w_k^i, \qquad i = 1, \ldots\ldots\ldots\ldots N_r \tag{5.26a}$$

Let $x_k^i = \sum_{j=1}^{M_t} h_k^{i,j}(k,\tau) s_k^j$

$$r_k^i = tanh\left(x_k^i\right) + w_k^i, \tag{5.26b}$$

$$r_k^i = x_k^i + 0.2\left(x_k^i\right)^2 - 0.1\left(x_k^i\right)^3 + w_k^i, \tag{5.26c}$$

Where,

s_k^j is the transmitted symbol in the time index k,

τ is the delay variable,

$h_k^{i,j}(k,\tau)$ is the channel impulse response between j^{th} transmitter and i^{th} receiver of MIMO channel with correlated Rayleigh processes whose Doppler spectrum is characterized by Gaussian Shape [Watterson 1970, Mastrangelo 1997].

w_k^i represent noise factor either Gaussian or non-Gaussian

A model adopted for the simulation to evaluate the performance of complete base-band system is shown in Figure 5.4. The model consists of the following blocks,

- Channel simulation block
- Base-band transmitter simulation block
- Non-linear system impairment
- Base-band receiver simulation block
- Performance metric

The following section presents a detailed discussion about the individual blocks adopted for simulation

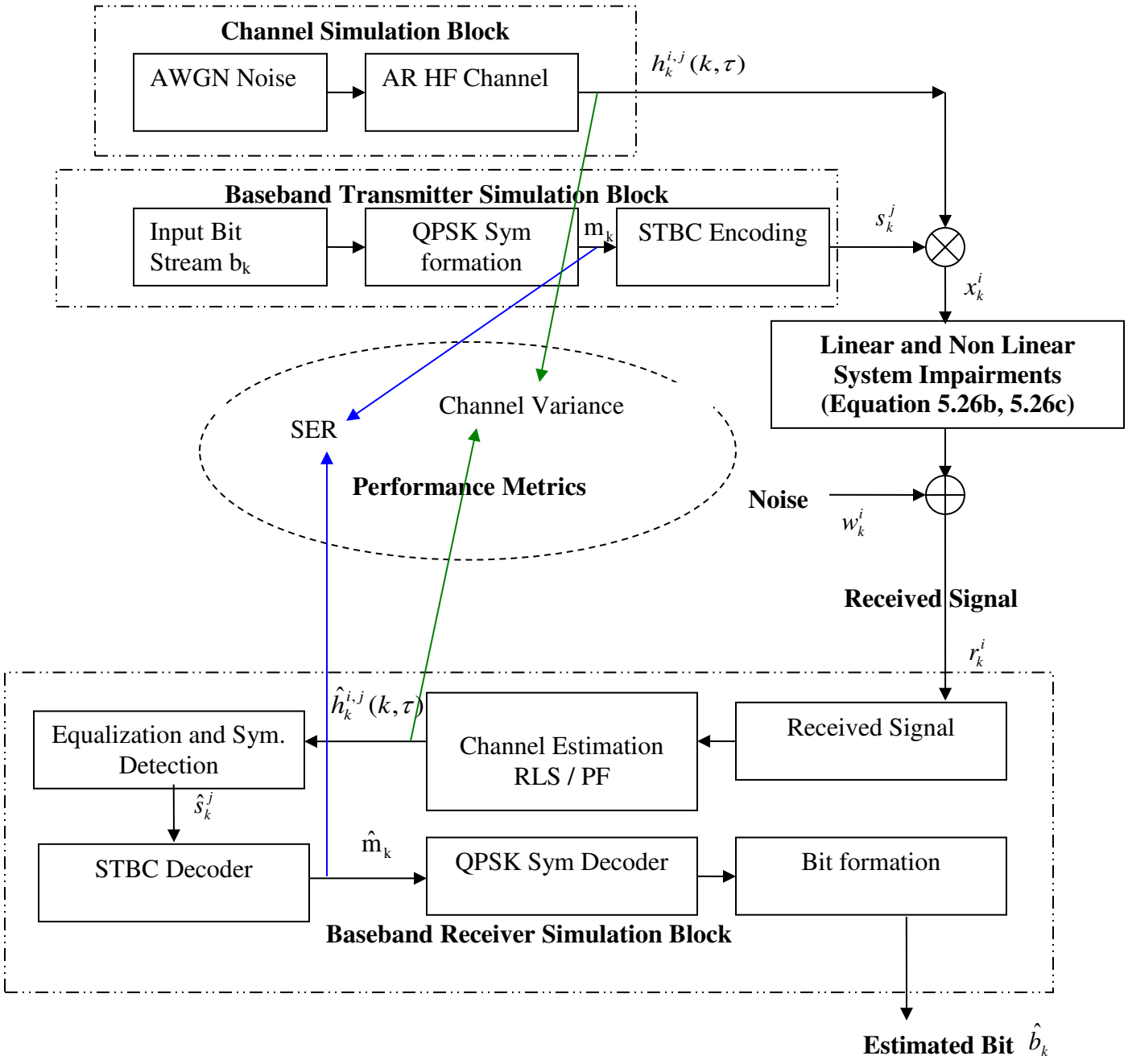

Figure 5. 4: Simulation Model for Performance Evaluation of Channel Estimation

5.3.1 Channel Simulation Block

In this block channel model is characterized based on HF fading channel parameters as discussed in chapter 4. The channel simulation consists of two blocks namely AWGN generation and AR channel filter. The input to AR channel filter is random time-varying AWGN subjected to AR HF channel model. The AR filter model is realized to characterize HF channel in terms of delay spread and Doppler spread based on the selection of parameters required for simulation. The output of this block is represented by the signal $h_k^{i,j}(k,\tau)$ that is multiplicative with modulated signal s_k^j to introduce the HF channel impairments (multipath fading).

5.3.2 Noise Simulation Block

The additive noise (w_k^i of Equation (5.26a)) can be modelled either as a complex-Gaussian distribution $p(z) = N(z: 0, \sigma_w^2)$ with argument z, zero mean, and variance σ_1^2, or as the Middleton class-A noise model [Wang 2004]. This latter model has been used to model the impulsive noise commonly generated in wireless environment [Wang 2004]. The probability density function of the noise model of [Wang 2004] is given by:

$$p(z) = (1-\varepsilon)N(z: 0, \sigma_1^2) + \varepsilon N(z: 0, \sigma_2^2) \tag{5.27}$$

Where $0 \leq \varepsilon \leq 1$. The first component $(1-\varepsilon)N(z: 0, \sigma_1^2)$ represents the ambient background noise with probability $(1-\varepsilon)$, while $\varepsilon N(z: 0, \sigma_2^2)$ denotes the presence of an impulsive component occurring with probability ε. In order to maintain a constant noise variance σ^2 for a particular Signal to Noise Ratio (SNR), the parameters ε, noise variance σ_1^2 and σ_2^2 are varied such that

$$\sigma_w^2 = (1-\varepsilon)\sigma_1^2 + \varepsilon\,\sigma_2^2 \tag{5.28}$$

If $\sigma_2^2 = 0$, then noise model represented through Equation (5.28) reverts to the usual Gaussian distribution.

5.3.3 Transmitter Simulation Block

From either a data or image file, the bit sequence b_k is generated by the information source in the form of binary bit which contains information to be communicated. After the encoding and Digital modulation (BPSK/QPSK), the bit sequence becomes the symbol stream (m_k). Modulation is the process that converts bit sequences to symbols, which are more amenable for transmission. Different modulation schemes enable trade-off between BER and rate of transmission. Modulation schemes supported in this simulation are BPSK and QPSK. The modulated symbols m_k are further processed in STBC encoder [Alamouti 1998] based on the antenna configuration to represent symbols s_k^j. In the simulation either 2x2 or 4x4 MIMO configuration is considered. The signal s_k^j which is subjected to multiplicative fading channel variations where the amplitude and phase are modified according to the random time varying phenomenon of HF channel parameter and the resulting signal are represented as x_k^i.

5.3.4 Non-Linear System Impairment

The signal x_k^i is subjected to either linear or non-linear impairment of front end (RF block) of Transceiver system. For the non-linear scenario, the signal x_k^i is model through Equations (5.26b) and (5.26c) before its passage through noise block detailed under section 5.3.2. The non-linear model of impairments caused by RF (front end) module is characterized according to the parameters such as level of non-linear distortion, phase noise and sensitivity which are required to analyse the performance of the system.

5.3.5 Base-band Receiver Simulation Block

The goal of base-band receiver blocks is the recovery the transmitted information bit (b_k). With the received signal at the receiver as input r_k^i , initial channel estimation is performed to know the impairment caused by HF channel on the transmitted symbol (s_k). Channel estimation $\hat{h}_k^{i,j}(k,\tau)$ parameter is used by equalization block to perform the inverse operation of channel impairments to recover the symbol $\hat{s}_k^j$ where j is the index for receiver antenna. The detected symbol $\hat{s}_k^j$ is performed by STBC decoder and QPSK

decoder to obtain $\hat{m}_k$. The estimated decoded mapper symbol $\widehat{m}_k$ is converted to estimated information bit $\hat{b}_k$.

5.3.6 Performance Metrics

To evaluate the validity of simulation of individual system blocks of Figure 5.3, and also to evaluate the performance of complete system against various impairments occurred during transmission of signal, key and appropriate performance metrics have been identified. The identified performance metrics facilitate the evaluation of the system performance under near practical conditions. The following system performance parameters have been considered in the simulation study.

- Channel variance
- Symbol Error Rate (SER)
- Capacity and Reliability

The choice of the identified metrics is conforming to the main emphasis (focus) of this thesis. In this thesis, the focus is mainly on channel characterization (analysis of impairments) and estimation (recovery of transmitted signal). The effectiveness of channel estimation algorithm with the consideration of channel impairments is measured through SER or BER. The SER defines mean square difference between encoder mapper symbols m_k and estimated symbols $\widehat{m}_k$ before mapper decoder. Whereas BER defines mean square difference between information bits b_k and estimated information bits $\hat{b}_k$. Channel variance is a measure of the accuracy of the channel estimation algorithm. Channel variance is a measure of the variance between channel model signal $h_k^{i,j}(k,\tau)$ and the estimated channel signal $\hat{h}_k^{i,j}(k,\tau)$.

Channel capacity defines the maximum data rate of transmission over a given channel. Capacity depends on the channel parameters and is given as

$$C = E\left[log_2 \, det\left(I_N + \frac{\rho}{M} HR_{ss} H^H \right) \right] \text{ bps/Hz} \qquad (5.29)$$

Where

E (.) denotes Expectation

ρ is referred as signal to noise ratio (SNR)

M is transmit antennas and N is receive antenna

H represents the channel matrix of dimension NXM at time index k.

R_{ss} is auto- covariance of symbol transmitted s_k^j

det (.) denotes determinant of matrix.

Superscript *H* represents Hermitian transpose

I_N is unity matrix of order N

As mentioned in Equation (5.29), the channel capacity depends on channel $h_k^{i,j}(k,\tau)$ and accuracy of estimated channel $\hat{h}_k^{i,j}(k,\tau)$. If channel is estimated exactly or it's near equivalence, the estimated symbol $\hat{s}_k^j$ will be same as transmitted symbol s_k^j. Hence auto-correlation factor R_{ss} increases. Also with known channel matrix *H,* the capacity C increases.

The term "reliability" refers to the degree of uninterrupted operation of communication links available to user during the course of signal transmission. This reliability of communication link depends on the accuracy and effectiveness of the chosen algorithms for various communication blocks in the receiver. Channel estimation algorithm is one such critical subsystem of a receiver block to counter the effect of channel impairments on the receiver performance. The development of channel estimation algorithms is a challenging task in the receiver design since the accuracy of the channel estimation technique plays a major role in determining both the capacity and reliability of communication link (system).

The above mentioned performance metrics (Channel variance, SER, Capacity and Reliability) are evaluated under on various conditions as discussed below.

Table 5. 1 Performance Metrics Evaluated under Various Conditions and Configurations.	
Channel impairments	Linear
Channel impairments and front end (RF) system impairments	Non-linear
Fading	Slow and fast ,
Noise	Gaussian and non-Gaussian
Antenna configuration	SISO and MIMO
MIMO configuration	2x2 and 4x4

The simulation study is also based on the following assumptions.

- Channel variation is quasi stationary during training period.
- Boundary detection is known
- Time and frequency synchronization is ideal

5.3.7 Input Parameters for Simulation Study

- **Channel Model**

i) HF Channel with three independent multipath using AR Filter of order 3
ii) Coefficient of the AR Filter is modeled as HF fading
iii) Power attenuation of 3 paths are 0, - 8, -10 dB respectively.
iv) Doppler spreads: 0.1 to 10 Hz

- **Noise Model**

For the noise model, $\varepsilon = 0.1$, $\sigma_2^2 = 10\sigma_1^2$ in Equation (5.28)

- **Channel Estimation Algorithms**

RLS and PF-EKF with particle length of 30.

- **MIMO Encoding Space Time Block Code (STBC) Matrix:**

For 2x2 MIMO configurations, STBC matrix is

$$A_{2x2} = \begin{bmatrix} s_1 & -s_2^* \\ s_2 & s_1^* \end{bmatrix} \tag{5.30}$$

Where s_1 and s_2 are QPSK symbol. Symbols [s_1 s_2] are transmitted over two antennas at time slot t_1 and Symbols [$-s_2^*$ s_1^*] are transmitted over two antennas at time slot t_2.

STBC matrix for 4x4 MIMO configurations is

$$A_{4x4} = \begin{bmatrix} s_1 & -s_2^* & s_1 & -s_2^* \\ s_2 & -s_1^* & s_2 & s_1^* \\ s_3 & -s_4^* & -s_3 & s_4^* \\ s_4 & s_3^* & -s_4 & -s_3^* \end{bmatrix} \tag{5.31}$$

Where, s_1, s_2, s_3 and s_4 are QPSK symbols. The symbols $[s_1 \;\; s_2 \;\; s_3 \;\; s_4]$ are transmitted over four antennas at time slot t_1, similarly symbols of other columns are transmitted in respective time slots t_2, t_3 and t_4.

- **Non-linear System Impairment:**

The Non-Linear (NL) system impairment is modelled as

$$r_k^i = tanh(\, x_k^i \,) + w_k^i \tag{5.32a}$$

$$r_k^i = x_k^i + 0.2(\, x_k^i \,)^2 - 0.1(\, x_k^i \,)^3 + w_k^i \tag{5.32b}$$

- **Spatial correlation Matrix:**

Spatial correlation matrix for 2x2 and 4x4 MIMO is

$$R_{2x2} = \begin{bmatrix} 1 & \alpha \\ \alpha^* & 1 \end{bmatrix} \otimes \begin{bmatrix} 1 & \beta \\ \beta^* & 1 \end{bmatrix} \tag{5.33a}$$

$$R_{4x4} = \begin{bmatrix} 1 & \alpha^{1/9} & \alpha^{4/9} & \alpha \\ \alpha^{1/9^*} & 1 & \alpha^{1/9} & \alpha^{4/9} \\ \alpha^{4/9^*} & \alpha^{1/9^*} & 1 & \alpha^{1/9} \\ \alpha^* & \alpha^{4/9^*} & \alpha^{1/9^*} & 1 \end{bmatrix} \otimes \begin{bmatrix} 1 & \beta^{1/9} & \beta^{4/9} & \beta \\ \beta^{1/9^*} & 1 & \beta^{1/9} & \beta^{4/9} \\ \beta^{4/9^*} & \beta^{1/9^*} & 1 & \beta^{1/9} \\ \beta^* & \beta^{4/9^*} & \beta^{1/9^*} & 1 \end{bmatrix} \tag{5.33b}$$

Where, $\otimes$ represents the Kronecker product,

α, β are the spatial correlation, * is complex conjugate

5.4 Simulation Results and Analysis

5.4.1 Effect of Doppler Spread on HF Channel Model

The Time- amplitude spectrum of a HF channel with SISO configuration under a Doppler spread of 2 Hz with a sampling rate of 100 Hz The results of Figure 5.5a illustrates normally encountered deep fading at random time intervals with a fading rate ($f_D T_s = 0.02$) and deep fading being observed at 2.7s ,5.8s ,7.2s , 11.6s and 18s.

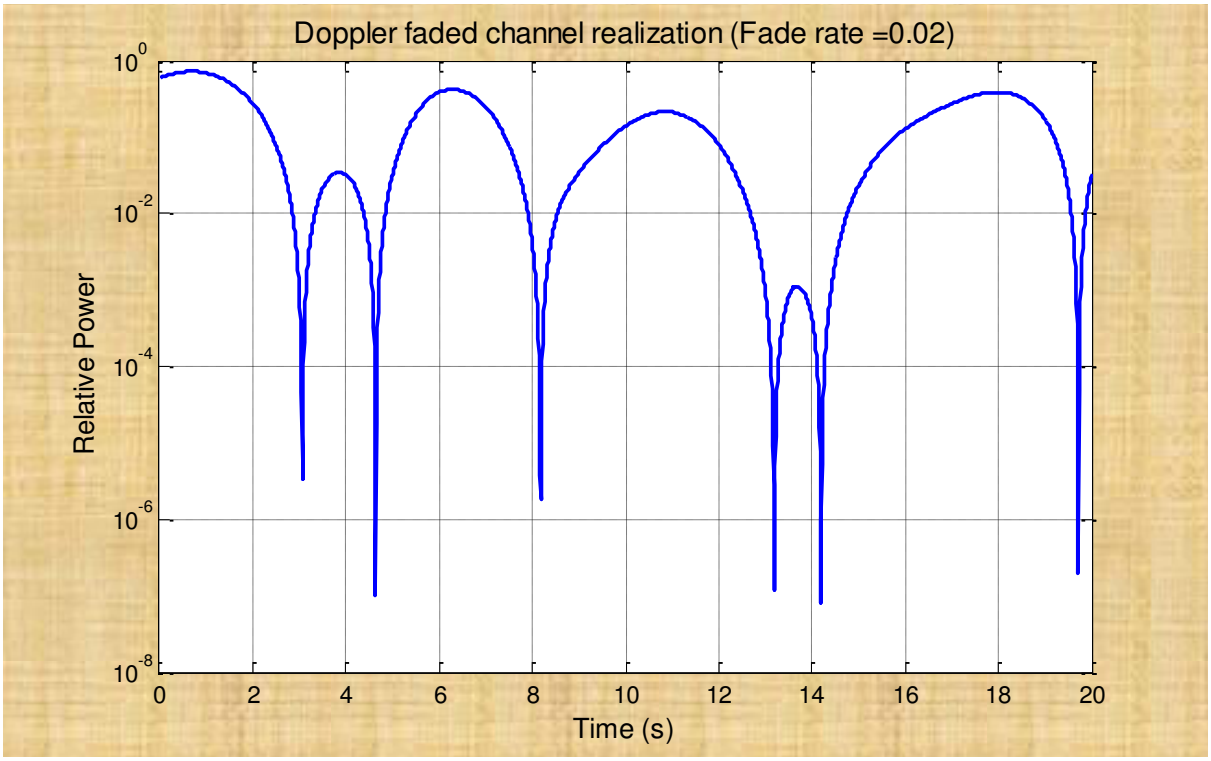

Figure 5.5(a):A typical Doppler faded channel realization at fade rate 0.02

Whereas amplitude spectrum with fading rate of 0.05 is shown in Figure 5.5b which corresponds to a Doppler spread of 5 Hz. As can be expected, one notices the rapidity in amplitude variations.

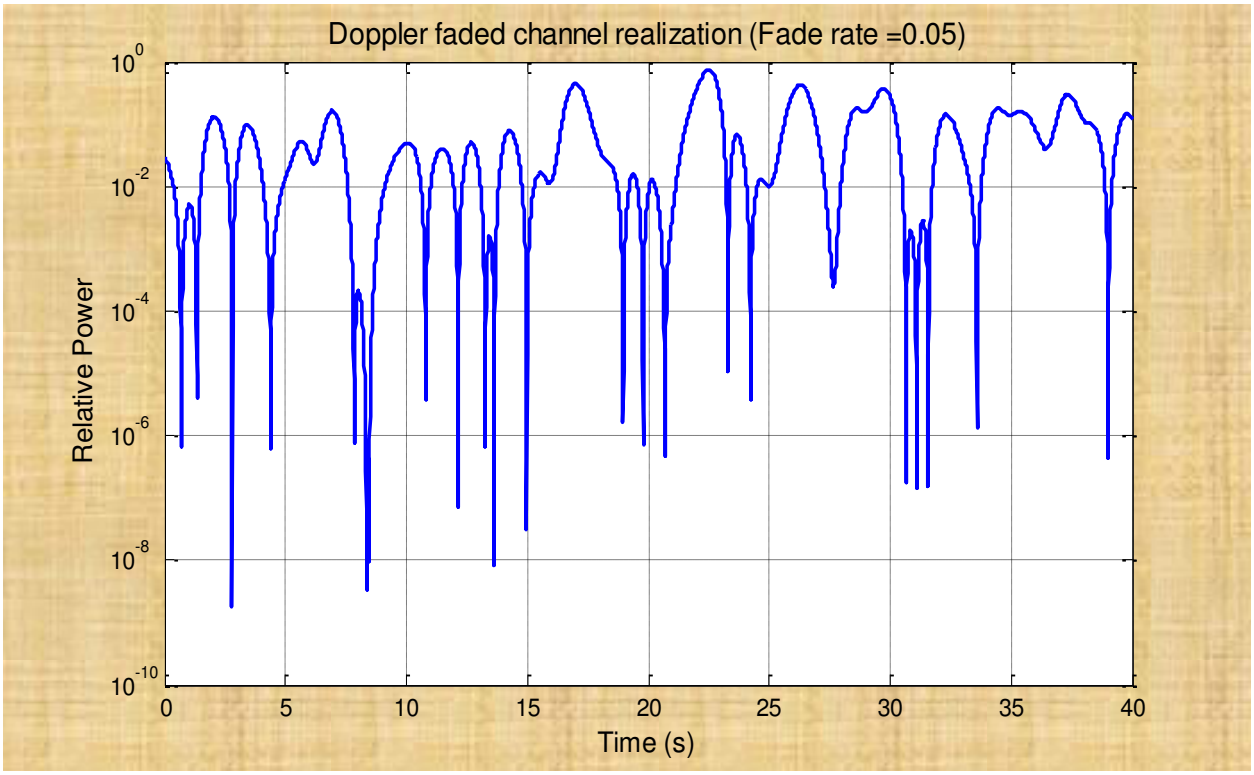

Figure 5.5 (b). A typical Doppler faded channel realization at fade rate 0.05

The time- amplitude spectrum of a HF channel with $2x2$ MIMO configuration under a Doppler spread of 2 Hz with a sampling rate of 100 Hz is shown in Figure 5.6a with fading rate ($f_D T_s = 0.02$). The results of Figure 5.6a illustrate the uncorrelated feature of random deep fading associated with 4 independent channel coefficients that characterize a rich scattering environment usually associated with HF channel.

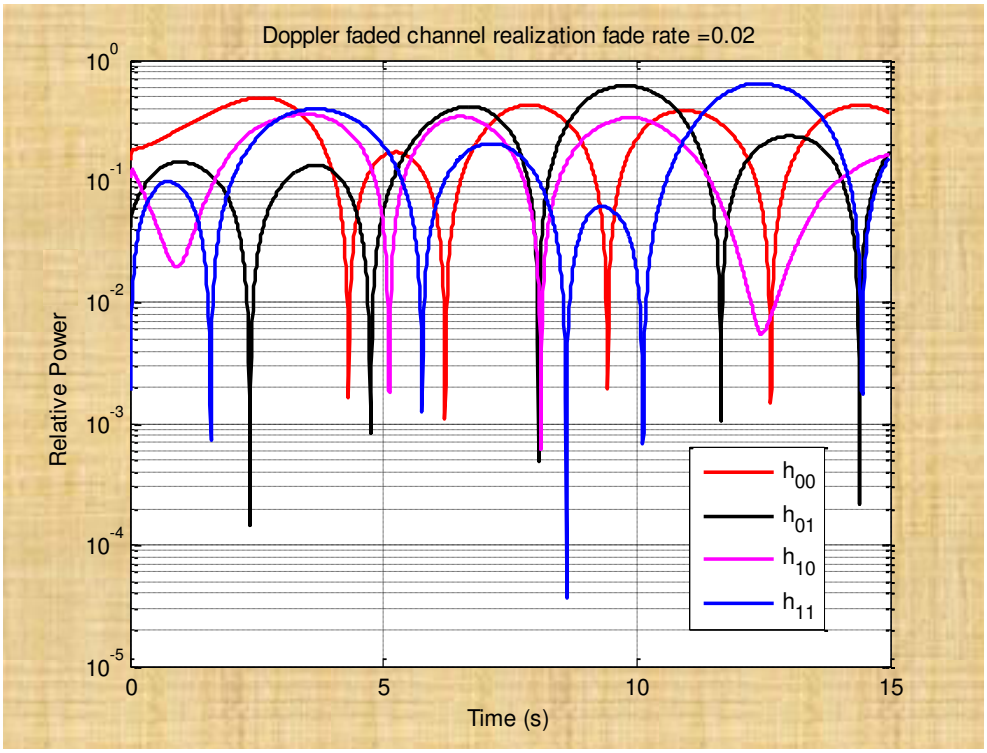

Figure 5.6(a): A typical Doppler faded channel realization for 2x2 MIMO at fade rate 0.02

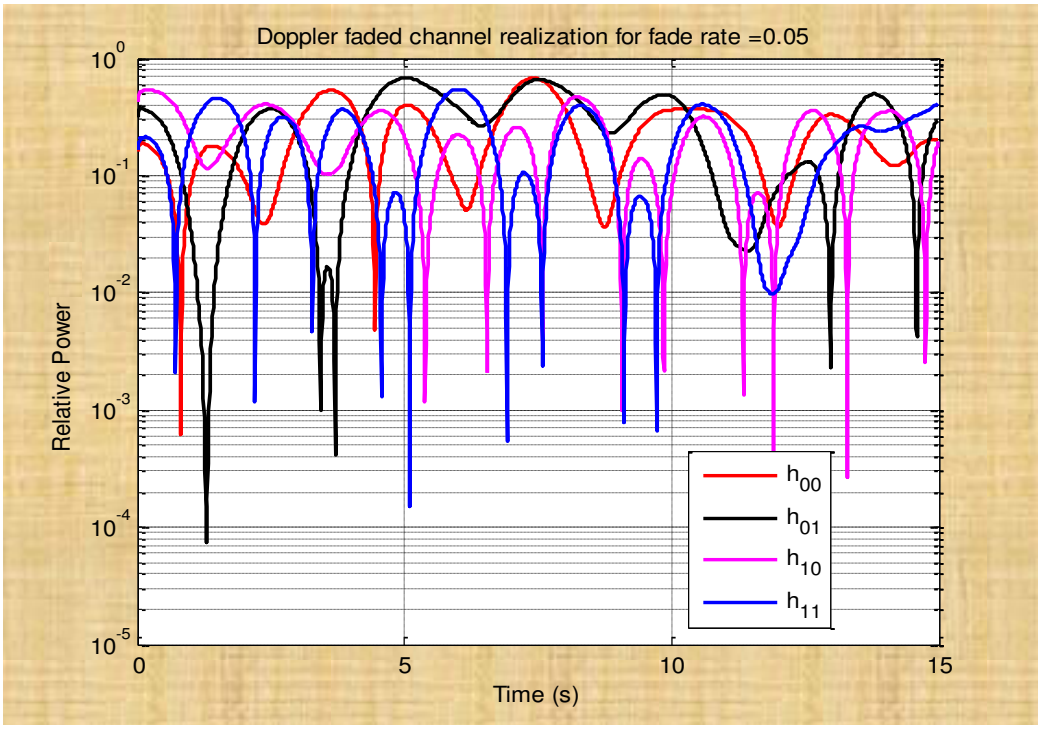

Figure 5.6 (b): A typical Doppler faded channel realization for 2x2 MIMO at fade rate 0.05

The influence of higher Doppler spread on amplitude spectrum of $2x2$ MIMO is illustrated in Figure 5.6b. As was observed with SISO, the higher Doppler spread increase the rate of rapidity in deep fading as inferred through Figure 5.6b.

5.4.2 Capacity Analysis for MIMO Configuration

Simulations were also carried out to perform relative comparison of capacity of an ideal HF channel versus HF channel undergoing fading. Both SISO and MIMO configurations have been considered in the simulations. Figures 5.7 (a) and (b) depict performance comparison for fading rates of $(f_D T_s = 0.01)$ and $(f_D T_s = 0.04)$ respectively. The relative performance difference between ideal and fading HF channel increase with increase in number of antennas in MIMO. The results of Figure 5.7 b indicate that with higher Doppler, the degradation in capacity of HF channel with SISO and MIMO is more pronounced. Also in MIMO configurations, the degradation of channel capacity is more with higher SNR scenario.

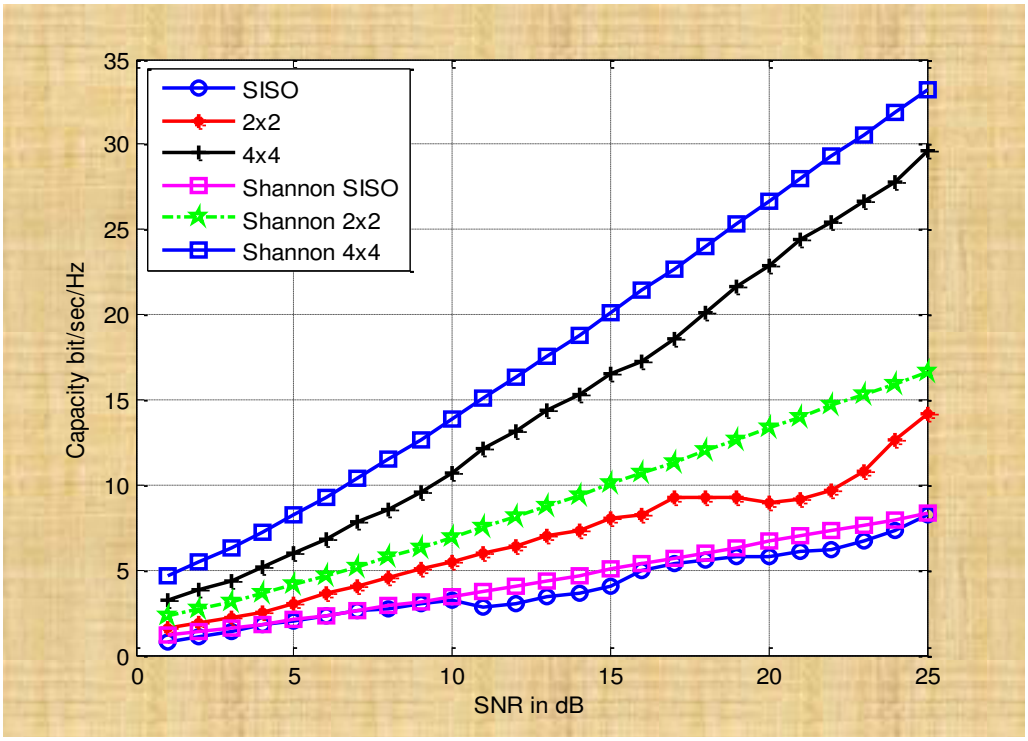

Figure 5.7 (a) : Capacity comparison between ideal Shannon capacity and HF fading channel for fading rate($f_D T_s = 0.01$)

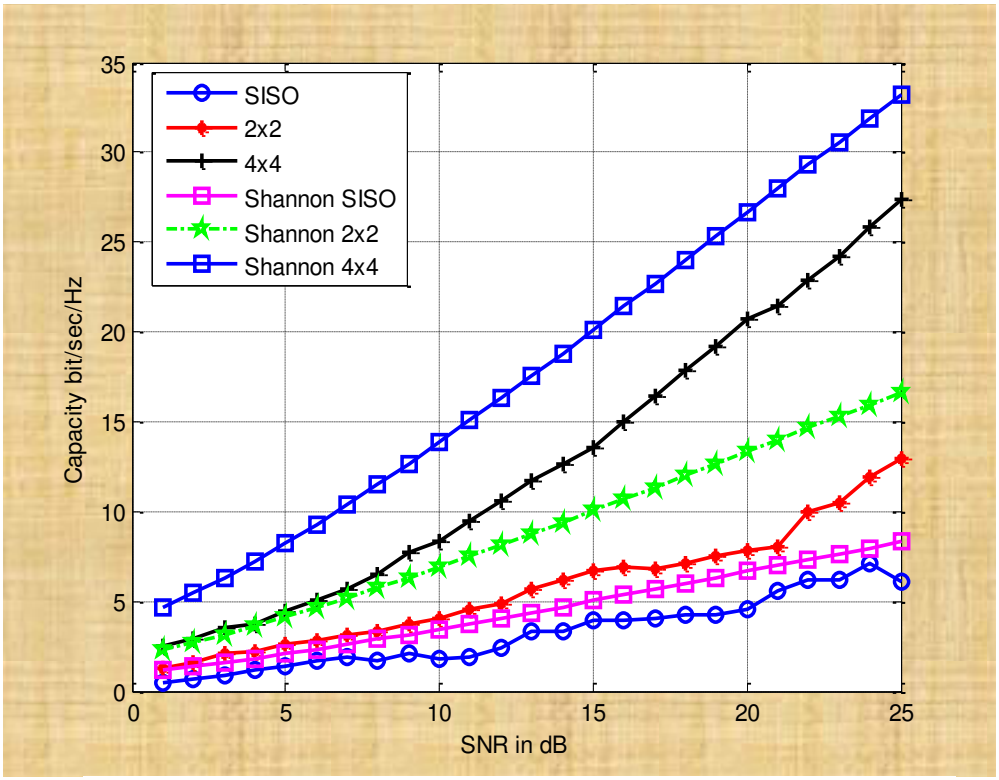

Figure 5.7(b) : Capacity comparison between ideal Shannon capacity and HF fading channel for fading rate ($f_D T_s = 0.04$)

5.4.3 Analysis of Influence of Linear Channel Impairments on HF Channel Estimation.

Extensive simulation studies have been carried out to analyse the influence of channel impairments on the performance of HF communication system. In this section, the performance improvement (BER, MSE and channel capacity) realized through various MIMO configurations such as $4x4$, $2x2$ has also compared with the SISO for a chosen HF channel model are presented. For the simulation results of this section, channel estimation error is analysed with error variance between the estimated channel matrix and simulated channel matrix as a performance parameter. Estimated symbol is obtained based on the estimated channel with zero force equalizer. The bit error probabilities have been estimated with a data symbol length of 2000 (4000 bits).

A. Simulation studies have been carried out on the BER performance realized through the SISO HF channel invoking the RLS as well as PF-EKF. The obtained simulated BER performance of the SISO HF channel has been compared with that published in [Eleftheriou 1987]. As can be seen from the results of the Table 5.2, it is evident that both the RLS and PF-EKF algorithms show improved performance relative to the method employed in [Eleftheriou 1987]. In this comparison, 40000 data bits were considered as employed in [Eleftheriou 1987]. However, even with reduced data bits of 4000, the simulation results continue to exhibit better performance relative to [Eleftheriou 1987].

Table 5.2 BER performance comparison with [Eleftheriou 1987] against simulated result under Doppler spread of 0.15, 0.5 and 1.1 Hz for SISO HF multipath channel

Doppler Spread Hz	SNR dB	BER		
		Ref [Eleftheriou 1987]	RLS	PF-EKF
1.1	5	0.8500	0.07158	0.0552
	10	0.7375	0.02837	0.0219
	15	0.6625	0.00420	0.0033
	20	0.6250	0.00135	0.0010
0.5	5	0.6250	0.06250	0.0459
	10	0.4000	0.01005	0.0063
	15	0.2500	0.00192	0.0012
	20	0.1375	0.00072	0.0005
0.15	5	0.325	0.01416	0.0051
	10	0.0775	0.00335	0.0012
	15	0.0550	0.00064	0.0002
	20	0.0325	0.00024	0.0001

B. The channel estimation Mean Square Error (MSE) of the SISO HF channel with varying Doppler spreads has been studied employing RLS and PF-EKF. The relative comparison of the MSE between the RLS and PF-EKF has been depicted in Figure 5.8, for SNR ranging from 0 to 25 dB. From the results shown in Figure 5.8, it is easy to infer that PF-EKF bears superior performance compared to RLS. Further, as one would expect, MSE decreases with lesser Doppler spread.

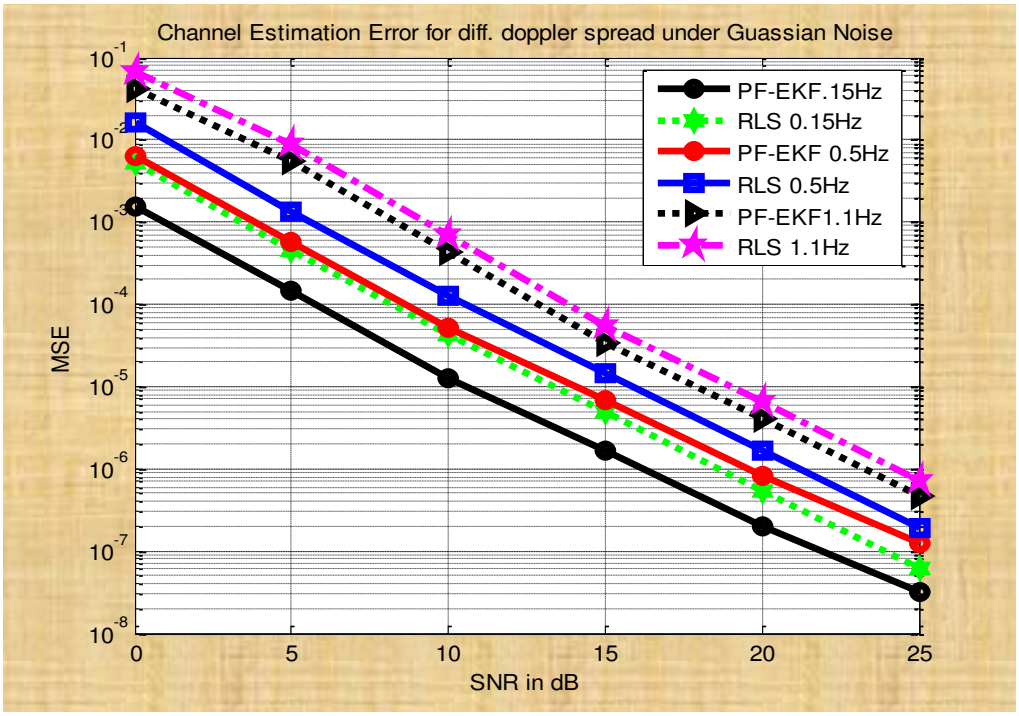

Figure 5.8 :MSE vs SNR for channel estimation under different Doppler spread for Gaussian noise HF channel

C. Simulation studies were conducted to analyze the performance of MIMO with different configurations of transmitter and receiver antennas. Figure 5.9 illustrate the relative comparison of MSE of MIMO and SISO configuration under Gaussian noise. In the simulation, the Doppler spread of 1.1 Hz has been assumed. From the results of Figure 5.9, it can be seen that MIMO configuration exhibits lower MSE compared to SISO. Further, MSE obtained through PF-EKF is lower compared to that of RLS algorithm.

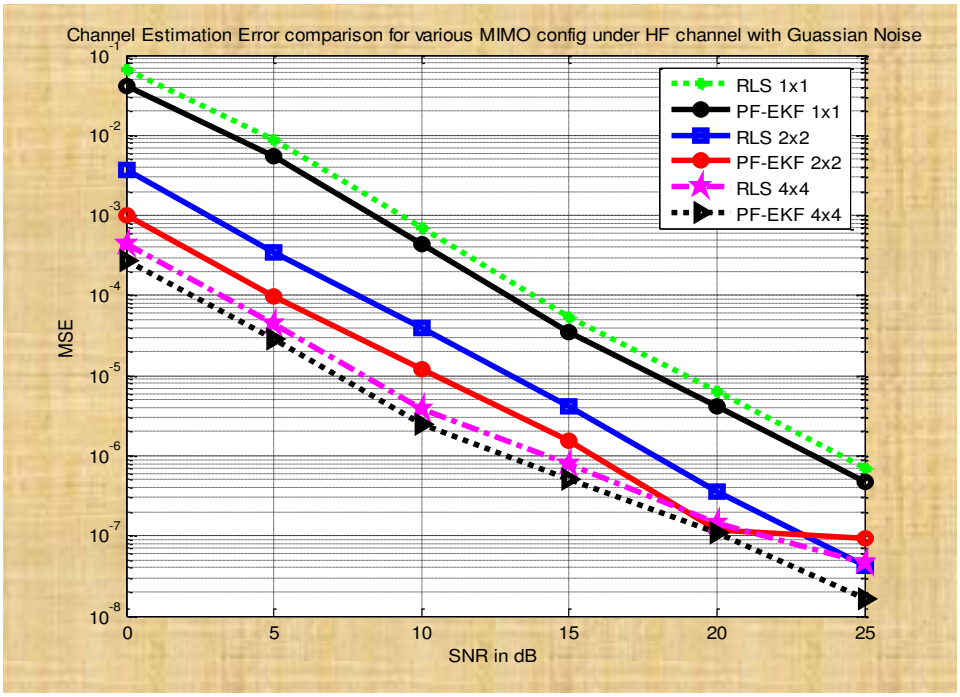

Figure 5.9: Channel estimated MSE vs. SNR for various MIMO configurations

D. Even with the non-Gaussian noise model, it can be seen that MIMO configuration exhibits lower MSE compared to SISO as shown in the results of Figure 5.10. Further, MSE obtained through PF-EKF is lower compared to that of RLS algorithm.

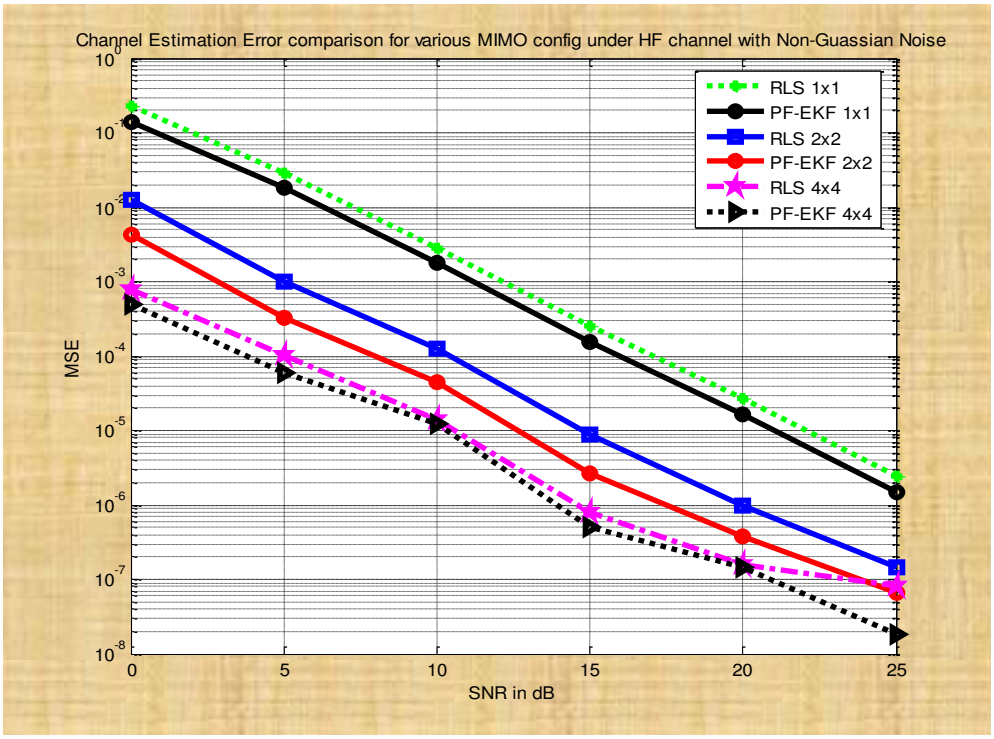

Figure 5.10: Channel estimated MSE vs. SNR for various MIMO configurations under non-Gaussian noise

The results on MSE illustrated in Figures 5.9 and 5.10 reveal that PF-EKF algorithm performs better than RLS. For higher MIMO configurations, there is an improvement in MSE. Comparison of MSE results of PF-EKF with RLS for 4x4 antenna configurations indicate a gain improvement of on average of 2-3 dB for Gaussian noise condition. Similarly for non-Gaussian scenario, the corresponding gain improvement is about 1-3 dB. It is pertinent to point that the above data on gain improvement of PF-EKF refers to low SNR (below 7dB).

E. In addition to the MSE performance, the symbol error rate is also computed for various MIMO configurations as well as SISO. The BER results are plotted in Figures 5.11 and 5.12 for Gaussian noise and non-Gaussian noise conditions respectively. The results of Figures 5.11 and 5.12 clearly demonstrate that MIMO configurations have desirable feature of lower BER relative to SISO. Also, the PF-EKF algorithm yields better performance than the RLS.

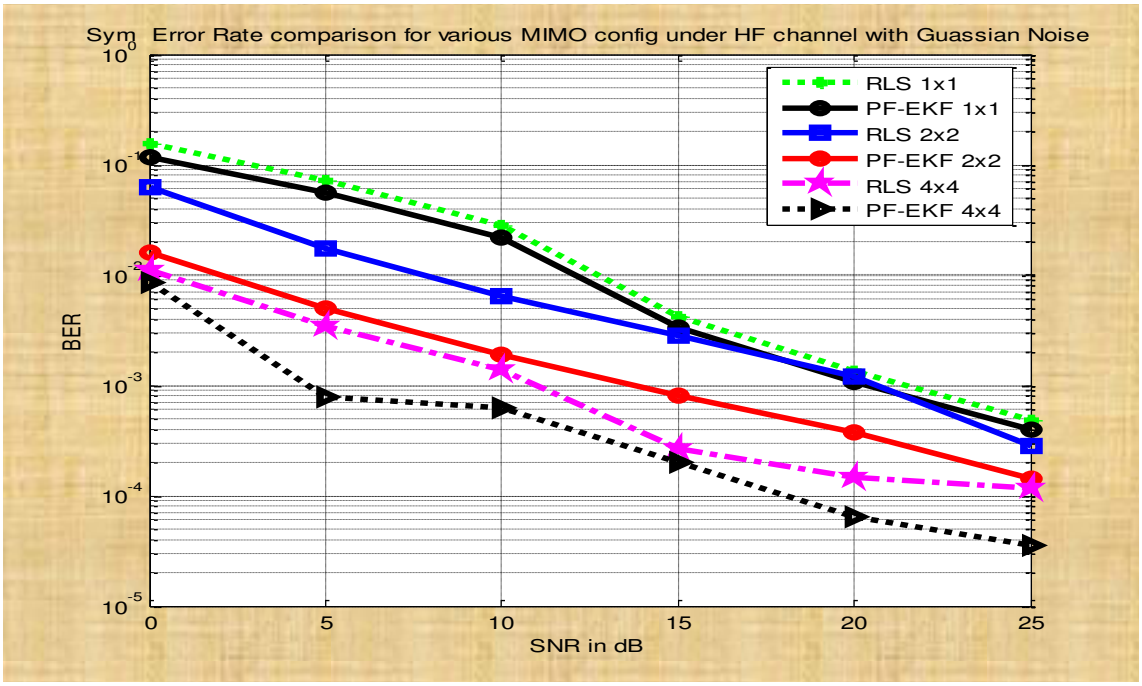

Figure 5.11: BER vs. SNR for various MIMO configurations under Gaussian noise

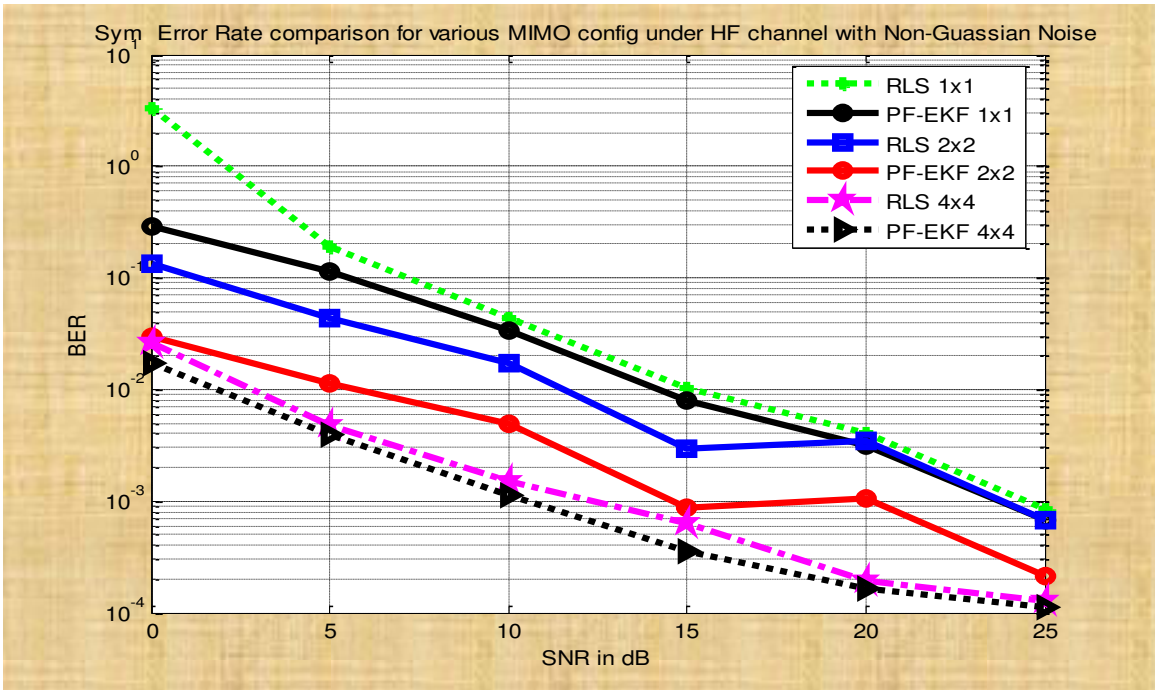

Figure 5.12: BER vs. SNR for various MIMO configurations under non-Gaussian noise

F. From the Figures 5.11 and 5.12, it is seen that PF-EKF algorithm performs better than RLS for both Gaussian and non-Gaussian noise conditions. There is an improvement in BER with higher MIMO configuration. This is to be expected due to diversity factor in STBC. A gain improvement of 0.8-1dB gain is noticed in the PF-EKF relative to RLS for 4x4 antenna configurations under Gaussian noise channel. For lower MIMO configuration (2x2), the corresponding improvement in the gain is of the order of 0.2 to 0.5 dB gain for Gaussian noise scenario. For non-Gaussian noise scenario the gain improvement is of the order of 0.5 to 0.8dB at lower SNR using PF- EKF.

G. A relative comparison of the Estimated Channel response obtained through the RLS and PF-EKF algorithms depicted in Figure 5.13 is for:

Normalized Doppler spread 1.1 Hz

Order of AR model 3

SNR =10 dB

Noise distribution: Gaussian noise.

Number of data bits=4000

Multipath=3

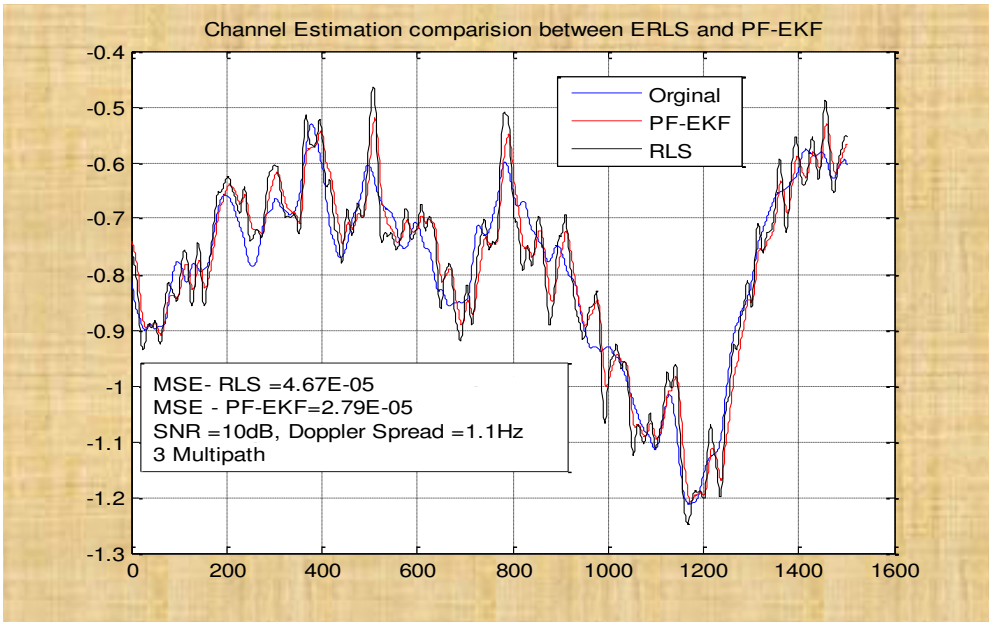

Figure 5.13: Comparison of channel estimation based RLS and PF-EKF

It is found that PF-EKF estimates the channel states more accurately compared to RLS. The variance of estimated channel state by RLS is 4.67E-05. The corresponding variance through PF-EKF is 2.79E-05 and thereby proving the better performance of PF-EKF.

H. The HF channel capacity estimated for 2x2 MIMO configurations is compared with an ideal Shannon channel capacity is shown in table II. In these simulations, Doppler spread of 1.1 Hz with 3 multipath has been assumed for the modeling of the simulated HF channel.

$$C = log_2\left(det\left(\frac{\rho}{M_T} HH^H + I_{N_R} \right)\right) bps/Hz \qquad (5.34)$$

Where, ρ the signal to noise ratio, H is the measured channel matrix, H^H is the conjugate transpose of this matrix.

Table 5.3 Capacity Comparison between RLS and PF-EKF for 2x2 MIMO

SNR dB	Capacity bit/sec/Hz		
	Ideal Shannon 2x2 MIMO	RLS	PF-EKF
0	2.0	1.7807	1.8113
5	4.1147	3.7391	3.76480
10	6.9188	6.32733	6.3491
15	10.055	8.91599	8.94696
20	13.3164	12.73805	12.74209
25	16.61875	15.76779	15.77185

The results illustrated in Table 5.3 clearly spell out the influence of the channel estimation on the channel capacity. From Table 5.3, it is evident that the PF-EKF exhibits a better channel estimation performance than the RLS algorithm for all MIMO configurations.

5.4.4 Analysis of Influence of System Non-Linearity with Channel Impairments on HF Channel Estimation

The simulation results presented in this section are extensions of those discussed in section 5.5.3 to demonstrate the capability of channel estimation based PF algorithm to deal with non-linear system and non-Gaussian noise channel impairments. The influence of channel impairments which exhibit non-linear and non-Gaussian nature on HF channel characterization is compared with the corresponding linear channel impairments. In all the simulation results presented in this section, the following parameters have been assumed: Doppler spread of 5 Hz; fade rate 0.05; Number of multipath = 3.

A. The variance performance HF channel estimation based on EKF -PF and RLS algorithms for 2x2 MIMO under various scenarios (Linear channel with Gaussian as well as non-Gaussian Noise, system non-linearity with Gaussian and non-Gaussian noise) is presented in Figures 5.14a to 5.14d.

Figure 5.14a shows the channel estimation variance for linear channel denoted as Channel L with Gaussian noise represented as Noise G. From the results of Figure 5.14a, it is inferred that EKF-PF exhibits superior performance compared to RLS with a gain improvement of 2 to 3 dB.

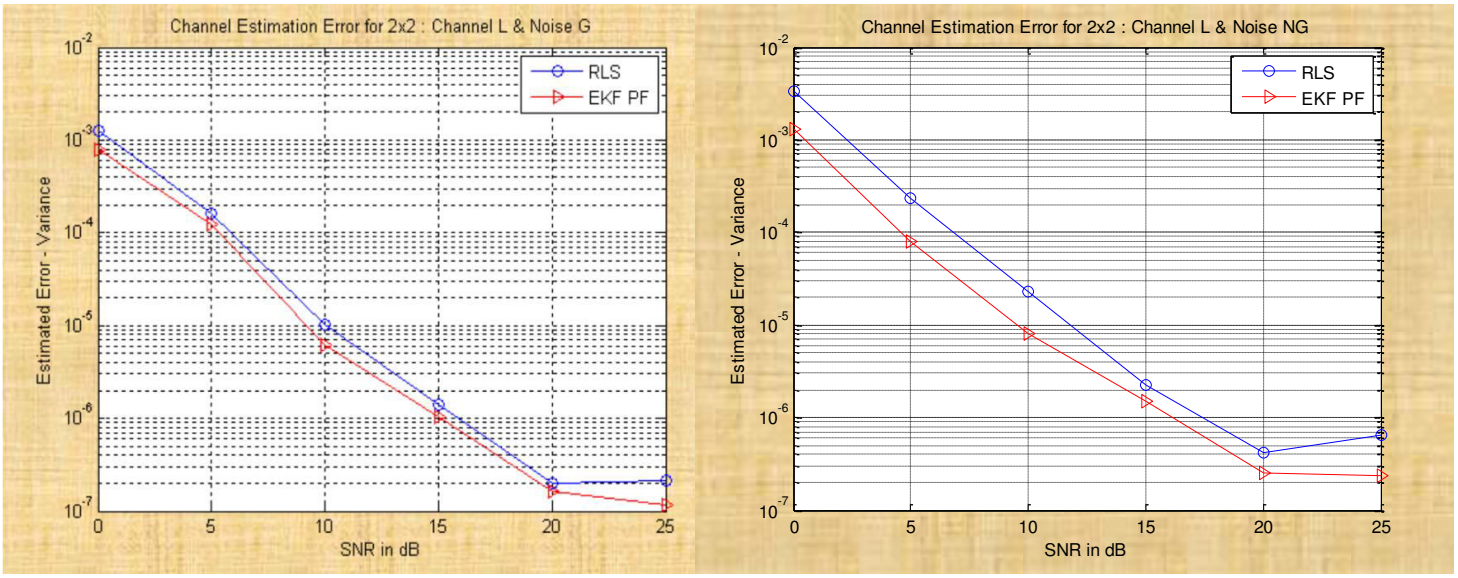

(a) Linear channel and Gaussian noise (b) Linear channel and non-Gaussian noise

Figure 5.14 (a) and (b): Channel estimation error variance for 2x2 MIMO under various conditions

The relative comparison of effect of Gaussian and non-Gaussian noise on a linear HF channel is the primary emphasis of Figure 5.14b. A comparison of the results of Figures 5.14a and 5.14b shows that under non-Gaussian (NG) noise condition, there is slight reduction in variance relative to Gaussian noise scenario. This is so for both the cases of EKF- PF and RLS algorithms. However, the above mentioned relative degradation with EKF-PF is very small but for the RLS algorithm, variance of channel estimation is degraded in the range of 0.01 to 0.5. This observation appears much more valid for lower SNR (less than 15 dB).

The variance of channel estimation for system non-linearity with HF channel (Channel NL) with Gaussian noise (Noise G) is the focus of Figure 5.14c. Compared to the results of Figure 5.14a, there is less reduction in variance that can be attributed to the system non-linearity of the HF channel. For lower SNR (< 10 dB), the steepness in the variance curve is evident. The difference in variance with linear and non -linear channel conditions is of the order of 0.01. For higher SNR, one notices a flattening in the variance curve due to contribution of non-linearity of the channel implying the dominance of non-linearity in the higher power of operation.

Figure 5.14d depicts the scenario of system non-linearity with HF channel (Channel NL) associated with non-Gaussian (Noise NG). A relative comparison of the results of Figure 5.14c and Figure 5.14d reveals degradation in variance of 0.01 to 0.6 due to non-Gaussian noise.

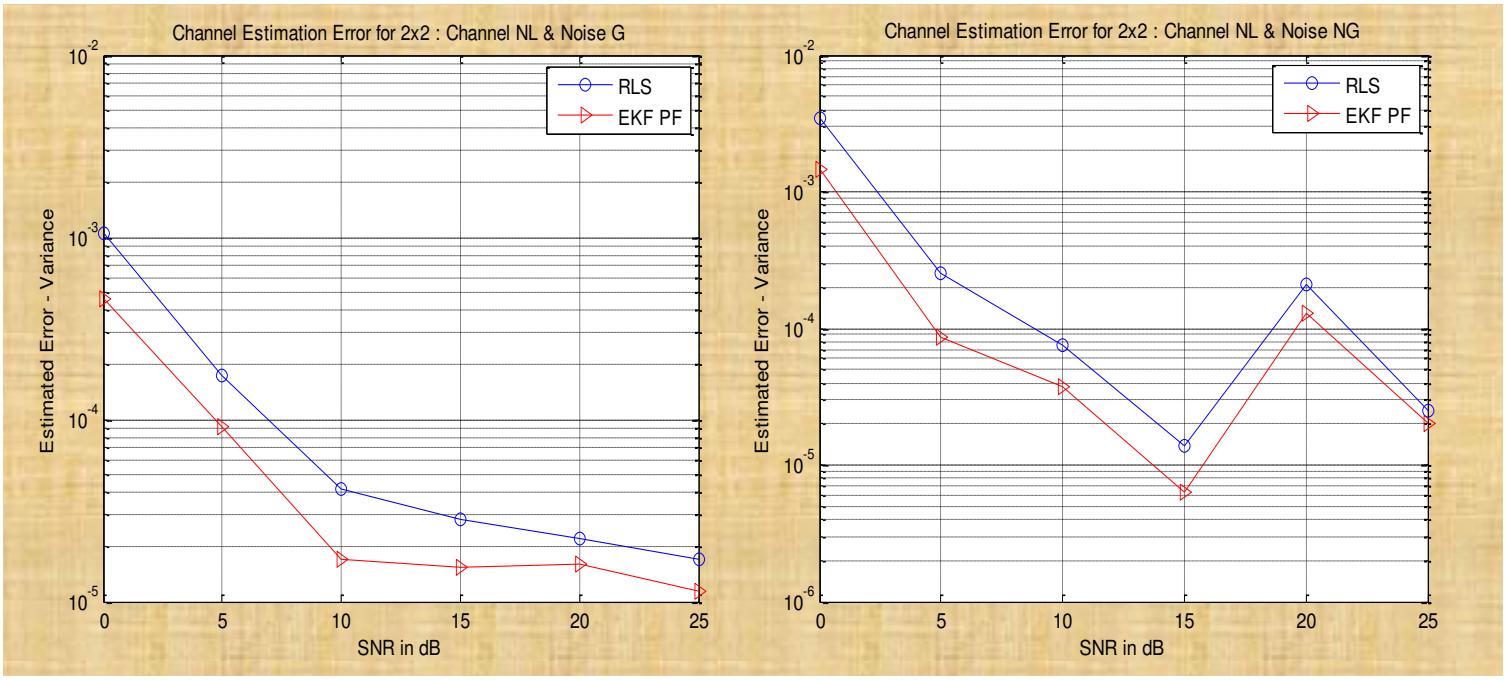

(c) System induced non-linear channel and Gaussian noise (b) System induced non-linear channel and NG noise

Figure 5.14 (c) and (d): Channel estimation error variance for 2x2 MIMO under various conditions

From the discussions on the results illustrated in the Figures 5.14 a to d, it is seen that the performance of EKP-PF based HF channel estimation is better than that based on RLS. This is true in all the scenarios considered in Figure 5.14 and EKPF- PF shows a minimum gain improvement of 2 to 3 dB implying the extended operation of the link without recharging of the battery system. Also even in the presence of non-linearity in system with channel impairments, EKPF- PF algorithm shows consistently better performance over that of RLS suggesting the enhanced reliability of the HF link.

B. Relative performance improvements derived in lieu of adaptation of MIMO have been analysed through extensive simulation studies. The results of Figure 5.15 are intended to highlight the superior performance of MIMO over conventional SISO under

varying HF channel conditions. Like in the previous subsection, the simulation studies have covered system linearity and non-linearity along with HF channel impairments associated with Gaussian as well as non- Gaussian noise of HF system. In Figure 5.15(a), variation of channel estimation variance as a function of SNR is shown for linear HF channel with Gaussian noise in the system. The results of Figure 5.15a indicate that higher MIMO configuration tend to reduce the channel estimation error because of the diversity gain feature of MIMO. The channel estimation with EKF-PF algorithm has an additional gain advantage of 2 to 4 dB over RLS. .

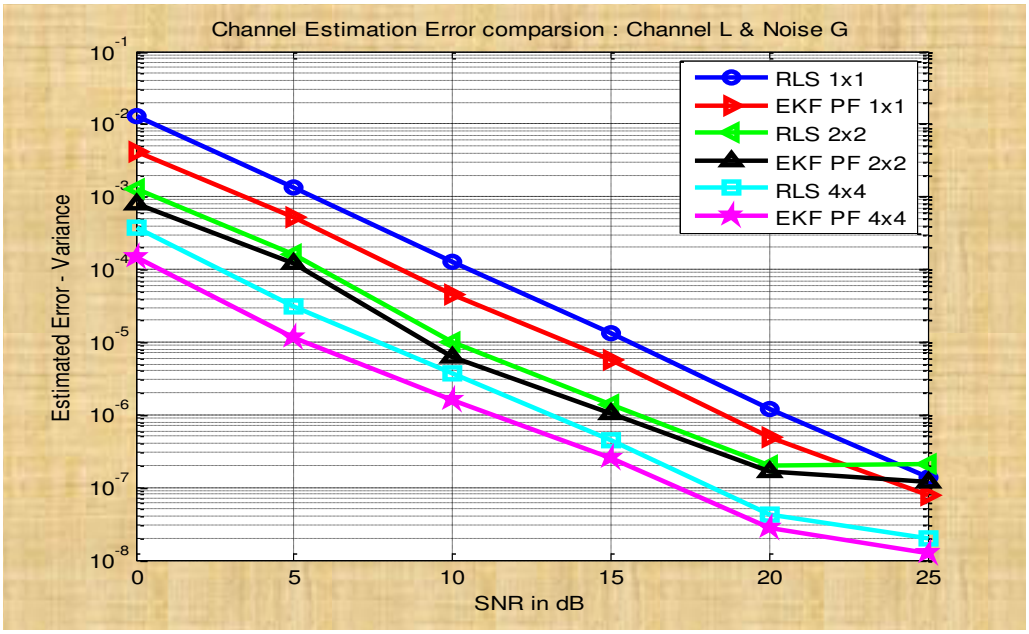

Figure 5.15 (a): Channel estimation error variance comparison for MIMO configuration under channel linear and Gaussian noise

Figure 5.15 (b) is analogous to Figure 5.15a, except that it encompasses non-Gaussian noise instead of Gaussian noise. The introduction of non-Gaussian in general degrades the estimation performance compared to Gaussian scenario. MIMO configuration continues to show relatively improved performance over SISO. The earlier remark on superior performance of EKF-PF over RLS also holds good even when non-Gaussian noise is considered in the simulation.

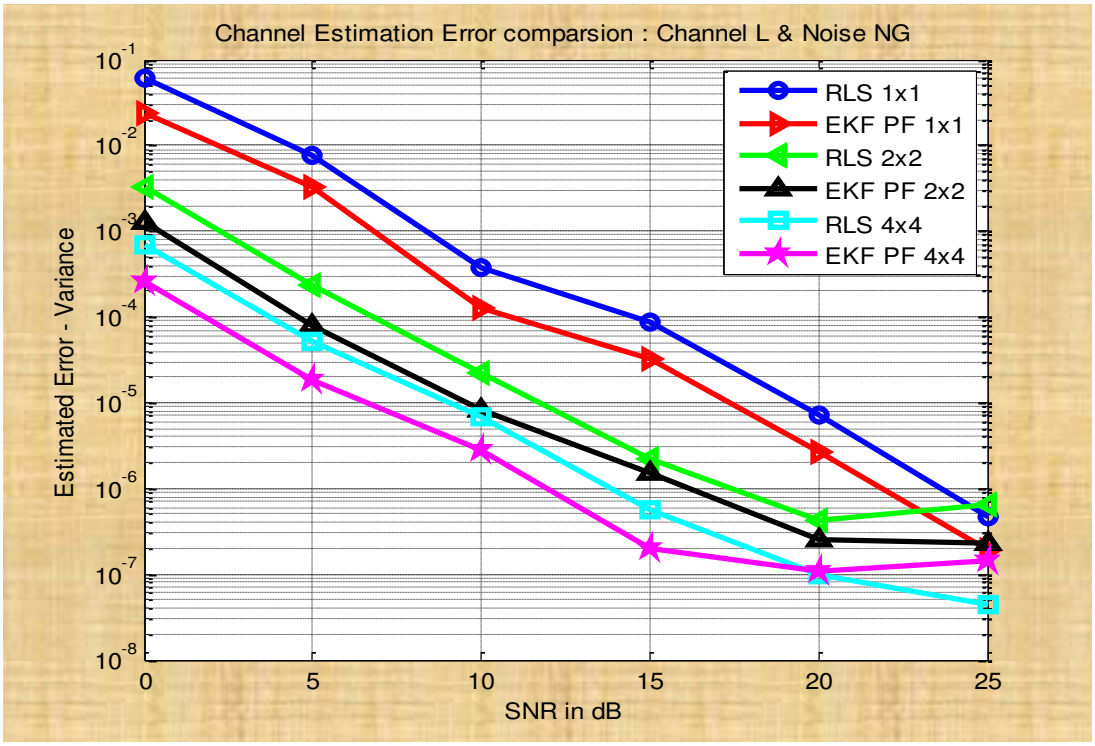

Figure 5.16 (b): Channel estimation error variance comparison for MIMO configuration under channel linear and Non-Gaussian noise

The analysis of influence of non-linearity in system with channel impairments on the channel estimation algorithm is one of the significant aspects of this research. In that sense, Figure 5.15 (c) is similar to Figure 5.15(a) except that it considers system non-linearity with channel impairments instead of linear channel conditions. The result of Figure 5.15c indicates that there is degradation in the performance of channel estimation algorithm under system non-linear conditions. The results of Figure 5.15c also suggest that RLS algorithm is not very effective to handle system non-linearity with channel conditions. However, channel estimation variance with EKF-PF algorithm is much lower relative to RLS even under system induced non-linearity with HF channel conditions.

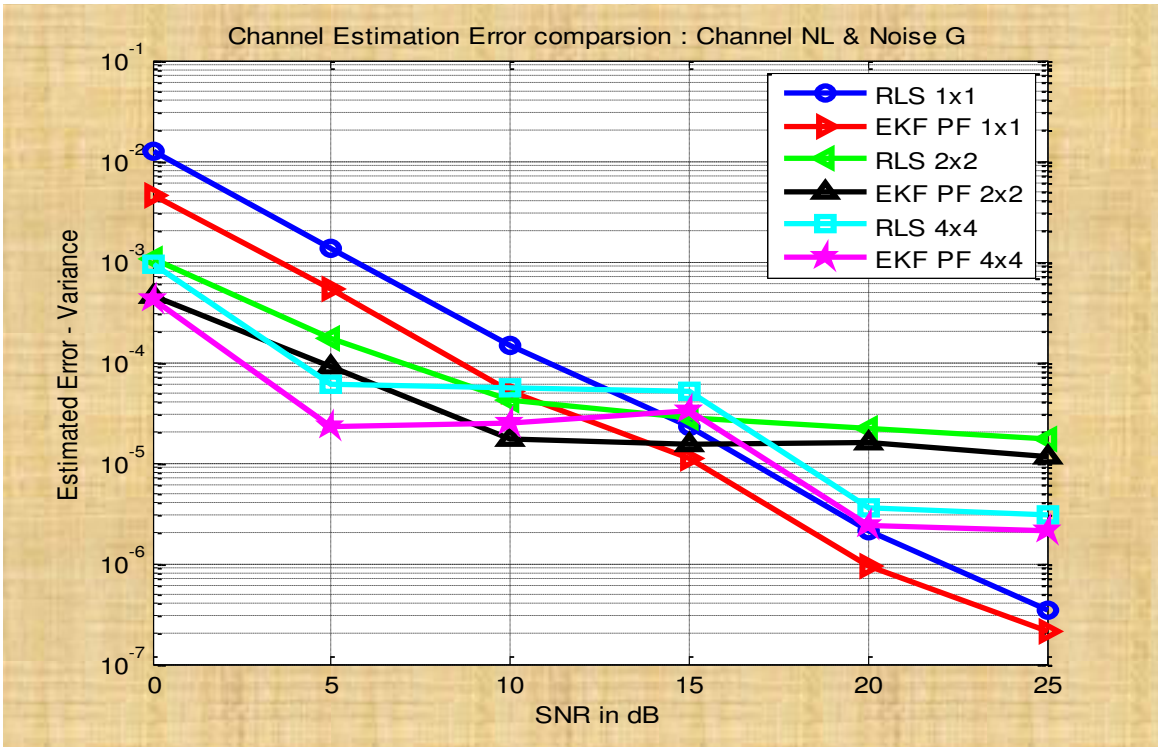

Figure 5.17 (c): Channel estimation error variance comparison for MIMO configuration under channel impairment with system induced non-linearity and Gaussian noise

The scenario of both the system non-linearity with channel impairments and non-Gaussian noise associated with HF system is by far the most severe conditions, to which the developed channel estimation algorithms have been subjected in their performance evaluation. The results of Figure 5.15 (d) depict such a scenario. The general trend of EKF-PF outperforming RLS continues to hold good. MIMO configurations exhibit improved performance over SISO.

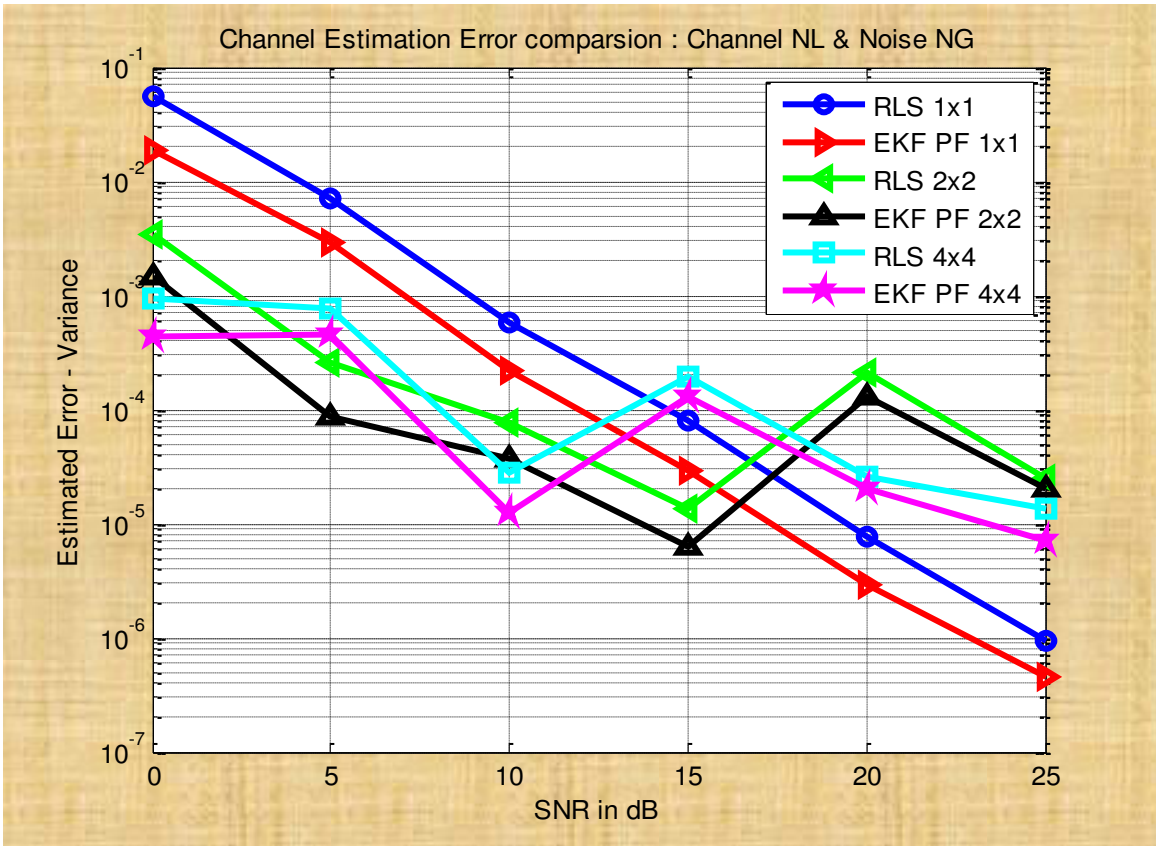

Figure 5.18 (d): Channel estimation error variance comparison for MIMO configuration under channel impairment with system induced non-linearity and Gaussian noise

C. In many of the discussions covered earlier in this chapter, the advantage of EKF-PF over RLS has been consistently emphasized with relevant illustrations wherever possible. The results of Figure 5.16 are meant to exclusively highlight the significance of PF algorithm in channel estimation techniques under non-linear and non-Gaussian conditions. From the results of simulation depicted in Figure 5.16, it is evident that at low SNR EKF-PF has gain advantage around 2 to 3.5 dB. For higher SNR, additional 1.5 to 2 dB gain advantage is achieved.

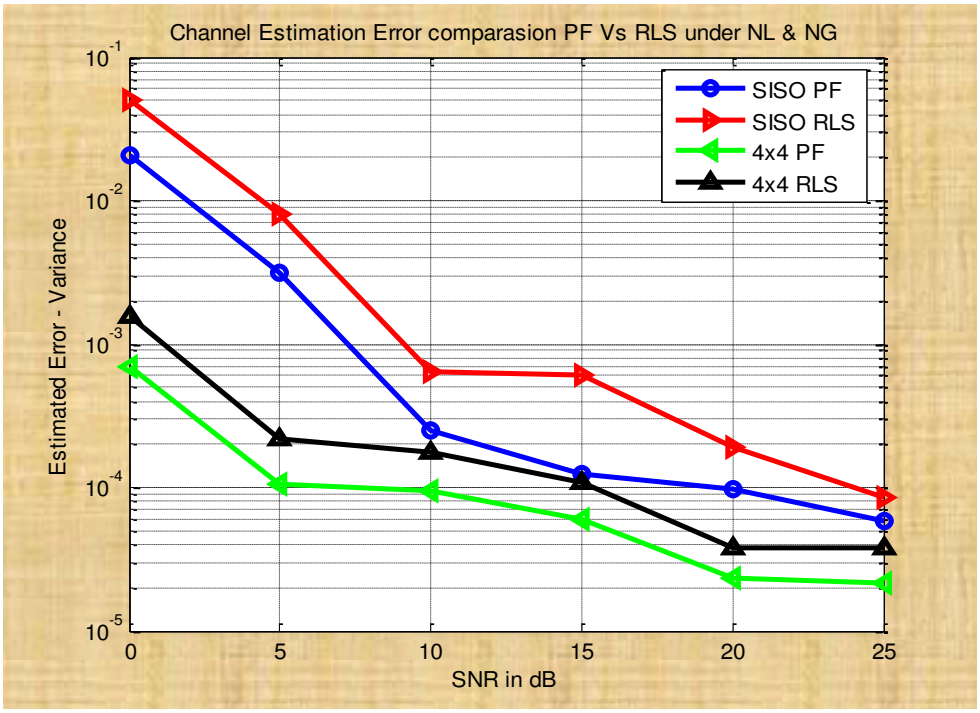

Figure 5.19: Channel estimation error variance comparison between PF and RLS for SISO and MIMO configuration under system non-linear and non-Gaussian noise conditions

D. The effect of non-linear channel conditions on the variance of channel estimation algorithms has been a topic of special emphasis in the discussions dealt in previous paragraphs. In continuation of the above, some typical simulation studies have also been performed to analyse the influence of specific type of non-linearity of the channel on the channel estimation algorithms. In particular the following two specific types of non-linear functions have been considered in the comparative analysis. The first type of non-linear function belongs to tan hyperbolic class such as $r_k^i = tanh(x_k^i) + w_k^i$ while the second category considers the 3rd order polynomial $r_k^i = x_k^i + 0.2(x_k^i)^2 - 0.1(x_k^i)^3 + w_k^i$. The results of Figure 5.17 infer the assumption that tan-hyperbolic type of non-linearity of HF channel may subject the HF system to a severe distortion of higher magnitude, compared to the 3rd order polynomial type of non-linearity.

.

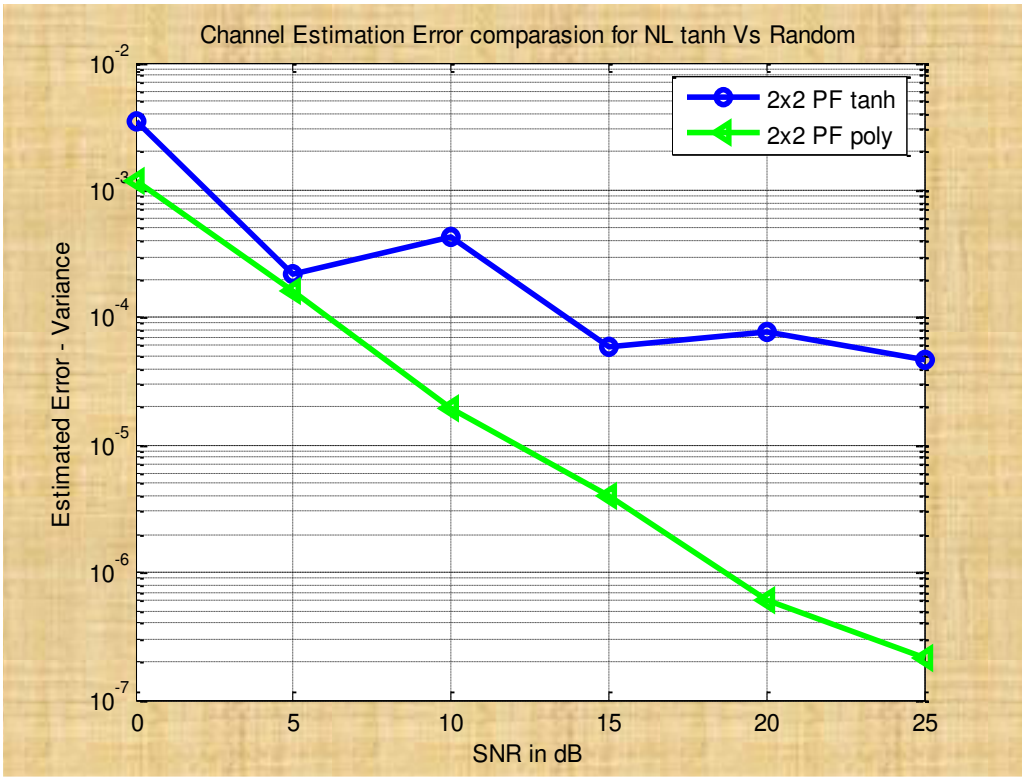

Figure 5.20: Effect of non- linearity in Channel estimation on 2x2 MIMO with Gaussian noise conditions

5.4.5 Analysis the Effect of MIMO Spatial Correlation on Channel Estimation

This section analyses the impact of spatial correlation of MIMO configuration on the performance of PF based channel estimation technique. As an example, spatial correlation for 2x2 MIMO is considered for the analysis. However, such an analysis can be extended to higher configuration of MIMO as well. The spatial correlation matrix for $\boldsymbol{2x2}$ MIMO configurations is given in Equation (5.33a). It is re-written as

$$R_{2x2} = \begin{bmatrix} 1 & \alpha \\ \alpha^* & 1 \end{bmatrix} \otimes \begin{bmatrix} 1 & \beta \\ \beta^* & 1 \end{bmatrix} = \begin{bmatrix} 1 & \beta & \alpha & \alpha\beta \\ \beta^* & 1 & \alpha\beta^* & \alpha \\ \alpha^* & \alpha^*\beta & 1 & \beta \\ \alpha^*\beta^* & \alpha^* & \beta^* & 1 \end{bmatrix} \tag{5.35}$$

Where $\otimes$ is Kronecker product. In Equation (5.35) α and β are the spatial correlation co-efficient's whose values are given in Table 4.2. For the analysis, the values of α and β are chosen to cover the three scenarios namely low, mid and high correlation of the

MIMO configuration. The effects of spatial correlation factors on the performance of the proposed channel estimation algorithm are illustrated through the simulation results of Figures 5.18 and 5.19. The simulation results of Figure 5.18 refer to the HF channel associated with channel impairment in the form of linear fading and the Gaussian noise. The results in Figure 5.19 correspond to the linear fading of the channel associated with the non-linearity of the system as well as non-Gaussian noise. As expected, high values of spatial correlation factors degrade the BER performance (Figures 5.18 and 5.19).

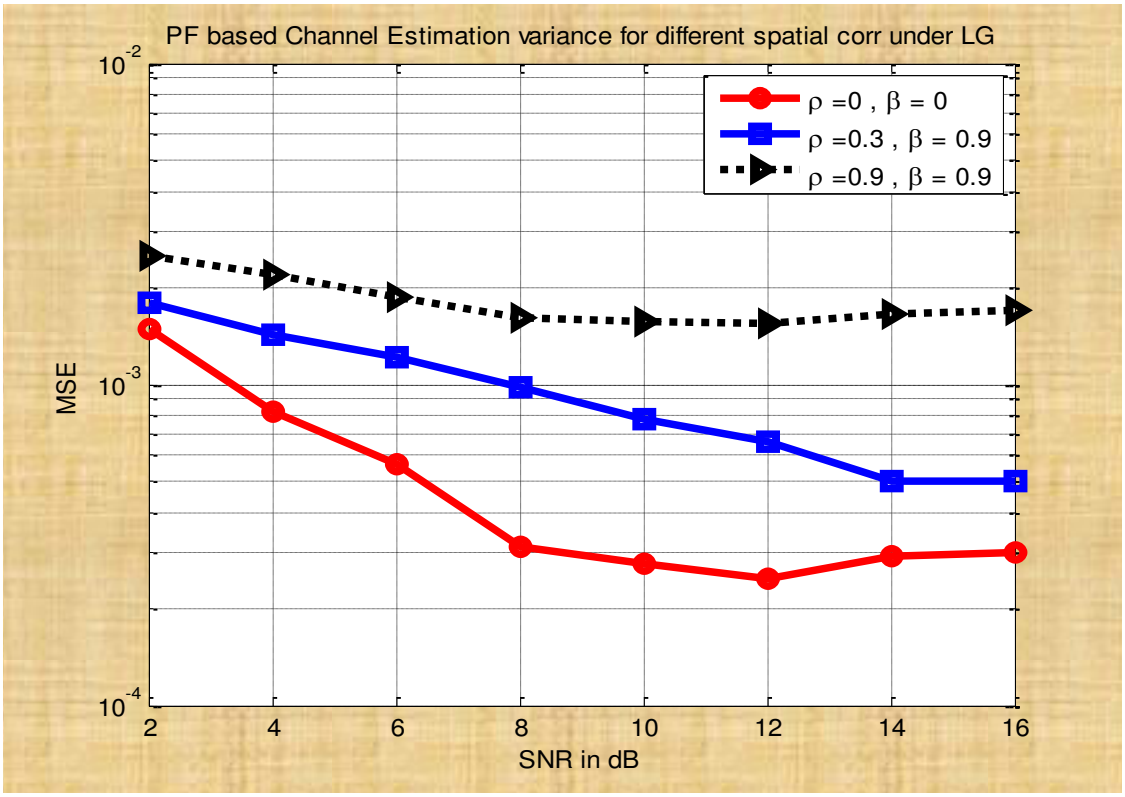

Figure 5.21: Effect of spatial correlation on channel estimation for linear HF channel with Gaussian noise

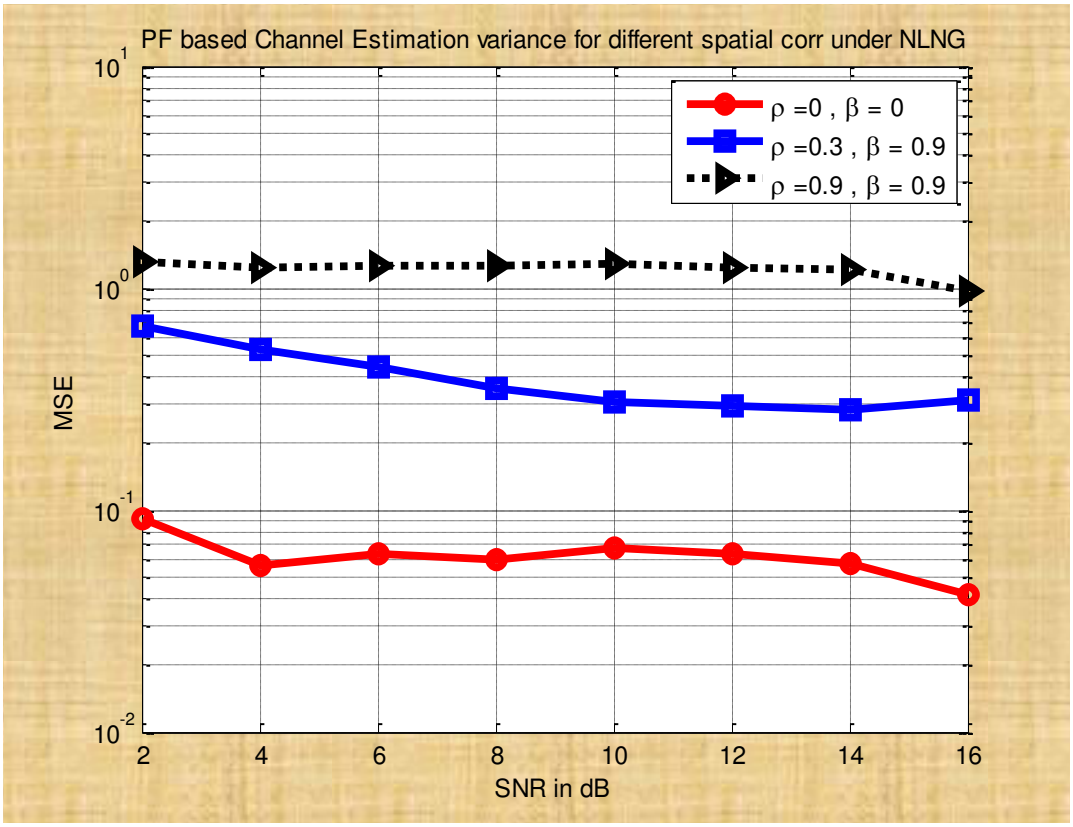

Figure 5.22 : Effect of spatial correlation on channel estimation for system non-linearity with non-Gaussian noise

5.4.6 Feasibility of Channel Estimation based on PF for Real Time MIMO-HF Channel

The improved performance of the proposed PF based channel estimation scheme over conventional estimation techniques using RLS has been substantiated for both SISO and MIMO configurations. However, it is necessary to examine the feasibility of invoking the proposed PF based channel estimation algorithms for real time applications of MIMO-HF channel since the adoption of PF for channel estimation in real-time systems is hampered by their computational complexity. The use of large number of particles and non-linear functions in PF algorithms increase their computational complexity and execution time. This sub section facilitates a snap shot view of the expected computational requirements of PF based channel estimation algorithms for its implementation on a proven hardware. The proposed feasibility study has been dealt through the well-known preamble symbol

and data symbol. The channel estimation is performed through block computations and these computations are performed during one preamble period. For real time applications, these block computations should be completed within the preamble period. For HF communication MIL STD 118-110 B each symbol period is 0.41 ms (Baud rate is 2400 bps). 16 or 32 symbols are used for preamble. While most stages in the particle filter algorithm can be parallelized, the resampling stage cannot be easily parallelized [Velmurugan 2007]. Parallelizing the various stages in the particle filter algorithm leads to faster execution time and efficient hardware architectures. [Miao 2011, El-Halym 2012] have proposed efficient hardware architectures for PF with minimum computation time (less than 6.8 μsec). As shown in Table 5.4, the preamble periods for 24 and 272 symbols are 9.84 msec and 14 msec respectively. These values have been arrived at by considering the MIL-STD 188-110C. According to it, the HF data waveforms use single contiguous bandwidths from 3 kHz to 24 kHz with baud rate 2.4 kbps to 19.2 kpbs. Number of preamble (mini-probe) symbol varies from 24 to 272 [Appendix D of MIL-STD 188-110C]. [El-Halym 2012] required 93cycles @ 74MHz = 1.25 μsec for an iteration of PF (with 64 particles). For 24 symbols, the computation time is 30 μsec which is far less than the allowed preamble period of 9.84 msec. Whereas [Miao 2011] requires 684 cycles @ 100MHz = 6.82 μsec for an iteration of PF (with 1000 particles) with computation time of 0.163 msec for 24 symbols.

Even for the case of 272 symbols in a preamble period, the expected computation time of 14 msec is still lower than the allowable preamble period of 1.85 msec. Since the computation time of PF (T_c) is much lower than that required for preamble period (T_p) $T_C < T_P$. This implies that the computations for PF based channel estimation can be completed well before the arrival of the next preamble or data. Therefore it can be concluded that the proposed PF based channel estimation algorithm is applicable for real time HF channel estimation also. The Table 5.4 depicts the finer details involved in various time estimates.

Table 5. 4 : Feasibility of PF Applicable for Real-Time HF Channel Estimation		
Description	Preamble period (T_P)	Computation time (T_c) available from literature
• For 3 kHz B.W, 2400 symbols per second Symbol Period = 0.41 msec	• For 24 symbols 24 *0.41 = 9.84 msec 272*0.41 = 111.5 msec	[El-Halym 2012] required 93cycle @ 74MHz = 1.25μs to compute an iteration of PF. For 24 symbols it requires 30μsec. For 272 symbols it requires 0.34msec
• For 24KHz B.W, 19200 symbols per second • Symbol Period = 52.08 μsec	• For 272 symbols 272 *52.08 = 14 msec	[Miao 2011] requires 684 cycles @ 100MHz =6.82 μs to compute an iteration of PF. For 24 symbols it requires 0.163 msec. For 272 symbols it requires 1.85 msec

5.5 Conclusion

Channel estimation is an important technique especially in HF communication system where the channel conditions change over time, usually caused by transmitter and/or receiver being in movement and rapid variation of ions in ionospheric layers. HF communication is adversely affected by the multipath interference resulting from reflection significantly from ionospheric layers and surroundings environments. The HF system needs an accurate estimate of the time-varying HF channel to ensure both the reliability and high data rate at the receiver. It is important to estimate the channel as close to the true channel as possible since the estimation has a direct impact on the performance of the receivers. Furthermore, MIMO-HF systems have been credited with potential to provide services such as data communication, voice, and video with high Quality of Service (QoS) in rich scattering environment. It is a real challenge in practical

MIMO systems, where the quality of data recovery is as important as attaining a high data throughput. The knowledge of the impulse response of HF propagation channels in the estimator is an aid in acquiring important information for testing, designing or planning HF communication systems.

This chapter presents both classical and Bayesian approaches to estimate the channel impulse response. Under classical supervised approach, RLS based HF channel estimator is discussed. PF, which falls under supervised Bayesian approach, has been analysed for its performance under adverse conditions, such as system non-linear, channel time-varying and non-Gaussian noise environments.

A performance analysis of MIMO based HF channel estimation invoking PF algorithm constitutes a key contribution of this chapter as well as the thesis. The proposed PF based analysis has been demonstrated to show an improved performance in comparison to that obtained with RLS algorithm. The noteworthy feature of this chapter is the treatment of system non-linearity with channel impairments and non-Gaussian noise scenario in estimating the HF channel estimation. Also, the influences of MIMO configurations on the performance of HF channel have also been investigated. The advantage of MIMO over classical SISO to enhance the channel capacity has been reiterated through extensive simulation studies. The performance of various MIMO configurations has been compared with that of SISO also. This chapter convincingly substantiates the benefit of incorporating dynamic Bayesian modelling technique for use in estimating a rapidly changing MIMO-HF wireless channel.

It is inferred from the simulation studies, that the performance of the channel estimation with the PF technique is superior to the RLS technique and other techniques with affordable computational complexity even in low SNR. The results presented in this chapter indicate that the PF techniques can be handled with a better trade-off between computational complexities and desirable performance suitable for HF communication system. The results derived out of the simulation studies indicate that the PF based HF channel estimation algorithm out performs the other algorithm like RLS in Gaussian

noise conditions. In the past, the prior algorithms have been found unable to treat either the system non-linearity with channel impairment or non-Gaussian noise condition. On the contrary, the proposed PF technique is demonstrated to successfully deal with these scenarios with affordable additional computations. The simulation results of the MIMO based HF channel with PF technique confirm that there is degradation in the channel performance under non-linear and non-Gaussian noise conditions and the degradation is relatively small. The simulation results conclusively suggest that the RLS based channel estimation algorithm is not very effective to handle system induced non-linearity conditions. However, channel estimation variance with EKF-PF algorithm is much lower relative to RLS, even under non-linearity conditions. The simulation studies indicate that under low SNR, EKF-PF has gain advantage around 2 to 3.5 dB over RLS. For higher SNR, additional 1.5 to 2 dB gain advantage is achievable. Further it is evident that feasibility of real time hardware implementation of PF for HF channel estimation is possible.

CHAPTER 6

CONCLUSIONS AND FUTURE WORK

This chapter is intended to facilitate recapitulation of succinct summary, inferences, and technical conclusions derived out of research study of this thesis. The potential scope for further research to extend simulation as well as analytical studies of this thesis is also highlighted.

6.1 Summary

In the past decade, MIMO technology has witnessed exciting developments in the wireless communication systems. Building upon the promising MIMO technology for HF transmission, this thesis proposes a computationally efficient approach for HF channel characterization and modelling based on Watterson HF channel model. This approach is valid for both SISO as well as MIMO configurations in HF channels environments. The modelling of channel characterization closely emulates the impulse response (transfer function) of a practical HF channel, by incorporating channel impairments comprising multipath fading, non- Gaussian noise and system non-linearity.

The channel parameters that characterize the channel conditions will have effect on the transmission of the data. The effects of channel conditions on the transmitted data must be estimated to recover the transmitted information correctly. The significance of channel estimation is to mitigate the effects of variation of statistical channel parameters for achieving the acceptable system performance at the receiver as specified by the designers. Over the past three decades, the RLS has become a standard technique in all branches of engineering disciplines and related applications that need estimation algorithms. However, recently, the novel and more accurate non-linear filters have been proposed as more accurate alternatives to the EKF within the framework of state and parameter estimation. Like most new algorithms, the new filtering methods are probably not widely known or understood and their application has been rather limited. In this thesis, non-linear filtering algorithm is invoked through PF for channel estimation. A study encompassing the application as well as the utility of PF for supervised channel

estimation has been undertaken and pursued to its logical conclusion. Under the framework of recursive Bayesian filtering, EKF with PF based efficient channel estimation algorithms have been developed in this thesis to address the commonly prevalent system non-linearity with channel impairments and non-Gaussian noise, which was hitherto not possible.

6.2 Conclusion

The conclusive observations, inferences, implicit and explicit novelties of research findings of this thesis are enlisted in this section.

6.2.1 Characterization and Modelling of HF Channel

The significant conclusive observations pertaining to the Characterisation and Modelling of
HF channel are as follows,

- In the proposed HF channel characterization scheme, system non-linear and random time-varying features have been imparted to the conventional Watterson channel model to capture both the time and frequency dispersion of a HF channel.

- The limitations associated in the application of FIR in modelling the HF channel and its inadequacy to represent the dynamic characteristics of the channel parameters have been analysed.

- This thesis demonstrates that HF channel modelled through IIR/AR filter can capture the dynamic characteristics of the channel with reduced computational complexity compared to FIR.

- Computational complexity involved in generating the AR function for different Doppler spreads and sampling frequencies is analysed. It is shown that computational complexity varies exponentially with the selected configuration of MIMO.

6.2.2 HF Channel Estimation

Under the topic "HF channel estimation", following are the salient research findings of the thesis.

- A noteworthy feature of this thesis is the ability of the EKF and PF based channel estimation algorithm to consider the adverse effects of multipath fading, system non-linearity and non-Gaussian noise scenario.
- It is inferred from the simulation studies, that the performance of the channel estimation with the PF technique is superior to the RLS technique with affordable computational complexity even in low SNR condition.
- The simulation results conclusively suggest that RLS based channel estimation algorithm is not very effective to handle system induced non- linear conditions.
- Variance of EKF-PF based channel estimation algorithm is much lower relative to RLS even under system induced non-linear conditions.
- The simulation studies indicate that under low SNR (5 to 15 dB), the channel estimation algorithm invoking EKF with PF has advantage of improvement in gain (2 to 3.5 dB) over the RLS algorithm.
- For higher SNR, the corresponding improvement in gain is 1.5 to 2 dB.

6.2.3 Contributions

The contributions of this thesis to the broad topic of modelling, characterization and estimation of HF channel can be summarized as follows:

- A generic framework to extend the concept of HF channel modelling, characterization and estimation techniques applicable to conventional SISO has been proposed for the emerging MIMO technology.
- The computational complexity and accuracy in the simulation of AR/IIR based HF channel model have been compared with the FIR based model.
- Methods of modelling HF channel to characterize the effects of system non-linearity with channel impairments and non-Gaussian noise have been proposed and validated.

- The channel estimation algorithms which can mitigate the effects of the multipath fading non-Gaussian noise the system induced non-linearity with channel impairments have been proposed and analysed for their functionality.
- The relative improvement in the overall performance of the HF communication system in lieu of adaptation of MIMO over SISO has been investigated through numerous analytical and simulation studies.

6.3 Future Work

As was stated in the earlier sections, a comprehensive analysis of channel characterization and estimation of HF channel with multiple antenna system has been presented. Viewed in totality, the research presented in this thesis is an incremental contribution in the overall developmental efforts to enhance the reliability and data handling capacity for HF system within the framework of MIMO-HF channel characterization and estimation.

6.3.1 Channel Characterization

The accuracy of the simulation model developed in this thesis is limited by the accuracy of the underlying mathematical model and the associated assumptions. The developed model for channel characterization, at best, provides merely a partial description of the system being modeled since, only certain aspects (such as short term fading effects that include time and frequency dispersive of the system, system induced non-linearity and non-Gaussian noise) have been considered. In order to develop a more accurate simulation model, it is recommended that the field measurements of the environment being modeled should also consider the following:

- Multidimensional (space, time, and frequency) characterization of HF propagation including time delay, angle of arrival, angle of departure profiles and time variance of the HF channel.
- Characterization that would deal with the effect of the interference of the environment.

- Analysis of climatic variations, mainly the effect of fading due to rain and other scintillations that are important in characterising the HF channel.
- Multidimensional analysis and modeling of multipath propagation for the waveform design of MIMO-HF or MIMO-OFDM HF system.

6.3.2 HF Channel Estimation

The research study presented in this thesis pertaining to the improved channel estimation algorithm for HF channel invokes recursive Bayesian technique that encompasses PF instead of conventional Kalman Filter. Any novelty aimed at reducing the computational burden as well as enhanced accuracy of PF based estimation algorithms can further supplement the analytical work of this thesis. The following aspects can be considered for further research,

- The PF based channel estimation algorithm can be further improved to deal with the higher degree of dynamics with narrow process or observation noise variance. In such a scenario, the particles set quickly collapses to one single point in the state space, leading to the severe performance degradation of the filtering performance. The kernel particle filter that invokes mean shift to allocate particles more efficiently and which also uses importance sampling to maintain fair samples from the posterior density function can be explored. It may be pertinent to point out that kernel method is a parametric model, whereas the PF belongs to the class of non-parametric estimation model. Non-parametric model requires relatively more accurate information on system and measurement.
- Particle generation and weight computation are computationally the most intensive steps in PF based channel estimation algorithms. The main challenges for accelerating the speed of execution of the algorithm lie not only in the reduction of the number of the operations but also in exploiting operational concurrency between the particle generation and weight computation steps. Further studies on architectural features of hardware to optimize the speed of computation through parallelization as well as recursion can be a significant contribution towards the development of a highly efficient real time HF communication system.

REFERENCES

Abbasi, N., Warrington, E., Gunashekar, S.D., Salous, S., Feeney, S., and Bertel, L. (2009) 'Capacity estimation of HF-MIMO system'. 11th IET International Conference on Ionospheric Radio Systems and Techniques, April 2009.

Alamouti, S. (1998) 'A simple transmit diversity technique for wireless applications'. IEEE Journal on Selected Areas on Communications, vol. 16, no. 8, pp. 1451-1458, 1998.

Alimohammad, A., and Cockburn, B.F. (2007) 'Modeling and hardware implementation aspects of fading channel simulators'. IEEE Transactions on Vehicular Technology, vol. 01, no. 1, Sep 2007.

Alimohammad, A., Fard, S.F., and Cockburn, B.F. (2012) 'Filter-based fading channel modeling'. Modelling and Simulation in Engineering, Hindawi Publishing Corporation, pp. 1-10, Aug 2012.

Alspach, D.L, and Sorenson, H.W (1972) 'Nonlinear Bayesian estimation using Gaussian sum approximations'. IEEE Transactions on Automatic Control, vol. 17, No. 4, pp. 439–448, Aug 1972.

Alvarez, I.P., Bello, S.Z., Ghogho, M., and Lopez-Perez, J. (2011) 'Experimental results on multicarrier MIMO HF communications'. XXX General Assembly and Scientific Symposium of the International Union of Radio Science, Istanbul, Turkey on August 13-20, 2011.

Apolinário, J.A. (2009) 'QRD-RLS Adaptive Filtering'. Springer 2009.

Arikan, L. (2004) 'A brief review of HF channel response estimation'. Journal of Electromagnetic. Waves and Appl., vol. 18, No. 6, pp.837–851, 2004.

Arulampalam, M.S, Maskell, S., Gordon, N., and Clapp, T. (2002) 'A tutorial on particle filters for online nonlinear/non-Gaussian Bayesian tracking'. IEEE Trans. on Signal Processing, pp. 174–188, Feb 2002.

Athans, M., Wishner, R.P., and Bertolini, A. (1968) 'Suboptimal state estimation for continuous–time nonlinear systems from discrete noisy measurements'. IEEE Transactions on Automatic Control, Vol. 13, No. 3, pp. 504–514, Oct 1968.

Aseeri, M.A., and Sobhy. (2001) 'Modelling and measurement of nonlinear amplifier system'. London Communications Symposium 2001, Proceedings, pp. 143 – 146, U C L Press Ltd.

Backeshoff, E. (2009) 'Sound samples for different types of transmissions' http://www.pervisell.com/download/soundsamplese.htm

Baddour, K.E., and Beaulieu, N.C. (2005) 'Autoregressive modelling for fading channel simulation'. IEEE Transactions on Wireless Communications, Vol. 4, No. 4, pp. 1650-1661, July 2005.

Bazzi, A. (2010) 'Radio communications chapter 6: Recent developments in channel estimation and detection for MIMO systems'. ISBN 978-953-307-091-9, April 1, 2010.

Bergman, N. (1999) 'Recursive Bayesian estimation: navigation and tracking applications'. Ph.D. Thesis Department of Electrical Engineering, Sweden, Dissertation No. 579, 1999.

Biglieri, E., Proakis, J., and Shamai, S. (1998) 'Fading channels: Information-theoretic and communications aspects'. IEEE Transactions on Information Theory, vol. 44, no. 6, pp. 2619-2692, Oct 1998.

Boroujeny, B.F., (1996) 'Channel equalization via channel identification: algorithms and simulation results for rapidly fading HF channels'. IEEE Transactions on Communications, vol. 44, No. 11, pp. 1409-1412, Nov 1996.

Bucy, R.S, and Senne, K.D. (1970) 'Realization of optimum discrete-time non-linear estimator'.1st Symposium on Nonlinear Estimation, San Diego, pp. 6–17, 1970.

Brine, N.L (2010) 'Capacity of MIMO wireless communication systems operating in the HF band'. PhD Thesis, University of Adelaide, Australia 2010.

Carlin, B.P., Polson, N.G., and Stoffer, D.S. (1992) 'A Monte Carlo approach to non-normal and nonlinear state-space modelling'. Journal of the American Statistical Association, vol. 87, No. 418, pp. 493–500, 1992.

Carpenter, J., Clifford, P., and Fearnhead, P. (1999) 'Improved particle filter for nonlinear problems'. IEE Proceedings - Radar, Sonar and Navigation, vol. 146, no. 1, pp. 2–7, Feb 1999.

Cannon, P.S., Angling, M.J., and Lundborg, B. (2002), 'Characterisation and modelling of the HF communications channel'. Reviews of Radio Science, edited by W. R. Stone, pp. 597-623, IEEE-Wiley, 1999-2002.

CCIR 322 (1986) 'CCIR (International Radio Consultative Committee), 'Characteristics and Applications of Atmospheric Radio Noise Data'. CCIR Report 322-3, 1986.

Chin, W.H., Ward, D.B., and Constantinides, A.G. (2002) 'Channel tracking for space-time block coded systems using particle filtering'. International Conference on Digital Signal Processing, 2002 14th Volume 2, pp.671-674, July 2002.

Cho, Y.S., Kim, J., Yang, W.Y., and Kang, C.G. (2010)'MIMO-OFDM wireless communications with Matlab'. John Wiley& sons (Asia) Pte Ltd, 2010.

Clark, A.P., and Hariharan, S. (1989) 'Adaptive channel estimation for an HF radio link', IEEE Transactions on Communications, vol. 37, No. 9, Sep 1989.

Clarke, R.H (1968) 'A statistical theory of mobile-radio reception'. Bell Syst. Tech. Journal., vol. 47, pp. 957-1000, July-Aug 1968.

Colman, G., Blostein, S., and Beaulieu, N.C. (1997) 'An ARMA multipath fading simulator'. Wireless Personal Communications: Improving Capacity, Services and Reliability. Boston, MA: Kluwer, 1997.

Cormick, J.M, and Blake, A. (2000) 'A Probabilistic exclusion for tracking multiple objects'. International Journal of Computer Vision, Vol. 39, No. 1, pp. 57–71, 2000.

Daniels, R.C., and Peters, S.W. (2013) 'A new MIMO HF data link: designing for high data rates and backwards compatibility'. Military Communications Conference, pp.1256 – 1261, MILCOM 2013.

Davies, K. (1965) ‘Ionospheric Radio Wave Propagation’. U.S. Department of Commerce. National Bureau of Standards, April 1965.

Delmas, J-P., Gazzah, H., Liavas, A. P., and Regalia, P. A. (2000) ‘Statistical analysis of some second-order methods for blind channel identification/equalization with respect to channel undermodeling’. IEEE Trans. Signal Processing, vol.48, no.7, pp.1984–1998, July 2000.

Durgin, G.D. (2003) ‘Space-time wireless channels’, Prentice Hall, New Jersey, 2003.

Djuri´c, P.M., Kotecha, J., Zhang, J., Huang, Y., Ghirmai, T., Bugallo, F., and Miguez, J. (2003) ‘Particle filtering’. IEEE Signal Processing Magazine, pp. 19–38, Sep 2003.

Doucet, A. (1998) ‘On sequential simulation-based methods for Bayesian filtering’. University of Cambridge CB2 1PZ Cambridge, Technical report CUED/F-INFENG/TR.310 ,1998.

Doucet, A., Godsill, S., and Andrieu, C. (2000) ‘On sequential Monte Carlo sampling methods for Bayesian filtering’. Statistical Computing, vol. 10, No. 3, pp. 197-208, 2000.

Ekman, T (2002) ‘Prediction of mobile radio channels: modelling and design’. PhD Thesis Uppsala University, 2002.

El-Halym, H.A.A., and Mahmoud, I.I. (2012) ‘Proposed hardware architectures of particle filter for object tracking’. EURASIP Journal on Advances in Signal Processing, Jan 2012.

Eleftheriou, E., and Falconer, D. (1987) ‘Adaptive equalization techniques for HF channels’. IEEE Journal on Selected Areas in Communications, vol.Sac-5, No. 2, pp. 238-246, Feb 1987.

Eyceoz, T., Duel-Hallen, A., and Hallen, H. (1998) ‘Deterministic channel modelling and long range prediction of fast fading mobile radio channels’. IEEE Comm. Lett., vol. 2, pp. 254-256, Sep 1998.

Fabrizio, G.A. (2000) ‘Space-time characterization and adaptive processing of ionospherically propagated HF signals’. PhD thesis, University of Adelaide Australia, 2000.

Freitas, N.D., Niranjan, M., and Gee, A. (1998) ‘Hierarchical Bayesian-Kalman models for regularization and ARD in sequential learning’. Technical Report CUED/FINFENG/TR 307, Cambridge University Engineering Department, University of Cambridge, Cambridge, UK, 1998.

Freitas, N.D. (1999) ‘Bayesian methods for neural networks’. Ph.D. Dissertation, Cambridge University Engineering Department, University of Cambridge, Cambridge, UK, 1999.

Fearnhead, P. 1998‘Sequential Monte Carlo methods in filter theory’. DPhil Dissertation, Merton College, University of Oxford, Oxford, UK, 1998.

Foschini, G.J., (1996) ‘Layered space-time architecture for wireless communications in a fading environment when using multi-element antennas’, Bell Labs Technical Journal, vol. 1, no. 2, pp. 41-59, 1996.

Foschini, G.J., and M.J Gans, M.J. (1998) ‘On limits of wireless communications in a fading environment when using multiple antennas’. Wireless Personal Communications, vol.6, pp. 311-315, 1998.

Frost, P.A., and T. Kailath, T. (1971) ‘An innovations approach to least-squares estimation-part iii: nonlinear estimation in white Gaussian noise’. IEEE Transactions on Automatic Control, vol. AC-16, No. 3, pp. 217–226, June 1971.

Gelb, A. (1974)‘Applied Optimal Estimation’. MIT Press, Cambridge, MA 1974.

Gesbert, D., Shafi, M.,Shiu,D., and Smith, P.J. (2003) ‘From theory to practice: an overview of MIMO space-time wireless systems’ IEEE Journal on Selected areas in communications, vol. 21, no. 3, pp. 281-301,Apr. 2003.

Gordon, N., Salmond, D., and Smith, A. F. M. (1993) ‘Novel approach to nonlinear/non-Gaussian Bayesian state estimation’. Radar and Signal Processing, IEE Proceedings F, vol. 140, no. 2, pp. 107–113, Apr 1993.

Gunashekar, S.D., Warrington, E.M., Salous, S., Kassem, W., Bertel, L., Lemur, D., Zhang, H., and Abbasi, N., (2007) 'An experimental investigation into the feasibility of MIMO Techniques within the HF band', in the second European Conference on Antenna and Propagation, pp. 1-5, Nov 2007.

Gunashekar, S.D., Warrington, E.M., Salous, S., Feeney, S.M., Abbasi, N. M., Bertel, L., Lemur, D., and Oger, M. (2009) 'Investigations into the feasibility of multiple input multiple output techniques within the HF band: Preliminary results' Radio Science, vol. 44, RS0A19, Aug 2009.

Harris Co. (1996) 'Radio communications in the digital age volume one: HF technology', Harris Corporation, RF Communications Division, May 1996.

Haykin, S., (1996) 'Adaptive filter theory'. Prentice-Hall, 3rd edition, 1996.

Haykin, S., Huber, K., and Chen, Z. (2004) 'Bayesian sequential state estimation for MIMO wireless communications'. Proceeding of IEEE, vol. 92, no. 3, pp. 439-454, Apr 2004

H¨oher, P. (1992) 'A Statistical discrete-time model for the WSSUS multipath channel'. IEEE Trans. Veh. Technol., vol. 41, pp. 461–468, Nov 1992.

Hoang, H.H, and Kwan, B.W. (2013) 'Suboptimal particle filtering for MIMO flat fading channel estimation' International Journal of Communication Systems, vol 26, Issue 3, pp. 356–368, March 2013.

Huber, K., and Haykin, S. (2003) 'Application of particle filters to MIMO wireless communications'. IEEE International Conference on Comm. volume 4, 11-15, pp.2311-2315, May 2003.

Ito, K., and K. Xiong, K. (2000) 'Gaussian filters for nonlinear filtering problems'. IEEE Transactions on Automatic Control, vol. 45, No. 5, pp. 910–927, May 2000.

ITU-R (2000) 'Testing of HF modems with bandwidths of up to about 12 KHz using Ionospheric channel simulators'. ITU-R F.1487 Recommendation, 2000.

Jantunrn, P. (2004) 'Modelling and measurement of nonlinear amplifier system', Master of Science in Espoo, Finland 2004.

Jeruchim, M.C., Balaban, P., Shanmugan, K.S. (1992) 'Simulation of communication systems'. Plenum Press, 1992.

Julier, S.J., Uhlmann, J.K., and Durrant-Whyte, H.F. (1995) 'A new approach for filtering nonlinear systems'. Proceedings of the American Control Conference, American Automatic Control Council, Evanston, IL, pp. 1628–1632, 1995.

Julier, S.J., and Uhlmann, J.K. (1997) 'A new extension of the Kalman filter to nonlinear systems'. The 11th International Symposium on Aerospace Defence Sensing, Simulation and Controls, Orlando, FL, 1997.

Kalman, R.E. (1960) 'A new approach to linear filtering and prediction problems'. Transactions on ASME, Journal of Basic Engineering, vol. 82, pp. 34–45, Mar 1960.

Karami, E., and Shiva. M (2006) 'Decision-directed recursive least squares MIMO channels tracking', EURASIP Journal on Wireless Communications and Networking, Article ID 43275, pp. 1–10, Mar 2006.

Kay, S.M. (1988) 'Modern spectral estimation'. Englewood Cliffs, NJ: Prentice-Hall, 1988.

Komninakis, C., Fragouli, C., Sayed, A.H., and Wesel, R.D. (2002) 'Multi-input multi-output fading channel tracking and equalization using Kalman estimation'. IEEE Trans on Signal Processing, pp. 1065 – 1076, May 2002.

Komninakis, C. 2003 'A Fast and Accurate Rayleigh Fading Simulator'. IEEE Globecom, pp. 3306-3311, 2003.

Kramer, S.C., and Sorenson, H.W. (1988) 'Recursive Bayesian estimation using piece-wise constant approximations'. Automatica, vol. 24, No. 6, pp. 789–801, May 1988.

Kermoal, J.P., Schumacher, L., Pedersen, K.I., Mogensen, P.E., and Frederiksen, F. (2002) 'A stochastic MIMO radio channel model with experimental validation', IEEE Journal on selected areas in communications, vol. 20, No.6, pp.1211-1226 Aug 2002.

Lee, D.J., (2005) 'Nonlinear Bayesian filtering with applications to estimation and navigation'. PhD Thesis, Texas A&M University May 2005.

Lemmon, J.J. (1997) 'Wideband model of man-man HF noise and interface' Radio Science vol. 32, Number 2, pp. 525-539, Mar-Apr 1997.

Lemmon, J.J. (2001) 'Wideband model of HF atmospheric radio noise'. Radio Science vol. 36, Issue 6, pp. 1385–1391, Nov-Dec 2001.

Liu, J.S., and Chen, R. (1998) 'Sequential Monte Carlo methods for dynamic systems'. Journal of the American Statistical Association, vol. 93, No. 443, pp. 1032–1044, Sep.1998.

Liu, Z., Ma, X., and Giannakis, G. B. (2002) 'Space-time coding and Kalman filtering for time-selective fading channels'. IEEE Trans on comm, vol 50(2), pp. 183–186, Feb 2002.

Loo, C., and Secord, N. (1991) 'Computer models for fading channels with applications to digital transmission'. IEEE Trans. Veh. Technol., vol. 40, pp. 700-707, Nov 1991.

Lui, G. (2011) 'The Sounds of HF' . http://goughlui.com/legacy/soundsofhf/index.htm

Malik, J.S., and Hemani, A. (2009) 'On the design of Doppler filters for next generation radio channel simulators', International Conference on Signals, Circuits and Systems, 2009.

Marzetta, T., and Hochwald, B. (1999) 'Capacity of a mobile multiple-antenna communication link in Rayleigh at fading', IEEE Transactions on Information Theory, vol. 45, no. 1, pp.139-157, Jan 1999.

Mastrangelo, J.F., Lemmon, J.J., Vogler, L.E., Hoffmeyer, J.A., Pratt, L.E., and Behm, C.J. (1997) 'A new wideband high frequency channel simulation system'. IEEE Transactions on Communications, vol. 45, No. 1, pp. 26-34 Jan 1997.

Merwe, R. V.D., Doucet, A., de Freitas, N., and Wan, E. (2000) 'The unscented particle filters'. Technical Report, CUED/F-INFENG/TR 380, Cambridge University Engineering Department, Cambridge, England, Aug 2000.

Miao, L., Zhang, J.J., Chakrabarti, C., and Suppappola, A.P. (2011) 'Algorithm and Parallel Implementation of Particle Filtering and its Use in waveform-agile sensing'. Springer Journal of Signal Processing Systems, vol. 65, pp. 211-227, Nov 2011.

Middleton, D. (1977) 'Statistical-Physical Models of Electromagnetic Interference'. IEEE transactions on electromagnetic compatibility, vol. EMC-19, No. 3, pp. 106-127 Aug 1977

MIL-STD-188-110C, (2011) 'Interoperability and performance standards for data modems', Sep 2011.

Naguib, A.F., Tarokh, V., Seshadri, N., and Calderbank, A.R. (1998) 'A space-time coding modem for high-data-rate wireless communications'. IEEE Journal on Selected Areas in Communications, vol. 16, pp. 1459 – 1478, Oct 1998.

Ndao, P.M., Lemur, D., and Braouseau, C. (2009) 'Capacity estimation of MIMO Ionospheric channels'.11th IET International Conference on Ionospheric Radio Systems and Techniques, Apr 2009.

Ndao, P.M., Erhel, Y., Lemur, D., and Masson, J.L. (2011) 'Design of a high-frequency (3 – 30 MHz) multiple-input multiple-output system resorting to polarization diversity' IET Microwave. Antennas Propag.vol.5, Issue.11, pp. 1310 – 1318, Aug 2011.

Ndao, P.M., Erhel, Y., Lemur, D., Oger, M., and Masson, J.L. (2013) 'Development and test of a trans-horizon communication system based on a MIMO architecture'. EURASIP Journal on Wireless Communications and Networking, vol. 167, pp.1687-1499, June 2013

Nordlund, P.J. (2002) 'Sequential Monte Carlo filters and integrated navigation'. Thesis, Department of Electrical Engineering, Link¨opings University, Link¨opings, Sweden, 2002

NTIA (1998) 'High frequency radio automatic link establishment (ale) application handbook' National Telecommunications and Information Administration (NTIA) Institute For Telecommunication Sciences (ITS) Boulder, Co September 1998.

Paulraj, A.J., Nabar, R. U., and Gore, D. (2003) 'Introduction to space-time wireless communications'. Cambridge University Press, Cambridge, UK, 2003.

Paulraj, A. J., Gore, D.A., Nabar, R. U and Bolcskei, H. (2004) 'An overview of MIMO communications a key to gigabit wireless'. Proceedings of the IEEE, vol. 92, no. 2, pp. 198–218, Feb. 2004.

Perrine, C., Erhel, Y., Lemur, D., and Bourdillon, A. (2005) 'Image transmission through the ionospheric channel', IEE Electron. vol. 41, (2), pp. 80–82, Feb 2005.

Pop, M.F., and Beaulieu, N.C., (2001) 'Limitations of sum-of-sinusoids fading channel simulators'. IEEE Trans Comm. vol. 49, pp. 699-708, Apr 2001.

Proakis, J.G. (1989) 'Digital Communications'. New York, McGraw-Hill, pp. 758-767, 1989.

Proakis, J.G., and Manolakis, D.K. (1997) 'Digital signal processing principles algorithms and applications'. Prentice Hall of India 1997.

Radenkovic, M., Bose, T., and Zhang, Z., (2003) 'Self-Tuning Blind Identification and Equalization of IIR Channels'. EURASIP Journal on Applied Signal Processing, vol. 9, pp. 930–937, 2003.

Rappaport, T. (1996) 'Wireless communications: principles and practice'. Prentice Hall, New Jersey, 1996.

Ristic, B., Arulampalam, S., and Gordon, N.J. (2004) 'Beyond the Kalman filter: particle filters for tracking applications', Artech House, Boston, MA, 2004.

Scheible, M.P., Teig, L. J., Fite, J.D., Cuomo, K.M., Werth, J.L., Meurer, G.W, Ferreira, N.C., Franzini, C.R. (2014) 'High Data Rate, Reliable Wideband HF Communications Demonstration'. Technical Paper, MITRE Corporation, 2014.

Shannon, C. (1948) 'A mathematical theory of communication'. Bell Labs Technical Journal, vol. 27, 379-423, 1948.

Shalom, Y.B., Li, X.R., and Kirubarajan, T. (2001) 'Estimation with applications to tracking and navigation'. John Wiley & Sons, Inc, New York, 2001.

Sklar, B. (1997a)'Rayleigh fading channels in mobile digital communication systems part I: characterization'. IEEE Communications Magazine July 1997.

Sklar, B. (1997b) 'Rayleigh fading channels in mobile digital communication systems part II: mitigation'. IEEE Communications Magazine July 1997.

Sorenson, H.W. and D.L. Alspach (1971). (1971) 'Recursive Bayesian estimation using Gaussian sums'. Automatica vol. 7, pp. 465–479, July 1971.

Spirent (2011) 'Correlation-based spatial channel modelling'. White paper 100, Spirent communication 2011.

Stangeways, H. J. (2006) 'Investigation of signal for spaced and co-located antennas on multipath HF links and implications for the design of SIMO and MIMO systems'. First European Conference on Antenna and Propagation pp. 1-6 Nov 2006.

Strangeways, H.J. (2007)'Estimation of signal correlation at spaced antennas for multi-mode ionospherically reflected signals and its effect on the capacity of SIMO and MIMO HF links', The 10th IET International Conference on IRST 2006, London, UK, pp. 306-310, 2007.

Su. K (2003) 'Space-time coding: from fundamentals to the future', Report, University of Cambridge, Sep 2003.

Tarokh, V., Jafarkhani, H., and Calderbank, A.R. (1999) 'Space-time block codes from orthogonal designs', IEEE Transactions on Information Theory, vol. 45, no. 5, 1456-1467, July 1999.

Telatar, I. E. (1999) 'Capacity of multi-antenna Gaussian channels'. European Transactions on Telecommunications, vol. 10, no. 6, pp.585-595, Nov. 1999.

Tomei, S., Coleman, C.J., Martorella, M., and Berizzi, F. (2013) 'The effect of Travelling Ionospheric Disturbances upon the performance of HF sky-wave MIMO radar'. IEEE radar conference, pp.1-6. 2013

Tugnait, J.K., Tong. L., and Ding. Z. (2000) 'Single-user channel estimation and equalization ', IEEE Signal Processing Magazine May 2000.

Velmurugan, R., Subramanian, S., Cevher, V., McClellan, J.H., and Anderson, D.V. (2007) 'Mixed-mode implementation of PFs'. IEEE Pacific Rim conference on communications, computers and signal processing, 2007.

Verdin, D., and Tozer,T. (1993) 'Generating a fading process for the simulation of land-mobile radio communications'. Electron. Lett., vol.29, pp. 2011-2012, Nov 1993.

Vucetic, B., and Yuan, J. (2003)'Space-time coding', John Wiley, 2003.

Wadsworth, M.A., and Dianat, S.D. (1999) 'Representation of HF atmospheric noise as a spherically invariant random process'. Proc. SPIE 3708, Digital Wireless Communication, 181, June 24, 1999.

Watterson, C. C., Juroshek, J. R., and Bensema, W.D. (1970) 'Experimental confirmation of an HF channel model'. Transactions on Communications, COM-18, No. 6, pp. 792–803, Dec. 1970.

Watterson, C.C (1979) 'Methods of Improving the performances of HF digital radios'. NTIA- Report -79-29, U. S Department of Commerce, Oct 1979

Wang, X., and Poor, H.V. (2004) 'Wireless communication system: advanced techniques for signal reception'. Pearson Education, 2004

Wheatley, M. (2000)'PathSim User and Technical Guide Ver. 1.0', Dec 2000.

Winters, J.H., Salz, J., and Gitlin, R.D. (1994) 'The impact of antenna diversity on the capacity of wireless communication systems'. IEEE Trans. Comm., vol. 42, pp. 1740 – 175, Feb/Mar/Apr 1994.

Wu, H., and Duel-Hallen, A. (2000) 'Multiuser detectors with disjoint Kalman channel estimators for synchronous CDMA mobile radio channels'. IEEE Trans. Comm., vol. 48, pp. 752-756, May 2000.

Xu, S., Zhang, H., Yang, H., and Wang, H. (2004)'New considerations for high frequency communications', 10th Asia-Pacific Conference on Communications and 5th International Symposium on Multi-Dimensional Mobile Communications, Beijing, China, pp. 444-447, 2004.

Young, D.J., and Beaulieu, N.C. (2000) 'The generation of correlated Rayleigh random variates by inverse Fourier transform'. IEEE Trans. Comm., vol. 48, pp. 1114-1127, July 2000.

Zhang, Q.T. (2000) 'A decomposition technique for efficient generation of correlated Nakagami fading channels'. IEEE J. Select. Areas Comm., vol. 18, pp. 2385-2392, Nov. 2000.

Zheng, Y.R and Xiao, C. (2002) 'Improved models for the generation of multiple uncorrelated Rayleigh fading waveforms'. IEEE Communication Letter, vol. 6, pp. 256-258, June 2002.

Zheng, Y.R and Xiao, C (2003) 'Simulation models with correct statistical properties for Rayleigh fading channels'. IEEE Trans. Comm., vol. 51, pp. 920-928, June 2003.

APPENDIX - 1

This appendix discusses the mathematical formulation to relate the channel impulse response and the tap-gain function. It deals with the characterisation of the channel parameters (both in time and frequency domain) to capture the HF channel impairments in the form of impulse response $g(\tau, t)$. These impulse responses are modelled as tap-delay filters. Each tap-delay is characterised to capture the channel impairment referred as tap-gain function. The summations of individual tap-gain function constitute the impulse response of channel. The variations channel parameters (Doppler, delay spread) are modelled as tap-gain function.

A.1.1 Characterization of Channel Impulse Response $g(\tau, t)$ in term of Tap-Gain Function

Ionospheric HF channel is non-stationary both in frequency and time. For scenarios comprising band-limited channel and impulse response $g(\tau, t)$ of the channel for a short time duration, the HF channel can be assumed to be merely stationary and accordingly it can be modelled [Watterson 1970]. A discrete stationary mode1 of a HF channel is illustrated in Figure A1.1. The input signal $x(t)$ whose propagation through a HF channel is of interest is fed to an ideal delay line and with finite number of taps along with adjustable delays. The signal at each tap is modulated in amplitude and phase by a suitable base-band tap-gain function $G_i(t)$ which represents the fading effect on the signal for particular paths. Several delayed and modulated signals are summed with additive noise (Gaussian, atmospheric, man-made) and interference (unwanted signals) to form the output signal y(t). Each tap corresponds to 'a' path and is used to model multipath components that are resolvable in time.

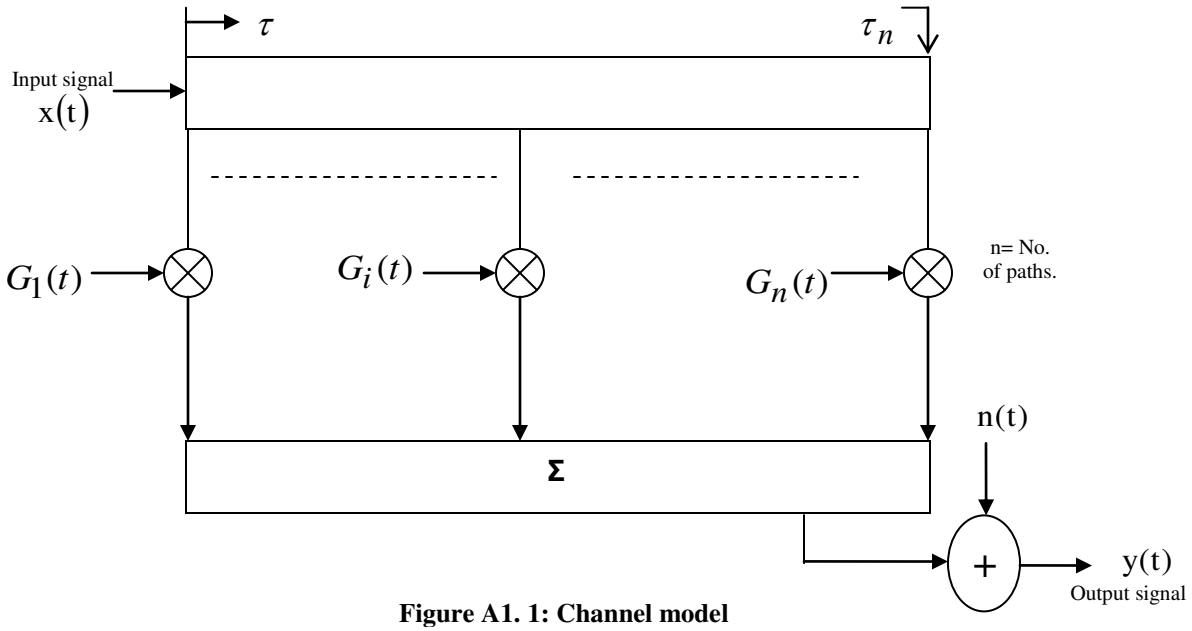

Figure A1. 1: Channel model

The channel model shown in Figure A1.1 is generic one for any wireless communication. The mathematical description of channel model illustrated in Figure A1.1 is as follows,

The time varying channel response $G(\tau, t)$ and its frequency response $H(f, t)$ of the model can be represented as

$$H(f,t) = \sum_{i=1}^{n} \exp(-j2\pi\tau_i f) G_i(t) \qquad \text{(A1.1)}$$

Where,

i is the index for a tap or path,

τ_i is time delay on the i^{th} path,

n is the total number of paths.

Statistical description for random process $G_i(t)$ and $H(f, t)$ is as follows,

The channel response, $G(\tau, t)$, is characterized in [Watterson 1970] as a wide sense-stationary complex-valued random process with the tap-gain auto-correlation function,

$$C_i(\tau_1, \tau_2, \Delta t) = E[G_i^*(\tau_1, t) G_i(\tau_2, t + \Delta t)] \qquad \text{(A1.2)}$$

In most radio communication media, the attenuation and phase shift of the channel associated with the signal delay τ_1 are uncorrelated with another signal delay τ_2. Then it follows from Equation (A1.2) that,

$$E[G_i^*(\tau_1, t)G_i(\tau_2, t + \Delta t)] = C_i(\tau_1 - \tau_2, \Delta t) \,.\, \delta(\tau_1 - \tau_2) \quad \text{(A1.3)}$$

Let $\tau' = \tau_1 - \tau_2$

Then Equation (A1.3) can re-written as,

$$C_i(\tau', \Delta t) = E[G_i^*(\tau_1, t)G_i(\tau_2, t + \Delta t)] \quad \text{(A1.4)}$$

Where,

E denotes expected or mean value

* denotes a complex conjugate

For Δt=0, the resulting autocorrelation function, $C_i(\tau') = C_i(\tau', 0)$ is referred as the multipath intensity profile of the channel. The range of values of delay τ over which $C_i(\tau') = 0$ is called the multipath delay spread of the channel and is denoted by T_m.

To simplify Equation (A1.4), the tap-gain correlation function is modified as follows,

$$C_i(\Delta t) = E[G_i^*(t)G_i(t + \Delta t)] \quad \text{(A1.5)}$$

Fourier transform of the tap-gain correlation function (Equation A1.5) is,

$$F[C_i(\Delta t)] = v_i(v) \quad \text{(A1.6)}$$

Where,

F denotes the Fourier transform

Since Fourier transform will not change the wide sense stationary properties of the channel. Considering the frequency response of channel Equation (A1.1), then correlation function of the channel referred as the spaced frequency correlation function $R(\Delta f, \Delta t)$ of the channel can defined as

$$R(\Delta f, \Delta t) = E[H^*(f, t)H(f + \Delta f\,, t + \Delta t)] \quad \text{(A1.7)}$$

Equation (A1.7) can also be represented by Fourier transform of tap-gain correlation function (Multipath profile), $C_i(\tau', \Delta t)$ of Equation (A1.4) with respect to τ since tap-gain functions are uncorrelated. Equation (A1.7) is written as

$$R(\Delta f, \Delta t) = \sum_{i=1}^{n} exp(-j2\pi\tau_i\Delta f)C_i(\Delta t) \quad \text{(A1.8)}$$

Based on some practical measurements [Watterson 1970], it has been noticed that the relation between the coherence bandwidth Δf_c and the multipath delay spread ΔT_m can be approximated by,

$$\Delta f_c \approx \frac{1}{T_m}$$

In order to illustrate the effects of the time variation of the channel, function $s(\tau, v)$ is defined as the Double Fourier transform of $R(\Delta f, \Delta t)$ with respect to the variables Δt and Δf. The function $s(\tau, v)$ is referred as channel scatter function. The channel scatter function is given as [Watterson 1970]

$$s(\tau, v) = \sum_{i=1}^{n} \delta(\tau - \tau_i) v_i(v) \qquad \text{(A1.9)}$$

Where,

$\delta(\tau)$ is the Dirac delta function.

$v_i(v)$ and $s(\tau, v)$ are power-ratio density functions;

v_i is the ratio of the output power per unit frequency offset over the i^{th} path to the channel input power

$s(\tau, v)$ is the ratio of the channel output power per unit frequency offset per unit time delay to the channel input power.

Scatter function $s(\tau, v)$ describes the relation between the time variation and the Doppler effects of channel. With $\tau = 0$ the function $s(v) = s(0, v)$ is referred as the Doppler power spectrum of the channel. The range of values of v over which $s(v \neq 0)$ is called the Doppler spread of the channel, f_d. The reciprocal of f_d is a measure of coherence time factor Δt_c of the channel,

$$\Delta t_c \approx \frac{1}{f_d} \qquad \text{(A1.10)}$$

Normally the tap-gain function for HF channel is considered to be an independent zero-mean complex-Gaussian function with Rayleigh amplitude and uniform phase density functions. The spectrum of tap-gain function will be of Gaussian shape. Even for single tap or path, two magneto-ionic components such as signal at low – ray, two Gaussian spectrums are considered [ITU-R 2000, Watterson 1970]. The tap-gain spectrum of two magneto-ionic components is illustrated in Figure A1.2.

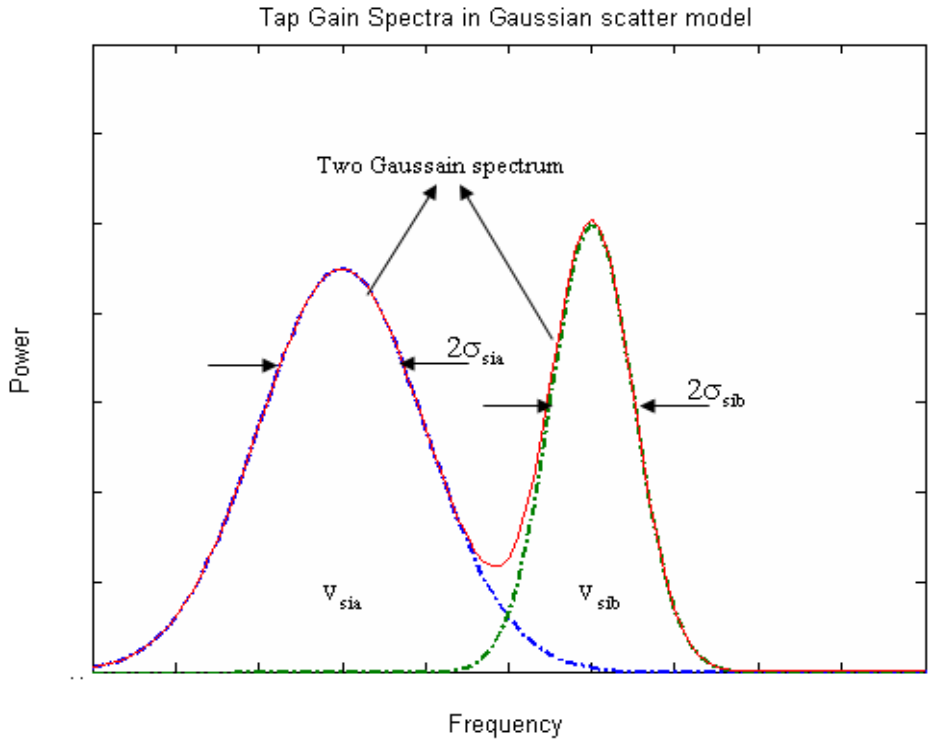

Figure A1. 2 : Tap-gain spectrums in channel model

The six parameters of Gaussian spectrums of tap-gain function are:

- Power ratios of the two magneto-ionic components $C_{sia}(0)$ and $C_{sib}(0)$
- Frequency shifts v_{sia} and v_{sib} ;
- Frequency spreads $2\sigma_{sia}$ and $2\sigma_{sib}$.

The subscripts 'a' and 'b' are meant to identify the magneto-ionic components. The subscript s denotes a specific channel model (particular channel parameter).

If the frequency shifts and spreads of the two magneto-ionic components are equal, they appear as one component and hence single Gaussian function is sufficient for the tap-gain spectrum. When separate taps are used, the two magneto-ionic components in the high ray are modelled through two different tap-gain Gaussian spectra.

For a HF channel that is band-limited and whose impulse response is of interest only with short time duration, the independent tap-gain functions can be defined as

$$G_{si}(t) = G_{sia}(t)exp(j2\pi v_{sia}t) + G_{sib}(t)exp(j2\pi v_{sib}t) \qquad \text{(A1.11)}$$

Where,

$G_{sia}(t)$ and $G_{sib}(t)$ are two independent complex (bivariate) Gaussian stationary ergodic random processes, with zero-mean values and independent quadrature components with equal rms values and identical spectrums. Specifically, $G_{sia}(t)$ is defined in terms of its real and imaginary components by

$$G_{sia}(t) = g_{sia}(t) + jg^{j}_{sia}(t) \qquad \text{(A1.12)}$$

Where $g_{sia}(t)$ and $g^{j}_{sia}(t)$ are independent real Gaussian processes, and are represented with the following single-time joint density function

$$p\left(g_{sia}, g^{j}_{sia}\right) = \frac{1}{\pi C_{sia}(0)} exp\left[-\frac{g^{2}_{sia}+g^{j^2}_{sia}}{C_{sia}(0)}\right] \qquad \text{(A1.13)}$$

In Equation (A1.13), $C_{sia}(0)$ is the autocorrelation of Equation (A1.12) at $\Delta t = 0$ and defines the ratio of the channel output power delivered by the magneto-ionic component to the channel input power.

Further, the Fourier spectra of $g_{sia}(t)$ and $g^{j}_{sia}(t)$ are equal implying,

$$F\{E[g_{sia}(t)g_{sia}(t+\Delta t)]\} = F\left\{E\left[g^{j}_{sia}(t)g^{j}_{sia}(t+\Delta t)\right]\right\} \qquad \text{(A1.14)}$$

Because $g_{sia}(t)$ and $g^{j}_{sia}(t)$ are independent, $G_{sia}(t)$ has a spectrum that is the sum of the identical spectrums of $g_{sia}(t)$ and $g^{j}_{sia}(t)$ and it has even symmetry about $v = 0$. Therefore, $exp(j2\pi v_{sia}t)$ factor has been included with $G_{sia}(t)$ in Equation (A1.11) to provide the desired frequency shift v_{sia} for this magneto-ionic component. With the '*a*' subscript replaced by '*b*', Equations (A1.12)-(A1.14) also apply for the other magneto-ionic components.

The tap-gain correlation function defined in Equation (A1.14) can be written as

$$C_{si}(\Delta t) = C_{sia}(0)exp[-2\pi^2\sigma^2_{sia}(\Delta t)^2 + j2\pi v_{sia}\Delta t] +$$
$$C_{sib}(0)exp[-2\pi^2\sigma^2_{sib}(\Delta t)^2 + j2\pi v_{sib}\Delta t] \qquad \text{(A1.15)}$$

and the corresponding tap-gain spectrum is

$$v_{si}(v) = \frac{C_{sia}(0)}{(2\pi)^{1/2}\sigma_{sia}} exp\left[-\frac{(v - v_{sia})^2}{2\sigma_{sia}^2}\right] + \frac{C_{sib}(0)}{(2\pi)^{1/2}\sigma_{sib}} exp\left[-\frac{(v - v_{sib})^2}{2\sigma_{sib}^2}\right] \quad \text{(A1.16)}$$

Where

$$C_{si} = C_{sia}(0) + C_{sib}(0) \quad \text{(A1.17)}$$

Figure.A1.2 depicts a typical tap-gain correlation function.

In view of the earlier stated assumption pertaining to near stationary feature of the HF channel, other than a Gaussian-scattering model, no additional statistical descriptions are necessary for modelling HF channel. It can be seen that the HF channel model involves three assumptions:

1) Gaussian-scattering hypothesis (each tap-gain function is a complex Gaussian process)
2) Independence hypothesis (each tap-gain function is independent)
3) Gaussian-spectrum hypothesis (each tap-gain spectrum in general is the sum of two Gaussian functions of frequency v_{sia} and v_{sib})

The establishment of the validity and appropriateness of the three assumptions stated above is also verification of the accuracy of the HF channel model. Propagation measurements and analyses of HF channel is aimed to test the validity of these three assumption and to determine the practical bandwidth limitations of the mode1 for typical channels. Because the discrete paths in the model only approximate the resolvable ionospheric model components with nonzero time spreads, the model, strictly speaking, can be valid only over an arbitrarily small band-width. Practically, however, it can be considered to be valid over a larger bandwidth *B*. Bandwidth B is inversely proportional to time spread *t* of the resolvable ionospheric components represented by each tap.

APPENDIX -2

This appendix highlights the comparison of simulation results on statistical parameters of HF channel obtained through open source channel simulators and the simulation model of HF channel proposed in this thesis. In view of the scope of the open source channel simulators, the comparison is limited to SISO configuration and the emphasis is on the Watterson model. In addition, this appendix presents a comparative analysis of atmospheric noise model appropriate for HF channel based on the analyses proposed by Middleton and Hall [Wadsworth 1999]. The atmospheric noise models of Middleton and Hall can be treated as derivatives of CCIR-322 model.

A2.1 Comparison of results on channel characteristics derived through the open source channel simulator and the simulation model of HF channel of this thesis

Following are the some of the available open source SISO-HF channel simulators.

- Pathsim
- Ionospheric Simulator V1.6
- Linsim

The modelling of channel in these channel simulators is based on the Watterson HF channel model. In this model, the ionospheric layers are assumed as fast moving reflecting media. The effect of these layers on reflected HF waves can be modelled by modulating the HF signal by a bivariate complex random process of Gaussian amplitude distribution resulting in modulated signal of Gaussian shape. Another effect of the simulated HF channel is to introduce the effect of multipath through delayed versions of transmitted signals arriving at the receiver.

The input to these simulators is the audio file. For analysis purpose, Linsim and Pathsim simulators are considered as reference to compare and validate the results obtained through the analysis presented in this thesis.

Screenshots of the three open source HF channel simulators are shown in Figures A2.1 to A2.3.

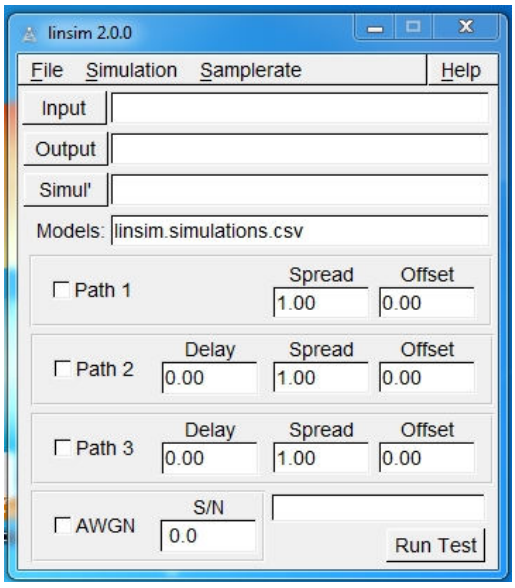

Figure A2. 1: Screen shot of Linsim HF channel simulator

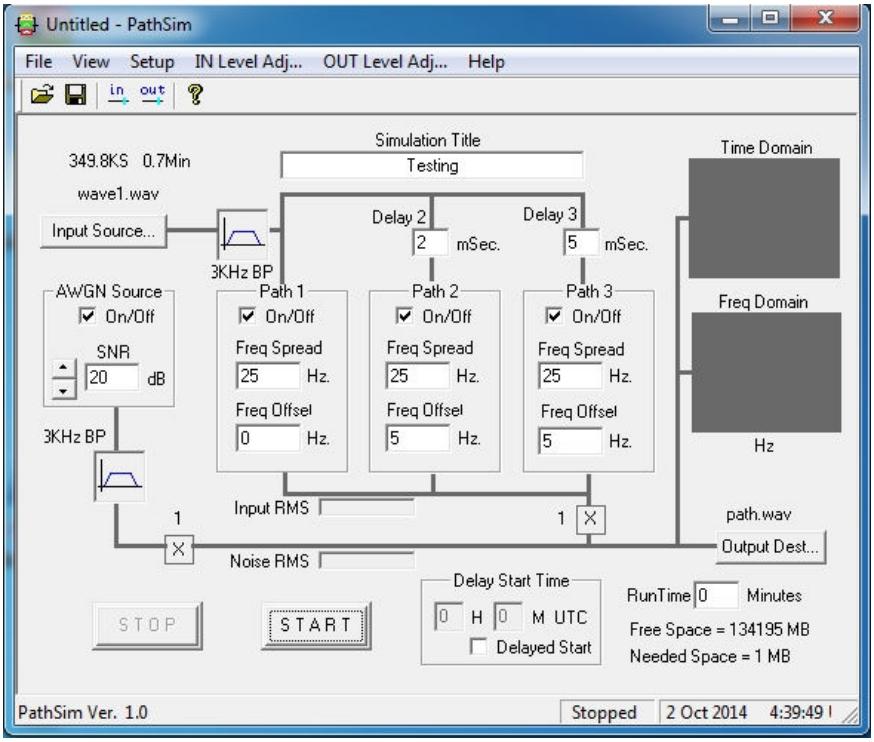

Figure A2. 2: Screenshot of PathSim HF channel simulator

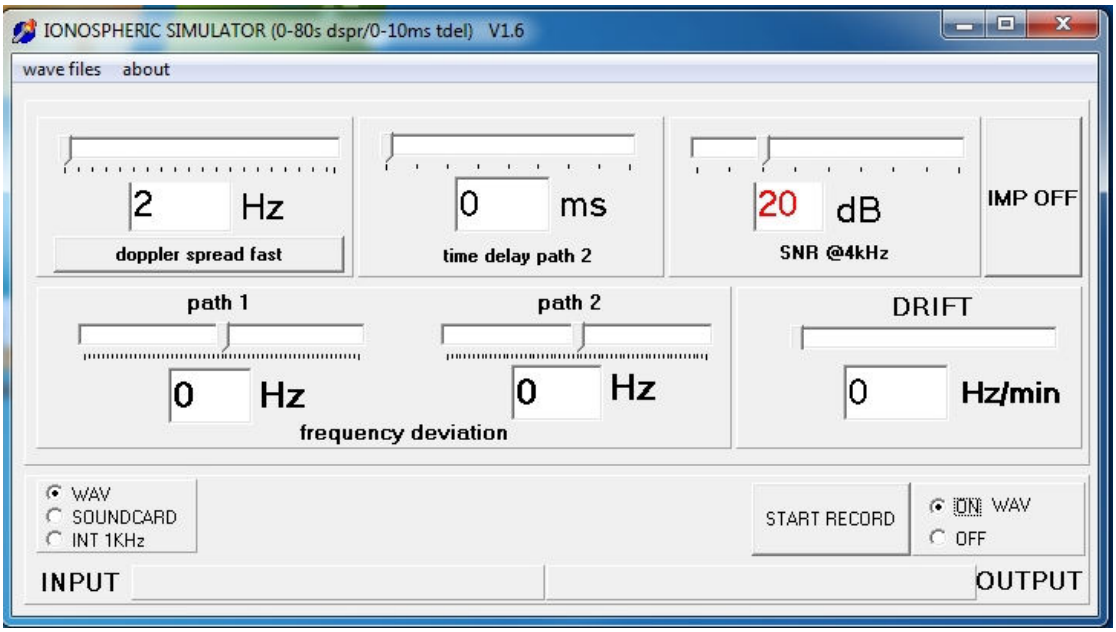

Figure A2. 3: Screen shot of ionospheric simulator

The channel parameters considered for the simulation of HF channel are:

- Doppler spread = 4Hz
- Multipath = 3 paths ; 0 ms , 3,ms , 5ms
- Noise = 10dB (Gaussian type)
- Input signal: QPSK modulated signal

The PSD of the impulse response of HF channel is simulated through simulators Linsim and Pathsim. The correlation between the simulation results of PSD obtained with Linsim and the simulation of Watterson model as proposed in the thesis is depicted in Figure A2.4. As can be seen from the results of Figure A2.4, there is a good agreement between the results derived through Linsim and the model proposed in this thesis. This in turn validates the analysis presented in the thesis. A similar comparison pertaining to ACF is shown in Figure A2.5

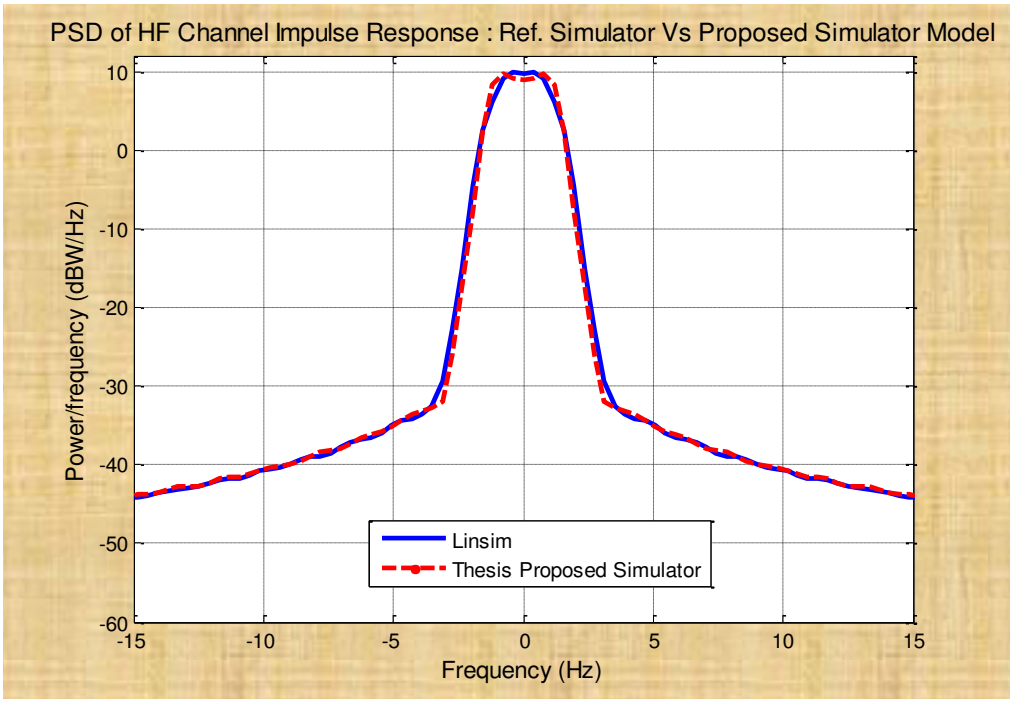

Figure A2. 4: PSD of HF channel impulse response: Linsim simulator Vs proposed channel simulator model

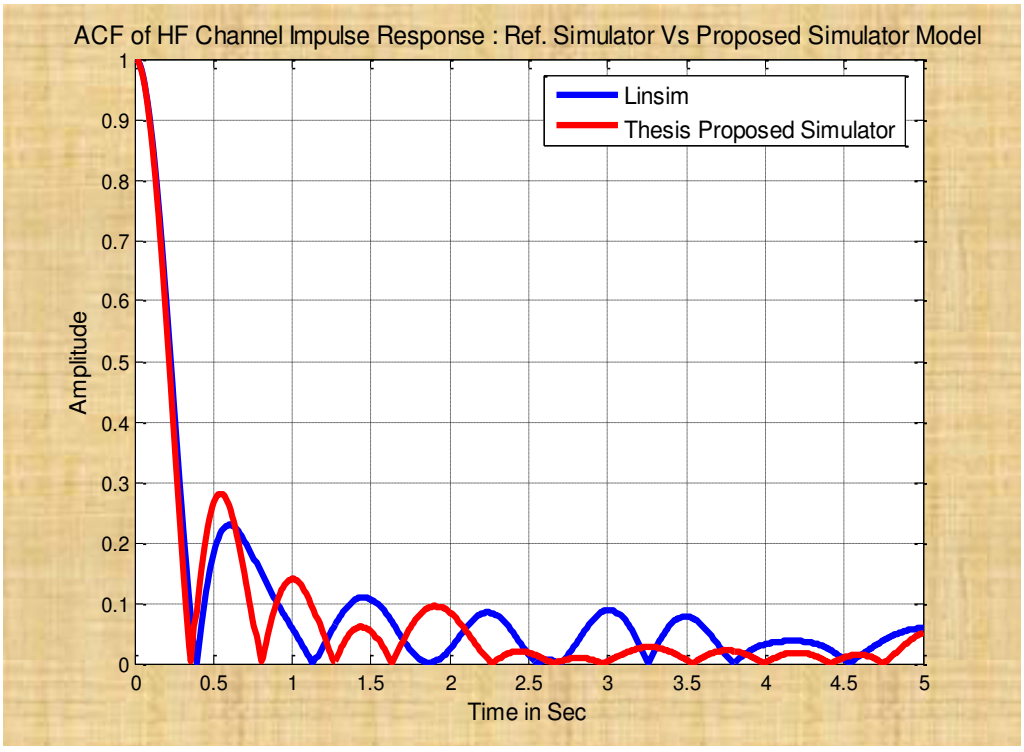

Figure A2. 5: ACF of HF channel impulse response: Linsim simulator Vs proposed channel simulator model

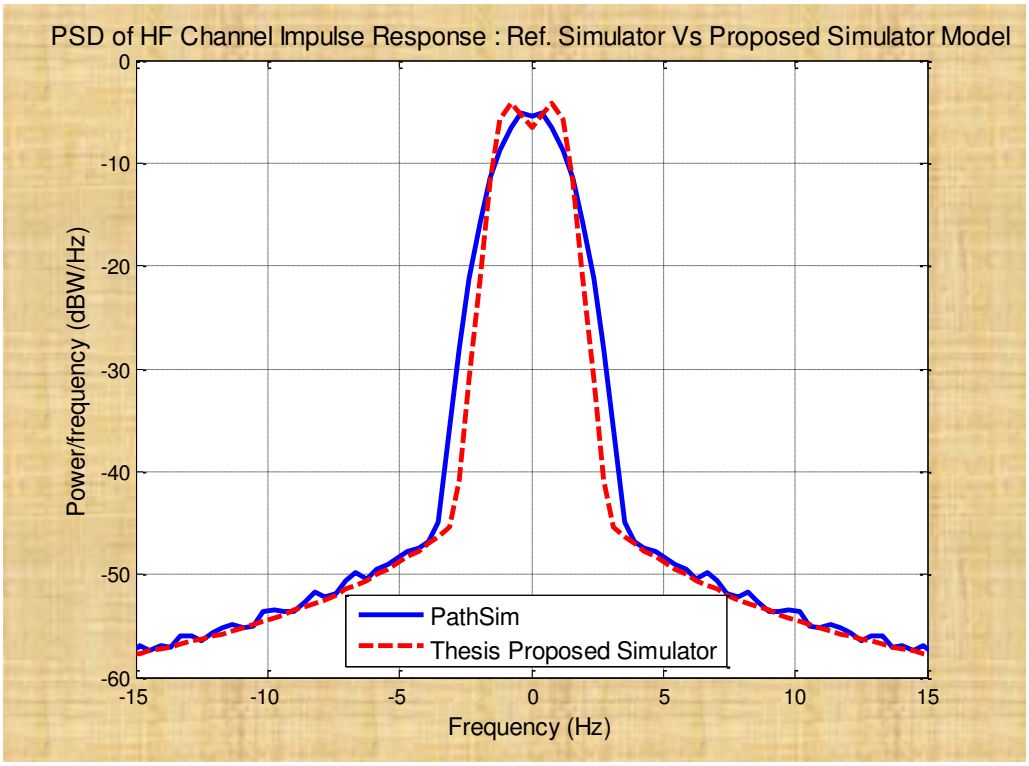

Figure A2. 6: PSD of HF channel impulse response: PathSim simulator Vs proposed channel simulator model

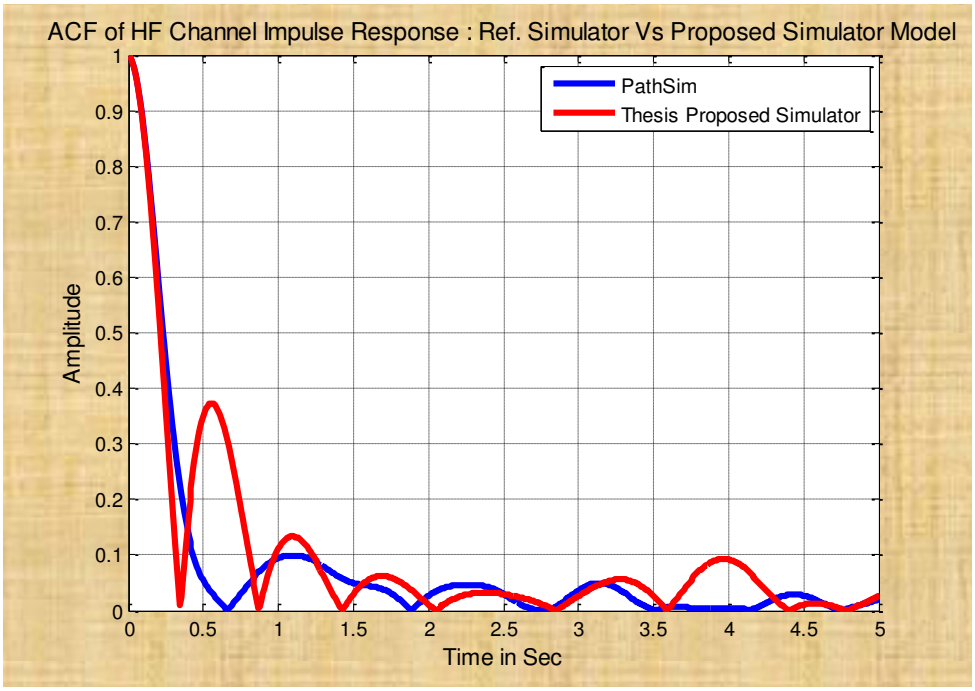

Figure A2. 7: ACF of HF channel impulse response: PathSim simulator Vs proposed channel simulator model

The Figures A2.6 and A2.7 show the comparison of the simulated results on PSD and ACF derived through the simulator Pathsim and the model of HF channel proposed in this thesis,The difference in the peaks of the curves pertaining to ACF can be attributed to the lack of precise information on order of Filters used in the open source simulators.

A.1.1 PSD and ACF for recorded HF signal

To facilitate a better appreciation about the statistical nature of real signal in a HF channel, data on real signals available in open literature is considered and its statistical parameters are also displayed. A data model commonly used by amateurs that employs FSK to modulate data in AX.25 frames at 300bps is considered. This is most commonly used for Automatic Packet Reporting System (APRS) [Lui 2011]. The statistical parameters PSD and ACF of sounding data'hfpacket.mp3' are plotted in Figures A2.8 and A2.9.

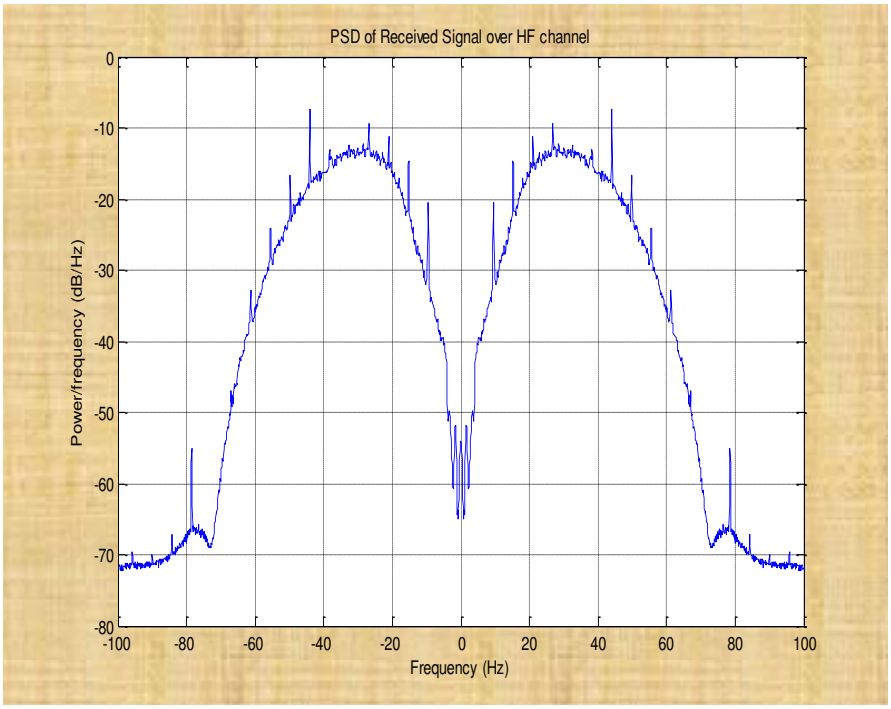

Figure A2. 8: PSD of recorded received HF channel signal

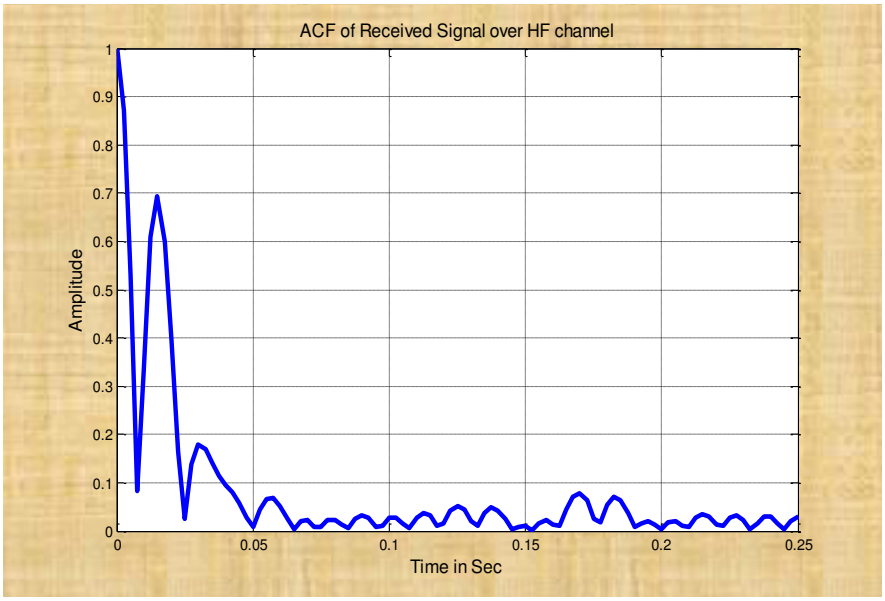

Figure A2. 9: ACF of recorded received HF channel signal

Another data model normally referred to as "Ionospheric Research Sounders and Over the Horizon Radars" is also studied**.** Ionosphere sounders are used to measure the channel state of the Ionosphere and provide important data which can be used to examine HF propagation [Lui 2011]. The statistical parameters (PSD and ACF) of sounding data 'iono-othr1.mp3' are plotted in Figures A2.10 and A2.11.

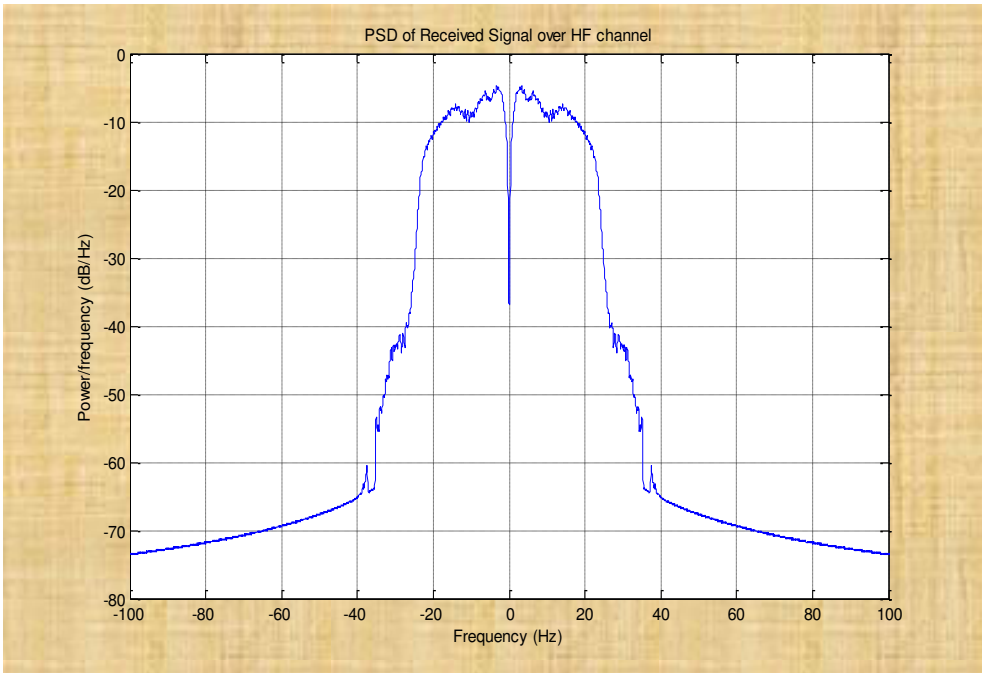

Figure A2. 10: PSD of recorded received HF channel signal

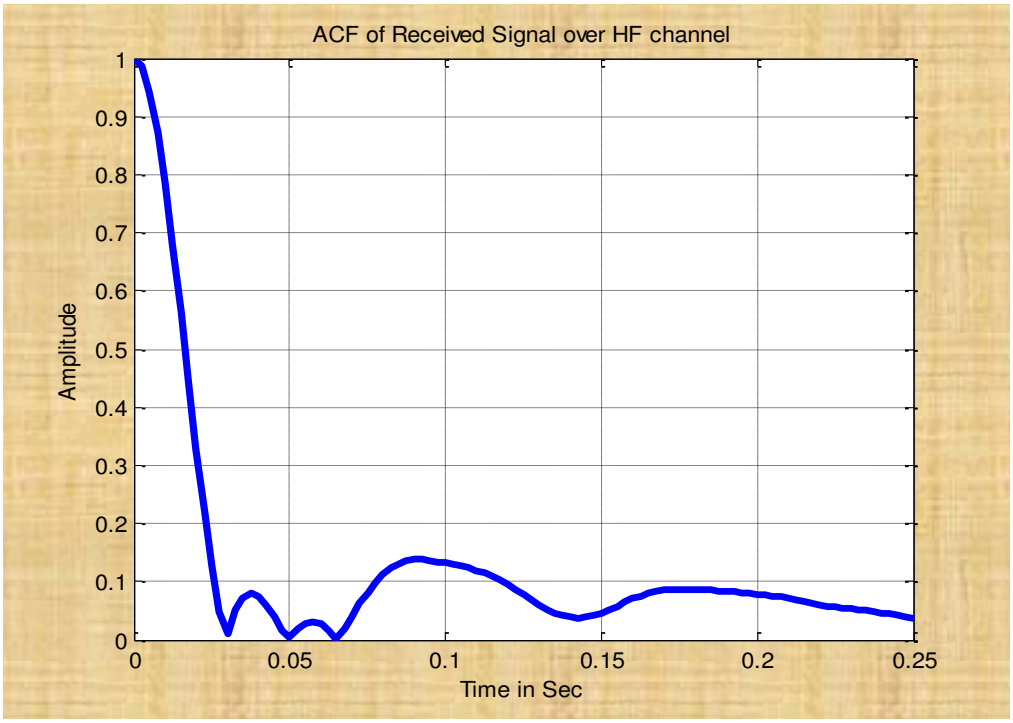

Figure A2. 11: ACF of recorded received HF channel signal

Referring back to the results in Figure 4.16, one can say that the statistical property of PSD of signal derived through simulation model of HF channel of this thesis resembles Gaussian spectral shape. The results in Figure 4.16 are based on a synthetic data. The results of open source simulators derived through real (recorded) data also exhibit Gaussian spectral shape as shown in Figures A2.4 and A2.6.

A.2 Comparison of Noise Models of Middleton and Hall

The determination of performance of a HF communication system is based on the availability of statistical properties of both the desired signal and the noise processes. System performance is highly dependent on the detailed statistical characteristics of signal, the noise and the signa1-to-noise ratio. The performance of a receiver depends on the optimal detector. An assumption of Gaussian distribution of noise is very common in an optimal detector. Based on this assumption, Probability of Bit error rate (P_e) is derived which is one of the important parameters in the assessment of the system performance of the communication link. However the HF atmospheric noise is non-Gaussian and this necessitates an alternate analysis of noise parameter. Usually CCIR-322 model is invoked

for the simulation of HF atmospheric noise. CCIR-322 model comprises the graphical and empirical models based on observations of HF atmospheric noise at numerous worldwide receive sites recorded over the period of many years.

CCIR-322 noise model is represented as

$$\eta(t) = V(t)\cos(\omega_c t + \emptyset(t)) \quad \text{(A2.1)}$$

Where,

$V(t)$ is voltage envelope whose the probability density function is a one-sided with two

parameters

$\emptyset(t)$ is phase which is uniformly distributed between 0 and 2π.

ω_c is centre frequency.

$\eta(t)$ is noise

[Lemmon 2001, Wadsworth 1999] have demonstrated that the CCIR 322 noise model can be approximated by a random process through a class of non-Gaussian random processes known as Spherically-Invariant Random Processes (SIRPs). Several models of HF atmospheric noise have been proposed by researchers [Wadsworth 1999] which have been considered as alternatives to CCIR-322. Following are the alternative atmospheric noise models.

- Middleton's canonical statistical-physical model of electromagnetic interference
- Shinde and Gupta's model of HF impulsive atmospheric noise
- Hall's model of impulsive phenomena

In subsequent subsection, Middleton and Halls models of HF atmospheric noise models are described to deal with non-Gaussian distribution of noise.

A.2.1 Middleton Model

A simplified distribution commonly used in the modelling of impulsive noise is the Gaussian mixture or contaminated Gaussian, defined by a $\varepsilon-$contamination density function of the form [Wang 2004]

$$f(x) = (1 - \varepsilon)f_p(x) + \varepsilon f_c(x), \quad \text{(A2.2)}$$

Where both f_p and f_c are zero-mean Gaussian densities with variances σ_p^2 and σ_c^2 respectively. Gaussian mixture models have been popular in communications mainly because of their mathematical tractability and their ease of conceptual interpretation. The parameter ε can be interpreted as the amount of contamination allowed in the model. Since $f(x)$ is the sum of two Gaussian densities, it is easy to generate a noise with pseudo random Gaussian–mixture for simulation studies. Figure A2.12 shows the PDF of noise based on Middleton model.

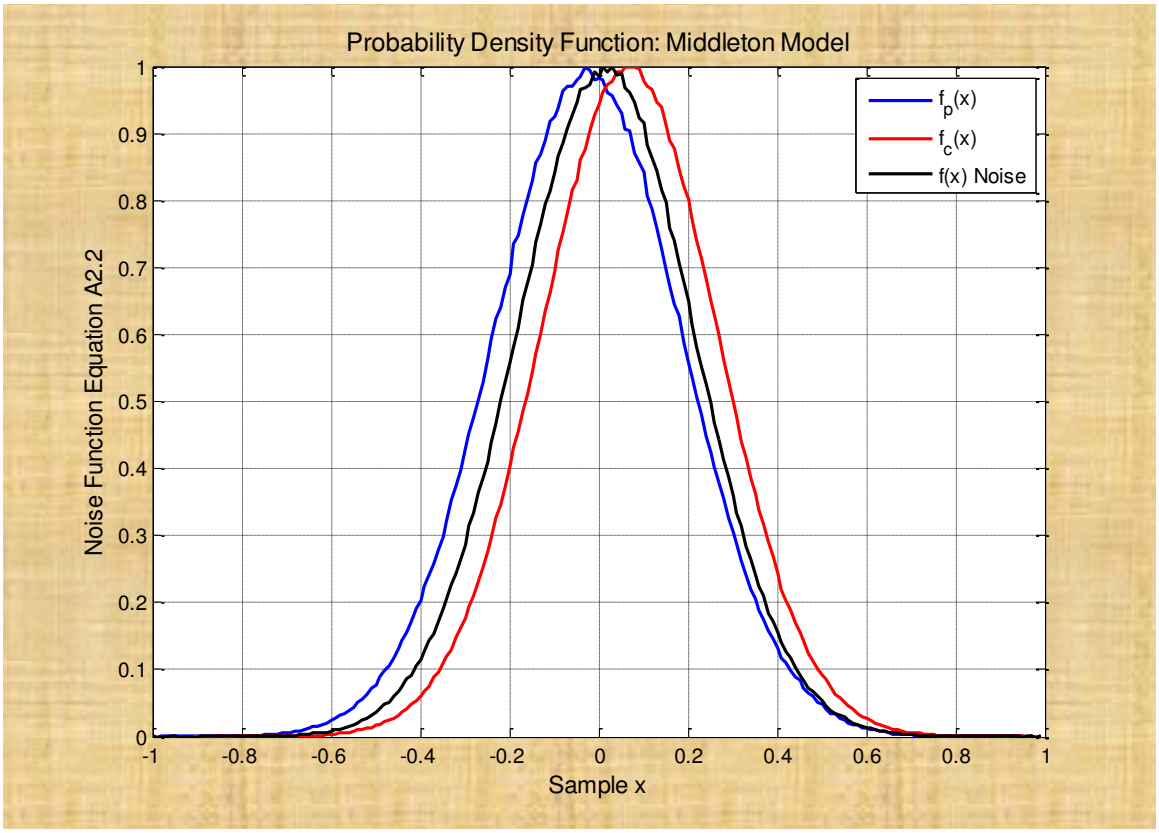

Figure A2. 12: PDF of noise generated through Middleton model

A2.2 Hall Model

In Hall model, it is assumed that the phase $\emptyset(t)$ is uniformly distributed and the PDF, $p_v(V)$ of the voltage envelope $V(t)$ of Equation (A2.1) is given as [Lemmon 2001]

$$p_v(V) = \frac{(\theta - 1)\gamma^{\theta-1}V}{(V^2 + \gamma^2)^{(\theta+1)/2}}, \tag{A2.3}$$

Where θ and γ are free parameters (with the constraint that $\theta > 1$, so that $p_v(V)$ is normalised).

The cumulative probability $P(V)$, is

$$P(V) = 1 - \frac{\gamma^{\theta-1}}{(V^2+\gamma^2)^{\frac{(\theta-1)}{2}}}, \quad \text{(A2.4)}$$

Rearranging the Equation (A2.4), $V(P)$ can be represented by

$$V(P) = \gamma\left(\frac{1}{(1-P)^{2/(\theta-1)}} - 1\right)^{1/2}, \quad \text{(A2.5)}$$

Where P is the cumulative probability of a random variable uniformly distributed between 0 and 1. The Figure A2.13 shows the PDF of noise generated based on Hall model. It is evident that phase $\emptyset(t)$ follows uniform distribution and envelope $V(t)$ *is* a one-sided with two parameters (γ and θ) and resultant noise $\eta(t)$ is whose distribution is Gaussian.

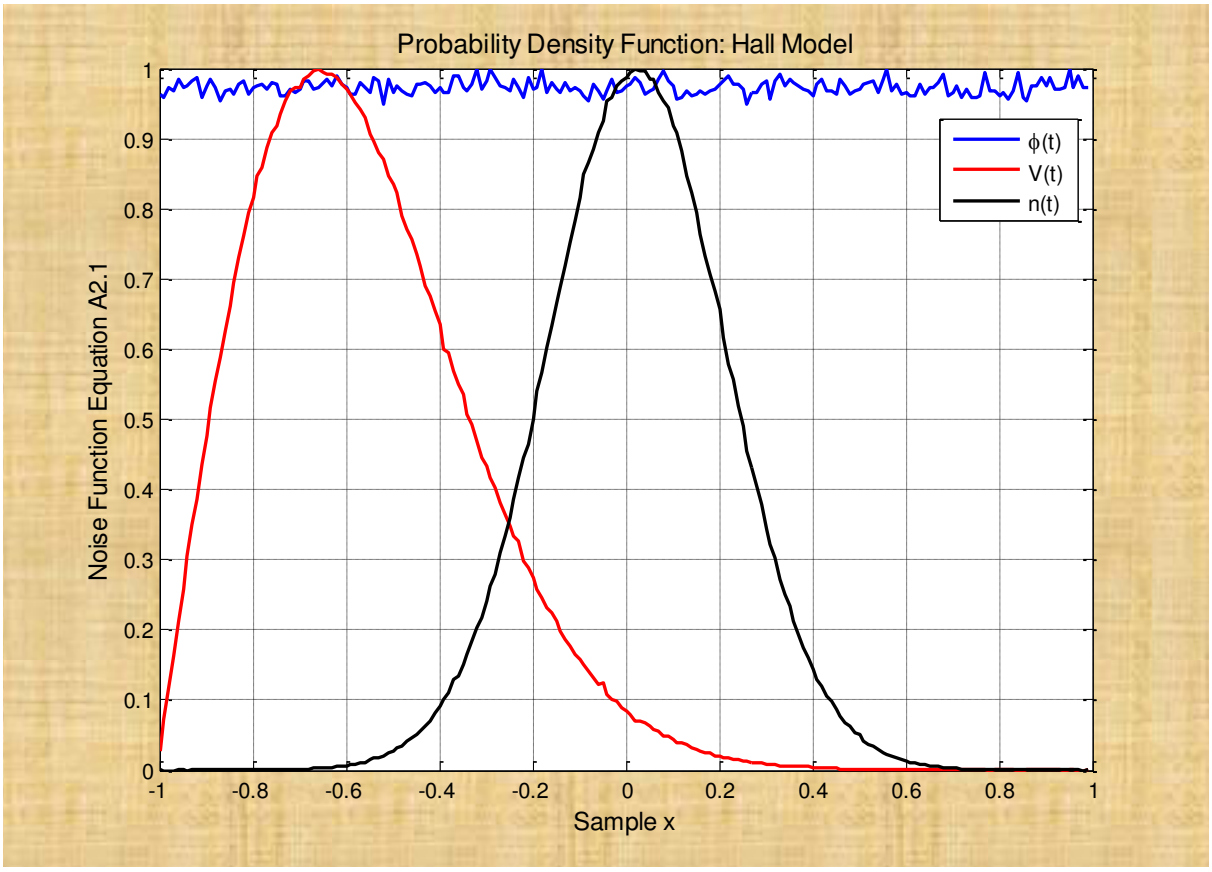

Figure A2. 13: PDF of noise generated through Hall model

A comparison of PDF of atmospheric noise derived through Middleton and Hall models is shown in Figure A2.14. In this comparison, $\varepsilon = 0.4$ for Middleton model: and $\theta = 60\,, \gamma = 5$ for Hall model have been assumed. To get a good correlation between these two models, a particular combination of respective parameters is needed.

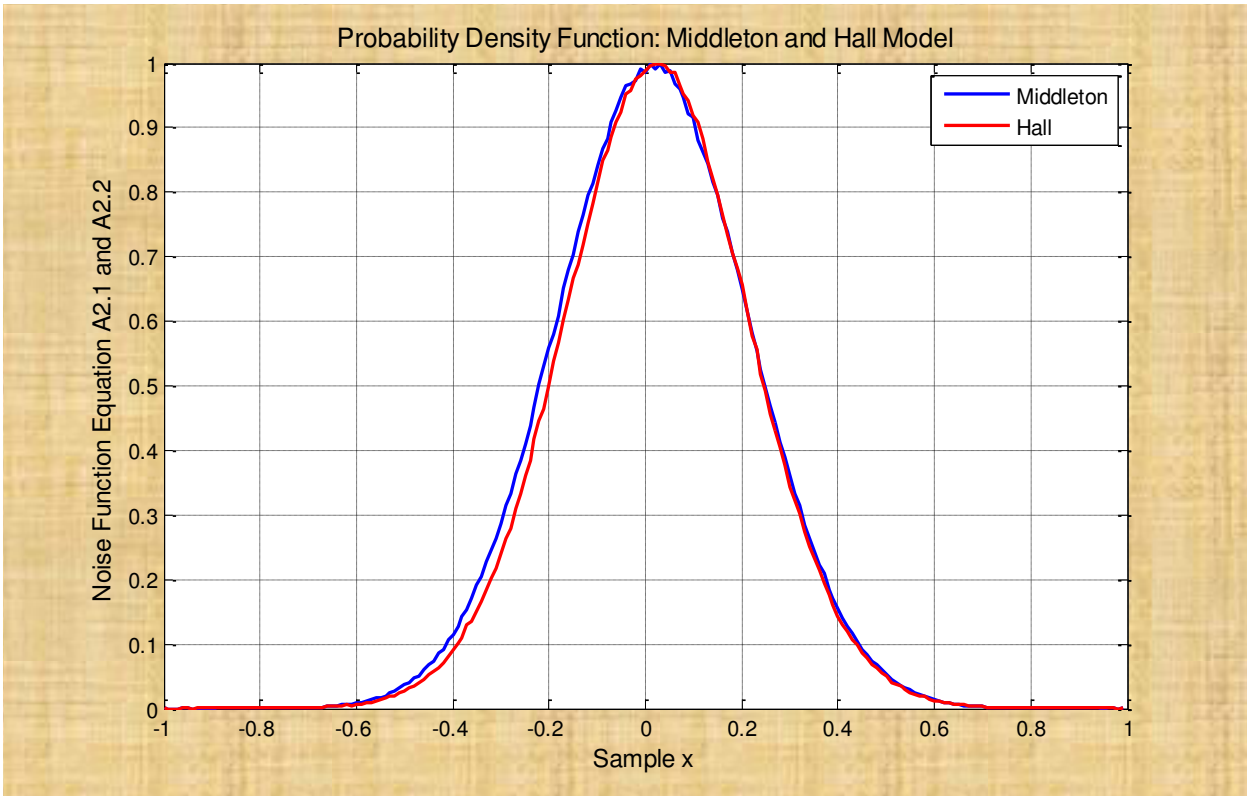

Figure A2. 14: PDF of noise generated through Middleton and Hall models

With different values of parameters for Middleton and Hall models of atmospheric noise, the variance and mean of noise distribution will vary but the resultant distribution is always Gaussian. The advantage for using Middleton model is to relate the probabilities of bit error and signal to noise ratio. The probability distribution of the instantaneous value of the received noise envelope is required to be known while formulating the probability of bit error (P_e). The required probability distribution can be obtained through model developed by Middleton model [Lemmon 1997].

APPENDIX -3

LOW RISK RESEARCH ETHICS APPROVAL

Low Risk Research Ethics Approval Checklist

Applicant Details

Name KUMARESH KRISHNIAN	E-mail K1_kumar@yahoo.com
Department	Date 01.04.2011
Course PhD	Title of Project Characterization & Estimation of High freq. channel with Multiple Antenna System

Project Details

Summary of the project in jargon-free language and in not more than 120 words:

- Research Objectives
- Research Design (e.g. Experimental, Desk-based, Theoretical etc)
- Methods of Data Collection

Participants in your research

1. Will the project involve human participants?	Yes	No ✓

If you answered **Yes** to this questions, this may **not** be a low risk project.

- If you are a student, please discuss your project with your Supervisor.
- If you are a member of staff, please discuss your project with your Faculty Research Ethics Leader or use the Medium to High Risk Ethical Approval or NHS or Medical Approval Routes.

Risk to Participants

2. Will the project involve human patients/clients, health professionals, and/or patient (client) data and/or health professional data?	Yes	No ✓
3. Will any invasive physical procedure, including collecting tissue or other samples, be used in the research?	Yes	No ✓
4. Is there a risk of physical discomfort to those taking part?	Yes	No ✓
5. Is there a risk of psychological or emotional distress to those taking part?	Yes	No ✓
6. Is there a risk of challenging the deeply held beliefs of those taking part?	Yes	No ✓
7. Is there a risk that previous, current or proposed criminal or illegal acts will be revealed by those taking part?	Yes	No ✓
8. Will the project involve giving any form of professional, medical or legal advice, either directly or indirectly to those taking part?	Yes	No ✓

If you answered **Yes** to **any** of these questions, this may **not** be a low risk project.

- If you are a student, please discuss your project with your Supervisor.
- If you are a member of staff, please discuss your project with your Faculty Research Ethics Leader or use the Medium to High Risk Ethical Approval or NHS or Medical Approval Routes.

Risk to Researcher

9. Will this project put you or others at risk of physical harm, injury or death?	Yes	No ✓
10. Will project put you or others at risk of abduction, physical, mental or sexual abuse?	Yes	No ✓
11. Will this project involve participating in acts that may cause psychological or emotional distress to you or to others?	Yes	No ✓
12. Will this project involve observing acts which may cause psychological or emotional distress to you or to others?	Yes	No ✓
13. Will this project involve reading about, listening to or viewing materials that may cause psychological or emotional distress to you or to others?	Yes	No ✓
14. Will this project involve you disclosing personal data to the participants other than your name and the University as your contact and e-mail address?	Yes	No ✓
15. Will this project involve you in unsupervised private discussion with people who are not already known to you?	Yes	No ✓
16. Will this project potentially place you in the situation where you may receive unwelcome media attention?	Yes	No ✓
17. Could the topic or results of this project be seen as illegal or attract the attention of the security services or other agencies?	Yes	No ✓
18. Could the topic or results of this project be viewed as controversial by anyone?	Yes	No ✓

If you answered **Yes** to **any** of these questions, this is **not** a low risk project. Please:

- If you are a student, discuss your project with your Supervisor.
- If you are a member of staff, discuss your project with your Faculty Research Ethics Leader or use the Medium to High Risk Ethical Approval route.

Informed Consent of the Participant

19. Are any of the participants under the age of 18?	Yes	No ✓
20. Are any of the participants unable mentally or physically to give consent?	Yes	No ✓
21. Do you intend to observe the activities of individuals or groups without their knowledge and/or informed consent from each participant (or from his or her parent or guardian)?	Yes	No ✓

If you answered **Yes** to **any** of these questions, this may **not** be a low risk project. Please:

- If you are a student, discuss your project with your Supervisor.
- If you are a member of staff, discuss your project with your Faculty Research Ethics Leader or use the Medium to High Risk Ethical Approval route.

Participant Confidentiality and Data Protection

22. Will the project involve collecting data and information from human participants who will be identifiable in the final report?	Yes	No ✓
23. Will information not already in the public domain about specific individuals or institutions be identifiable through data published or otherwise made available?	Yes	No ✓
24. Do you intend to record, photograph or film individuals or groups without their knowledge or informed consent?	Yes	No ✓
25. Do you intend to use the confidential information, knowledge or trade secrets gathered for any purpose other than this research project?	Yes	No ✓

If you answered **Yes** to **any** of these questions, this may **not** be a low risk project:

- If you are a student, discuss your project with your Supervisor.
- If you are a member of staff, discuss your project with your Faculty Research Ethics Leader or use the Medium to High Risk Ethical Approval or NHS or Medical Approval routes.

Gatekeeper Risk

26. Will this project involve collecting data outside University buildings?	Yes	No ✓
27. Do you intend to collect data in shopping centres or other public places?	Yes	No ✓
28. Do you intend to gather data within nurseries, schools or colleges?	Yes	No ✓
29. Do you intend to gather data within National Health Service premises?	Yes	No ✓

If you answered **Yes** to **any** of these questions, this is **not** a low risk project. Please:

- If you are a student, discuss your project with your Supervisor.
- If you are a member of staff, discuss your project with your Faculty Research Ethics Leader or use the Medium to High Risk Ethical Approval or NHS or Medical Approval routes.

Other Ethical Issues

30. Is there any other risk or issue not covered above that may pose a risk to you or any of the participants?	Yes	No ✓
31. Will any activity associated with this project put you or the participants at an ethical, moral or legal risk?	Yes	No ✓

If you answered **Yes** to these questions, this may **not** be a low risk project. Please:

- If you are a student, discuss your project with your Supervisor.
- If you are a member of staff, discuss your project with your Faculty Research Ethics Leader.

Principal Investigator Certification

If you answered **No** to **all** of the above questions, then you have described a low risk project. Please complete the following declaration to certify your project and keep a copy for your record as you may be asked for this at any time.

Agreed restrictions to project to allow Principal Investigator Certification

Please identify any restrictions to the project, agreed with your Supervisor or Faculty Research Ethics Leader to allow you to sign the Principal Investigator Certification declaration.

Participant Information Leaflet attached.
Informed Consent Forms attached.

Principal Investigator's Declaration

Please ensure that you:

- Tick all the boxes below and sign this checklist.
- Students must get their Supervisor to countersign this declaration.

I believe that this project **does not require research ethics approval**. I have completed the checklist and kept a copy for my own records. I realise I may be asked to provide a copy of this checklist at any time.	
I confirm that I have answered all relevant questions in this checklist honestly.	
I confirm that I will carry out the project in the ways described in this checklist. I will immediately suspend research and request a new ethical approval if the project subsequently changes the information I have given in this checklist.	

Signatures

If you submit this checklist and any attachments by e-mail, you should type your name in the signature space. An email attachment sent from your University inbox will be assumed to have been signed electronically.

Principal Investigator

Signed..... (Principal Investigator or Student)

Date ..... 01.04.2011 .....

Students storing this checklist electronically must append to it an email from your Supervisor confirming that they are prepared to make the declaration above and to countersign this checklist. This-email will be taken as an electronic countersignature.

Student's Supervisor

Countersigned..... (Supervisor)

Date ..... 01.04.2011 .....

I have read this checklist and confirm that it covers all the ethical issues raised by this project fully and frankly. I also confirm that these issues have been discussed with the student and will continue to be reviewed in the course of supervision.